UNIVERSITA' DEGLI STUDI DI CATANIA
Ph.D. in Biotechnology
Curriculum Molecular Biotechnology
(XXXIV cycle)

STEFANO CONTI NIBALI

Electrophysiological analysis of human VDAC proteins incorporated into the Nanodiscs and investigation of VDAC isoform 3 cysteine residues in mitochondrial functionality and ROS buffering

Ph.D. thesis

Supervisor: Professor Vito De Pinto

Coordinator: Professor Vito De Pinto

2018-2021

Affiliations:

1.Department of Biomedical and Biotechnological Sciences, University of Catania, Catania, Italy.

2.Membrane Biophysics and Center for Synthetic Biology, Technische Universitat Darmstadt, Darmstadt, Germany.

Research experience abroad:

6 months in the laboratory of Prof Dr. Gerhard Thiel at the Technical University of Darmstadt (Germany).

Keywords:

VDAC; Planar Lipid Bilayer; Cell-free expression; Nanodisc; Mitochondria; ROS; HAP1 knock-out cell lines; Cysteines.

Abbreviation:

ATP	*Adenosine triphosphate*
ADP	*Adenosine diphosphate*
NAD	*Nicotinamide adenine dinucleotide*
mtDNA	*Mitochondrial DNA*
IMM	*Inner Mitochondrial Membrane*
IMS	*Intermembrane Space*
AIF	*Apoptosis-Inducing Factor*
OMM	*Outer Mitochondrial Membrane*
VDAC	*Voltage-Dependent Anion-selective Channel*
ROS	*Reactive oxygen species*
NMR	*Nuclear magnetic resonance*
PLB	*Planar Lipid Bilayer*
DPhPC	*Di-phytanoyl-phosphatidyl-choline*
CFPS	*Cell-Free protein expression system*
ND	*Nanodisc*
MSP	*Membrane Scaffold Protein*
APO-1	*Apolipoprotein 1*
DMPC	*Di-myristoyl-phosphatidylcholine*
DPPC	*Di-palmitoyl-phosphatidylcholine*
POPC	*Palmitoyl-oleoyl-glycerol-phosphocholine.*
PS	*Phosphatidyl-serine*
PG	*Phosphatidyl-glycerol*

PE	*Phosphatidyl-ethanolamine*
Cyt C	*Cytochrome C*
Bax	*Bcl-2-associated X protein*
HK	*Hexokinase*
Bak	*Bcl-2 homologous antagonist/killer*
RyR2	*Ryanodine Receptor type-2*
StAR	*Steroidogenic Acute Respiratory protein*
ER	*Endoplasmic Reticulum*
MAM	*Mitochondria-Associated endoplasmic reticulum Membrane*
Ox-PTM	*Oxidative post-translational modification*
Cys	*Cysteine*
MS	*Mass Spectrometry*
MDV	*Mitochondrial-Derived Vesicle*
PKA	*Protein kinase A*
GSK3β	*Glycogen synthase kinase 3-beta*
TSPO	*translocator protein*
HBV	*Hepatitis B virus*
HHV-8	*Human Gamma-herpesvirus 8*

Sommario

I mitocondri sono organelli essenziali per le cellule eucariotiche poiché sostengono l'enorme richiesta energetica, necessaria per mantenere l'omeostasi cellulare. La comunicazione tra il citosol e i mitocondri è consentita dalle porine mitocondriali, note anche come Voltage-Dependent Anion Selective Channels (VDACs), localizzate nella membrana mitocondriale esterna di tutti gli eucarioti. Le proteine VDAC permettono gli scambi di metaboliti e partecipano a numerose vie cellulari grazie all'interazione con specifici enzimi citosolici e fattori apoptotici. Nei mammiferi esistono tre diverse isoforme, conosciute come VDAC1, VDAC2 e VDAC3. Pur condividendo un'alta omologia di sequenza, le tre isoforme presentano funzioni e caratteristiche diverse.

La prima parte di questa tesi di dottorato si focalizza sull'analisi elettrofisiologica delle proteine VDAC prodotte utilizzando un sistema di espressione *cell-free* associato a nanodisc. Questo nuovo metodo di espressione rappresenta una potente alternativa per evitare le procedure di ripiegamento *in vitro* delle proteine. In questo lavoro, il sistema di sintesi proteica *in vitro* è stato usato per la prima volta per esprimere le tre isoforme VDAC. In particolare, è stato investigato se il sistema *cell-free* associato ai nanodisc, mantenesse inalterate le caratteristiche elettrofisiologiche dei canali VDAC. Inoltre, è stato valutato l'impatto sulle caratteristiche biofisiche di VDAC3 in seguito a pre-trattamento della proteina con agente riducente (DTT) e dopo la rimozione dei residui di cisteina nella sequenza amminoacidica mediante mutagenesi sito-diretta. I nostri risultati hanno dimostrato che questo nuovo sistema mantiene immutate le caratteristiche elettrofisiologiche delle proteine VDAC e inoltre ha convalidato l'estrema importanza dei residui di cisteina sull'attività canale di VDAC3.

La seconda parte della tesi riguarda l'indagine del contributo di VDAC3 nella risposta allo stress ossidativo. VDAC3 rappresenta la meno abbondante e la più enigmatica isoforma ed è stata a lungo l'argomento di ricerca del gruppo di De Pinto. L'isoforma 3 presenta proprietà biofisiche atipiche che sono state attribuite allo stato ossidativo dei suoi residui di cisteina. Inoltre, alcune evidenze in letteratura hanno suggerito che VDAC3 potrebbe essere un *sensore redox*, sottolineando il suo coinvolgimento nell'omeostasi mitocondriale delle specie reattive dell'ossigeno. Una prova diretta, tuttavia, manca. Lo scopo di questo lavoro è stato quello di valutare il ruolo di VDAC3 sulla funzionalità mitocondriale utilizzando la linea cellulare umana HAP1 knock-out di VDAC3. Questo lavoro ha rivelato che VDAC3 previene il deterioramento mitocondriale indotto dallo stress ossidativo. Inoltre, è stato dimostrato, per la prima volta, che i residui di cisteina di VDAC3 sono responsabili della capacità della proteina di contrastare l'eccesso dei ROS mitocondriali.

Abstract

Mitochondria are crucial organelles for eukaryotic cells since they support the huge energy demand required to maintain cellular homeostasis. Communication between cytosol and mitochondria is allowed by mitochondrial porins, also known as Voltage-Dependent Anion selective Channels (VDACs), localized in the outer mitochondrial membrane of all eukaryotes. VDACs allow metabolite exchanges across the organelle and participate in numerous cellular pathways due to the interaction with cytosolic enzymes and apoptotic factors. There are three different isoforms in mammals: VDAC1, VDAC2, and VDAC3. Although sharing a high sequence homology, the three isoforms present different functions and characteristics.

The first part of this Ph.D. thesis focuses on the electrophysiological analysis of VDAC proteins produced using a cell-free expression system associated with nanodiscs (NDs), which offer a native-like environment. This new expression method represents a powerful alternative to avoid protein refolding procedures. In this work, the *in vitro* protein synthesis system was used for the first time to express the three human VDAC isoforms. After their reconstruction into Planar Lipid Bilayer, the electrophysiological features were compared with those obtained by canonical expression protocol. Furthermore, we analyzed the impact of both reducing agents in the buffer and cysteine removal on the biophysical characteristics of human VDAC3. Our results showed that this new system did not change the electrophysiological features of VDACs, and additionally validated the extreme importance of cysteine residues in the channel functionality of VDAC3.

The second part of the thesis concerns the investigation of human VDAC3 contribution in oxidative stress response. Among the three isoforms in mammals, VDAC3 has long been the research topic of De Pinto's group as it represents the least abundant and the most enigmatic one. It features untypical biophysical properties that have been attributed to the specific oxidative status of its cysteine residues. Moreover, clues within the literature have suggested VDAC3 as a putative redox sensor, stressing its involvement in mitochondrial reactive oxygen species homeostasis. A direct proof, however, is missing. This work aimed to evaluate the role of VDAC3 on mitochondrial functionality using the near-haploid human HAP1 cell line devoid of VDAC3. This work revealed that VDAC isoform 3 prevents mitochondrial impairment induced by oxidative stress. For the first time, we have also proved that cysteine residues of VDAC3 are responsible for the ability of the protein to counteract mitochondrial ROS overload.

TABLE OF CONTENTS

1. Introduction

1.1 Mitochondria

Mitochondria are critical organelles in eukaryotic cells due to their essential role in regulating several processes and pathways. They are considered *the cell's powerhouse* since they supply the cells with more than 90% of the required ATP energy [1]. They also play a crucial role in the biosynthesis of required molecules for proliferation, production of reactive oxygen species (ROS), calcium signaling, apoptotic activation, and cell death [2–4]. Given the different functions, it is not surprising that the mitochondria are involved in various disorders and diseases, including cancer [5–7]. Mitochondria resemble α-proteobacteria, from which they are speculated to have originated by endocytosis about 1.6 billion years ago [8]. The most unmistakable evidence of this evolutionary relationship is the closely related homology of the bacterial and mitochondrial respiratory chain complexes [9]. Mitochondria also have their genetic system (known as mitochondria DNA or mtDNA), which uses a distinct DNA code that differs from their bacterial ancestors and their eukaryotic hosts [10]. During evolution, they have transferred up to 99 % of their genes to the nucleus [9]. The vast majority of mitochondrial proteins are produced in the cytoplasm and imported into the organelle by specific protein translocases. In mammals, only 13 mitochondrial proteins are encoded by the mtDNA; most of the hydrophobic subunits of respiratory chain complexes or the ATP synthase [10,11].

Structurally, mitochondria are organelle with a diameter of about 0.75-3 μm and bounded by a double membrane [12]. Their peculiar structural conformation allows distinguishing five different compartments: the outer membrane, intermembrane space, inner membrane, cristae, and matrix [13–16]. The outer membrane separates mitochondria from the cytoplasm (see below). The inner mitochondrial membrane (IMM) is a tight diffusion barrier to all ions and molecules. These can cross the IMM thanks to specific membrane transport proteins, each highly selective for a particular ion or molecule. Because of its ion selectivity, an electrochemical membrane potential of about 180 mV accumulates across the inner membrane [17]. Unlike the outer membrane, the inner membrane has a very high protein/phospholipid ratio due to the large number of proteins required for the metabolic pathway [18,19]. Moreover, the inner membrane forms invaginations (called cristae) that extend deeply into the matrix, defining the third mitochondrial compartment, which contains most electron transport chain complexes and the ATP synthase [14,16,20]. Outer and inner mitochondrial membranes delimit the intermembrane space, which is biochemically similar to the cytosol. This space also

contains enzymes that utilize ATP and different cell death-promoting factors, including caspases, apoptosis-inducing factor (AIF), and cytochrome C [21,22]. The displacement of these proapoptotic factors from the intermembrane space to the cytosol is the critical function of mitochondria to trigger the cell death cascade. The mitochondrial matrix, bounded by the IMM, is considered the innermost compartment. Matrix is characterized by a high pH value required to create the transmembrane electrochemical gradient that drives ATP synthesis [17]. In the mitochondrial matrix is placed the mtDNA (estimated 2-10 copies per organelle) [23], which is compacted by the mitochondrial transcription factor into supramolecular assemblies called nucleoids [24]. The matrix is also the site of organellar DNA replication, transcription, protein biosynthesis, and numerous enzymatic reactions (including the citric acid cycle) [10,15].

1.2 The Outer Mitochondrial membrane

The outer mitochondrial membrane (OMM) mediates numerous interactions between the mitochondrial and the rest of the cell. It typically contains ~ 8% of the total proteins of the organelle. Unlike the IMM, the outer membrane is more homogenous in structure and contains less cardiolipin and a lower proportion of proteins [25,26]. All proteins in the outer membrane encode in the nucleus and synthesize by cytosolic ribosomes. The insertion of these proteins into the outer membrane is promoted by internal targeting sequences and the activity of specific proteins [23]. OMM proteins include various enzymes, components of precursor protein translocation and insertion machinery, pore-forming proteins, and proteins mediating mitochondrial fusion and fission [27]. Hence, the outer membrane plays a crucial role in the biogenesis, metabolism, and morphology of the organelle.

Two different types of integral outer membrane proteins exist, proteins embedded by a single or multiple α-helices and proteins with a transmembrane β-barrel [23], as shown in Fig. 1. Most of these proteins are anchored to the membrane by a single helix, which crosses the membrane and can be located either at the N- or C-terminus of the polypeptide chain. Generally, most of these proteins are exposed to the cytosol, and only a short segment is located in the IMS (Fig.1 A and B). Tom22 and Mim1 belong to the second group of proteins with a single transmembrane segment; they have an orientation in which the N-terminal domain is in the cytosol, and the C-terminal part faces the IMS (Fig. 1C). In yeast, two different proteins were found anchored in the membrane through multiple α-helices: Fzo1, a GTPase involved in mitochondrial fusion, displays the largest part of the protein directed toward the cytosol, and the two helices embedded in the membrane are

connected via a short loop in the IMS (Fig. 1D); and Ugo1, an interaction partner of Fzo1, is organized as a multi-pass membrane protein and has been suggested to possess at least three transmembrane helices (Fig. 1E) [28,29].

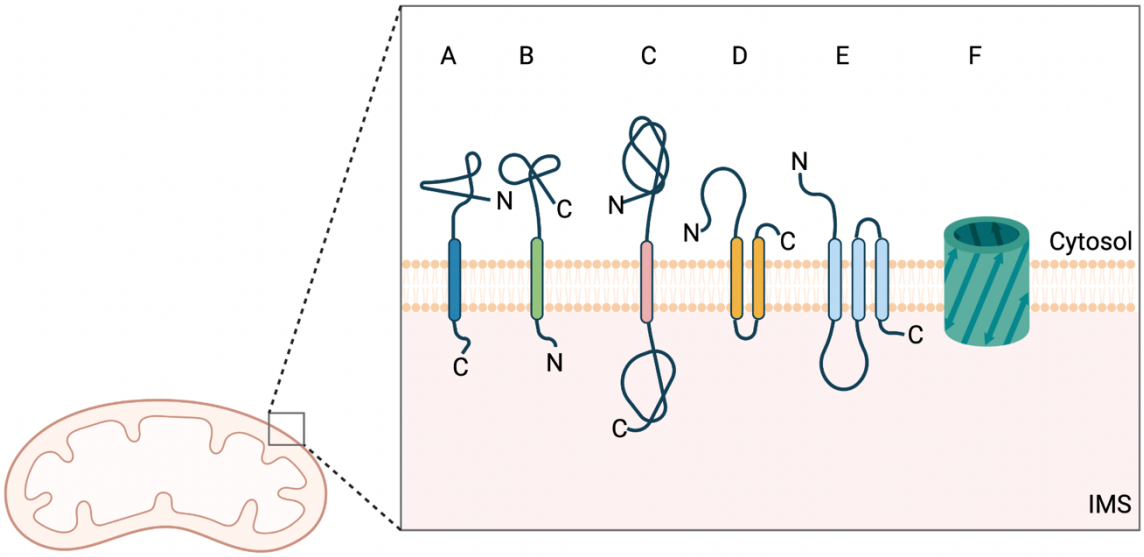

Figure 1. Topologies of proteins in the mitochondrial outer membrane. Integral outer membrane proteins are anchored either by a transmembrane β-barrel or single or multiple α-helices. A and B: proteins are inserted with the bulk of the polypeptide is exposed to the cytosol, and only a minor C- or N-terminal segment crosses the outer membrane. C: proteins traverse the outer membrane once, with an N-terminal domain localized to the cytosol and a soluble C-terminal domain to the intermembrane space. D and F: proteins span the membrane twice or several times. F: proteins cross the outer membrane as a series of antiparallel β-strands, forming a β-barrel structure. (Picture modified from: [23])

β-barrel proteins are exclusively found in the outer membranes of Gram-negative bacteria and in eukaryotic organelles of endosymbiotic origin. Unlike the other proteins mentioned above, they form a cylindrical structure consisting of antiparallel β-strands that are interconnected by loops (Fig. 1 F). Individual filaments are usually 9-11 amino acids long and are inclined at approximately 45° to the membrane plane. The pore structure is stabilized by hydrogen bonds between the peptide backbones of neighboring β-strands [23]. Compared to bacteria, the number of known mitochondrial β-barrel proteins is relatively small. Six proteins are predicted to form β-barrel structures in yeast, including two isoforms of porin. Regarding porins, in mammalian cells, they are also known as Voltage-Dependent Anion-Selective Channel [30].

1.3 Voltage-Dependence Anion-Selective Channels (VDACs)

VDACs are the most abundant pore-forming proteins of the OMM. In mammals, high conserved through evolution, three distinct genes encode for three different VDAC isoforms, known as VDAC1, VDAC2, and VDAC3 [31]. The isoforms are characterized

by similar molecular weight (28–32 kDa) and by approximately 70% of sequence similarity. Despite the high sequence homology, VDAC isoforms display different roles in physiological and pathological conditions, expression levels, and tissue-specificity [32]. VDAC channels are required for the metabolic cross-talk between cytosol and mitochondria, allowing the exchanges of many Krebs's cycle intermediates, ATP & ADP, NAD^+/NADH [33–35], also regulate the flux of small ions (Cl^-, K^+, Na^+, and Ca^{2+}), participate in fatty acid transport and cholesterol distribution in mitochondrial membranes [36]. Furthermore, VDACs maintain the physiological level of cytosolic calcium and are considered the main escape route for mitochondrial superoxide anion (O^{2-}) to the cytosol. [37]. Beyond the metabolic functions, the peculiar position of VDACs, at the interface between cytosol and mitochondria, makes them the mitochondrial docking site for several cytosolic proteins (e.g., hexokinases, glycerol kinase, glucokinase, and creatine kinase), including molecules involved in the regulation of cell life and death [38]. The main VDACs cellular functions are summarized in Fig. 2.

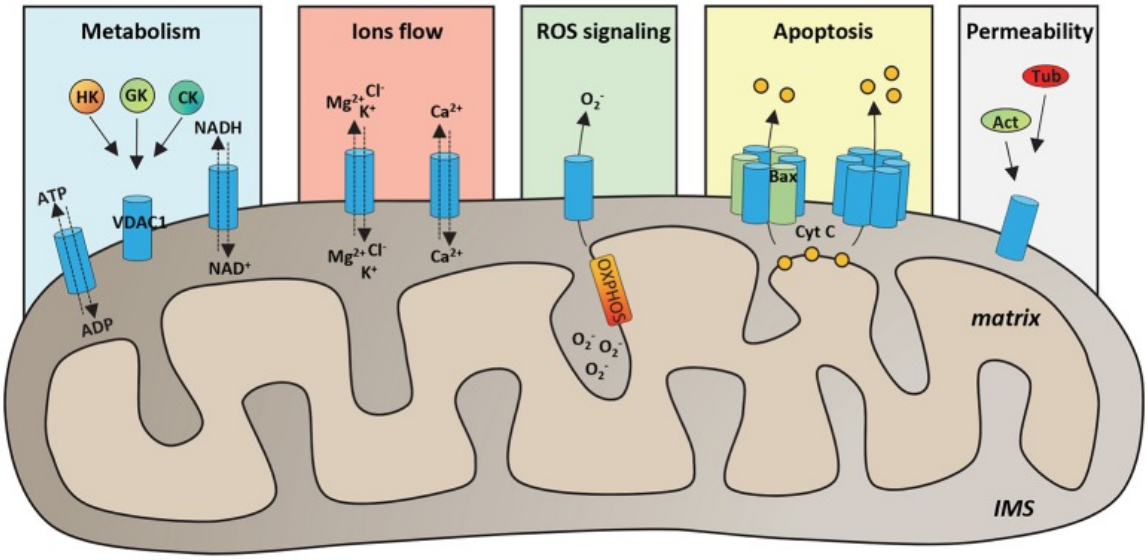

Figure 2: Schematic representation of VDAC functions. VDACs allow metabolite and ions exchanges across the OMM. VDACs mediates cellular energy production by transporting ATP/ADP, NADH, and Krebs cycle's intermediates. VDAC1 controls the flux of Mg^{2+}, Cl^- and K^+ ions across the OMM and maintains cytosolic Ca^{2+} levels in the physiological range. Furthermore, VDAC proteins are responsible for superoxide anion release to the cytosol. VDACs participate in numerous cellular pathways thanks to interacting with cytosolic enzymes and apoptotic factors. It has been shown that many cytoskeleton proteins, such as Actin (Act) or Tubulin (Tub), bind VDAC and regulate channel permeability. (Picture from: [39]).

1.4 Structure and electrophysiological features

Structure

In 2008, the 3D structure of VDAC1 was determined simultaneously in three independent laboratories using NMR spectroscopy [40], X-ray crystallography [41], or a combination

of both techniques [30] (Figure 3A, 3B, and 3C). All three structures showed a 19-stranded β-barrel, with the N-terminal tail positioned inside the pore, confirming the dimensions of the VDAC pore previously observed by electron microscopy. Although the three structures differed in some details (e.g., the NMR structure did not fully resolve the alpha-helix), the number and tilt of β-strands and overall dimensions were almost identical. The β-strands are arranged in an antiparallel bunch strengthened by hydrogen bridges between each couple, albeit, the odd number of β-strands causes β1 and β19 to run in parallel (Figure 3D). This structural shape is a peculiarity of mitochondrial VDACs since bacterial porins form complete antiparallel β-barrels [42]. An odd number of beta-strands is also shared by Tom40, indicating that this superfamily is evolutionarily relatively young, and this peculiar feature has emerged in the context of mitochondrial evolution [43]. The N-terminal segment of VDAC is a sequence of 25–36 amino acids predicted to form an α-helix in a whole β-strands structure. It is considered to play an essential role in protein stability and functionality. Indeed, the N-terminal domain is crucial for channel stabilization in the open state and in the molecular mechanism that drives the gating of VDAC. The structure of VDAC2 is very similar to that of VDAC1, as shown by X-ray crystallography and solid-state NMR spectroscopy [44,45]. However, VDAC2 shows a unique 11–12 amino acid extension at the N-terminal. This extension is not conserved in other chordates and could only be necessary for some functions confined to mammals. The structure of VDAC3 has not yet been obtained. Nonetheless, several bioinformatic predictions have been proposed based on the extensive sequence similarity; VDAC3 showed β-barrel almost identical to other VDAC isoforms [46].

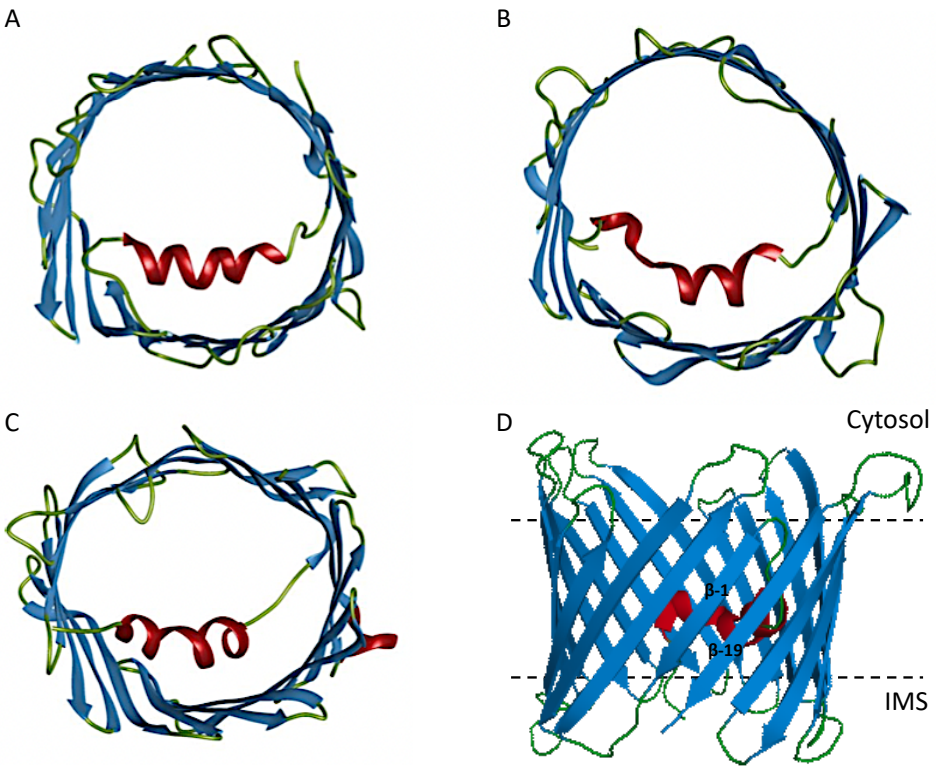

Figure 3: 3D structure of VDAC1. A: The structure of human VDAC1 determined by the combination of NMR spectroscopy and X-ray crystallography; **B:** the structure of mouse VDAC1 determined via X-ray crystallography; **C**: The structure of human VDAC1 as determined by NMR spectroscopy. The structures are colored according to secondary structural elements (helix: red, β-strand: blue, unstructured region: green). **D:** The structure of hVDAC side view (PDB code: 2jk4). The parallel orientation of the first (β1, blue) and last (β19, red) β-strands is clearly visible. (Picture modified from: [47])

Electrophysiological features

Electrophysiological technics are designed to evaluate ion channels' physical properties and features. Planar lipid bilayer (PLB) is one of the unique electrophysiological techniques that is developed to analyze specific channels features in a controlled artificial system [48,49]. This technique allows the analysis of ion channels behavior at the single-molecule level, monitoring the transport of ions across membranes through incorporated ion channels. Furthermore, this method is widely useful for analyzing protein-protein interaction or investigating the direct effects of drugs on the electrophysiological properties of VDAC channels. PLB set up consists of a chamber made of cis- and trans-compartments that are separated by a small aperture with a diameter ranging from ~50 to 250 µm and connected by Ag-AgCl electrodes. *Cis* and *trans* compartments are filled with symmetric saline solution (e.g., 1 M KCl), and pure or mixtures of lipids are applied to the small aperture with subsequent formation of a planar bilayer membrane on the hole. Synthetic phosphatidylcholine DPhPC (di-phytanoyl-phosphatidyl-choline) is widely used because of its high purity and chemical stability [50,51]. The lipid bilayer represents a

capacitor capable of storing charge in the electric field. Capacitance (C) of the bilayer formed across circular aperture is directly proportional to its surface area and dielectric constant (ε), and it is inversely proportional to the thickness of the bilayer (d). The capacitance can be calculated using the following formula C= ε πr2/d (where r is the radius of the bilayer) [52] (e.g., a phospholipid membrane dissolved in n-decane should have a capacitance in the range of 0.3-0.6 μF/cm2). The capacitance should also be monitored frequently during the electrophysiology experiment to confirm that the membrane area remains constant. After that, ion channel proteins can be reconstituted into the artificial lipid membrane directly from lipid membrane mimics such as detergent micelles, lipid/detergent mixtures, and liposomes. The ion current (with pico-amperes (pA) amplitude) through incorporated VDAC channels is measured upon application of a membrane potential (Vm). Conductance (G) of ions at a single-channel level is obtained from the ratio between the recorded current (I) value and the voltage (V) applied (I/V); it is usually measured in a range of 10 to 1000 pico-siemens (pS). Generally, ion selectivity analysis of VDAC proteins is performed in the presence of an asymmetric salt solution across the membrane (e.g., a ten-fold KCl concentration ratio (1M (Trans)/ 0.1 M (Cis)) and applying a potential range of ± 50 mV. Under these experimental conditions, it is possible to calculate the reversion potential (Vrev), corresponding to the potential value at which there is no net flux through the channel (I=0). A negative Vrev value indicates an anion selectivity, while a positive value corresponds to cation selectivity. Starting from reversion potential values it is possible to calculate with the Goldman-Hodgkin-Katz equation the permeability ratio of anions over cations (P_{Cl^-}/ P_{K+}) [53]. The permeability ratio (P_{Cl^-}/ P_{K+}) provides information about the propensity of ion channels to promote the passage of one ion species over another. In addition, it can be used to assess differences in ion selectivity between VDAC isoforms [54] or between different mutants [55].

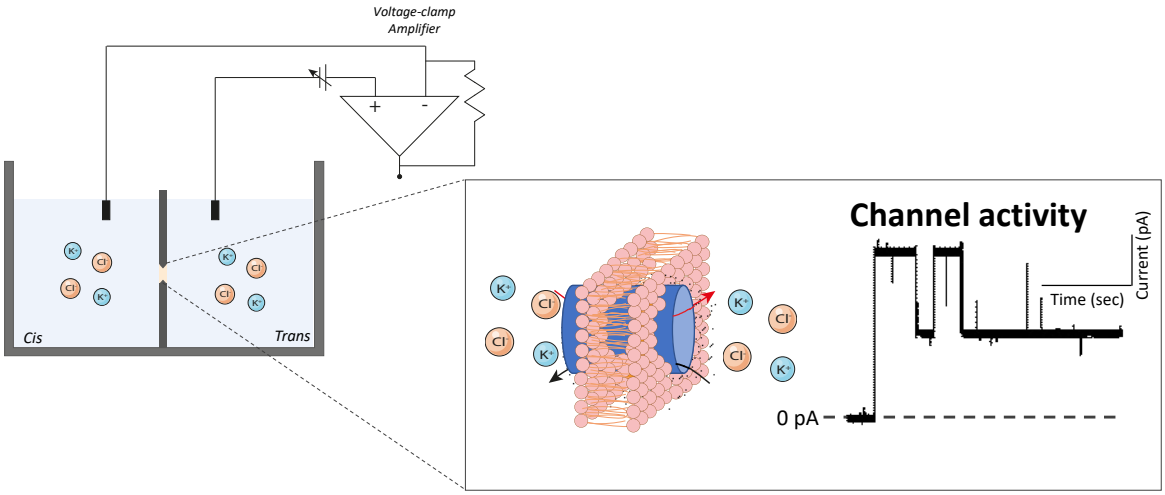

Figure 4: Schematic representation of planar lipid bilayer and channel activity. Schematic representation of PLB reconstitution (left) and the channel conductance assay system (right) for assessing the single-channel activity. Channel activity is measured following its reconstitution into a PLB and measuring the current passing through the channel when a salt concentration gradient or voltage is applied across the bilayer. The membrane serves as a capacitor, whereas the ions carry the current. Currents can be recorded under voltage-clamp by using a bilayer clamp amplifier. (Picture modified from: [56]).

Planar Lipid Bilayer is widely used to characterize the electrophysiological features of VDACs from many organisms [54,57–60] (Fig.5A). Different conductance values characterize VDAC proteins according to the applied voltage, and this phenomenon is known as voltage-dependence. Accordingly, at low membrane voltages (0 ± 20 mV) VDACs exhibit a high-conductive state (known as "open" state) with an average conductance value of about 3.5-4.0 nS in 1 M KCl [58] (Fig 5B). In this conductive state, VDACs show a slight preference for anions over cations ($P_{Cl^-}/ P_{K^+} > 1$), and the channel is also permeable to large anions, such as ATP. However, at increasing membrane potentials of > ± 30 mV, conductance drops to about half [58] (Fig B). In this low-conductive state (known as "closed state"), the channel remains permeable to small ions, with a moderate preference of cations over anions ($P_{Cl^-}/ P_{K^+} < 1$) [34,58], but no longer permeable to ATP [61]. There are different ways to display the voltage dependency of VDAC protein in single-channel recordings. One of these is the G/G_{Max} (or G/G_0) ratio, where G denotes average conductance at a given Vm and G_{Max} denotes average conductance values calculated in the presence of the lowest applied potential (Fig. 1C) [62]. Whereas the open channel shows a conductance of G_{Max} = 4 nS, the conductance decreases gradually at values below 2 nS (referred to as 'closed' states), if the transmembrane potential exceeds ± 30 mV. In the example shown in Fig. 1B, G/ G_{Max} = 1.6 nS/4.0 nS = 0.4. However, the bell-shaped curve (G/G_{Max}) depends on the preparation details, including lipid [63]. VDAC channels from yeast to human have remarkably conserved biophysical properties.

Mammalian VDAC1 [64,65] and VDAC2 insert into membranes readily and present similar voltage dependence and ion selectivity [66], while VDAC3 has a low propensity for membrane insertion and distinctive features (see below) [67–69].

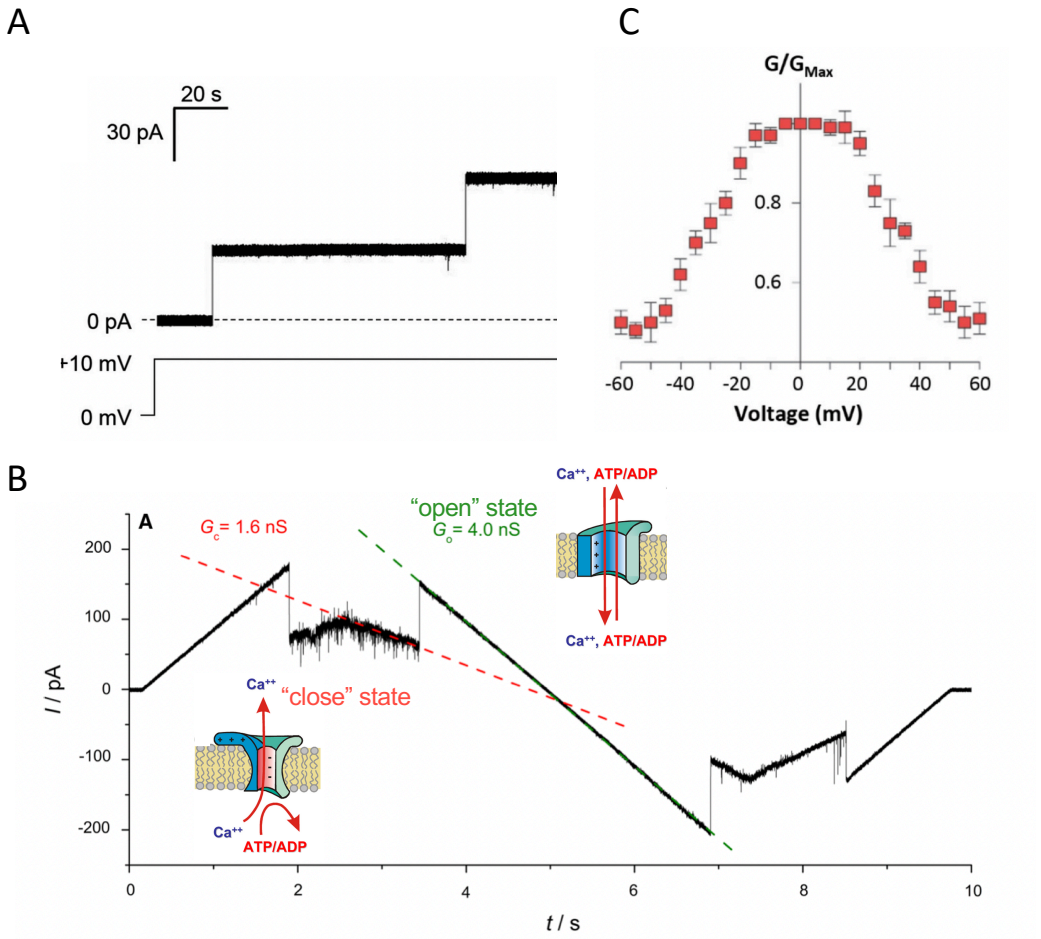

Figure 5: Electrophysiological features of VDAC1. A: Representative trace of recombinant hVDAC1 insertion in artificial membrane measured at the PLB. The trace indicates that VDAC1 can easily form channels of about 4 nS in 1 M KCl. The experiment was performed at the constant voltage of + 10 mV, in 1 M KCl. **B**: Representative triangular curve of recombinant VDAC1 showing changes in channel conductance upon application of a voltage ramp between ± 50 mV. As shown, VDAC1 remains in a stable high-conductive state at low voltages, between ± 30 mV; conversely, at higher voltages, VDAC1 switches into low-conductive states. The slopes show the difference between the open state conductance of Go = 4.0 nS (green dotted line) and a 'closed' state conductance of Gc = 1.6 nS (red dotted line). The experiment was performed in 1 M KCl. **C**: Bell-shaped curve of hVDAC1 voltage dependence, showing the channel's open probability (G/G_{Max}) in relation to the voltage applied. The experiment was performed in 1 M KCl in a voltage range of ± 60 mV. (Picture modified from: [39,47,61]).

VDAC Voltage-gating

As previously reported, recombinant and native VDAC exhibits voltage gating in lipid bilayers. Nevertheless, the underlying mechanism of voltage gating of VDAC is not yet fully understood, although several models exist. Early electrophysiology studies of VDAC

reconstituted in artificial lipid bilayers suggested changes in channel diameter during gating, from ~3 nm to 1.8 nm [70,71]. More than two decades ago, mutagenesis studies identified several residues throughout the protein sequence that appear to influence gating behavior. Song et al. proposed a model according to which the gating of VDAC is achieved by a complex rearrangement of the protein that involves the movement of a large region (called the voltage sensor) whit consequence in pore reduction [72]. Since the publication of the high-resolution structure of VDAC, several models for gating have been proposed. Early models suggest pore closure would occur by moving the N-terminal helix from the barrel wall toward the center of the channel, reducing the pore diameter. The movement could involve the entire α-helix (residues 1-20) [41] or, as suggested by Hiller et al. only a few residues (from 11 to 20) could be involved in porin voltage gating [73]. Otherwise, Zachariae et al. proposed that the movement of the N-terminal domain could include unwinding of the helix (Fig. 6 C) [74]. Finally, the Villinger et al. model suggests more extensive conformational rearrangements that also involve the β-barrel structure without dislodging of the helix [75] (Fig. 6 D). However, there are still many controversies regarding the mechanism of voltage gating.

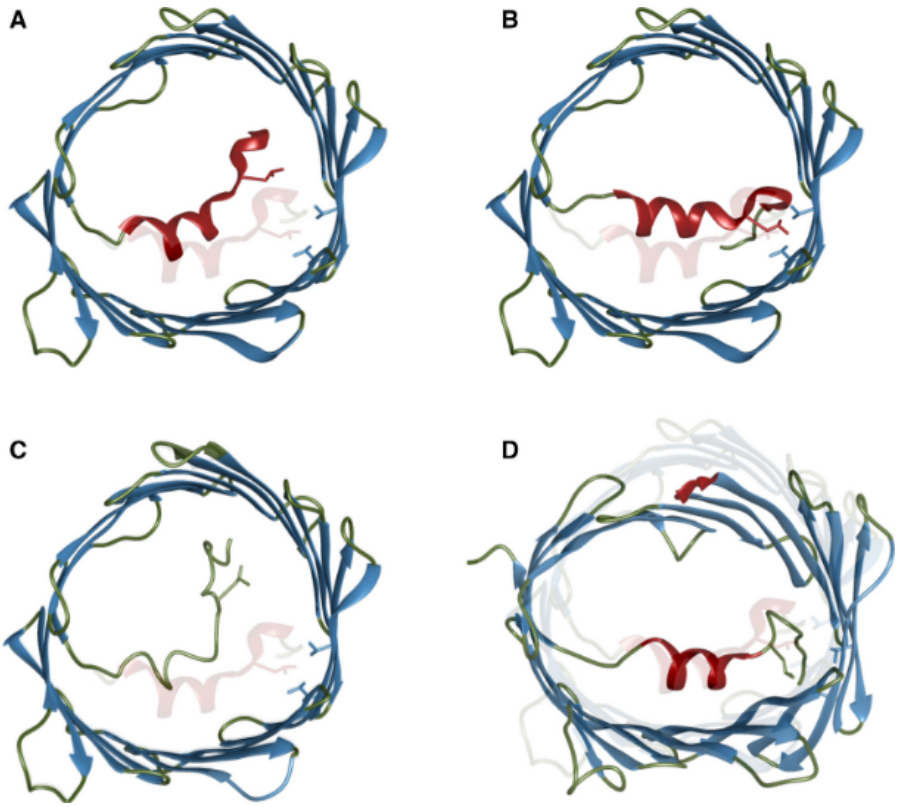

Figure 6: Models for VDAC's voltage gating mechanism. A: Voltage gating by the movement of the helix to the center of the pore [41]. **B**: Voltage gating thorough dislodging of the α2-helix from the barrel wall [73]. **C**: Unwinding of the helix upon gating [74]. **D**: Voltage gating upon elliptic deformation of the barrel without dislodging the helix [75]. (Picture from: [47])

1.5 Nanodisc technology

In all the major bilayer methods, the proteins of interest are either isolated directly from cells [76] or produced as recombinant proteins [67,68,77]. *Escherichia coli* is the most frequently used bacterial system because of its rapid growth and cost-effectiveness. Despite its wide use, this technology has limitations related to protein folding failure, especially for highly hydrophobic membrane proteins that can aggregate into inclusion bodies [78]. Since functional and structural studies need bioactive proteins, numerous strategies have been established to counteract any denaturation process. Regarding VDAC proteins, these methods include column refolding [77] or droplet dilution in the presence of detergents [40,67]; all these procedures are well established and have been extensively used for structural/functional study of VDAC proteins. However, an alternative strategy to a heterologous expression is provided by recent progress in the cell-free translation of proteins (CFPS), which represent a valid and powerful alternative to avoid protein refolding procedures. Initially used for solely producing soluble proteins, CFPS systems emerged as tools for the expression of membrane proteins [79] thanks the development of lipid membrane mimics. Nanodiscs (NDs) are the most recent class of model membrane systems, and they generate a biomimetic phospholipid bilayer environment for incorporating transmembrane proteins [80–82]. NDs conceptually derive from high-density lipoprotein particles, especially Apolipoprotein 1 (Apo-1). Structurally, they are formed of a discoidal patch of a lipid bilayer that is stabilized by two amphipathic helical membrane scaffold proteins (MSPs) [83], which emulate the function of Apo-1; the hydrophobic side of the helix interacts with the hydrocarbon tails of the bilayer, while the hydrophilic side of the helix interacts with the aqueous solution [84]. Fig. 7 illustrated a 3D representation of nanodisc.

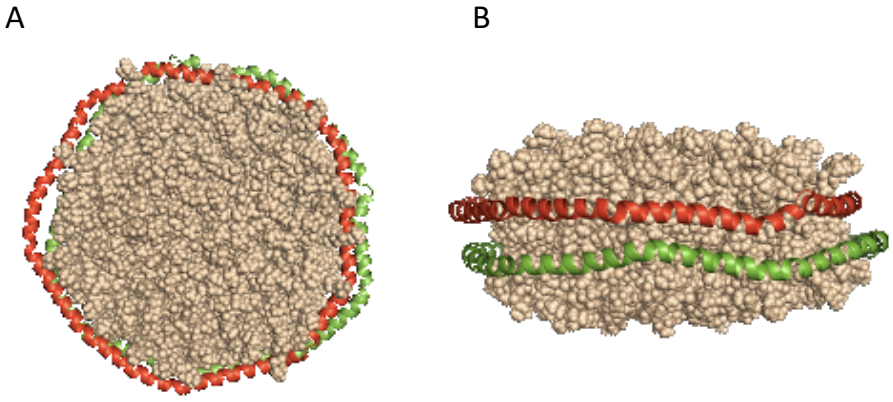

Figure 7: Nanodisc representation. Nanodiscs are discoidal lipid bilayers stabilized by encircling amphipathic helical scaffold proteins termed membrane scaffold protein (MSP). Model of Nanodiscs structure viewed (A) perpendicular to the bilayer and (B) in the bilayer plane. (Picture modified from: [85]).

The original Apo-1 sequence was modified, removing single or multiple helices, to obtain a series of scaffold proteins of different lengths [84]. In Fig. 8, various MSPs are reported based on the original human Apo-1 sequence. The size of the NDs is controlled not only by the length of the MSPs but especially by the stoichiometry of the lipid/MSP-protein ratio used in the self-assembly process. The most popular synthetic lipids used for nanodisc assembly include phosphatidylcholine (PC- lipids) DMPC, DPPC, POPC, and mixtures of PC with charged phospholipids as PS, PG, PE [84].

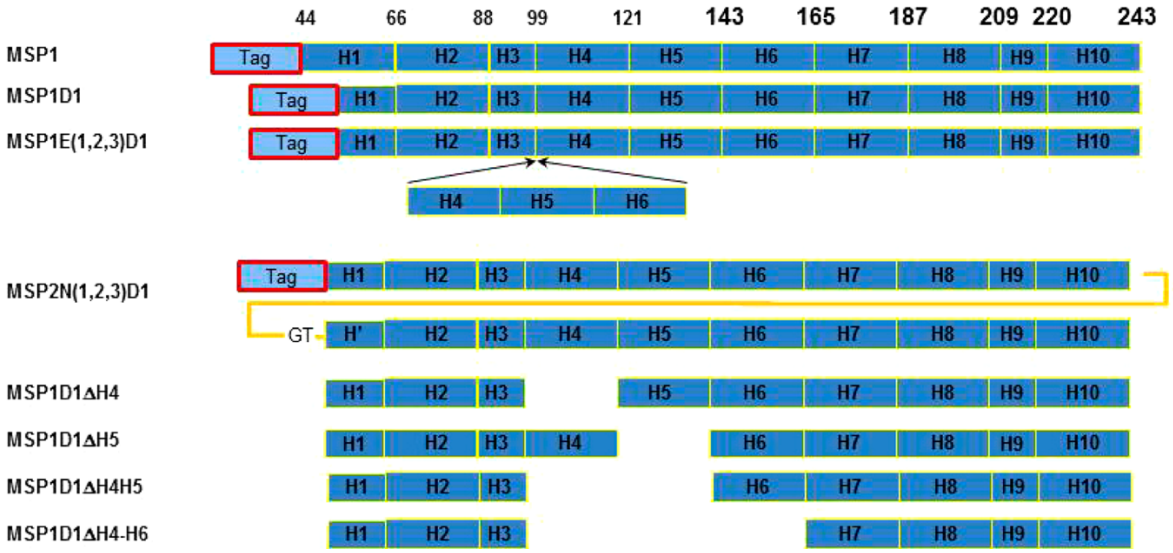

Figure 8: Modularity of the MSP helices. The MSPs consist of a series of helices that can be treated as modular units, and these units can be removed or repeated to change the length of the protein. The figure shows the architecture of MSP2N2, MSP1D1, and some mutants where single or multiple helices have been removed to make smaller particles. (Picture from: [84]).

The classical application of nanodisc technology remains the stabilization of membrane proteins in an aqueous solution for structural analysis and electrophysiological recordings in PLBs. Several membrane proteins from different protein families with various transmembrane domains have already been successfully incorporated into nanodiscs and analyzed [86–95]. In the specific case of VDAC, the literature already contains some examples of ND-stabilized VDACs, which concern only the characterization of functional and structural properties of human VDAC1 and VDAC2 reconstituted in nanodisc using solution NMR spectroscopy [96,97].

1.6 Mammalian VDACs

In mammals, the genes encoding VDAC isoforms are located in different chromosomes and share a similar exon organization, conserved among the whole eutherian group. Specifically, the genes have the same number of coding exons, characterized by the same

size [32]. VDAC2 represents an exception since it contains an additional first exon encoding for the short pre-sequence of 11 amino acids, as shown in Figure 9. The three isoforms of mammalian VDAC are expressed ubiquitously, although at varying levels in different tissues [31,98], and they are considered functionally distinct, despite they show high sequence and structure similarity.

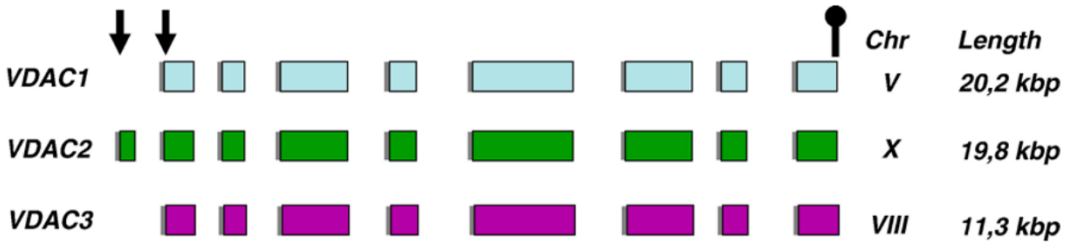

Figure 9: Structure of genes coding for VDAC isoforms in humans. VDAC1, VDAC2, and VDAC3 show similar gene organization. The genes have the same number of coding exons, characterized by the same size. VDAC2 represents an exception since it contains an additional first exon encoding for the short pre-sequence of 11 amino acids. (Picture from: [32]).

VDAC1

VDAC1 is the most abundant and best-characterized isoform. Its location allows the control of metabolic cross-talk between mitochondria and cytosol, playing a crucial role in regulating mitochondrial metabolic and energetic function (Fig 10A). VDAC1 deficiency indeed reduces mitochondria metabolism in *vdac1*$^{-/-}$ mice [99], confirming the importance of this protein as a carrier of metabolites across the OMM. Mitochondria are essential for both intrinsic and extrinsic pathways of apoptosis. VDACs participate in the regulation of mitochondrial-mediated apoptosis in different ways. VDAC1 is widely considered a pro-apoptotic protein due to its binding to Bax (Fig 10 B). Notably, this interaction influences channel activity [100] and leads to the formation of VDAC1-Bax hetero-oligomers involved in releasing Cytochrome C (Cyt c). In addition, apoptotic stimuli can induce oligomerization of VDAC1, likewise participating in the passage of Cyt c to the cytosol. The two main isoforms of hexokinases (HK), known as HK1 and HK2, bind to VDAC1 with a different level of affinity to obtain direct access to mitochondrial ATP [38]. Specifically, HKs compete with Bax for binding to VDAC1 by reducing the formation of VDAC1-Bax complexes [101,102]. Apoptosis stimuli result in the detachment of HKs from VDAC1, increasing the propensity of the porin to bind Bax, thereby initiating the apoptotic process. [101,102]. Overall, it is not surprising that VDAC1 has become interesting from a pharmacological point of view, and recently many molecules targeted to VDAC1 have been developed [39,103].

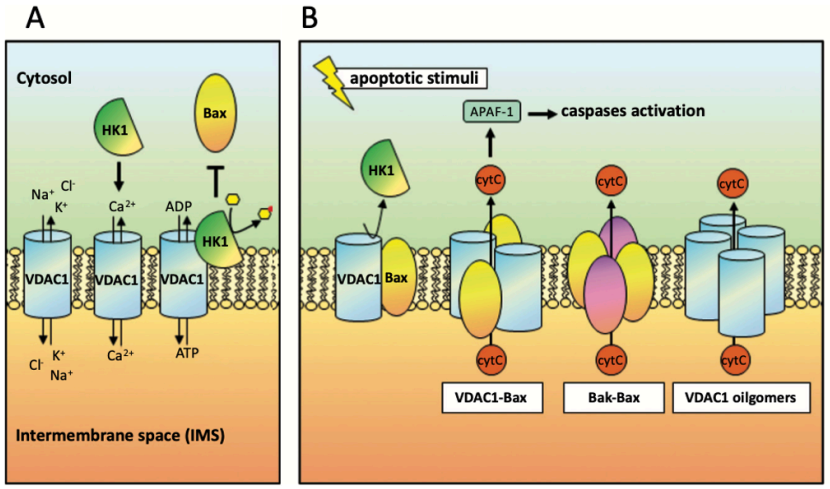

Figure 10: VDAC1 functions in physiological condition and apoptosis. Schematic representation of VDAC1 functions in the cell and its involvement in apoptosis. **A:** VDAC1 mainly participates in the transport of ions and small hydrophilic molecules. Furthermore, VDAC1 is the principal mitochondrial receptor of HK1. The binding VDAC1-HK1 impairs the interaction with Bax (a pro-apoptotic factor). **B:** VDAC1 participation in apoptosis. In the presence of apoptotic stimuli, the detachment of HK1 from VDAC1 leads to the recruitment of Bax in the OMM and its interaction with VDAC1. The active Bax can also associate with Bak, forming hetero-oligomers that increase the OMM's permeability. In Addition, VDAC1 homo-oligomers participate in the cytochrome c (Cyt C) release to the cytosol. (Picture modified from: [103]).

VDAC also interacts with TSPO to contribute to mitochondrial quality control [104]. The translocator protein (TSPO) is a highly hydrophobic 18 kDa protein located in the OMM. TSPO is involved in various functions, such as cholesterol import and regulation of the mitochondrial membrane potential, mitochondrial metabolism, apoptosis, cell proliferation, immunomodulation, inflammation, Ca^{2+} signaling, and oxidative stress regulation [104–107]. Specifically, VDAC1-TSPO interaction inhibits mitophagy downstream of the PINK1/PARK2 pathway, thus preventing essential ubiquitination of VDAC proteins [108]. TSPO has also been suggested to activate the mitochondrial permeability transition pore (PTP) opening, representing a non-specific pore activated by ROS, Ca^{2+} overload, and other agents, leading to mitochondrial swelling and the release of Cyt c into the cytosol [109]. Changes in VDAC1-TSPO interactions have been observed in several pathological conditions, so much so that it has become a possible pharmacological target [104].

VDAC1-Tubulin interaction: the impact on mitochondrial respiration

Mitochondrial outer membrane permeability regulation is essential in normal metabolite and energy exchange between mitochondria and cytoplasm. Indeed, the balance in the closing/opening mechanism of VDAC plays a critical role in proper mitochondrial

function. It is known that the mitochondrial porin permeability strongly depends on the applied electrical potential. However, the outer mitochondrial membrane potential generation mechanisms are not known yet, except for the Donnan potential (i.e., the difference in ions and chemicals across a semipermeable membrane, such as the OMM [110,111]. A Donnan potential of 43 mV was measured between the cytosol and IMS, which shows potential for a closed VDAC conductance state [112]; but this measurement depends on the conditions of the cell. It is more likely that proteins and metabolites (e.g., NADH) bind to the inside of VDAC's pore, promoting reversible porin closure. This closure due to ligand binding is more physiologically relevant than voltage-only dependent closure [110].

Nevertheless, numerous studies have reported interactions of some proteins with VDACs, which could lead to a reversibly closed channel, resulting in some disease conditions. Rostovtseva and coworkers found that the cytoskeletal protein tubulin plays a crucial role in regulating OMM permeability [113,114]. Furthermore, the authors established that nanomolar concentrations of dimeric αβ-tubulin close VDAC1 reconstituted into planar lipid bilayers and suppressed respiration of isolated mitochondria and permeabilized cells [113,114]. The tubulin dimer of 100-kDa molecular mass is far too large (approx. dimensions of 8 nm × 4.5 nm × 6.5 nm), and it cannot permeate through the VDAC pore of 2.5- to 3.0-nm diameter [41]. Hence, it has been proposed as permeation blocking site the anionic C-terminal tails (CTTs) of tubulin that both sterically and electrostatically fit in the positively charged VDAC lumen [115]. Furthermore, experimental evidence supports the requirement of intact CTT on the tubulin body for blocking VDAC. Tubulin with truncated CTTs does not block VDAC [116], demonstrating that CTTs induce the characteristic VDAC blockage. A model of VDAC-tubulin interaction has been proposed, wherein a negatively charged tubulin CTT partially blocks the positively charged VDAC lumen, making the net channel charge more negative, thus shifting channel ion selectivity towards more cationic (Fig. 12 A) [113,115]. However, as reported in [115] tubulin-induced closed state is different from voltage-induced closed. In fact, untreated VDAC1 exhibits a wide variety of closed states after applying high potentials (Fig 12 B and D). On the contrary, tubulin induces a single closed state of VDAC, as shown Fig. 12 C and D.

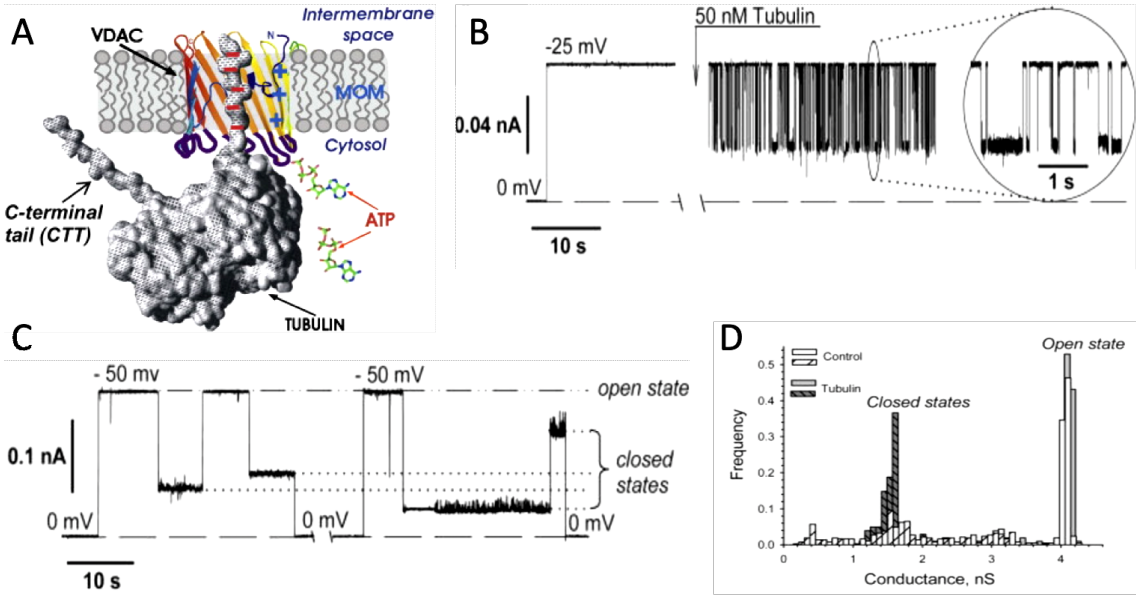

Figure 12: Model of tubulin-VDAC1 interaction and impact on electrophysiological features. A. Model of tubulin–VDAC interaction. The CTT tubulin domain partially blocks channel conductance by entering the VDAC pore. B. Tubulin at nanomolar concentrations induces reversible blockage of VDAC. Single-channel representative current record after adding 50 nM tubulin to the cis side (at −25 mV). **C.** VDAC1 voltage gating in tubulin-free solution under periodically applied −50 mV voltage impulses. In this experimental condition, porin conductance moves from a single high-conducting open state to various low-conducting closed states. D. Distribution of conductances. Tubulin induces a single well-resolved closed state of VDAC1. In contrast, untreated VDAC1 exhibits a wide variety of closed states. The experiment was performed in 1 M KCl buffered, 5 mM Hepes, pH 7.4. (Picture modified from: [115]).

The immediate implications of VDAC blockage by tubulin is its potential involvement in metabolism and multiple cells signaling pathway. VDAC in an open state maintains efficient ATP/ADP exchange across the OMM, thus promoting normal mitochondrial functioning. On the contrary, when VDAC is blocked by tubulin, fluxes of ATP/ADP across the outer mitochondrial membrane are restricted, reducing mitochondrial metabolism and contributing to the Warburg effect. Sheldon et al. showed that VDAC blockage by tubulin is extremely sensitive to the state of VDAC phosphorylation [113,117]. Indeed, phosphorylation of VDAC in vitro by PKA (protein kinase A) and GSK3β (Glycogen synthase kinase 3-beta) resulted in an increased VDAC–tubulin-binding rate. In detail, reconstitution experiments into PLB showed that VDAC was blocked symmetrically when tubulin is added to both sides of the membrane (cis and trans side). However, VDAC phosphorylation with PKA and GSK3β changes its behavior. The sensitivity of VDAC to tubulin increases when tubulin is added to the cis side of the channel [117], suggesting that the phosphorylation sites are positioned on one side of the channel only. Hence, activation or inhibition of kinase activity might modulate VDAC blockage by tubulin and consequently affect OMM permeability.

Overall, VDAC–tubulin interaction might represent a hallmark of cancer cells. It has been hypothesized that the state of VDAC phosphorylation and the intracellular distribution of

β-tubulin isoforms could be different in normal and cancer cells, which might modulate VDAC-tubulin interaction and, as a consequence the mitochondrial activity and cell death [113,115,117]. Therefore, some molecules target the VDAC-tubulin interaction, such as erastin, a VDAC-binding small molecule selectively lethal to some cancer cells [118]. Maldonado et al., evaluated the role of specific VDAC isoforms in mitochondrial metabolism by HepG2 cells and the effect of erastin on tubulin-VDAC interactions. Their results showed that erastin prevents and reverses tubulin-induced VDAC blockage, thus it promotes mitochondrial metabolism and antagonizes Warburg metabolism [119].

VDAC2

Aside from transporting metabolites across the OMM, VDAC2 exhibits peculiar and distinct functions. Several proofs indicate an anti-apoptotic function for VDAC2. Genetic studies have shown that *vdac2*$^{-/-}$ mice are embryonic lethal, whereas both *vdac1*$^{-/-}$ and *vdac3*$^{-/-}$ mice are viable [120–123]. Furthermore, the effect of VDAC2 knockout on embryonic lethality cannot be compensated by overexpression of VDAC1 and 3 [120]. In 2003, Cheng et al. showed that VDAC2 binds the pro-apoptotic protein Bak (Bcl-2 homologous antagonist/killer) in the OMM and prevents its oligomerization, inhibiting Bak-dependent mitochondrial apoptosis [123]. Therefore, VDAC2 is considered essential for cell survival. Mitochondria play a significant role in Ca^{2+} homeostasis in eukaryotic cells; VDAC2, in particular, has been shown to regulate Ca^{2+} homeostasis in cardiac cells [124–126]. In cardiomyocytes, co-localization studies indicated an interaction between VDAC2 and ryanodine receptor type-2 (RyR2) at the sarcoplasmic reticulum (SR)–mitochondrial junctions in the sub-sarcolemmal regions. These junctions are indispensable for Ca^{2+} transfer from the sarcoplasmic reticulum to the mitochondria [126]. Moreover, human VDAC2 shows higher cation-selectivity than VDAC1 [46]; the less affinity to Cl^{-} ions might increase the affinity for Ca^{2+} ions, allowing this isoform to play a major role in Ca^{2+} homeostasis [127]. VDAC2 is also involved in steroidogenesis via interaction with steroidogenic acute respiratory protein (StAR) in the mitochondria-associated endoplasmic reticulum (ER) membrane (MAM) [128]. Several other VDAC2-interaction partners have been implicated in multiple cellular functions [129], summarized in Fig. 12.

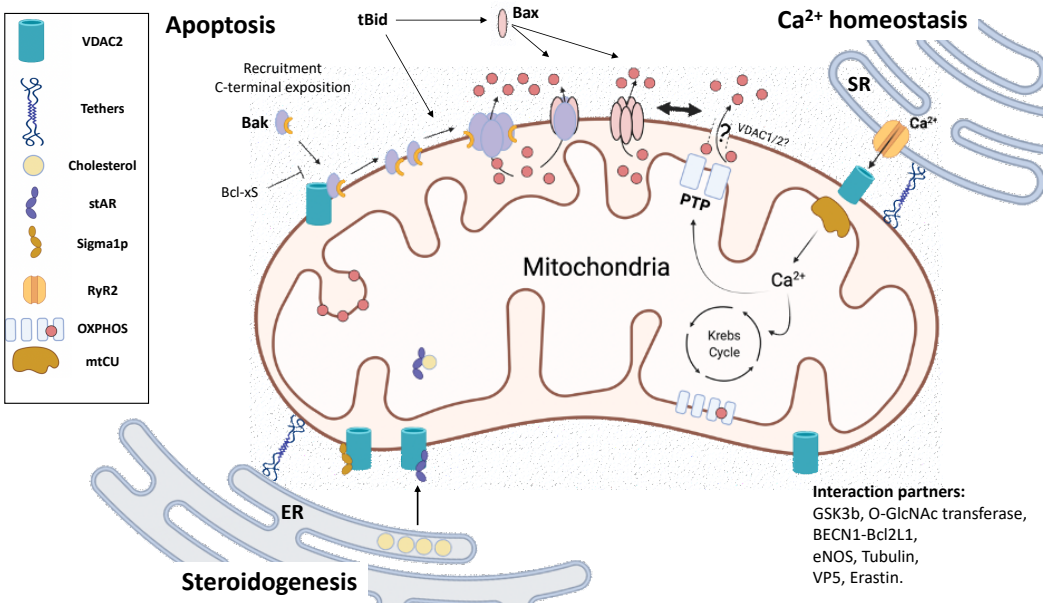

Figure 12: Function and interaction of VDAC2. Schematic representation of VDAC2 function and interaction partners in the cell. **Apoptosis**: VDAC2 plays a crucial role in apoptosis. In the healthy cells, VDAC2 sequesters Bak into the OMM in an inactive conformer, while Bax is present in the cytosolic fraction. When apoptosis is induced, truncated Bid form (tBid) translocates into OMM, where it displaces Bak from VDAC2 [123] (tBID shows stronger affinity to VDAC2 as compared to Bak [130]). Both Bax and Bak can homo- or hetero-oligomerize in the OMM to produce pores large enough for the release of cytochrome c. **Ca_{2+} homeostasis**: In cardiac cells, VDAC2 plays a major role in transferring Ca^{2+} from SR to the mitochondria by interacting with RyR2. **Steroidogenesis:** Cholesterol is the substrate for steroid hormones, and it needs to be transported from ER to IMM for the first step of steroidogenesis. The transport of cholesterol in a hydrophilic environment is facilitated by stAR. Prasad et al., showed that stAR interacts with VDAC2, thus increasing the residence time of StAR at the MAM before it is transported across the mitochondrial membranes. (Picture modified from: [129]).

VDAC3

VDAC3 is the least known isoform. Unlike VDAC1 and VDAC2, which are ubiquitously expressed in all eukaryotes, VDAC3 exhibits a restricted organ distribution, and it prevails in the cerebral cortex, liver, heart, testes, and spermatozoa [122]. Isoform 3 is essential in sperm mobility since VDAC3 knockout mice show an ultrastructural modification in the epididymal axoneme [122] and disassembly of cilia during the cell cycle by targeting Mps1 protein kinase to centrosomes [131]. Literature available to date reveals that VDAC3 considerably differs from isoforms 1 and 2. The complementation assay in *Saccharomyces cerevisiae* strain devoid of endogenous porin (*Δpor1*) has been extensively exploited for functional studies on VDAC proteins [68,132–134]. Δ*por1* cells are unable to grow on glycerol-based media at elevated temperature (37°C), a condition where the yeast cells are mitochondrial-dependent for its survival. As reported, the heterologous expressions of mammalian VDAC1 and VDAC2 fully complement the growth defect associated with

gene loss, while VDAC3 only partially rescues the porin-less phenotype [68,132] (Fig. 13).

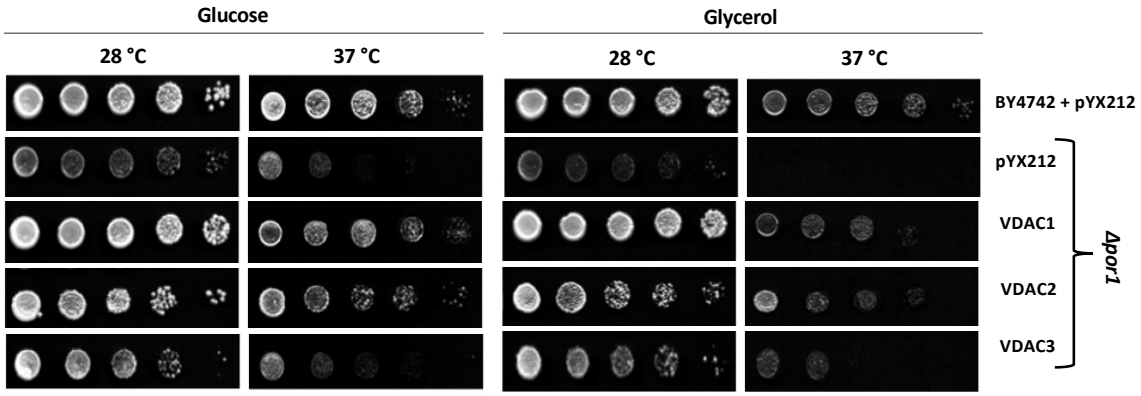

Figure 13: Yeast growth phenotype analysis of Δpor1 cells overexpressing human VDAC (hVDAC) isoforms. A representative panel of drop-serial dilutions assay of WT or Δpor1 yeast, transformed with empty vector (pYX212) or constructs carrying the three VDAC isoforms (pYX212+hVDAC1, pYX212+hVDAC2 and pYX212+hVDAC3). Yeast samples were plated on YPD (Glucose) or YPY (Glycerol) and incubated at 28 °C or 37 °C. As shown, no significant difference between the strain WT and those transformed with different constructs is detected in glucose as substrate (28 °C). On glycerol, while Δpor1 transformed with pYX142 vector shows a significative impairment of the growth rate, the addition of the plasmid expressing hVDAC1 and hVDAC2, but not hVDAC3, restores the yeast growth defect. (Picture modified from: [132])

Initially, VDAC3 was considered unable to form channels since its pore-forming activity has long been quite hard to be detected [65]. Subsequently, Checchetto et al. reported that under non-reducing conditions, VDAC3 inserts into artificial membranes as small and ungated channels with an average conductance of about 0.09 nS in 1 M KCl [67]. Nevertheless, when refolded under highly reducing conditions [55] or pre-treated with reducing agent (e.g., DTT) [56,69], VDAC3 forms typical voltage-dependent pores displaying similar channel behavior with VDAC1 and VDAC2 (Fig. 14). As reported in [68,69], replacement of specific cysteine residues in human VDAC3 (as well as the replacement of all cysteines to alanine [55]) affects both electrophysiological features and its ability to complement the growth defect in *Δpor1* yeast cells. Overall, these results suggest that the cysteine residues of VDAC3 are involved in modulating channel activity.

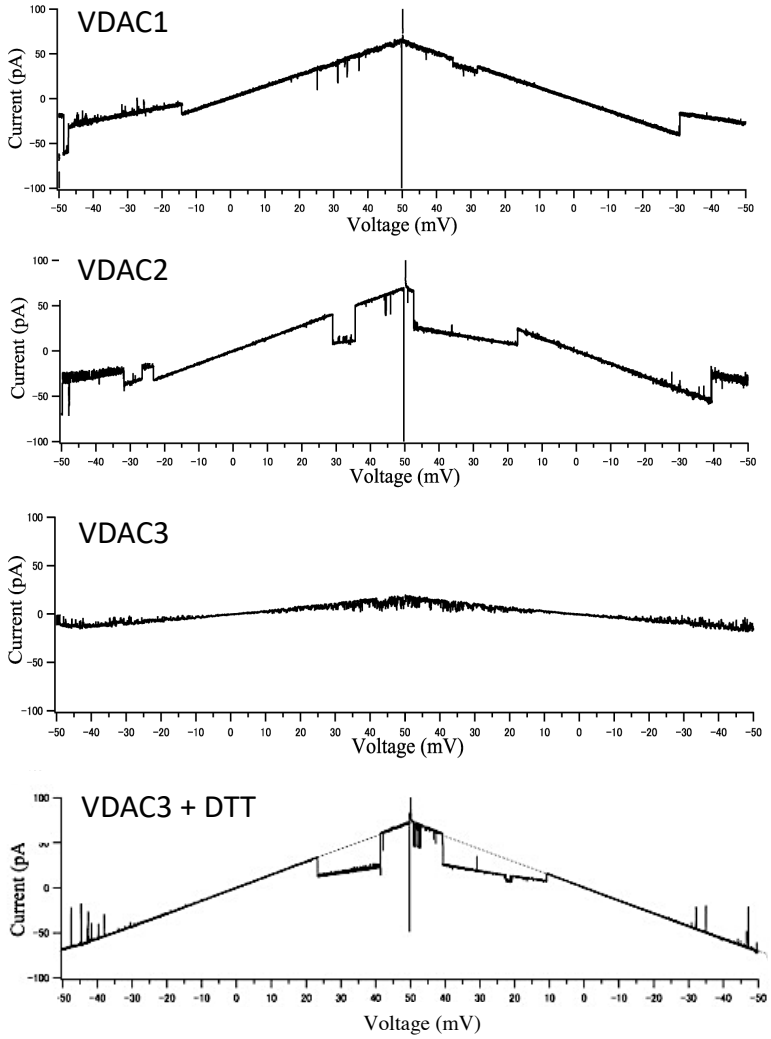

Figure 14: Voltage-dependence of VDAC isoforms. Representative triangular curves of recombinant VDAC1, VDAC2, VDAC3, and VDAC3 treated with DTT. VDAC1 and VDAC2 remain in a stable high-conductive state at low voltages, between ± 20-30 mV; conversely, at higher voltages, VDAC1 and VDAC2 switch into low-conductive states. VDAC3 has no voltage sensitivity. However, the treatment of VDAC3 with 5 mM DTT makes it similar to the other two isoforms. (Picture modified from: [69])

1.7 Cysteine oxidation in VDAC isoforms

Cysteine residues are reactive amino acids that, through their redox-reactive thiol group (-SH), can undergo various oxidative post-translational modifications (Ox-PTMs), as reported in Fig. 15; except for sulfonic acid, all the others reported modifications are reversible and ruled by specific enzymes [135–137]. Mitochondria are responsible for maintaining cellular redox homeostasis through the continuous generation and wasting of ROS. Under physiological conditions, ROS generated by mitochondria regulates mitochondrial protein interactions and activity via oxidative modification of cysteine residues [138].

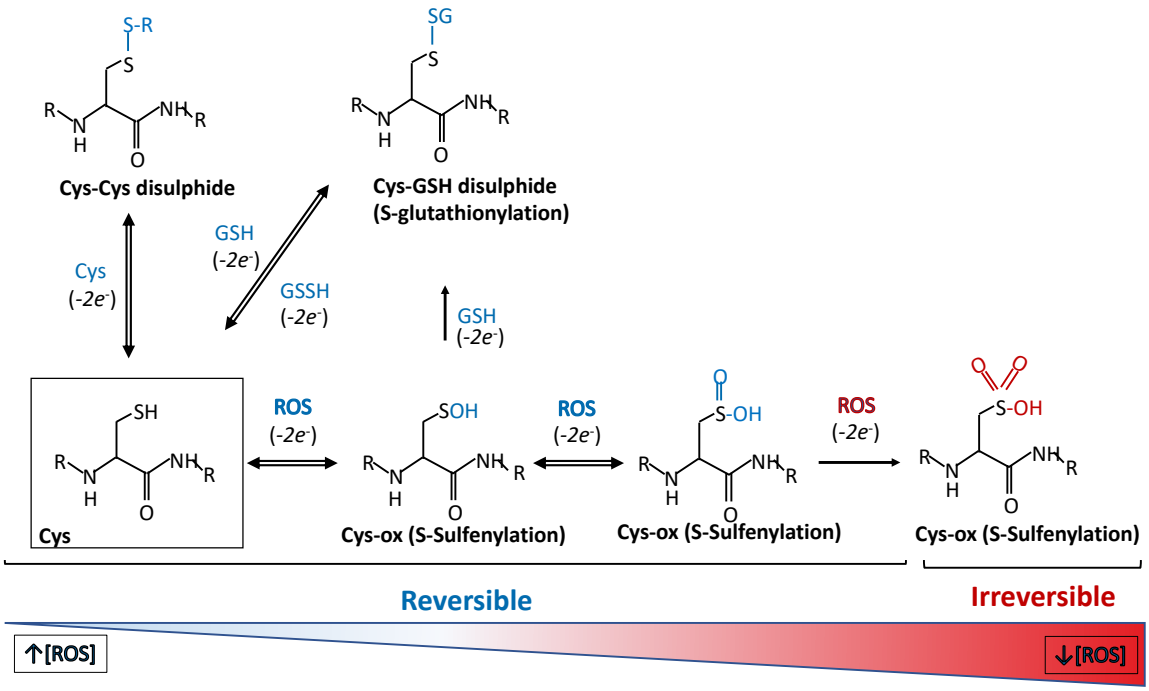

Figure 15: Oxidative post-translational modifications (Ox-PTMs) on cysteine. Cysteines are amino acids characterized by the property to undergo reversible redox reactions. At physiological pH, cysteine sulfur shows a pKa value > 8.0, which means that the sulfur is present in the protonated state or reduced, –SH. The cysteine sulfur can be deprotonated, becoming a highly reactive –S− in the presence of factors lowering the cysteine pKa, like proximity of basic residues or a general oxidative environment. Cys residues are likely subjected to various Ox-PTMs including: S-nitrosylation (SNO), sulfhydration (SSH), S-acylation, S-glutathionylation (SG), disulfide bonds (RS-SR), sulfenylation (SOH), sulfinic acid (SO_2H), and sulfonic acid (SO_3H). Except for sulfonic acid, all the reported Ox-PTMs are readily reversible and ruled by specific enzymatic activities [135–138].

VDAC isoforms differ in number and distribution of cysteine residues: in humans, VDAC1, VDAC2, and VDAC3 have two, nine, and six cysteines, respectively [139]. VDAC3 is considered the oldest isoform. In this regard, it has been hypothesized that evolution has reduced cysteines number in VDAC1 due to its ubiquitous expression and pro-apoptotic function and concurrently increased Cys content in VDAC2, possibly to favor anti-apoptotic functions [139]. Many of these residues are located in protein loops exposed to IMS (Fig. 16A), which is known to be one of the most oxidizing environments in the cell. Therefore, it has been speculated that the redox status of VDAC cysteine residues exposed to IMS might be affected by the abundance of radical species in this compartment [68]. Recently, mass spectrometry (MS) analyses have shown that all these cysteine residues follow an evolutionarily conserved redox modification pattern. In both human and rat VDACs (rVDACs), indeed, some cysteine residues are exclusively found in the reduced form, while others are constantly and irreversibly overoxidized to sulfonic acid (as shown in Fig 16B) [139–141]. Specifically, in hVDAC1, Cys 127 (located in β8 and exposed towards the hydrophobic layer of the OMM) was consistently detected in the trioxidized form of $–SO_3H$, whereas Cys 232 (embedded in β16 facing the water-accessible

side of the channel) was found exclusively in the reduced and carboxyamido-methylated form [142]. In rVDAC1, both these residues have been moderately oxidized [121,122]. As mentioned above, VDAC2 possesses the highest cysteine content: 11 and 9 in rat and human, respectively. This difference is due to two additional cysteines in the N-terminal domain of rat isoform [140]. In hVDAC2, cysteines in positions 8, 13, and 133 (all exposed to the IMS) were reported in the reduced form [139]. Interestingly, the corresponding residues in the rat ortholog (Cys9, Cys14, and Cys134) have also been identified as wholly reduced or not determined (Cys134). Moreover, in rVDAC2, the additional Cys4 and Cys5 in the N-terminal domain were also found in the reduced form; thus, VDAC2 presents a cluster of cysteines oriented towards the IMS, which are available to reversible oxidation [140]. Cys227 was detected exclusively in the carboxyamido-methylated form, similar to Cys228 in rVDAC2. Unlike the other residues, Cys227 is the only cysteine predicted to be in a cytosol-exposed loop, so it has been hypothesized to be a docking site for possible interactors [142]. On the contrary, hVDAC2 cysteine residues 47, 76, 103, and 210 (all located in IMS loops) were identified as partially oxidated to $–SO_3H$, likewise to Cys 48, 77, 104, and 211 in rVDAC2. Finally, hVDAC2 Cys138, which faces the lipid environment of the OMM, was found fully trioxidized to sulfonic acid as the homologous residue in hVDAC1 (Cys127) [139,140]. As reported in [139,141,142], the preferred redox state of cysteines is also conserved between rat and human VDAC3 [139,141,142]. Except for Cys8, located within the pore, all cysteine residues of VDAC3 protrude toward the IMS. In particular, Cys2, Cys8, Cys122, and Cys229 were identified in the carboxyamido-methylated form, while the N-terminal Cys2 was found acetylated. Cys36 and Cys65 were detected in the reduced form and trioxidized to sulfonic acid. Hence, MS data demonstrate that, at least in mammals, the oxidative state of cysteine reflects a physiological condition and could be correlated to a specific structural or functional role of the protein [138,142].

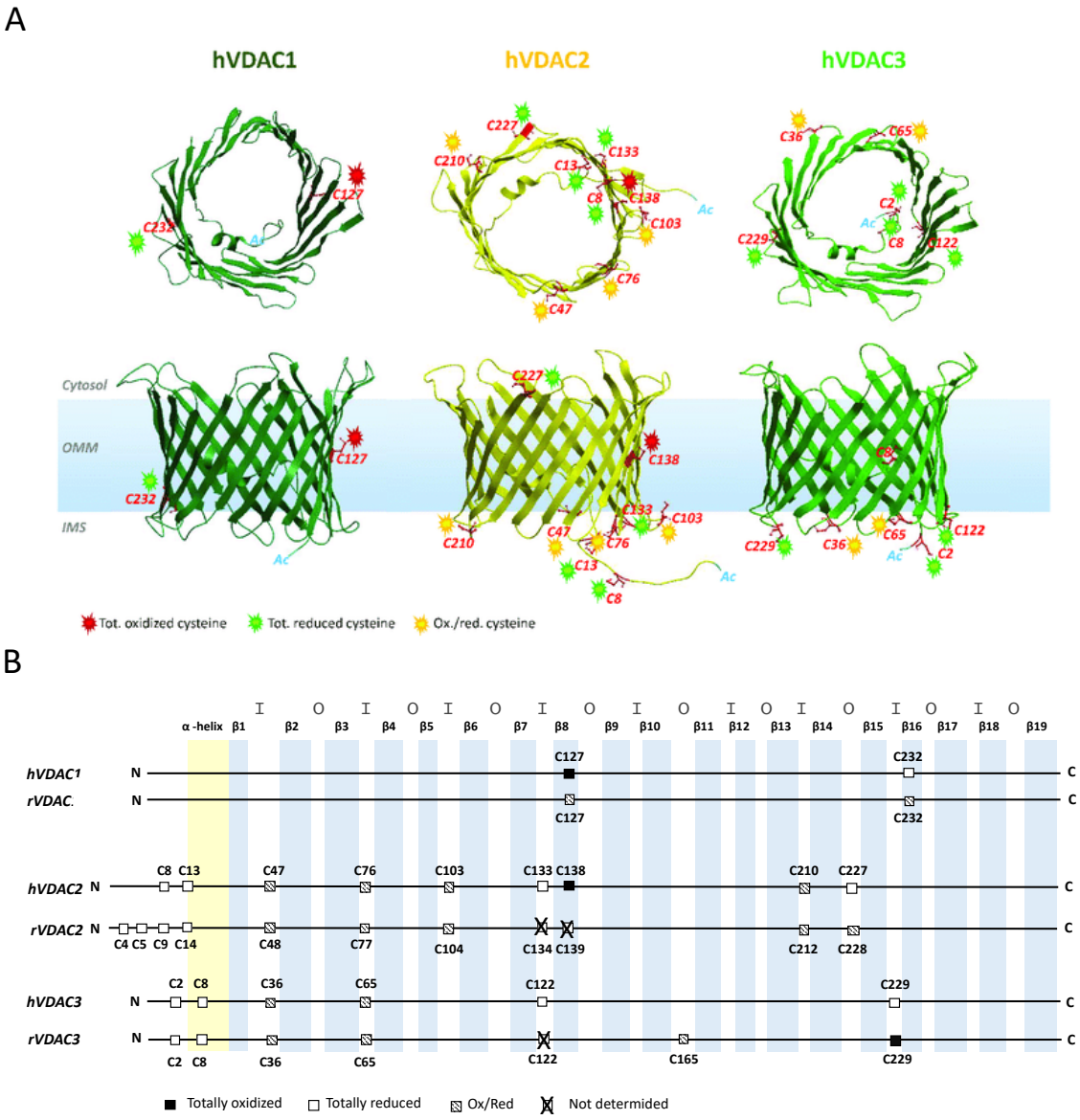

Figure 16: Cysteine residues in VDAC isoforms. A: Structure of human VDAC isoforms highlighting cysteine residues and their oxidation states. Top view and side view of hVDACs. The cysteine residues are highlighted (in red), and colored sparks indicate their oxidative state: green (totally reduced), red (totally oxidized), or yellow (red/ox, i.e., partially oxidized). There are no VDAC cysteines exposed toward the cytosol. **B:** Cysteine localization in the aligned sequences of human and rat VDACs. The N-terminal α-helix is shown in yellow, and β-strands are in light blue. The loops exposed to the intermembrane space are indicated with I. The loops exposed to the cytosol are indicated with O. (Picture modified from: [138]).

1.8 VDAC3 involvement in mitochondrial quality control

In order to guarantee efficient energy provision and proper integration of intracellular signaling, mitochondria are subject to quality control systems, by means of which cells eliminate defective organelles to maintain cellular homeostasis. The mitochondrial-lysosomal axis is recognized as the main actor in the deployment of mitochondrial quality control, where the single affected organelle is targeted to lysosomes and destroyed [143]. An alternative degradative pathway identifies slightly damaged mitochondrial components (such as proteins or membrane patches) and destroys them by a process involving the

formation of mitochondrial-derived vesicles (MDVs) that are subsequently targeted to lysosomes. This mechanism contributes to organelle homeostasis before triggering total mitochondrial degradation [144]. As reported above, post-translational modifications of VDAC3 cysteines have been precisely determined. Since these amino acids have never been detected as totally oxidized, it has been speculated that changes in their redox status could be regulated by ROS-levels in the intermembrane space [145]. Hence, thought cysteines, VDAC3 could "perceive" and "buffer" the excess of mitochondrial ROS, playing a role in mitochondrial quality control [138,145]. In this regard, cysteine at the N-terminal domain is subjected to the so-called "N-end rule pathway", a destructive process wherein the presence of an oxidized N-terminal cysteine in several mammalian proteins is required for arginylation by ATE1 R-transferases and subsequent ubiquitin-dependent degradation [146,147]. In VDAC3, post-translational modification deletes the first methionine (Met1) in the sequence, replacing the first amino acid with the second cysteine (Cys2) [139,141] . Because the oxidized form of Cys2 was never detected, it is plausible that the Cys2-oxidized could function as a marker for VDAC3 removal from OMM and degradation. Hence, it has been supposed that small amounts of mitochondrial ROS might oxidize some cysteine residues of VDAC3 (including Cys2) and lead to eliminating the protein by the N-end rule pathway [138]. In these terms, VDAC3 could buffer the ROS excess and "sacrifice" itself in an early step of mitochondrial control quality [138,145]. However, due to mitochondrial stress, the progressive accumulation of ROS increases the amounts of oxidized cysteines in VDAC3, which could modify the channel structure or the mobility of the N-terminus. These modifications might signal the redox state of the mitochondria to the rest of the cell, leading to the incorporation of individual damaged proteins (or membrane patches containing damaged proteins) into MDVs or the elimination of the mitochondria through mitophagy [145]. Until now, some studies support the idea that VDAC3 may function as a redox-sensing protein [148–151]; however, the involvement of its cysteine residues has not yet been established.

1.9 Interactome of VDAC3

Messina and coworkers defined the VDAC3 interactome *in vivo* by a TAP-Tag immunoprecipitation strategy and mass spectrometry identification [152]. VDAC3 was found associated with proteins from the endoplasmic reticulum (Grp75, Hsp70, GRP, and calreticulin) and MAM, proteins correlated with the response to oxidative stress (GSTO-1, PRDX, and GSTK-1), proteins involved in response to misfolded or unfolded proteins (YWHAQ, KCIP1, or SFN), proteasomal components and chaperons (PDI and Erp5), and

proteins related to ribosome contact and control [151]. It has recently been reported that the main difference between VDAC3 and the other VDAC isoforms concerns associations with cytosolic proteins involved in mitochondrial metabolism, especially alpha-synuclein (α-syn) and the dimeric tubulin [55,115,153]. Data from PLB analysis shown that monomeric α-syn reversibly blocks VDAC1 conductance in a voltage-dependent manner already at very low concentrations and reverses its ion selectivity from anionic to cationic [153]. Specifically, the C-terminal domain would appear to be the specific domain of α-syn responsible for the interaction with VDAC1. The C-domain could be due to the high content of negatively charged amino acids at the C-terminus of α-Syn [55,153]. α-Syn can induce two distinct blocked states: a blocked state with a conductance of about 40% the open state and a second deeper state with a conductance of 17% the open state (≥ +30 mV) [55]. Furthermore, data has shown that similarly to VDAC1, α-syn interacts with VDAC3 10–100 times less effectively (Fig. 17 A) [55]. This indicates that, despite the high similarity between the two isoforms, slight differences in cytosolic-exposed domains of VDAC3 could change the lipid-VDAC interface and, consequently, the ability of the pore to capture α-syn [55]. The different affinity of VDAC3 towards α-syn could also be explained by the different content, position, and oxidation pattern of cysteine residues. Indeed, data obtained using a cysteine-less human VDAC3 mutant showed that the cysteine residues do not significantly affect VDAC3 stability or functionality, but they are responsible for the voltage asymmetry in the on-rate of α-syn/VDAC3 interaction (Fig. 17 B) [55]. This result reinforces the concept that cysteines play a crucial role in regulating VDAC3 function and that modification of cysteines oxidation state might interfere with the interaction of the physiological binding partners. In addition to α-syn, VDAC interacts with other cytosolic proteins such as dimeric tubulin, implicated in mitochondrial metabolism [115]. Queralt-Martín reported that VDAC3 is blocked by tubulin 10 times less effective than VDAC1(Fig. 17 C), supporting the hypothesis that VDAC3 is primarily open when VDAC1 is closed via tubulin interaction [55]. In this regard, Gurnev [118] proposed that VDAC3 is critical for maintaining mitochondrial metabolism in cancer cells. However, further investigations are needed to better understand the VDAC isoform 3 roles.

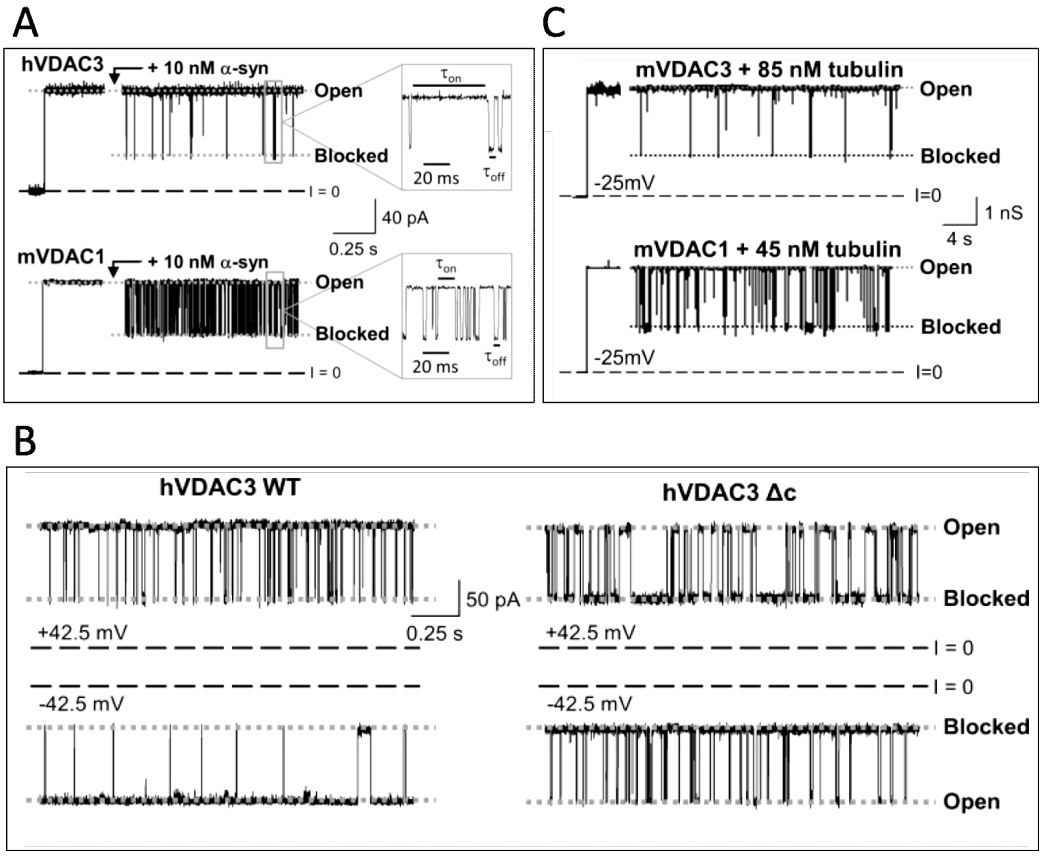

Figure 17: VDAC3 interaction. A. α-Syn blocks hVDAC3 less efficiently than mVDAC1. Representative current traces of hVDAC3 and mVDAC1 before and after addition of 10 nM α-syn (at +30 mV). Nanomolar concentrations of α-syn, added to either side of the membrane, induce rapid transitions of VDAC from the high-conductance open state to the low-conductance blocked state. The difference between hVDAC3 and mVDAC1 is in the frequency of α-syn–induced blockage events **B.** Cysteines affect hVDAC3 interaction with α-syn. Representative current traces of hVDAC3 WT and hVDAC3-Δc after adding 20 nM α-syn (at ± 42.5 mV). α-Syn is capable of blocking hVDAC3-Δc from both sides of the channel, similarly to WT protein, but the on-rate of α-syn–hVDAC3-Δc interaction is approx. 10 times higher than the WT hVDAC3 at negative voltage polarities. **C.** Tubulin blocks hVDAC3 less efficiently than mVDAC1. Representative current traces of hVDAC3 and mVDAC1 before and after adding of tubulin (at -25 mV). Tubulin induces characteristic blockage events for both mVDAC3 and mVDAC1. The efficiency of tubulin interaction with mVDAC3 is significantly lower than with mVDAC1. 85 nM of tubulin led to fewer blockage events in mVDAC3 compared to the number of blockages induced by 45 nM of tubulin in mVDAC1 (Picture modified from: [55]).

VDAC3 is also involved in the recruitment of the PINK1/Parkin pathway, which regulates mitochondrial quality control and promotes the selective autophagy of depolarized mitochondria [154,155]. Loss of mitochondrial quality control regulation causes morphological and functional alterations in the organelles, associated with the pathogenesis of Parkinson's disease. Sun et al. proposed that VDACs are part of the machinery that recruits Parkin to the organelle [156]. The authors observed that in the absence of all three VDAC isoforms, the recruitment of Parkin to defective mitochondria and mitophagy was compromised [155]. Furthermore, Reina and coworkers hypothesized that changing mitochondrial ROS amount could lead to the over-oxidation of cysteines or other modifications, which can modify the structure of the pore or mobility of the N-

terminus of VDAC3 [145]. Hence, these conformational changes might recruit the PINK/Parkin system that ubiquitinates VDAC3. Another relevant VDAC3-interactor is the VCP (TER-ATPase), a member of the ERAD pathway [152]. It is involved in extracting proteins from the OMM to be directed to ubiquitination and degradation through ER [157]. VCP alterations are implicated in numerous neurodegenerative disorders. Overall, these interactions have significant implications for mitochondrial bioenergetics and may pave the way for discovering new specific functions for VDAC isoform 3.

1.10 Voltage Dependence Anion Channel 3 in diseases

Due to its crucial role in cellular metabolism and apoptosis, VDACs are implicated in several diseases, including cancer [39,158,159] and neurodegenerative disorders [103,153,160]. However, the knowledge about VDAC3 involvement in pathologies is very restricted. For example, Zhang et al. [161] proposed a role of VDAC3 in the hepatocarcinogenesis induced by HBV (Hepatitis B virus) infection. In particular, the authors reported that a specific miRNA (miR-3928v) directly targets and down-regulates VDAC3 expression and promotes hepatocarcinoma malignancy, but the molecular mechanism is still not completely clear. VDAC3 also seems to be involved in HHV-8 (Human Gamma-herpesvirus 8) infection, an oncogenic human herpesvirus that has been identified in all types of Kaposi's sarcoma [162]. Furthermore, Wang and coworkers [163] showed that the HHV-8 K7 protein could interact with VDAC3. Recently, Józwiak [149] reported a remarkable change in VDAC3 expression in non-metastatic endometrial cancers. In detail, the authors displayed an increase of VDAC3 in non-metastatic endometrial cancers compared to normal cells. On the contrary, a reduction of VDAC3 expression in endometrial tumors with metastasis has been shown [149]. However, some reports in the literature show alterations in VDAC isoform 3 mRNA levels in diseases different from cancer. Indeed, variations in VDAC3 expression levels have also been reported in cerebral malaria [164], the most severe neurological complication of infections by *Plasmodium falciparum*. The over-expression of VDAC3 is also accompanied by alterations of many other genes whose dysfunction is associated with neurological disorders. However, the brain injury mechanisms are still unclear [164].

Furthermore, Chronic Unpredictable Stress (CUS), one of the most clinically relevant stress in rodents, mimics several behavioral characteristics of patients affected by depression, anxiety, and mood disorders [165]. In a zebrafish model of CUS, Chakravarty et al. showed a remarkable variation in VDAC3 expression. The authors hypothesized that

the increase in mRNA VDAC3 levels in the stressed fish brain might increase the efficiency of bioenergetic metabolism or protection against ROS [165].

In conclusion, a peculiar expression of VDAC3 was observed in cells and tissue in the germinal lines of different organisms. Genetic variants of VDAC3 are correlated with infertility [166]. Indeed, male mice lacking VDAC3 are infertile. It has also been assumed [98] that VDAC3 might affect the energy supply for spermatogenesis and Leydig cell steroidogenesis so that it affects spermatogenesis. Very recently, the group of De Pinto performed a systematic analysis of human VDAC genes [167]. The authors found several factors that binding sites in the VDAC3 promoter involved in developing germinal tissues, organogenesis, and sex determination, confirming the experimental evidence of its crucial role in fertility. However, the molecular mechanisms in which VDAC3 is involved in pathophysiological conditions are not fully understood. Therefore, in the future, the study of this protein could allow the acquisition of deeper basic knowledge to develop diagnostic and therapeutic approaches for different diseases.

2. Aim of the Ph.D. thesis

The first part of this Ph.D. thesis concerns the electrophysiological measurements of human VDACs incorporated into nanodiscs and reconstituted into planar lipid bilayers. For this purpose, I spent six months in the laboratory of Prof Dr. Gerhard Thiel at the Technical University of Darmstadt (Germany), during which I successfully performed a protocol for *in vitro* translation of different members of the VDAC family directly into nano-membranes scaffold (Conti Nibali et al. Biophys Rep. 2021; **Article 1**). In this work, the *in vitro* protein synthesis system with the Nanodisc (ND) technology was used for the first time to express and reconstitute the three human VDAC isoforms into artificial lipid membranes, and their electrophysiological features were compared with those obtained by canonical recombinant production and protein isolation protocols. In addition, the impact of reducing agents in the buffer and replacement of cysteines on the biophysical features of human VDAC3 were analyzed.

The second part of the thesis focuses on investigating the involvement of VDAC isoform 3 in mitochondrial ROS homeostasis (Reina, Conti Nibali et al. Submitted to Redox Biology; **Article 2**). As reported above, it has been recently reported that VDAC3 cysteines were never detected in totally oxidized states: changes in oxidation/reduction states of these residues could be regulated by intermembrane space ROS levels. The aim of this project was to evaluate the role of VDAC3 cysteine residues in mitochondrial functionality and their buffering capacity to prevent the excess of mitochondrial ROS. For this work, near-haploid human HAP1 cell line devoid of VDAC3 (HAP1-ΔVDAC3) was compared to VDAC1 knockout (HAP1-ΔVDAC1) and wild-type cell lines to test VDAC3 contribution in oxidative stress response. In addition, the HAP1-ΔVDAC3 cell line was transfected with a cysteine null (C0A) VDAC3 to analyze the involvement of these residues in mitochondrial redox-regulating networks.

3. Results and Discussions

This Ph.D. thesis includes two different papers, each of which deserves its paragraph summarizing the results obtained. The two articles ("Cell-free electrophysiology of human VDACs incorporated into nanodiscs: An improved method" and "Voltage-Dependent Anion Channel 3 (VDAC3) protects mitochondria from oxidative stress") are annexed to the thesis.

3.1 Cell-free electrophysiology of human VDACs incorporated into nanodiscs: An improved method.

In this work, human VDAC proteins were expressed using the Cell-Free protein expression system in the presence of a ND, namely MSP2N2. After purification, the VDAC-NDs complexes were reconstituted into PLBs to test whether this new procedure retained the electrophysiological properties of VDACs as reported in [60,67,68,168]. VDAC-NDs complexes were therefore added to the trans side of a PLB, and their channel-forming activity was analyzed. Channel insertion was studied in an ionic buffer (1 M KCl, 10 mM Hepes, pH 7.4) by applying an electric potential of +10 mV to the membrane. At this voltage, hVDAC1 and hVDAC2 were inserted quickly into Diph-PC membranes as fully open-state pores, displaying the same conductance values obtained with conventional expression and reconstitution systems. Nonetheless, VDAC channels registered a higher probability to insert into artificial membranes when compared with VDAC proteins expressed via the heterologous system.

In addition, the new expression system maintained the same characteristics of voltage dependence and ion selectivity reported in the literature. Human VDAC isoform 3 deserves a separate discussion: in the absence of any reductants (as observed with protein refolded according to the traditional protocols [67–69]), hVDAC3 indeed adopted a lower conductance state compared to hVDAC1 and hVDAC2. Furthermore, VDAC isoform 3 did not show any voltage dependence in this experimental condition. The untreated hVDAC3, due to insensitivity to the voltage applied, exhibited cation selectivity exclusively; this could be conceivable from the fact that a channel with a small conductance promotes the passage of cations (K+) over anions (Cl-). On the other hand, pre-incubation with DTT, before bilayer reconstitution, as well as the removal of all cysteine residues and their substitution by mutagenesis with alanine (hVDAC3 C0A mutant) made VDAC3 channels almost indistinguishable from VDAC1 and VDAC2; the mean current through hVDAC3 indeed increased both in hVDAC3 pre-treated with 5 mM

DTT and C0A mutant. Under the aforementioned experimental conditions, hVDAC3 displayed sensitivity to the voltage applied and ion selectivity similar to the other two isoforms. Overall, these results showed that the proposed new expression protocol perfectly replicates the data obtained with the traditional method. In addition, data obtained from the reconstitution of hVDAC3 using the new expression method strongly support the essential role of cysteine residues in channel gating, as has been previously demonstrated by conventional protocols. [55,67–69].

3.2 Voltage-Dependent Anion Channel 3 (VDAC3) protects mitochondria from oxidative stress.

In this work, human HAP1 cells lacking VDAC3 were compared whit VDAC1 knock-out and parental cell lines to analyze the contribution of isoform 3 in mitochondrial ROS metabolism and signaling. The preliminary characterization of HAP1-ΔVDAC1 and HAP1-ΔVDAC3 cells demonstrated a remarkable decrease in VDAC1 and a concomitant increase in VDAC2 expression when VDAC3 is knocked out, whereas the lack of VDAC1 does not significantly affect the expression of the other two isoforms. Moreover, both knock-out cell lines significantly reduced mitochondrial content compared to the parental cell line. It is reasonable to assume that the cells entirely reorganize their mitochondrial asset in response to the lack of proteins primarily involved in mitochondrial permeability and functionality. Under physiological conditions, our human VDAC3 knock-out model exhibited a severe increase in the amount of ROS, accompanied by a remarkable overexpression of main antioxidant enzymes. In addition, we found the extreme susceptibility of VDAC3-deficient cells to treatment with different ROS-inducing factors (i.e., Rotenone, Menadione, and Paraquat), suggesting the enormous role of VDAC3 in oxidative stress response. Furthermore, after exposure of the parental HAP1 cell line to the aforementioned drugs, the relative quantification of VDAC isoforms revealed the highest increase in VDAC3 expression compared with isoform 1, demonstrating that VDAC3 expression is mainly affected by reactive oxygen species. Maurya et al. have speculated a role for VDAC2 cysteines in regulating mitochondrial ROS, although no experimental evidence has yet demonstrated this [169]. However, our results showed that, following the above treatments, the increase in expression of VDAC3 is more remarkable even than isoform 2, which has the highest number of cysteines. Overall, these data support the hypothesis that VDAC3 and not VDAC2 plays a role in maintaining mitochondrial ROS homeostasis.

In order to analyze the involvement of VDAC3 cysteines in modulating mitochondrial ROS content, HAP1-ΔVDAC3 cells were transiently transfected with plasmids encoding VDAC3 or VDAC3 C0A (a mutant where all cysteine residues were replaced with alanine residues). Our results showed that, after treatment with 50 and 100 μM of rotenone, only the expression of VDAC3 induced a significant increase in the viability of HAP1-ΔVDAC3 cells. In contrast, VDAC3 C0A did not affect the sensitivity of VDAC3 knock-out cells to the drug. These results are notable because neither VDAC3 nor VDAC3 C0A transfections altered mitochondrial content and VDAC1 protein level, covering the lack of VDAC3. Finally, we tested the ability of VDAC3 to protect mitochondrial function during rotenone exposure, which increases mitochondrial ROS production by inhibiting the activity of complex I [170,171]. To this purpose, High-Resolution Respirometry was used to assess the oxygen consumption of HAP1 cell lines exposed to a low dose of rotenone (10 nM). We found that at the nanomolar concentration of the drug, there is only partial inhibition of complex I activity, with limited impact on cell functionality, in the parental HAP1 cell line. However, the lack of VDAC3 significantly impacted mitochondrial function in the HAP1 cells after treatment with 10 nM rotenone. Under these experimental conditions, only HAP1-ΔVDAC3 cells transfected with a plasmid encoding VDAC3 exhibited recovery of the main analyzed parameters roughly to the levels measured in the parental HAP1 cell line. On the other hand, complementation experiments with the VDAC3 mutant provided evidence that the antioxidant feature of the protein is related to its cysteines. VDAC3 C0A has not been able to recover the oxygen flux like wild-type protein. Overall, the results suggest that cysteine depletion suppresses the protective effect of VDAC3 against mitochondrial oxidative injury.

4. Conclusions

In conclusion, the data obtained in the present Ph.D. work concern the electrophysiological measurements of nanodisc-embedded human VDACs reconstituted in artificial membrane and the analysis of the involvement of human VDAC isoform 3 in mitochondrial ROS homeostasis. In the first part, we introduced a new protocol for VDAC expression and reconstitution into the artificial membrane, based on cell-free expression combined with nanodisc technology, which allowed to obtain human VDAC isoforms directly integrated into a native-like bilayer. Our results revealed that measurements (conductance, voltage dependence, and ion selectivity) of the three human VDACs, obtained by cell-free expression and incorporated into the planar lipid bilayer, completely reproduced and even improved the results reported in conventional expression and reconstitution systems [60,67,68,168]. In addition, the electrophysiological characteristics of human VDAC3 were studied through a mutant without cysteine, validating the extreme importance of these residues in pore function. The new method also displayed extraordinary advantages in reproducibility and experimental effectiveness. It is quicker and easier than the previous protocols [60,67,68,168] because it takes only a few hours from the expression of VDACs to their reconstitution in PLB; this is mainly due to the lack of all those complex and lengthy steps necessary for the refolding of the channels. In addition, VDAC channels presented excellent stability, more than what was obtained with previous protocols [60,67,68,168] (i.e., exhibiting higher insertion efficiency into the artificial membrane). We believe that this new protocol will open up new opportunities in the electrophysiology of VDAC channels. The future perspective is that a combination of cell-free protein expression with NDs may lead the way for site-specific incorporation of non-canonical amino acids, which could be used in functional and structural studies.

The second part concerns the investigation of the human HAP1 cell lines devoid of VDAC1 or VDAC3 in response to oxidative stress. The three VDAC isoforms exhibit different electrophysiological properties, and in particular, the importance of VDAC3 cysteine residues in channel functionality has been validated [55,56,67–69]. According to mass spectrometry investigation, these residues follow an evolutionarily conserved redox modification pattern [139,141]. Notably, the entire set of cysteine residues was never detected as fully oxidized [139], suggesting that specific residues may be subjected to continuous oxidation-reduction cycles, which could be regulated by IMS ROS levels [138]. We found that VDAC3 depletion makes cells extremely sensitive to drugs that promote the buildup of mitochondrial superoxide, enhancing the hypothesis that VDAC3

plays a crucial role in protecting mitochondria from induced oxidative stress. For the first time, we have also demonstrated that the functional antioxidant feature of VDAC3 is linked to its cysteines. Indeed, transient transfection experiments of the HAP1-ΔVDAC3 cell line, with the VDAC3 Cys-less mutant, revealed that the lack of cysteines abrogates the protective action of this protein against the damaging effects of mitochondrial oxidative stress. Therefore, we assume that VDAC3 could perceive changes in the amount of mitochondrial ROS through its cysteines. Specifically, the modification in the redox state of these residues could be used as a marker that promotes the elimination of defective mitochondria to counteract the damaging effects of oxidative stress.

Finally, our results also revealed an over-expression of VDAC3 in response to mitochondria-originated ROS, highlighting the importance of isoform 3 in countering oxidative stress. Regardless, the molecular pathway that induces VDAC3 up-regulation has not yet been determined. Hence, the most exciting perspective is to investigate the mechanism by which VDAC3 is up-regulated, studying the potential involvement of a non-canonical initiation site, called the TCT motif (polypyrimidine initiator) identified in the VDAC3 promoter [167], which is a target for oxidative and metabolic stress translation regulation. Furthermore, it is interesting to note that the expression of VDAC3 varies in some forms of cancer. Jóźwiak et al. demonstrated for the first time that changes in VDAC3 expression are significantly associated with the progression of endometrial cancer. Their results indicated a significant increase in VDAC3 expression in moderately and poorly differentiated endometrial cancers compared to normal tissue [149]. However, a decreased level of VDAC3 expression in endometrial tumors with metastasis has been reported. Metastasis involves the spread of cancer cells from the primary tumor to the surrounding tissues and to distant organs [45]. Studies reveal that tumor metastasis is not an autonomous program but a complex and multifaceted event, where an increase of ROS plays an essential role in the migration and invasion of cancerous cells [172]. Therefore, it could be speculated that endometrial cancer cells might reduce VDAC3 expression by promoting a remarkable increase in mitochondrial ROS, promoting the spread of malignant cells. Overall, variation in VDAC3 expression might depend on the physio-pathological state of the cell to respond appropriately to a change in mitochondrial ROS. Thus, further studies are needed to explain the mechanisms of regulation of VDAC3 expression.

5. Other activities

During my Ph.D., I joined the team and performed the electrophysiological characterization of the recombinant protein Voltage-Dependent Anion Channel isoform 2 of the yeast *Saccharomyces cerevisiae* (yVDAC2), which was believed for many years to be devoid of channel activity. Recently, yVDAC2 has been isolated directly from yeast mitochondria and showed channel-forming activity in the planar lipid bilayer system [157]. This work described an alternative strategy for yVDAC2 isolation through heterologous expression in bacteria and refolding in vitro (described in **Article 3**). I also worked on the review that recapitulates known information about VDAC isoforms in yeast *S. cerevisiae* (**Article 4**) and on the review summarizing data on post-translational modifications of VDAC proteins obtained using nano-Reversed Phase Ultra-High Performance Liquid Chromatography and ultra-sensitive High-Resolution Mass Spectrometry methods (**Article 5**).

6. References

[1] M. Giacomello, A. Pyakurel, C. Glytsou, L. Scorrano, The cell biology of mitochondrial membrane dynamics, Nat Rev Mol Cell Biol. 21 (2020) 204–224. https://doi.org/10.1038/s41580-020-0210-7.

[2] E. Holzerová, H. Prokisch, Mitochondria: Much ado about nothing? How dangerous is reactive oxygen species production?, Int J Biochem Cell Biol. 63 (2015) 16–20. https://doi.org/10.1016/j.biocel.2015.01.021.

[3] P.J. Burke, Mitochondria, Bioenergetics and Apoptosis in Cancer, Trends Cancer. 3 (2017) 857–870. https://doi.org/10.1016/j.trecan.2017.10.006.

[4] D. De Stefani, A. Raffaello, E. Teardo, I. Szabò, R. Rizzuto, A forty-kilodalton protein of the inner membrane is the mitochondrial calcium uniporter, Nature. 476 (2011) 336–340. https://doi.org/10.1038/nature10230.

[5] P.M. Herst, M.R. Rowe, G.M. Carson, M.V. Berridge, Functional Mitochondria in Health and Disease, Frontiers in Endocrinology. 8 (2017) 296. https://doi.org/10.3389/fendo.2017.00296.

[6] C.S. Ahn, C.M. Metallo, Mitochondria as biosynthetic factories for cancer proliferation, Cancer Metab. 3 (2015) 1. https://doi.org/10.1186/s40170-015-0128-2.

[7] J. Nunnari, A. Suomalainen, Mitochondria: In Sickness and in Health, Cell. 148 (2012) 1145–1159. https://doi.org/10.1016/j.cell.2012.02.035.

[8] W.F. Martin, S. Garg, V. Zimorski, Endosymbiotic theories for eukaryote origin, Philos Trans R Soc Lond B Biol Sci. 370 (2015) 20140330. https://doi.org/10.1098/rstb.2014.0330.

[9] B.E. Christian, L.L. Spremulli, Mechanism of protein biosynthesis in mammalian mitochondria, Biochim Biophys Acta. 1819 (2012) 1035–1054. https://doi.org/10.1016/j.bbagrm.2011.11.009.

[10] J.-W. Taanman, The mitochondrial genome: structure, transcription, translation and replication, Biochimica et Biophysica Acta (BBA) - Bioenergetics. 1410 (1999) 103–123. https://doi.org/10.1016/S0005-2728(98)00161-3.

[11] R.C. Scarpulla, R.B. Vega, D.P. Kelly, Transcriptional integration of mitochondrial biogenesis, Trends Endocrinol Metab. 23 (2012) 459–466. https://doi.org/10.1016/j.tem.2012.06.006.

[12] L.L. Lackner, Determining the shape and cellular distribution of mitochondria: the integration of multiple activities, Curr Opin Cell Biol. 25 (2013) 471–476. https://doi.org/10.1016/j.ceb.2013.02.011.

[13] H.J. Harmon, J.D. Hall, F.L. Crane, Structure of mitochondrial cristae membranes, Biochimica et Biophysica Acta (BBA) - Reviews on Biomembranes. 344 (1974) 119–155. https://doi.org/10.1016/0304-4157(74)90002-1.

[14] C.A. Mannella, The relevance of mitochondrial membrane topology to mitochondrial function, Biochimica et Biophysica Acta (BBA) - Molecular Basis of Disease. 1762 (2006) 140–147. https://doi.org/10.1016/j.bbadis.2005.07.001.

[15] J.R. Friedman, J. Nunnari, Mitochondrial form and function, Nature. 505 (2014) 335–343. https://doi.org/10.1038/nature12985.

[16] T.G. Frey, C.A. Mannella, The internal structure of mitochondria, Trends in Biochemical Sciences. 25 (2000) 319–324. https://doi.org/10.1016/S0968-0004(00)01609-1.

[17] W. Kühlbrandt, Structure and function of mitochondrial membrane protein complexes, BMC Biology. 13 (2015) 89. https://doi.org/10.1186/s12915-015-0201-x.

[18] F. Joubert, N. Puff, Mitochondrial Cristae Architecture and Functions: Lessons from Minimal Model Systems, Membranes. 11 (2021) 465.

https://doi.org/10.3390/membranes11070465.
[19] S.E. Horvath, G. Daum, Lipids of mitochondria, Prog Lipid Res. 52 (2013) 590–614. https://doi.org/10.1016/j.plipres.2013.07.002.
[20] M. Picard, M.J. McManus, G. Csordás, P. Várnai, G.W. Dorn II, D. Williams, G. Hajnóczky, D.C. Wallace, Trans-mitochondrial coordination of cristae at regulated membrane junctions, Nat Commun. 6 (2015) 6259. https://doi.org/10.1038/ncomms7259.
[21] I.F. Sevrioukova, Apoptosis-Inducing Factor: Structure, Function, and Redox Regulation, Antioxid Redox Signal. 14 (2011) 2545–2579. https://doi.org/10.1089/ars.2010.3445.
[22] H.K. Lorenzo, S.A. Susin, J. Penninger, G. Kroemer, Apoptosis inducing factor (AIF): a phylogenetically old, caspase-independent effector of cell death, Cell Death Differ. 6 (1999) 516–524. https://doi.org/10.1038/sj.cdd.4400527.
[23] D.M. Walther, D. Rapaport, Biogenesis of mitochondrial outer membrane proteins, Biochimica et Biophysica Acta (BBA) - Molecular Cell Research. 1793 (2009) 42–51. https://doi.org/10.1016/j.bbamcr.2008.04.013.
[24] N. Lecrenier, P. Van Der Bruggen, F. Foury, Mitochondrial DNA polymerases from yeast to man: a new family of polymerases, Gene. 185 (1997) 147–152. https://doi.org/10.1016/s0378-1119(96)00663-4.
[25] E. Zinser, C.D. Sperka-Gottlieb, E.V. Fasch, S.D. Kohlwein, F. Paltauf, G. Daum, Phospholipid synthesis and lipid composition of subcellular membranes in the unicellular eukaryote Saccharomyces cerevisiae, J Bacteriol. 173 (1991) 2026–2034. https://doi.org/10.1128/jb.173.6.2026-2034.1991.
[26] A.I. de Kroon, D. Dolis, A. Mayer, R. Lill, B. de Kruijff, Phospholipid composition of highly purified mitochondrial outer membranes of rat liver and Neurospora crassa. Is cardiolipin present in the mitochondrial outer membrane?, Biochim Biophys Acta. 1325 (1997) 108–116. https://doi.org/10.1016/s0005-2736(96)00240-4.
[27] Y.J. Liu, R.L. McIntyre, G.E. Janssens, R.H. Houtkooper, Mitochondrial fission and fusion: A dynamic role in aging and potential target for age-related disease, Mechanisms of Ageing and Development. 186 (2020) 111212. https://doi.org/10.1016/j.mad.2020.111212.
[28] M. Rojo, F. Legros, D. Chateau, A. Lombès, Membrane topology and mitochondrial targeting of mitofusins, ubiquitous mammalian homologs of the transmembrane GTPase Fzo, J Cell Sci. 115 (2002) 1663–1674.
[29] S. Fritz, D. Rapaport, E. Klanner, W. Neupert, B. Westermann, Connection of the Mitochondrial Outer and Inner Membranes by Fzo1 Is Critical for Organellar Fusion, Journal of Cell Biology. 152 (2001) 683–692. https://doi.org/10.1083/jcb.152.4.683.
[30] M. Bayrhuber, T. Meins, M. Habeck, S. Becker, K. Giller, S. Villinger, C. Vonrhein, C. Griesinger, M. Zweckstetter, K. Zeth, Structure of the human voltage-dependent anion channel, Proc Natl Acad Sci U S A. 105 (2008) 15370–15375. https://doi.org/10.1073/pnas.0808115105.
[31] V. Shoshan-Barmatz, V. De Pinto, M. Zweckstetter, Z. Raviv, N. Keinan, N. Arbel, VDAC, a multi-functional mitochondrial protein regulating cell life and death, Mol Aspects Med. 31 (2010) 227–285. https://doi.org/10.1016/j.mam.2010.03.002.
[32] A. Messina, S. Reina, F. Guarino, V. De Pinto, VDAC isoforms in mammals, Biochim Biophys Acta. 1818 (2012) 1466–1476. https://doi.org/10.1016/j.bbamem.2011.10.005.
[33] R. Benz, Permeation of hydrophilic solutes through mitochondrial outer membranes: review on mitochondrial porins, Biochim Biophys Acta. 1197 (1994) 167–196. https://doi.org/10.1016/0304-4157(94)90004-3.
[34] T. Hodge, M. Colombini, Regulation of metabolite flux through voltage-gating of VDAC channels, J Membr Biol. 157 (1997) 271–279. https://doi.org/10.1007/s002329900235.

[35] A.C. Lee, X. Xu, E. Blachly-Dyson, M. Forte, M. Colombini, The role of yeast VDAC genes on the permeability of the mitochondrial outer membrane, J Membr Biol. 161 (1998) 173–181. https://doi.org/10.1007/s002329900324.
[36] K. Lee, J. Kerner, C.L. Hoppel, Mitochondrial carnitine palmitoyltransferase 1a (CPT1a) is part of an outer membrane fatty acid transfer complex, J Biol Chem. 286 (2011) 25655–25662. https://doi.org/10.1074/jbc.M111.228692.
[37] E. Simamura, H. Shimada, T. Hatta, K.-I. Hirai, Mitochondrial voltage-dependent anion channels (VDACs) as novel pharmacological targets for anti-cancer agents, J Bioenerg Biomembr. 40 (2008) 213–217. https://doi.org/10.1007/s10863-008-9158-6.
[38] C. Fiek, R. Benz, N. Roos, D. Brdiczka, Evidence for identity between the hexokinase-binding protein and the mitochondrial porin in the outer membrane of rat liver mitochondria, Biochim Biophys Acta. 688 (1982) 429–440. https://doi.org/10.1016/0005-2736(82)90354-6.
[39] A. Magrì, S. Reina, V. De Pinto, VDAC1 as Pharmacological Target in Cancer and Neurodegeneration: Focus on Its Role in Apoptosis, Frontiers in Chemistry. 6 (2018) 108. https://doi.org/10.3389/fchem.2018.00108.
[40] S. Hiller, R.G. Garces, T.J. Malia, V.Y. Orekhov, M. Colombini, G. Wagner, Solution structure of the integral human membrane protein VDAC-1 in detergent micelles, Science. 321 (2008) 1206–1210. https://doi.org/10.1126/science.1161302.
[41] R. Ujwal, D. Cascio, J.-P. Colletier, S. Faham, J. Zhang, L. Toro, P. Ping, J. Abramson, The crystal structure of mouse VDAC1 at 2.3 A resolution reveals mechanistic insights into metabolite gating, Proc Natl Acad Sci U S A. 105 (2008) 17742–17747. https://doi.org/10.1073/pnas.0809634105.
[42] K. Zeth, M. Thein, Porins in prokaryotes and eukaryotes: Common themes and variations, The Biochemical Journal. 431 (2010) 13–22. https://doi.org/10.1042/BJ20100371.
[43] K. Zeth, U. Zachariae, Ten Years of High Resolution Structural Research on the Voltage Dependent Anion Channel (VDAC)—Recent Developments and Future Directions, Frontiers in Physiology. 9 (2018) 108. https://doi.org/10.3389/fphys.2018.00108.
[44] Z. Gattin, R. Schneider, Y. Laukat, K. Giller, E. Maier, M. Zweckstetter, C. Griesinger, R. Benz, S. Becker, A. Lange, Solid-state NMR and Molecular Dynamics Characterization of human VDAC2, J Biomol NMR. 61 (2015) 311–320. https://doi.org/10.1007/s10858-014-9876-5.
[45] J. Schredelseker, A. Paz, C.J. López, C. Altenbach, C.S. Leung, M.K. Drexler, J.-N. Chen, W.L. Hubbell, J. Abramson, High resolution structure and double electron-electron resonance of the zebrafish voltage-dependent anion channel 2 reveal an oligomeric population, J Biol Chem. 289 (2014) 12566–12577. https://doi.org/10.1074/jbc.M113.497438.
[46] G.F. Amodeo, M.A. Scorciapino, A. Messina, V. De Pinto, M. Ceccarelli, Charged residues distribution modulates selectivity of the open state of human isoforms of the voltage dependent anion-selective channel, PLoS One. 9 (2014) e103879. https://doi.org/10.1371/journal.pone.0103879.
[47] E.E. Najbauer, S. Becker, K. Giller, M. Zweckstetter, A. Lange, C. Steinem, B.L. de Groot, C. Griesinger, L.B. Andreas, Structure, gating and interactions of the voltage-dependent anion channel, Eur Biophys J. 50 (2021) 159–172. https://doi.org/10.1007/s00249-021-01515-7.
[48] J. Maher, M. Allen, Planar lipid bilayers in recombinant ion channel research, Methods. 147 (2018) 206–212. https://doi.org/10.1016/j.ymeth.2018.03.003.
[49] S. Oiki, M. Iwamoto, Lipid Bilayers Manipulated through Monolayer Technologies for Studies of Channel-Membrane Interplay, Biological and Pharmaceutical Bulletin. 41 (2018) 303–311. https://doi.org/10.1248/bpb.b17-00708.

[50] S. Oiki, Planar Lipid Bilayer Method for Studying Channel Molecules, in: Y. Okada (Ed.), Patch Clamp Techniques: From Beginning to Advanced Protocols, Springer Japan, Tokyo, 2012: pp. 229–275. https://doi.org/10.1007/978-4-431-53993-3_16.
[51] M. Iwamoto, S. Oiki, Physical and Chemical Interplay Between the Membrane and a Prototypical Potassium Channel Reconstituted on a Lipid Bilayer Platform, Front Mol Neurosci. 14 (2021) 634121. https://doi.org/10.3389/fnmol.2021.634121.
[52] E. Zakharian, Ion channel reconstitution in lipid bilayers, Methods Enzymol. 652 (2021) 273–291. https://doi.org/10.1016/bs.mie.2021.03.001.
[53] E.-M. Krammer, H. Saidani, M. Prévost, F. Homblé, Origin of ion selectivity in Phaseolus coccineus mitochondrial VDAC, Mitochondrion. 19 (2014) 206–213. https://doi.org/10.1016/j.mito.2014.04.003.
[54] C. Guardiani, A. Magrì, A. Karachitos, M.C. Di Rosa, S. Reina, I. Bodrenko, A. Messina, H. Kmita, M. Ceccarelli, V. De Pinto, yVDAC2, the second mitochondrial porin isoform of Saccharomyces cerevisiae, Biochim Biophys Acta Bioenerg. 1859 (2018) 270–279. https://doi.org/10.1016/j.bbabio.2018.01.008.
[55] M. Queralt-Martín, L. Bergdoll, O. Teijido, N. Munshi, D. Jacobs, A.J. Kuszak, O. Protchenko, S. Reina, A. Magrì, V. De Pinto, S.M. Bezrukov, J. Abramson, T.K. Rostovtseva, A lower affinity to cytosolic proteins reveals VDAC3 isoform-specific role in mitochondrial biology, J Gen Physiol. 152 (2020) e201912501. https://doi.org/10.1085/jgp.201912501.
[56] S. Conti Nibali, M.C. Di Rosa, O. Rauh, G. Thiel, S. Reina, V. De Pinto, Cell-free electrophysiology of human VDACs incorporated into nanodiscs: An improved method, Biophys Rep. 1 (2021) None. https://doi.org/10.1016/j.bpr.2021.100002.
[57] S.J. Schein, M. Colombini, A. Finkelstein, Reconstitution in planar lipid bilayers of a voltage-dependent anion-selective channel obtained from paramecium mitochondria, J Membr Biol. 30 (1976) 99–120. https://doi.org/10.1007/BF01869662.
[58] R. Benz, Permeation of hydrophilic solutes through mitochondrial outer membranes: review on mitochondrial porins, Biochim Biophys Acta. 1197 (1994) 167–196. https://doi.org/10.1016/0304-4157(94)90004-3.
[59] M. Colombini, Measurement of VDAC permeability in intact mitochondria and in reconstituted systems, Methods Cell Biol. 80 (2007) 241–260. https://doi.org/10.1016/S0091-679X(06)80012-9.
[60] A. Magrì, A. Karachitos, M.C. Di Rosa, S. Reina, S. Conti Nibali, A. Messina, H. Kmita, V. De Pinto, Recombinant yeast VDAC2: a comparison of electrophysiological features with the native form, FEBS Open Bio. 9 (2019) 1184–1193. https://doi.org/10.1002/2211-5463.12574.
[61] T. Rostovtseva, M. Colombini, ATP flux is controlled by a voltage-gated channel from the mitochondrial outer membrane, J Biol Chem. 271 (1996) 28006–28008. https://doi.org/10.1074/jbc.271.45.28006.
[62] S.Y. Noskov, T.K. Rostovtseva, A.C. Chamberlin, O. Teijido, W. Jiang, S.M. Bezrukov, Current state of theoretical and experimental studies of the voltage-dependent anion channel (VDAC), Biochim Biophys Acta. 1858 (2016) 1778–1790. https://doi.org/10.1016/j.bbamem.2016.02.026.
[63] M. Queralt-Martín, L. Bergdoll, D. Jacobs, S.M. Bezrukov, J. Abramson, T.K. Rostovtseva, Assessing the role of residue E73 and lipid headgroup charge in VDAC1 voltage gating, Biochim Biophys Acta Bioenerg. 1860 (2019) 22–29. https://doi.org/10.1016/j.bbabio.2018.11.001.
[64] M. Colombini, Structure and mode of action of a voltage dependent anion-selective channel (VDAC) located in the outer mitochondrial membrane, Ann N Y Acad Sci. 341 (1980) 552–563. https://doi.org/10.1111/j.1749-6632.1980.tb47198.x.
[65] X. Xu, W. Decker, M.J. Sampson, W.J. Craigen, M. Colombini, Mouse VDAC isoforms expressed in yeast: channel properties and their roles in mitochondrial outer

membrane permeability, J Membr Biol. 170 (1999) 89–102. https://doi.org/10.1007/s002329900540.
[66] V.A. Menzel, M.C. Cassará, R. Benz, V. de Pinto, A. Messina, V. Cunsolo, R. Saletti, K.-D. Hinsch, E. Hinsch, Molecular and functional characterization of VDAC2 purified from mammal spermatozoa, Biosci Rep. 29 (2009) 351–362. https://doi.org/10.1042/BSR20080123.
[67] V. Checchetto, S. Reina, A. Magrì, I. Szabo, V. De Pinto, Recombinant human voltage dependent anion selective channel isoform 3 (hVDAC3) forms pores with a very small conductance, Cell Physiol Biochem. 34 (2014) 842–853. https://doi.org/10.1159/000363047.
[68] S. Reina, V. Checchetto, R. Saletti, A. Gupta, D. Chaturvedi, C. Guardiani, F. Guarino, M.A. Scorciapino, A. Magrì, S. Foti, M. Ceccarelli, A.A. Messina, R. Mahalakshmi, I. Szabo, V. De Pinto, VDAC3 as a sensor of oxidative state of the intermembrane space of mitochondria: the putative role of cysteine residue modifications, Oncotarget. 7 (2016) 2249–2268. https://doi.org/10.18632/oncotarget.6850.
[69] M. Okazaki, K. Kurabayashi, M. Asanuma, Y. Saito, K. Dodo, M. Sodeoka, VDAC3 gating is activated by suppression of disulfide-bond formation between the N-terminal region and the bottom of the pore, Biochim Biophys Acta. 1848 (2015) 3188–3196. https://doi.org/10.1016/j.bbamem.2015.09.017.
[70] M. Colombini, C.L. Yeung, J. Tung, T. König, The mitochondrial outer membrane channel, VDAC, is regulated by a synthetic polyanion, Biochim Biophys Acta. 905 (1987) 279–286. https://doi.org/10.1016/0005-2736(87)90456-1.
[71] J. Zimmerberg, V.A. Parsegian, Polymer inaccessible volume changes during opening and closing of a voltage-dependent ionic channel, Nature. 323 (1986) 36–39. https://doi.org/10.1038/323036a0.
[72] J. Song, C. Midson, E. Blachly-Dyson, M. Forte, M. Colombini, The sensor regions of VDAC are translocated from within the membrane to the surface during the gating processes, Biophys J. 74 (1998) 2926–2944. https://doi.org/10.1016/S0006-3495(98)78000-2.
[73] S. Hiller, G. Wagner, The role of solution NMR in the structure determinations of VDAC-1 and other membrane proteins, Curr Opin Struct Biol. 19 (2009) 396–401. https://doi.org/10.1016/j.sbi.2009.07.013.
[74] U. Zachariae, R. Schneider, R. Briones, Z. Gattin, J.-P. Demers, K. Giller, E. Maier, M. Zweckstetter, C. Griesinger, S. Becker, R. Benz, B.L. de Groot, A. Lange, β-Barrel mobility underlies closure of the voltage-dependent anion channel, Structure. 20 (2012) 1540–1549. https://doi.org/10.1016/j.str.2012.06.015.
[75] S. Villinger, R. Briones, K. Giller, U. Zachariae, A. Lange, B.L. de Groot, C. Griesinger, S. Becker, M. Zweckstetter, Functional dynamics in the voltage-dependent anion channel, Proc Natl Acad Sci U S A. 107 (2010) 22546–22551. https://doi.org/10.1073/pnas.1012310108.
[76] D. Gincel, H. Zaid, V. Shoshan-Barmatz, Calcium binding and translocation by the voltage-dependent anion channel: a possible regulatory mechanism in mitochondrial function, Biochem J. 358 (2001) 147–155. https://doi.org/10.1042/0264-6021:3580147.
[77] Y. Shi, C. Jiang, Q. Chen, H. Tang, One-step on-column affinity refolding purification and functional analysis of recombinant human VDAC1, Biochem Biophys Res Commun. 303 (2003) 475–482. https://doi.org/10.1016/s0006-291x(03)00359-0.
[78] A. Singh, V. Upadhyay, A.K. Upadhyay, S.M. Singh, A.K. Panda, Protein recovery from inclusion bodies of Escherichia coli using mild solubilization process, Microb Cell Fact. 14 (2015) 41. https://doi.org/10.1186/s12934-015-0222-8.
[79] T.H. Bayburt, S.G. Sligar, Self-assembly of single integral membrane proteins into soluble nanoscale phospholipid bilayers, Protein Sci. 12 (2003) 2476–2481. https://doi.org/10.1110/ps.03267503.

[80] X. Jiang, Y. Ookubo, I. Fujii, H. Nakano, T. Yamane, Expression of Fab fragment of catalytic antibody 6D9 in an Escherichia coli in vitro coupled transcription/translation system, FEBS Lett. 514 (2002) 290–294. https://doi.org/10.1016/s0014-5793(02)02383-9.
[81] L.A. Ryabova, D. Desplancq, A.S. Spirin, A. Plückthun, Functional antibody production using cell-free translation: effects of protein disulfide isomerase and chaperones, Nat Biotechnol. 15 (1997) 79–84. https://doi.org/10.1038/nbt0197-79.
[82] A.S. Spirin, V.I. Baranov, L.A. Ryabova, S.Y. Ovodov, Y.B. Alakhov, A continuous cell-free translation system capable of producing polypeptides in high yield, Science. 242 (1988) 1162–1164. https://doi.org/10.1126/science.3055301.
[83] I.G. Denisov, Y.V. Grinkova, A.A. Lazarides, S.G. Sligar, Directed self-assembly of monodisperse phospholipid bilayer Nanodiscs with controlled size, J Am Chem Soc. 126 (2004) 3477–3487. https://doi.org/10.1021/ja0393574.
[84] I.G. Denisov, S.G. Sligar, Nanodiscs for structural and functional studies of membrane proteins, Nat Struct Mol Biol. 23 (2016) 481–486. https://doi.org/10.1038/nsmb.3195.
[85] A. Nath, W.M. Atkins, S.G. Sligar, Applications of phospholipid bilayer nanodiscs in the study of membranes and membrane proteins, Biochemistry. 46 (2007) 2059–2069. https://doi.org/10.1021/bi602371n.
[86] N. Akkaladevi, S. Mukherjee, H. Katayama, B. Janowiak, D. Patel, E.P. Gogol, B.L. Pentelute, R. John Collier, M.T. Fisher, Following Natures Lead: On the Construction of Membrane-Inserted Toxins in Lipid Bilayer Nanodiscs, J Membr Biol. 248 (2015) 595–607. https://doi.org/10.1007/s00232-014-9768-3.
[87] B.J. Baas, I.G. Denisov, S.G. Sligar, Homotropic cooperativity of monomeric cytochrome P450 3A4 in a nanoscale native bilayer environment, Arch Biochem Biophys. 430 (2004) 218–228. https://doi.org/10.1016/j.abb.2004.07.003.
[88] M. Etzkorn, T. Raschle, F. Hagn, V. Gelev, A.J. Rice, T. Walz, G. Wagner, Cell-free expressed bacteriorhodopsin in different soluble membrane mimetics: biophysical properties and NMR accessibility, Structure. 21 (2013) 394–401. https://doi.org/10.1016/j.str.2013.01.005.
[89] L.-M. Winterstein, K. Kukovetz, U.-P. Hansen, I. Schroeder, J.L. Van Etten, A. Moroni, G. Thiel, O. Rauh, Distinct lipid bilayer compositions have general and protein-specific effects on K+ channel function, J Gen Physiol. 153 (2021) e202012731. https://doi.org/10.1085/jgp.202012731.
[90] L.-M. Winterstein, K. Kukovetz, O. Rauh, D.L. Turman, C. Braun, A. Moroni, I. Schroeder, G. Thiel, Reconstitution and functional characterization of ion channels from nanodiscs in lipid bilayers, J Gen Physiol. 150 (2018) 637–646. https://doi.org/10.1085/jgp.201711904.
[91] O. Rauh, U.P. Hansen, D.D. Scheub, G. Thiel, I. Schroeder, Site-specific ion occupation in the selectivity filter causes voltage-dependent gating in a viral K+ channel, Sci Rep. 8 (2018) 10406. https://doi.org/10.1038/s41598-018-28751-w.
[92] M. Krajewska, P. Koprowski, Solubilization, purification, and functional reconstitution of human ROMK potassium channel in copolymer styrene-maleic acid (SMA) nanodiscs, Biochim Biophys Acta Biomembr. 1863 (2021) 183555. https://doi.org/10.1016/j.bbamem.2021.183555.
[93] A. Viegas, T. Viennet, M. Etzkorn, The power, pitfalls and potential of the nanodisc system for NMR-based studies, Biol Chem. 397 (2016) 1335–1354. https://doi.org/10.1515/hsz-2016-0224.
[94] H. Ghazarian, W. Hu, A. Mao, T. Nguyen, N. Vaidehi, S. Sligar, J.E. Shively, NMR analysis of free and lipid nanodisc anchored CEACAM1 membrane proximal peptides with Ca2+/CaM, Biochim Biophys Acta Biomembr. 1861 (2019) 787–797. https://doi.org/10.1016/j.bbamem.2019.01.004.
[95] M. Walter, R. Schlesinger, Nanodisc Reconstitution of Channelrhodopsins

Heterologously Expressed in Pichia pastoris for Biophysical Investigations, Methods Mol Biol. 2191 (2021) 29–48. https://doi.org/10.1007/978-1-0716-0830-2_3.
[96] T. Raschle, S. Hiller, T.-Y. Yu, A.J. Rice, T. Walz, G. Wagner, Structural and functional characterization of the integral membrane protein VDAC-1 in lipid bilayer nanodiscs, J Am Chem Soc. 131 (2009) 17777–17779. https://doi.org/10.1021/ja907918r.
[97] T.-Y. Yu, T. Raschle, S. Hiller, G. Wagner, Solution NMR spectroscopic characterization of human VDAC-2 in detergent micelles and lipid bilayer nanodiscs, Biochim Biophys Acta. 1818 (2012) 1562–1569. https://doi.org/10.1016/j.bbamem.2011.11.012.
[98] K.-D. Hinsch, V. De Pinto, V.A. Aires, X. Schneider, A. Messina, E. Hinsch, Voltage-dependent anion-selective channels VDAC2 and VDAC3 are abundant proteins in bovine outer dense fibers, a cytoskeletal component of the sperm flagellum, J Biol Chem. 279 (2004) 15281–15288. https://doi.org/10.1074/jbc.M313433200.
[99] S.F. Okada, W.K. O'Neal, P. Huang, R.A. Nicholas, L.E. Ostrowski, W.J. Craigen, E.R. Lazarowski, R.C. Boucher, Voltage-dependent anion channel-1 (VDAC-1) contributes to ATP release and cell volume regulation in murine cells, J Gen Physiol. 124 (2004) 513–526. https://doi.org/10.1085/jgp.200409154.
[100] M.G. Vander Heiden, N.S. Chandel, P.T. Schumacker, C.B. Thompson, Bcl-xL prevents cell death following growth factor withdrawal by facilitating mitochondrial ATP/ADP exchange, Mol Cell. 3 (1999) 159–167. https://doi.org/10.1016/s1097-2765(00)80307-x.
[101] J.G. Pastorino, N. Shulga, J.B. Hoek, Mitochondrial binding of hexokinase II inhibits Bax-induced cytochrome c release and apoptosis, J Biol Chem. 277 (2002) 7610–7618. https://doi.org/10.1074/jbc.M109950200.
[102] S. Abu-Hamad, H. Zaid, A. Israelson, E. Nahon, V. Shoshan-Barmatz, Hexokinase-I protection against apoptotic cell death is mediated via interaction with the voltage-dependent anion channel-1: mapping the site of binding, J Biol Chem. 283 (2008) 13482–13490. https://doi.org/10.1074/jbc.M708216200.
[103] A. Magri, A. Messina, Interactions of VDAC with Proteins Involved in Neurodegenerative Aggregation: An Opportunity for Advancement on Therapeutic Molecules, Curr Med Chem. 24 (2017) 4470–4487. https://doi.org/10.2174/0929867324666170601073920.
[104] V. Shoshan-Barmatz, S. Pittala, D. Mizrachi, VDAC1 and the TSPO: Expression, Interactions, and Associated Functions in Health and Disease States, Int J Mol Sci. 20 (2019) 3348. https://doi.org/10.3390/ijms20133348.
[105] L. Veenman, V. Papadopoulos, M. Gavish, Channel-like functions of the 18-kDa translocator protein (TSPO): regulation of apoptosis and steroidogenesis as part of the host-defense response, Curr Pharm Des. 13 (2007) 2385–2405. https://doi.org/10.2174/138161207781368710.
[106] S. Galiègue, P. Casellas, A. Kramar, N. Tinel, J. Simony-Lafontaine, Immunohistochemical assessment of the peripheral benzodiazepine receptor in breast cancer and its relationship with survival, Clin Cancer Res. 10 (2004) 2058–2064. https://doi.org/10.1158/1078-0432.ccr-03-0988.
[107] V. Papadopoulos, M. Baraldi, T.R. Guilarte, T.B. Knudsen, J.-J. Lacapère, P. Lindemann, M.D. Norenberg, D. Nutt, A. Weizman, M.-R. Zhang, M. Gavish, Translocator protein (18kDa): new nomenclature for the peripheral-type benzodiazepine receptor based on its structure and molecular function, Trends Pharmacol Sci. 27 (2006) 402–409. https://doi.org/10.1016/j.tips.2006.06.005.
[108] J. Gatliff, D. East, J. Crosby, R. Abeti, R. Harvey, W. Craigen, P. Parker, M. Campanella, TSPO interacts with VDAC1 and triggers a ROS-mediated inhibition of mitochondrial quality control, Autophagy. 10 (2014) 2279–2296. https://doi.org/10.4161/15548627.2014.991665.

[109] V. Giorgio, L. Guo, C. Bassot, V. Petronilli, P. Bernardi, Calcium and regulation of the mitochondrial permeability transition, Cell Calcium. 70 (2018) 56–63. https://doi.org/10.1016/j.ceca.2017.05.004.
[110] V.V. Lemeshko, Model of the Outer Membrane Potential Generation by the Inner Membrane of Mitochondria, Biophysical Journal. 82 (2002) 684–692. https://doi.org/10.1016/S0006-3495(02)75431-3.
[111] S.V. Lemeshko, V.V. Lemeshko, Metabolically derived potential on the outer membrane of mitochondria: a computational model., Biophys J. 79 (2000) 2785–2800.
[112] A.M. Porcelli, A. Ghelli, C. Zanna, P. Pinton, R. Rizzuto, M. Rugolo, pH difference across the outer mitochondrial membrane measured with a green fluorescent protein mutant, Biochem Biophys Res Commun. 326 (2005) 799–804. https://doi.org/10.1016/j.bbrc.2004.11.105.
[113] T.K. Rostovtseva, S.M. Bezrukov, VDAC inhibition by tubulin and its physiological implications, Biochimica et Biophysica Acta (BBA) - Biomembranes. 1818 (2012) 1526–1535. https://doi.org/10.1016/j.bbamem.2011.11.004.
[114] E.N. Maldonado, VDAC-Tubulin, an Anti-Warburg Pro-Oxidant Switch, Front Oncol. 7 (2017) 4. https://doi.org/10.3389/fonc.2017.00004.
[115] T.K. Rostovtseva, K.L. Sheldon, E. Hassanzadeh, C. Monge, V. Saks, S.M. Bezrukov, D.L. Sackett, Tubulin binding blocks mitochondrial voltage-dependent anion channel and regulates respiration, Proceedings of the National Academy of Sciences. 105 (2008) 18746–18751. https://doi.org/10.1073/pnas.0806303105.
[116] A. Priel, J.A. Tuszynski, N.J. Woolf, Transitions in microtubule C-termini conformations as a possible dendritic signaling phenomenon, Eur Biophys J. 35 (2005) 40–52. https://doi.org/10.1007/s00249-005-0003-0.
[117] K.L. Sheldon, E.N. Maldonado, J.J. Lemasters, T.K. Rostovtseva, S.M. Bezrukov, Phosphorylation of voltage-dependent anion channel by serine/threonine kinases governs its interaction with tubulin, PLoS One. 6 (2011) e25539. https://doi.org/10.1371/journal.pone.0025539.
[118] P.A. Gurnev, T.K. Rostovtseva, S.M. Bezrukov, Tubulin-blocked state of VDAC studied by polymer and ATP partitioning, FEBS Letters. 585 (2011) 2363–2366. https://doi.org/10.1016/j.febslet.2011.06.008.
[119] E.N. Maldonado, K.L. Sheldon, D.N. DeHart, J. Patnaik, Y. Manevich, D.M. Townsend, S.M. Bezrukov, T.K. Rostovtseva, J.J. Lemasters, Voltage-dependent anion channels modulate mitochondrial metabolism in cancer cells: regulation by free tubulin and erastin, J Biol Chem. 288 (2013) 11920–11929. https://doi.org/10.1074/jbc.M112.433847.
[120] W.J. Craigen, B.H. Graham, Genetic strategies for dissecting mammalian and Drosophila voltage-dependent anion channel functions, J Bioenerg Biomembr. 40 (2008) 207–212. https://doi.org/10.1007/s10863-008-9146-x.
[121] K. Anflous-Pharayra, N. Lee, D.L. Armstrong, W.J. Craigen, VDAC3 has differing mitochondrial functions in two types of striated muscles, Biochim Biophys Acta. 1807 (2011) 150–156. https://doi.org/10.1016/j.bbabio.2010.09.007.
[122] M.J. Sampson, W.K. Decker, A.L. Beaudet, W. Ruitenbeek, D. Armstrong, M.J. Hicks, W.J. Craigen, Immotile sperm and infertility in mice lacking mitochondrial voltage-dependent anion channel type 3, J Biol Chem. 276 (2001) 39206–39212. https://doi.org/10.1074/jbc.M104724200.
[123] E.H.Y. Cheng, T.V. Sheiko, J.K. Fisher, W.J. Craigen, S.J. Korsmeyer, VDAC2 inhibits BAK activation and mitochondrial apoptosis, Science. 301 (2003) 513–517. https://doi.org/10.1126/science.1083995.
[124] K.P. Subedi, J.-C. Kim, M. Kang, M.-J. Son, Y.-S. Kim, S.-H. Woo, Voltage-dependent anion channel 2 modulates resting Ca^{2}+ sparks, but not action potential-induced Ca^{2}+ signaling in cardiac myocytes, Cell Calcium. 49 (2011) 136–143.

https://doi.org/10.1016/j.ceca.2010.12.004.
[125] H. Shimizu, J. Schredelseker, J. Huang, K. Lu, S. Naghdi, F. Lu, S. Franklin, H.D. Fiji, K. Wang, H. Zhu, C. Tian, B. Lin, H. Nakano, A. Ehrlich, J. Nakai, A.Z. Stieg, J.K. Gimzewski, A. Nakano, J.I. Goldhaber, T.M. Vondriska, G. Hajnóczky, O. Kwon, J.-N. Chen, Mitochondrial Ca(2+) uptake by the voltage-dependent anion channel 2 regulates cardiac rhythmicity, Elife. 4 (2015). https://doi.org/10.7554/eLife.04801.
[126] C.K. Min, D.R. Yeom, K.-E. Lee, H.-K. Kwon, M. Kang, Y.-S. Kim, Z.Y. Park, H. Jeon, D.H. Kim, Coupling of ryanodine receptor 2 and voltage-dependent anion channel 2 is essential for Ca^{2}+ transfer from the sarcoplasmic reticulum to the mitochondria in the heart, Biochem J. 447 (2012) 371–379. https://doi.org/10.1042/BJ20120705.
[127] S.R. Maurya, R. Mahalakshmi, Mitochondrial VDAC2 and cell homeostasis: highlighting hidden structural features and unique functionalities, Biol Rev Camb Philos Soc. 92 (2017) 1843–1858. https://doi.org/10.1111/brv.12311.
[128] M. Prasad, J. Kaur, K.J. Pawlak, M. Bose, R.M. Whittal, H.S. Bose, Mitochondria-associated endoplasmic reticulum membrane (MAM) regulates steroidogenic activity via steroidogenic acute regulatory protein (StAR)-voltage-dependent anion channel 2 (VDAC2) interaction, J Biol Chem. 290 (2015) 2604–2616. https://doi.org/10.1074/jbc.M114.605808.
[129] S. Naghdi, G. Hajnóczky, VDAC2-specific cellular functions and the underlying structure, Biochim Biophys Acta. 1863 (2016) 2503–2514. https://doi.org/10.1016/j.bbamcr.2016.04.020.
[130] V.G. Veresov, A.I. Davidovskii, Structural insights into proapoptotic signaling mediated by MTCH2, VDAC2, TOM40 and TOM22, Cell Signal. 26 (2014) 370–382. https://doi.org/10.1016/j.cellsig.2013.11.016.
[131] S. Majumder, H.A. Fisk, VDAC3 and Mps1 negatively regulate ciliogenesis, Cell Cycle. 12 (2013) 849–858. https://doi.org/10.4161/cc.23824.
[132] V. De Pinto, F. Guarino, A. Guarnera, A. Messina, S. Reina, F.M. Tomasello, V. Palermo, C. Mazzoni, Characterization of human VDAC isoforms: a peculiar function for VDAC3?, Biochim Biophys Acta. 1797 (2010) 1268–1275. https://doi.org/10.1016/j.bbabio.2010.01.031.
[133] L. Leggio, F. Guarino, A. Magrì, R. Accardi-Gheit, S. Reina, V. Specchia, F. Damiano, M.F. Tomasello, M. Tommasino, A. Messina, Mechanism of translation control of the alternative Drosophila melanogaster Voltage Dependent Anion-selective Channel 1 mRNAs, Sci Rep. 8 (2018) 5347. https://doi.org/10.1038/s41598-018-23730-7.
[134] A. Magrì, M.C. Di Rosa, M.F. Tomasello, F. Guarino, S. Reina, A. Messina, V. De Pinto, Overexpression of human SOD1 in VDAC1-less yeast restores mitochondrial functionality modulating beta-barrel outer membrane protein genes, Biochim Biophys Acta. 1857 (2016) 789–798. https://doi.org/10.1016/j.bbabio.2016.03.003.
[135] M.T. Forrester, J.S. Stamler, A classification scheme for redox-based modifications of proteins, Am J Respir Cell Mol Biol. 36 (2007) 135–137. https://doi.org/10.1165/rcmb.2006-001ED.
[136] C.I. Murray, J.E. Van Eyk, Chasing cysteine oxidative modifications: proteomic tools for characterizing cysteine redox status, Circ Cardiovasc Genet. 5 (2012) 591. https://doi.org/10.1161/CIRCGENETICS.111.961425.
[137] L.J. Alcock, M.V. Perkins, J.M. Chalker, Chemical methods for mapping cysteine oxidation, Chem Soc Rev. 47 (2018) 231–268. https://doi.org/10.1039/c7cs00607a.
[138] S. Reina, M.G.G. Pittalà, F. Guarino, A. Messina, V. De Pinto, S. Foti, R. Saletti, Cysteine Oxidations in Mitochondrial Membrane Proteins: The Case of VDAC Isoforms in Mammals, Front Cell Dev Biol. 8 (2020) 397. https://doi.org/10.3389/fcell.2020.00397.
[139] M.G.G. Pittalà, R. Saletti, S. Reina, V. Cunsolo, V. De Pinto, S. Foti, A High Resolution Mass Spectrometry Study Reveals the Potential of Disulfide Formation in Human Mitochondrial Voltage-Dependent Anion Selective Channel Isoforms (hVDACs),

Int J Mol Sci. 21 (2020) E1468. https://doi.org/10.3390/ijms21041468.
[140] R. Saletti, S. Reina, M.G.G. Pittalà, A. Magrì, V. Cunsolo, S. Foti, V. De Pinto, Post-translational modifications of VDAC1 and VDAC2 cysteines from rat liver mitochondria, Biochim Biophys Acta Bioenerg. 1859 (2018) 806–816. https://doi.org/10.1016/j.bbabio.2018.06.007.
[141] R. Saletti, S. Reina, M.G.G. Pittalà, R. Belfiore, V. Cunsolo, A. Messina, V. De Pinto, S. Foti, High resolution mass spectrometry characterization of the oxidation pattern of methionine and cysteine residues in rat liver mitochondria voltage-dependent anion selective channel 3 (VDAC3), Biochim Biophys Acta Biomembr. 1859 (2017) 301–311. https://doi.org/10.1016/j.bbamem.2016.12.003.
[142] M.G.G. Pittalà, S. Conti Nibali, S. Reina, V. Cunsolo, A. Di Francesco, V. De Pinto, A. Messina, S. Foti, R. Saletti, VDACs Post-Translational Modifications Discovery by Mass Spectrometry: Impact on Their Hub Function, Int J Mol Sci. 22 (2021) 12833. https://doi.org/10.3390/ijms222312833.
[143] S.A. Killackey, D.J. Philpott, S.E. Girardin, Mitophagy pathways in health and disease, J Cell Biol. 219 (2020) e202004029. https://doi.org/10.1083/jcb.202004029.
[144] V. Soubannier, P. Rippstein, B.A. Kaufman, E.A. Shoubridge, H.M. McBride, Reconstitution of mitochondria derived vesicle formation demonstrates selective enrichment of oxidized cargo, PLoS One. 7 (2012) e52830. https://doi.org/10.1371/journal.pone.0052830.
[145] S. Reina, F. Guarino, A. Magrì, V. De Pinto, VDAC3 As a Potential Marker of Mitochondrial Status Is Involved in Cancer and Pathology, Frontiers in Oncology. 6 (2016) 264. https://doi.org/10.3389/fonc.2016.00264.
[146] T. Tasaki, Y.T. Kwon, The mammalian N-end rule pathway: new insights into its components and physiological roles, Trends in Biochemical Sciences. 32 (2007) 520–528. https://doi.org/10.1016/j.tibs.2007.08.010.
[147] M. Eldeeb, R. Fahlman, The-N-End Rule: The Beginning Determines the End, Protein Pept Lett. 23 (2016) 343–348. https://doi.org/10.2174/0929866523666160108115809.
[148] L. Zou, V. Linck, Y.-J. Zhai, L. Galarza-Paez, L. Li, Q. Yue, O. Al-Khalili, H.-F. Bao, H.-P. Ma, T.L. Thai, J. Jiao, D.C. Eaton, Knockout of mitochondrial voltage-dependent anion channel type 3 increases reactive oxygen species (ROS) levels and alters renal sodium transport, J Biol Chem. 293 (2018) 1666–1675. https://doi.org/10.1074/jbc.M117.798645.
[149] P. Jóźwiak, P. Ciesielski, E. Forma, K. Kozal, K. Wójcik-Krowiranda, Ł. Cwonda, A. Bieńkiewicz, M. Bryś, A. Krześlak, Expression of voltage-dependent anion channels in endometrial cancer and its potential prognostic significance, Tumour Biol. 42 (2020) 1010428320951057. https://doi.org/10.1177/1010428320951057.
[150] L. Bleier, I. Wittig, H. Heide, M. Steger, U. Brandt, S. Dröse, Generator-specific targets of mitochondrial reactive oxygen species, Free Radic Biol Med. 78 (2015) 1–10. https://doi.org/10.1016/j.freeradbiomed.2014.10.511.
[151] C. Lee, J.S. Nam, C.G. Lee, M. Park, C.-M. Yoo, H.-W. Rhee, J.K. Seo, T.-H. Kwon, Analysing the mechanism of mitochondrial oxidation-induced cell death using a multifunctional iridium(III) photosensitiser, Nat Commun. 12 (2021) 26. https://doi.org/10.1038/s41467-020-20210-3.
[152] A. Messina, S. Reina, F. Guarino, A. Magrì, F. Tomasello, R.E. Clark, R.R. Ramsay, V. De Pinto, Live cell interactome of the human voltage dependent anion channel 3 (VDAC3) revealed in HeLa cells by affinity purification tag technique, Mol Biosyst. 10 (2014) 2134–2145. https://doi.org/10.1039/c4mb00237g.
[153] T.K. Rostovtseva, P.A. Gurnev, O. Protchenko, D.P. Hoogerheide, T.L. Yap, C.C. Philpott, J.C. Lee, S.M. Bezrukov, α-Synuclein Shows High Affinity Interaction with Voltage-dependent Anion Channel, Suggesting Mechanisms of Mitochondrial Regulation

and Toxicity in Parkinson Disease, J Biol Chem. 290 (2015) 18467–18477. https://doi.org/10.1074/jbc.M115.641746.
[154] D. Narendra, A. Tanaka, D.-F. Suen, R.J. Youle, Parkin is recruited selectively to impaired mitochondria and promotes their autophagy, J Cell Biol. 183 (2008) 795–803. https://doi.org/10.1083/jcb.200809125.
[155] S. Geisler, K.M. Holmström, D. Skujat, F.C. Fiesel, O.C. Rothfuss, P.J. Kahle, W. Springer, PINK1/Parkin-mediated mitophagy is dependent on VDAC1 and p62/SQSTM1, Nat Cell Biol. 12 (2010) 119–131. https://doi.org/10.1038/ncb2012.
[156] Y. Sun, A.A. Vashisht, J. Tchieu, J.A. Wohlschlegel, L. Dreier, Voltage-dependent Anion Channels (VDACs) Recruit Parkin to Defective Mitochondria to Promote Mitochondrial Autophagy, J Biol Chem. 287 (2012) 40652–40660. https://doi.org/10.1074/jbc.M112.419721.
[157] A. Raturi, T. Simmen, Where the endoplasmic reticulum and the mitochondrion tie the knot: the mitochondria-associated membrane (MAM), Biochim Biophys Acta. 1833 (2013) 213–224. https://doi.org/10.1016/j.bbamcr.2012.04.013.
[158] S. Reina, V. De Pinto, Anti-Cancer Compounds Targeted to VDAC: Potential and Perspectives, Curr Med Chem. 24 (2017) 4447–4469. https://doi.org/10.2174/0929867324666170530074039.
[159] E.N. Maldonado, J. Patnaik, M.R. Mullins, J.J. Lemasters, Free tubulin modulates mitochondrial membrane potential in cancer cells, Cancer Res. 70 (2010) 10192–10201. https://doi.org/10.1158/0008-5472.CAN-10-2429.
[160] A. Magrì, P. Risiglione, A. Caccamo, B. Formicola, M.F. Tomasello, C. Arrigoni, S. Zimbone, F. Guarino, F. Re, A. Messina, Small Hexokinase 1 Peptide against Toxic SOD1 G93A Mitochondrial Accumulation in ALS Rescues the ATP-Related Respiration, Biomedicines. 9 (2021) 948. https://doi.org/10.3390/biomedicines9080948.
[161] Q. Zhang, G. Song, L. Yao, Y. Liu, M. Liu, S. Li, H. Tang, miR-3928v is induced by HBx via NF-κB/EGR1 and contributes to hepatocellular carcinoma malignancy by down-regulating VDAC3, Journal of Experimental & Clinical Cancer Research. 37 (2018) 14. https://doi.org/10.1186/s13046-018-0681-y.
[162] L. Corey, S. Brodie, M.-L. Huang, D.M. Koelle, A. Wald, HHV-8 infection: a model for reactivation and transmission, Rev Med Virol. 12 (2002) 47–63. https://doi.org/10.1002/rmv.341.
[163] H.-W. Wang, T.V. Sharp, A. Koumi, G. Koentges, C. Boshoff, Characterization of an anti-apoptotic glycoprotein encoded by Kaposi's sarcoma-associated herpesvirus which resembles a spliced variant of human survivin, EMBO J. 21 (2002) 2602–2615. https://doi.org/10.1093/emboj/21.11.2602.
[164] M.A. Mubaraki, T.A. Hafiz, S. Al-Quraishy, M.A. Dkhil, Oxidative stress and genes regulation of cerebral malaria upon Zizyphus spina-christi treatment in a murine model, Microb Pathog. 107 (2017) 69–74. https://doi.org/10.1016/j.micpath.2017.03.017.
[165] S. Chakravarty, B.R. Reddy, S.R. Sudhakar, S. Saxena, T. Das, V. Meghah, C.V. Brahmendra Swamy, A. Kumar, M.M. Idris, Chronic unpredictable stress (CUS)-induced anxiety and related mood disorders in a zebrafish model: altered brain proteome profile implicates mitochondrial dysfunction, PLoS One. 8 (2013) e63302. https://doi.org/10.1371/journal.pone.0063302.
[166] M.J. Sampson, R.S. Lovell, W.J. Craigen, The murine voltage-dependent anion channel gene family. Conserved structure and function, J Biol Chem. 272 (1997) 18966–18973. https://doi.org/10.1074/jbc.272.30.18966.
[167] F. Zinghirino, X.G. Pappalardo, A. Messina, G. Nicosia, V. De Pinto, F. Guarino, VDAC Genes Expression and Regulation in Mammals, Front Physiol. 12 (2021) 708695. https://doi.org/10.3389/fphys.2021.708695.
[168] A. Magrì, R. Belfiore, S. Reina, M.F. Tomasello, M.C. Di Rosa, F. Guarino, L. Leggio, V. De Pinto, A. Messina, Hexokinase I N-terminal based peptide prevents the

VDAC1-SOD1 G93A interaction and re-establishes ALS cell viability, Sci Rep. 6 (2016) 34802. https://doi.org/10.1038/srep34802.
[169] S.R. Maurya, R. Mahalakshmi, VDAC-2: Mitochondrial outer membrane regulator masquerading as a channel?, FEBS J. 283 (2016) 1831–1836. https://doi.org/10.1111/febs.13637.
[170] N. Li, K. Ragheb, G. Lawler, J. Sturgis, B. Rajwa, J.A. Melendez, J.P. Robinson, Mitochondrial complex I inhibitor rotenone induces apoptosis through enhancing mitochondrial reactive oxygen species production, J Biol Chem. 278 (2003) 8516–8525. https://doi.org/10.1074/jbc.M210432200.
[171] A.A. Starkov, G. Fiskum, Regulation of brain mitochondrial H2O2 production by membrane potential and NAD(P)H redox state, J Neurochem. 86 (2003) 1101–1107. https://doi.org/10.1046/j.1471-4159.2003.01908.x.
[172] J.G. Gill, E. Piskounova, S.J. Morrison, Cancer, Oxidative Stress, and Metastasis, Cold Spring Harb Symp Quant Biol. 81 (2016) 163–175. https://doi.org/10.1101/sqb.2016.81.030791.

The results present in this thesis work are derived from the papers:

Article 1: Cell-free electrophysiology of human VDACs incorporated into nanodiscs: An improved method.

Article 2: Voltage Dependent Anion Channel 3 (VDAC3) protects mitochondria from oxidative stress.

Other activities:

Article 3: Recombinant yeast VDAC2: a comparison of electrophysiological features with the native form. FEBS Open Bio. 2019

Article 4: Voltage-Dependent Anion Selective Channel Isoforms in Yeast: Expression, Structure, and Functions. Front Physiol. 2021.

Article 5: VDACs Post-Translational Modifications Discovery By Mass Spectrometry: Impact On Their Hub Function. Int. J. Mol. Sci. 2021.

Article 1.

Biophysical Reports

Cell-free electrophysiology of human VDACs incorporated into nanodiscs: An improved method.

Stefano Conti Nibali,[1] Maria Carmela Di Rosa,[1] Oliver Rauh,[2] Gerhard Thiel,[2] Simona Reina,[3,4] and Vito De Pinto[1,4]

[1]Department of Biomedical and Biotechnological Sciences, University of Catania, Catania, Italy; [2]Membrane Biophysics and Center for Synthetic Biology, Technische Universitat Darmstadt, Darmstadt, Germany; [3]Department of Biological, Geological and Environmental Sciences, Section of Molecular Biology, University of Catania, Catania, Italy; [4]we.MitoBiotech.srl, Catania, Italy

Biophysical Reports

ARTICLE

Cell-free electrophysiology of human VDACs incorporated into nanodiscs: An improved method

Stefano Conti Nibali,[1] Maria Carmela Di Rosa,[1] Oliver Rauh,[2] Gerhard Thiel,[2] Simona Reina,[3,4,*] and Vito De Pinto[1,4]

[1]Department of Biomedical and Biotechnological Sciences, University of Catania, Catania, Italy; [2]Membrane Biophysics and Center for Synthetic Biology, Technische Universität Darmstadt, Darmstadt, Germany; [3]Department of Biological, Geological and Environmental Sciences, Section of Molecular Biology, University of Catania, Catania, Italy; and [4]we.MitoBiotech.srl, Catania, Italy

ABSTRACT Voltage-dependent anion-selective channel (VDAC) is one of the main proteins of the outer mitochondrial membrane of all eukaryotes, where it forms aqueous, voltage-sensitive, and ion-selective channels. Its electrophysiological properties have been thoroughly analyzed with the planar lipid bilayer technique. To date, however, available results are based on isolations of VDACs from tissue or from recombinant VDACs produced in bacterial systems. It is well known that the cytosolic overexpression of highly hydrophobic membrane proteins often results in the formation of inclusion bodies containing insoluble aggregates. Purification of properly folded proteins and restoration of their full biological activity requires several procedures that considerably lengthen experimental times. To overcome these restraints, we propose a one-step reaction that combines in vitro cell-free protein expression with nanodisc technology to obtain human VDAC isoforms directly integrated in a native-like lipid bilayer. Reconstitution assays into artificial membranes confirm the reliability of this new methodological approach and provide results comparable to those of VDACs prepared with traditional protein isolation and reconstitution protocols. The use of membrane-mimicking nanodisc systems represents a breakthrough in VDAC electrophysiology and may be adopted to further structural studies.

WHY IT MATTERS This work demonstrates the extraordinary advantages in terms of reproducibility and experimental effectiveness in combining in vitro VDAC translation with nanodisc technology. Accordingly, single-channel recordings as well as voltage dependence and selectivity measurements of the three human VDAC isoforms in planar lipid bilayer completely reproduced and even improved results obtained with conventional expression and reconstitution systems. In particular, electrophysiological features of human VDAC3 were in-depth investigated by means of a cysteine-less mutant that validated the extreme importance of cysteine residue in pore functionality, as already reported in literature.

INTRODUCTION

VDACs (voltage-dependent anion-selective channels) are aqueous pore-forming proteins that mediate communication across the outer mitochondrial membrane of all eukaryotes (1). Interactions with cytosolic enzymes (2,3) and both antiapoptotic and proapoptotic factors make VDAC a key protein in regulating mitochondrial metabolism and apoptosis (4–7). In mammals, evolution led to three isoforms: VDAC1, VDAC2, and VDAC3, encoded by three genes located on different chromosomes (8). Although sharing ~70% sequence homology, VDAC isoforms fulfill distinctly different physiological roles. VDAC1 is the main isoform responsible for membrane permeability and additionally interacts with Bcl-2 proapoptotic proteins and with hexokinase (9,10); VDAC2 was initially considered an antiapoptotic protein (11) before later contrasting evidence showed that it interacts with Bax, a proapoptotic protein (12). However, there is no doubt that they play a relevant role in the control of cell death. VDAC3 has been proposed to be involved in reactive oxygen species (ROS) homeostasis and mitochondria quality control (13,14). According to the three-dimensional structure, VDAC1 exhibits a transmembrane β-barrel architecture composed of 19 amphipathic β-strands together with a N-terminal α-helix moiety folded inside the pore (15–17). The α-helix is part of the voltage sensor and is essential for channel gating (18). Electrophysiological properties of VDACs have been extensively examined exploiting the planar lipid bilayer (PLB) technique (19–21). VDACs spontaneously insert

Submitted April 7, 2021, and accepted for publication June 25, 2021.

*Correspondence: simona.reina@unict.it

Editor: Erdinc Sezgin.

https://doi.org/10.1016/j.bpr.2021.100002

into PLBs, where they form pores with an average conductance of ~4 nS in 1 M KCl. Low membrane potentials (0 ± 20 mV) maintain channels in a full conducting "open state" that features a considerable preference for anions over cations. Potentials exceeding ±30 mV mediate transition to multiple cation-selective "closed states" with a drastic drop in pore conductance (22–24). VDAC1 and VDAC2 routinely show this prototypic behavior, whereas VDAC3 reconstitution into PLB has been challenging (25). Checchetto and co-workers first, to our knowledge, described human isoform 3 as a low-conducting pore (conductance ~100 pA) with no voltage-dependence (26). Further studies uncovered the critical role of cysteine residues in VDAC3 modulating channel activity (14,27,28). Data available so far were derived from the successful membrane incorporation of VDACs isolated from tissue mitochondria (29) or from reconstitution of recombinant proteins (14,26,30). For the latter approach, *Escherichia coli* is the host of choice because of its fast growth and cost-effectiveness, albeit heterologous protein folding failure is not uncommon especially for highly hydrophobic membrane proteins that can aggregate into inclusion bodies (31). Cell-free (CF) protein synthesis (CFPS) systems represent a valid and powerful alternative to avoid protein refolding procedures (32,33). They were initially employed for the exclusive production of soluble proteins (34–36): CFPS systems have subsequently emerged as a suitable tool also for the high-throughput expression of membrane proteins thanks to the development of lipid membrane mimics (e.g., detergent micelles, lipid/detergent mixtures, liposomes, and nanodiscs (NDs)) (37,38). NDs are the most recent class of model membrane systems, structurally composed of a discoidal phospholipid bilayer which is stabilized in solution by two pairs of amphipathic helical membrane scaffold proteins (MSPs) (39). In the last decades, useful application of NDs for CF expression of membrane proteins has been reported. NDs offer a native-like environment for maintaining the structure and functionality of membrane proteins in solution (40), providing a worthy condition for functional analysis in PLBs (41–44). ND-embedded VDAC1 and VDAC2 were already investigated in (45) and (46) for structural studies by solution NMR and functional assays with PLBs, respectively. In both cases it appeared that the structural and functional properties of the VDACs in NDs were not different from micelle-embedded VDACs. To date, however, reports about the use of the CFPS-NDs binomial technique in VDAC electrophysiology are missing. In this work, we combine for the first time the in vitro protein synthesis system with the ND technology to express and reconstitute the three human VDAC isoforms ($VDAC_{CF/ND}$) into artificial lipid membranes. In addition, we compared the impact of reducing agents in the buffer and the removal of cysteines on the biophysical properties of hVDAC3 from the combined in vitro translation/ND method ($hVDAC3_{CF/ND}$) with those obtained by canonical recombinant production and protein isolation protocols (14,28). Our results clearly indicate that this innovative method keeps the electrophysiological properties of VDAC unchanged, although it reduces experimental times and increases production yield. Despite a vast literature with detailed biophysical analysis of functional properties of VDAC channels, the technical approach proposed here represents a novel, to our knowledge, and promising method for an easier, quicker, and more reliable investigation of VDAC function in PLBs.

MATERIALS AND METHODS

CF cloning of hVDAC1, hVDAC2, hVDAC3, and hVDAC3 C0A

The coding sequence of human VDAC1, VDAC2, VDAC3, and VDAC3 C0A obtained from pET21a vector (Novagen) were amplified by PCR and cloned into the pET24Δlac vector (Merck, Darmstadt, Germany) with the NEBuilder HiFi DNA Assembly Master Mix (New England BioLabs). The following pairs of primers were used for cloning (Table 1).

Protein expression and purification

Heterologous expression of recombinant human VDAC1 cloned in pET21a vector was performed as already reported in (14,26,47). The C-terminal His-tagged VDAC1 was purified by a single-step affinity chromatography using a Ni-NTA agarose (Qiagen, Hilden, DE) packed column according to the manufacturer's instructions and then refolded as described in (14,26,47). CF expression of human VDAC1, VDAC2, VDAC3, and VDAC3C0A was achieved using the MembraneMax HN Protein Expression Kit (Invitrogen, Carlsbad, CA) in the presence of NDs with a DMPC (1,2-dimyristoyl-sn-glycero-3-phosphocholine) bilayer. The scaffold proteins of the NDs contained

TABLE 1 List of primers used for cloning

Primer	Sequence
Fw hVDAC1	5′-GTTTAACTTTAAGAAGGAGATATACATA TGGCTGTGCCACCCACGT-3′
Rev hVDAC1	5′-CAGCATGGACCACAGCAGTCGACCTATGCT TGAAATTCCAGTCCTA-3′
Fw hVDAC2	5′-GTTTAACTTTAAGAAGGAGATATACATA TGGCGACCCACGGACAGACT-3′
Rev hVDAC2	5′-CAGCATGGACCACAGCAGTCGACCTAAG CCTCCAACTCCAGGGCGA-3′
Fw hVDAC3	5′-GTTTAACTTTAAGAAGGAGATATACATA TGTGTAACACACCAACGT-3′
Rev hVDAC3	5′-CAGCATGGACCACAGCAGTCGACCTAAG CTTCCAGTTCAAATCCCA-3′
Fw hVDAC3 C0A	5′-GTTTAACTTTAAGAAGGAGATATACATAT GGCTAACACACCAACGT-3′
Rev hVDAC3 C0A	5′-CAGCATGGACCACAGCAGTCGACCTAAGC TTCCAGTTCAAATCCCA-3′

a His-tag for purification. Briefly, 35 μM of MSP2N2-his or MSP1D1-his NDs (Cube Biotech, Monheim, DE) were added to the CFPS mixture and incubated at 37°C for 3.5 h in an orbital shaker at 1000 rpm. VDAC-ND complexes were then purified using Ni-NTA affinity chromatography and every purification step was carried out in the absence of any reductant. After the addition of 400 μL of equilibration buffer (10 mM imidazole, 300 mM KCl, 20 mM NaH_2PO_4, pH 7.4) the whole reaction mix was loaded onto a pre-equilibrated 0.2 HisPur Ni-NTA agarose spin column (Thermo Fisher Scientific, Rockford, IL) and incubated for 1 h at room temperature at 200 rpm. Afterwards, the buffer was removed by centrifugation at 700 $\times$ g for 2 min and the column was washed three times with 400 μL of washing buffer (20 mM imidazole, 300 mM KCl, 20 mM NaH_2PO_4, pH 7.4) to remove unspecific binders. The His-tagged NDs containing VDAC were eluted with 600 μL of elution buffer (250 mM imidazole, 300 mM KCl, 20 mM NaH_2PO_4, pH 7.4) and collected in three 200 μL fractions. Purified hVDACs assembled into NDs were diluted in NuPage LDS buffer with reducing agent, heated at 95°C for 5 min and separated onto a 4–12% NuPage Bis-Tris gel (Thermo Fisher Scientific, Carlsbad, CA) in MES running buffer at 200 V. Samples were stored at 4°C for up to 12 days.

PLB

Electrophysiological analysis of recombinant hVDAC1 was performed as previously described (14,26,47,48). Briefly, an artificial PLB made of 1% DiPhPC (Avanti Polar Lipids, Alabaster, AL) in n-decane was formed on an aperture of 200 μm in a Derlin cuvette (Warner Instruments, Hamden, CT). Membrane capacitances of 110–150 pF were accepted for proper lipid bilayers. Channel insertion was obtained by addition of ~40 ng of refolded protein solution to the *cis* side of the cuvette containing 3 mL of KCl solution. Data were acquired using a Bilayer Clamp amplifier (Warner Instruments) at 100 μs/point, filtered at 300 Hz and analyzed using the pClamp software (Ver-10; Molecular Devices, San Jose, CA). Electrophysiological analysis of human $VDAC_{CF/ND}$s was performed using the Innovation setup. An artificial PLB was formed on a hole with a diameter of 100 μm in a 25-μm thick Teflon foil separating two Teflon chambers with a volume of 2.5 mL each. First, the rim of the hole was treated with 1 μL of 1% hexadecane in n-hexane and both chambers were filled to the lower edge of the hole with an electrolyte solution. Subsequently, 35 μL of 15 mg/mL phospholipids dissolved in n-pentane were added to each side of the chamber and bilayers were built using a folding technique that consists in elevating the buffer level of each chamber as reported in (49). Both chambers were connected to the amplifier via Ag/AgCl electrodes. All measurements were performed at RT in 1,2-diphytanoyl-sn-glycero-3-phosphocholine (DPhPC; Avanti Polar Lipids) membranes with symmetrical KCl solution (1 M KCl, 10 mM Hepes, pH 7.0). Membrane capacitances of 100–140 pF were accepted for proper lipid bilayers. Reconstitution of VDAC proteins was observed after the addition of ~5 μL of the purified channel-ND complex directly below the bilayer in the *trans* compartment with a bent 25 μL Hamilton syringe. The currents were acquired with a sampling frequency of 10 kHz after low-pass-filter at 3 kHz and digitized using an EPC 7 Patch Clamp Amplifier and Patchmaster software (HEKA). Channel conductance (G) was calculated from current (I) measurements in the presence of the applied constant voltage (V) of +10 mV, according to the following equation: conductance (G) = current (I)/voltage (V).

Voltage dependence analysis

VDAC voltage dependence was measured in symmetrical KCl solution (1 M KCl, 10 mM Hepes, pH 7.0) by applying 10 mHz triangular voltage waves of $\pm$50 mV, time 100 s. At least three independent experiments were performed for each protein. Plots of the average VDAC conductance as a function of voltage were obtained by the application of a voltage range of $\pm$50 mV with discrete steps of $\pm$5 mV for 15 s. The relative conductance was calculated as G/G_0, where G denotes average conductance at a given Vm and G_0 denotes average conductance values calculated in the presence of the lowest applied potential. Three independent experiments were performed for each protein. Data are shown as the mean $\pm$ SEM and graphited using prism 8.0 software (GraphPad Software).

Ion selectivity measurement

Ion selectivity measurements were performed in 0.1 M/1 M *cis*/*trans* gradient of KCl and permeability ratios of cation K^+ (P_{K+}) over anion Cl^- (P_{Cl^-}) was calculated from the reversal potential (V_{rev}) using the Goldman-Hodgkin-Katz equation. Channel insertion was initially achieved in symmetrical 1 M KCl. After the insertion of at least one channel, solution in *cis* was changed perfusing ~10 chamber volumes and 10 mHz triangular voltage wave ($\pm$50 mV; time, 100 s) was applied. The channel conductance in 0.1 M/1 M *cis*/*trans* gradient of KCl was calculated from the current measurements when a voltage Vm is applied, using equation: $I = G\ (Vm - V_{rev})$.

RESULTS

Human $VDAC_{CF/ND}$ isoforms insert into membrane with typical channel conductance

NDs are widely used to mimic a native-like bilayer environment for membrane proteins, thus rendering them soluble in aqueous solutions for structural and functional analysis (50). NDs conceptually arise from high density lipoprotein particles, in particular the apolipoprotein 1 (Apo-1). They consist of a discoidal lipid bilayer which is stabilized and made highly soluble by two pairs of amphipathic membrane scaffold proteins (MSPs), which mimic the function of Apo-1 (51). The length of the MSPs and the stoichiometry of lipid/MSP ratio used in the self-assembly process control the size of the ND structure (39). In recent years, NDs with different lipid composition and size have been developed. In this work, human VDAC proteins were expressed using the CF expression system in the presence of two different commercially available NDs: MSP1D1 and MSP2N2. They share the same dimyristoylphosphatidylcholine (DMPC) bilayer but differ in diameter from ~9.7 to ~17 nm, respectively, as measured by solution x-ray scattering (52,53). After the CF expression in the presence of NDs, $hVDAC_{CF/ND}$s were eluted from Ni-NTA columns. The samples were analyzed by NuPAGE (Fig. 1). As shown in Fig. 1, the treatment with the anionic detergent LDS provided two most relevant bands at ~30 kDa (monomeric hVDACs) and ~45 kDa (the scaffold protein of MSP2N2 NDs). hVDAC1, hVDAC2, hVDAC3, and hVDAC3 C0A were thus successfully incorporated into MSP2N2 NDs. The experiment was intended to

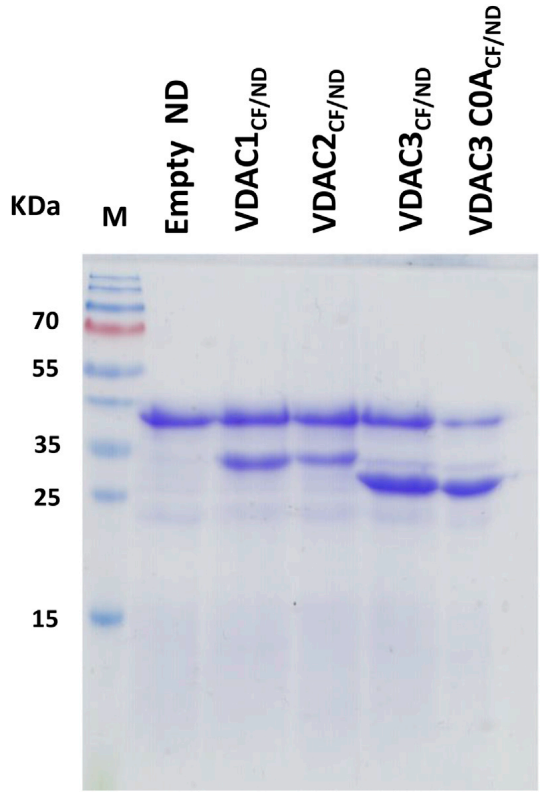

FIGURE 1 Incorporation of human VDACs into MSP2N2 NDs. 4–12% NuPAGE gel of $hVDAC_{CF/ND}$ isoforms eluted from Ni-NTA columns. The first lane is loaded with 0.5 μL of empty NDs as a control. Lanes 2–5 were loaded with MSP2N2-hVDAC1, -hVDAC2, -hVDAC3, and -hVDAC3 C0A, respectively. In each lane, the protein bands corresponding to the scaffold protein of MSP2N2 NDs (~45 kDa) and those of monomeric human VDACs (~30 kDa) are visible. As expected, VDAC3 wild-type and C0A proteins migrate faster than isoform 1 and 2.

verify the ability of VDAC proteins to incorporate as functional pore into the PLB. The successful electrophysiological recording of typical VDAC channel activity reported below underpins proper assembly and folding of hVDACs produced by the CF protocol in NDs (called from here on $hVDAC_{CF/ND}$). Fig. 1 shows the presence of all three VDAC isoform in the ND preparations, together with the scaffold protein. Hence, the concentration of functional channels in the NDs resulting from this protocol is ideal for reconstituting single VDAC channels into a PLB and for recording its electrophysiological properties. Although the functional reconstitution of human VDACs in MSP2N2 NDs was successful, the same procedure did not generate any channel activity when VDACs were translated in the presence of the smaller MSP1D1 NDs. The absence of channel activity in these experiments can be traced back to the failure of incorporation of VDAC proteins into the smaller MSP1D1 NDs. This is demonstrated by electrophoresis, where in this case exclusively the protein band corresponding to the scaffold protein was detected indicating that these empty NDs did not contain VDACs (data not shown). It is reasonable to speculate that MSP1D1 may form NDs with a diameter too small for hosting a folded VDAC pore.

Next, we examined the efficiency of the purification protocol and the membrane insertion procedure described above and we tested whether these preparations have the same functional properties of hVDACs prepared by the traditional protocol as in (14,26,47). The VDAC isoforms in NDs were therefore added to the *trans* side of a PLB at a concentration of 100 ng/μL and their channel forming activity analyzed by electrophysiological methods. Channel insertion was studied by applying an electric potential of +10 mV to the membrane. At this voltage, $hVDAC1_{CF/ND}$ and $hVDAC2_{CF/ND}$ inserted as fully open state pores with discrete current steps of 3.47 $\pm$ 0.43 nS ($n = 35$) and 3.28 $\pm$ 0.36 nS ($n = 30$), respectively (Fig. 2, *A, B, and F*). Fig. 2, *C and F* show that, in the same experimental conditions, $hVDAC3_{CF/ND}$ channels adopted a lower conductance state of 0.64 $\pm$ 0.28 nS ($n = 29$), as already noticed in (26). It is worth noting that this state is more frequently observed upon VDAC isoform 3 reconstitution in PLB (14,26,27) and totally differs, as demonstrated below, from the canonical high-conducting state recorded most of the time for VDAC1 and VDAC2 (23,54). Preincubation with 5 mM DTT before bilayer reconstitution significantly increased the mean current through $hVDAC3_{CF/ND}$ (i.e., 3.01 $\pm$ 0.47nS ($n = 30$)), albeit the incorporation rate, as empirically observed, was still far below that of isoform 1 and 2 (Fig. 2, *D and F*). Removal of all cysteine residues and their substitution by mutagenesis with alanine (C0A) also causes $hVDAC3_{CF/ND}$ to form channels with the typical VDAC conductance (3.57 nS $\pm$ 0.64 ($n = 33$)), and improves the rate of insertion (Fig. 2, *E and F*). These results confirm what was previously reported about the influence of the oxidative state of cysteine residues in VDAC3 on channel conductance (14,26,27).

NDs preserve the voltage dependence of human VDAC isoforms

VDAC pores show a typical feature, from which their name derives, in that they are voltage dependent. For VDACs this means that, after reconstitution in artificial membranes, the channel conductance does not proportionally raise but begins to decay in response to voltages above 20–30 mV. This phenomenon corresponds to a partial closure of the pore: indeed, such partial "closure" does not allow the passage of large molecules such as ATP and the ion selectivity is modified (24). It is hypothesized that VDAC closure might have relevant functional consequences on the

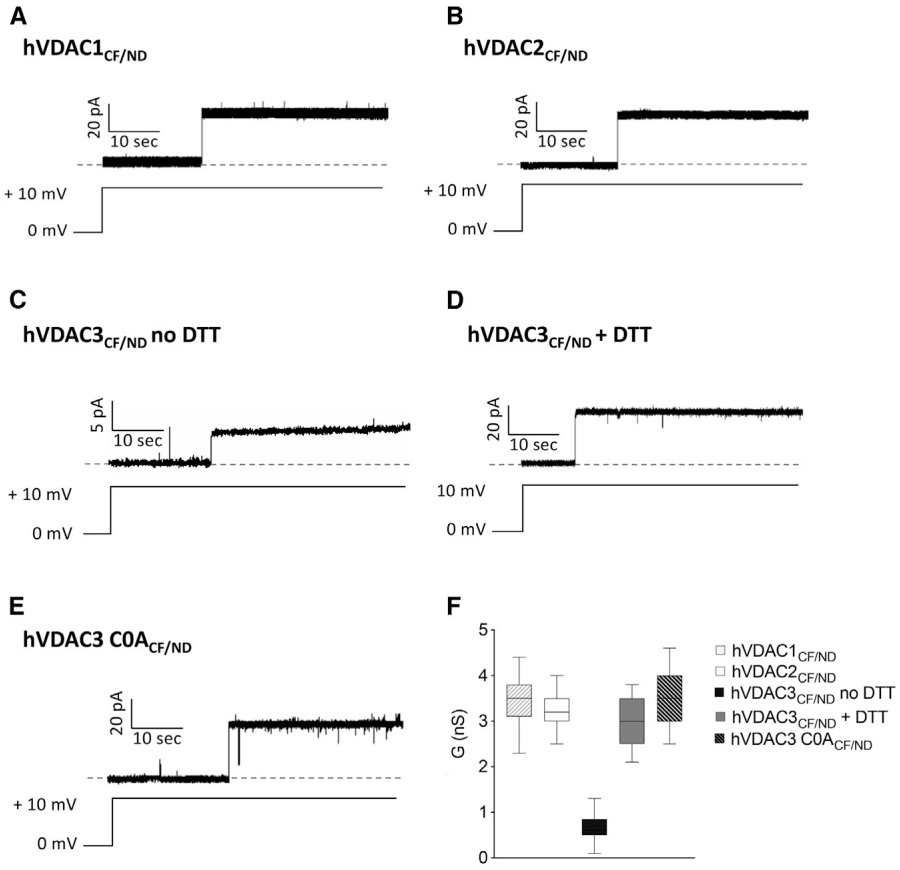

FIGURE 2 Single-channel recordings of $VDAC_{CF/ND}$. (*A–E*) Representative current traces of $hVDAC1_{CF/ND}$ (*A*), $hVDAC2_{CF/ND}$ (*B*), $hVDAC3_{CF/ND}$ no DTT (*C*), $hVDAC3_{CF/ND}$ preincubated with 5 mM DTT (*D*), and hVDAC3 $C0A_{CF/ND}$ (*E*) recorded at +10 mV in 1 M KCl/10 mM HEPES, pH 7.0. (*F*) Distribution of channel conductance events as a function of (G).

mitochondria activity (1,7,55,56). We aimed to check whether such electrophysiological feature was kept by $hVDAC_{CF/ND}$.

After successful incorporation of VDAC channels from NDs into a host bilayer, we monitored their voltage dependence by applying a triangular voltage ramp from 0 to ±50 mV in 100 s (Fig. 3). At low membrane potentials, $hVDAC1_{CF/ND}$ and $hVDAC2_{CF/ND}$ current traces increased linearly with voltage. Higher voltages of either polarity induced step-like transitions to a single and stable closed substate in $hVDAC1_{CF/ND}$. $hVDAC2_{CF/ND}$ was more responsive to positive voltages than to negative ones: during the short time of the voltage ramp, the channel rapidly shifted to a stable lower conductance substate already at +20 mV. At negative potentials, the channel exhibited first some fast fluctuations at voltages more negative than −30 mV before reaching a steady closed substate between −40 and −50 mV). As found with protein refolded in the traditional way (26), $hVDAC3_{CF/ND}$ did not display any voltage dependence in the absence of reductants. In Fig. 3 *G*, it can be appreciated how current constantly increases and decreases as a function of the driving force (voltage) without showing any gating events. The addition of DTT, as well as the removal of all cysteine residues, made $hVDAC3_{CF/ND}$ sensitive to the membrane potential. As shown in Fig. 3, *I and K*, the application of voltages higher than ±30 mV elicited closures of $hVDAC3_{CF/ND}$ in the presence of 5 mM DTT. The same was observed in the Cys-free hVDAC3 $C0A_{CF/ND}$.

These results, obtained by reconstituting recombinant hVDAC3 from membrane mimetic NDs, support the essential role of cysteines in channel gating, as was previously shown by conventional protocols. Within the applied voltage range +20/−30 mV and +20/−40 mV, $hVDAC1_{CF/ND}$, and $hVDAC2_{CF/ND}$, respectively, are fully open; the linear trajectory of the current follows the voltage ramp. As expected for symmetrical buffers, both in the *cis* and *trans* side the current reverses at 0 mV. At voltages positive and negative outside these windows, partial channel closures can be observed. The voltage-dependent reduction in channel open probability reduces the slope of the I/V curve which translates into a decreased conductance; the decrease in conductance becomes evident at voltages ±20 to 30 mV for $hVDAC1_{CF/ND}$ (Fig. 3 *D*). $hVDAC2_{CF/ND}$ switched to a stable lower conductance substate at positive potentials (+25 mV), whereas at negative potentials, ranging from −30 to −40 mV, the channel exhibited fast open-closed transitions before going into a permanent partially closed substate at

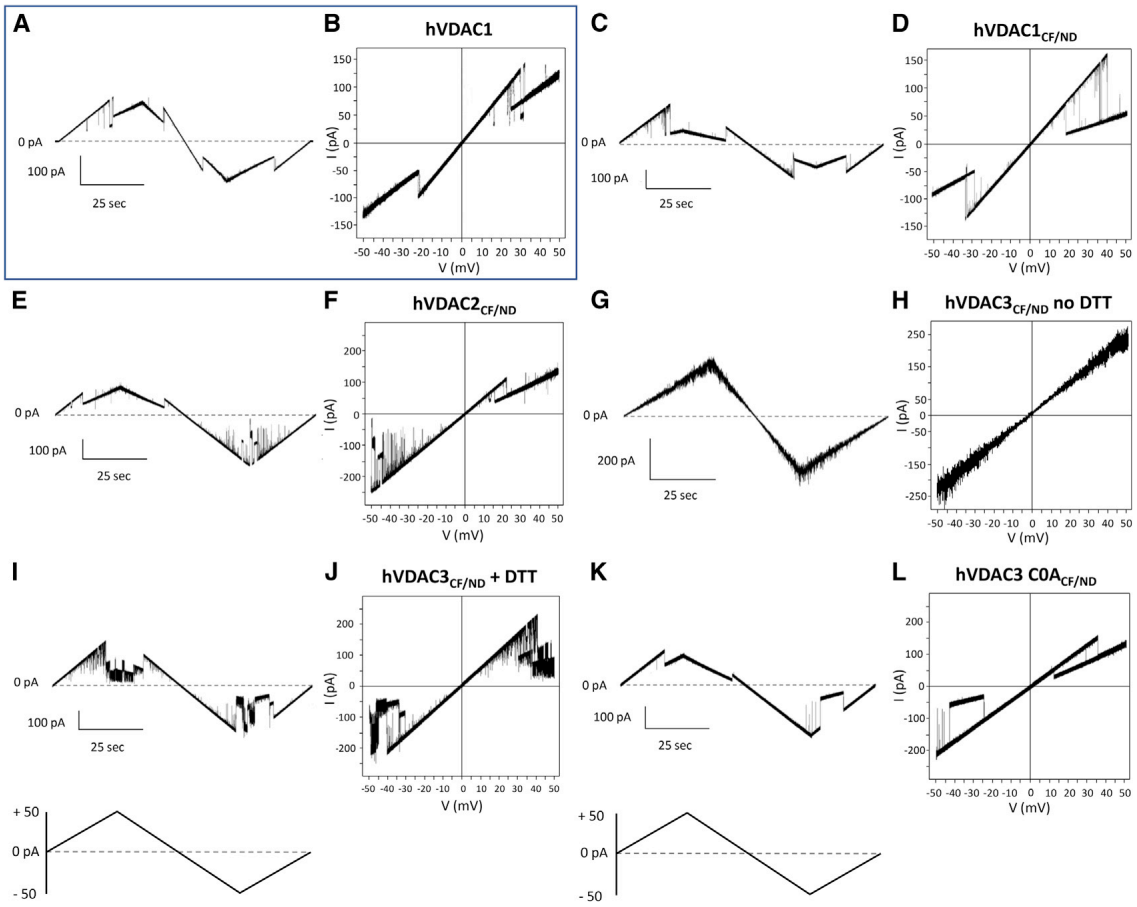

FIGURE 3 Voltage dependence of human VDAC isoforms analyzed by triangular voltage ramps in PLB in different reconstitution methods. In each experiment, current traces were obtained by applying to the reconstituted VDAC a triangular voltage protocol. The corresponding I–V plots were obtained by plotting the current as a function of clamp voltage. The experiments were performed in symmetrical 1 M KCl solution. (*A* and *B*) hVDAC1: channel refolded and reconstituted as in (14,26,47). (*C* and *D*) $hVDAC1_{CF/ND}$: channel incorporated in NDs as described in Materials and methods. (*E* and *F*) $hVDAC2_{CF/ND}$: conditions as in (*C* and *D*). (*G* and *H*) $hVDAC3_{CF/ND}$ no DTT: multichannel analysis in the absence of any reducing agent; other conditions as in (*C* and *D*). (*I* and *J*) $hVDAC3_{CF/ND}$ + DTT: channel analyzed in the presence of 5 mM DTT; other conditions as in (*C* and *D*). (*K* and *L*) hVDAC3 $C0A_{CF/ND}$: mutagenized hVDAC3 lacking any cysteine, mutated in alanine; other conditions as in (*C* and *D*).

voltages higher than −40 mV (Fig. 3 *F*). The I/V plot of $hVDAC3_{CF/ND}$ shows that the channels do not display dependence on the entire voltage range tested because no conductance decrease was recorded. (Fig. 3 *H*). Channel closures at positive and negative voltages are only observed after preincubating hVDAC3 with DTT or after removing its cysteines from the sequence. Under these conditions $hVDAC3_{CF/ND}$ exhibits distinct partial closures at extreme positive and negative voltages. Such closures are evident applying more than ±30 mV to incorporated $hVDAC3_{CF/ND}$ + 5 mM DTT and more than ±35 to 40 mV to hVDAC3 $C0A_{CF/ND}$, respectively (Fig. 3, *J and L*). All data were compared with an experiment in which the triangular voltage wave was applied to hVDAC1 reconstituted by canonical recombinant production and purification from *E. coli* as in (14,26,47) (Fig. 3, *A and B*). The experimental traces of human VDAC isoforms conductance in response to 15 s voltage steps of ±10 mV over a range of ±50 mV, are also shown (Fig. 4). When the normalized conductance G/G_0 is plotted as a function of V_m, $hVDAC1_{CF/ND}$, and $hVDAC2_{CF/ND}$ exhibit the characteristic bell-shaped curve. This result indicates a symmetrical voltage-dependent channel closure at both positive and negative potentials (Fig. 4, *A, B, and F*). In the same plot the G/G_0 ratio of $hVDAC3_{CF/ND}$ remains nearly constant over the entire voltage window (Fig. 4, *C and F*). When the latter channel was incubated under reducing conditions (+DTT) before reconstitution in the bilayer, also $hVDAC3_{CF/ND}$ exhibited a similar bell-shaped voltage dependence as the two other isoforms $hVDAC1_{CF/ND}$ and $hVDAC2_{CF/ND}$; even though the voltage dependence of $hVDAC3_{CF/ND}$ was less steep than for the other isoforms (Fig. 4, *D and F*). An almost perfect overlap of the voltage dependence between all three isoforms was obtained only when the

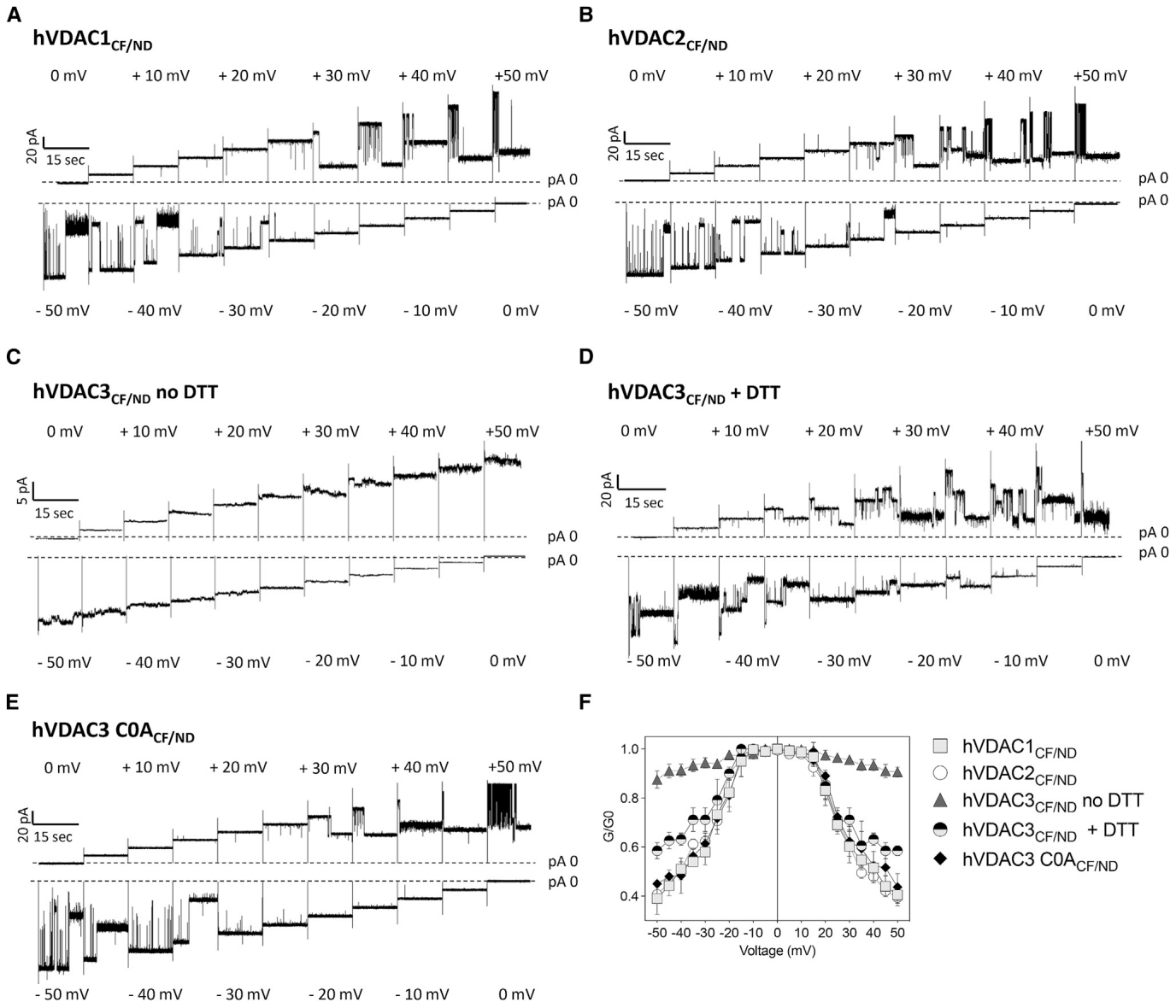

FIGURE 4 Current traces of reconstituted VDAC isoforms. (*A–E*) Current traces of reconstituted $hVDAC_{CF/ND}$ isoforms described as in Fig. 3 were obtained by clamping membrane 15 s voltage steps of ± 5 mV over voltage window of ± 50 mV. (*F*) Conductance G/G_0 of VDAC isoforms as a function of the applied voltage. The voltage dependence of most isoforms exhibits a bell shape; only $hVDAC3_{CF/ND}$ shows, in the absence of reducing agents, almost no voltage dependence.

cysteines were removed from the hVDAC3 sequence ($hVDAC3\ C0A_{CF/ND}$) (Fig. 4, *E and F*).

Ion selectivity of VDAC isoforms reconstituted in NDs

A typical feature of VDACs is that they have a slight preference for anions over cations in the so-called "open state" (20,21) but a cations over anions preference in the "closed state" (24,25). Here, the ion selectivity of the three human VDAC isoforms has been investigated using a 10-fold KCl gradient, as described in Materials and methods. When *cis* and *trans* sides of the membrane contain buffers with different concentrations, the I/V curve of a "selective" channel reverses at a voltage different from zero. The "reversal potential" (V_{rev}) at which the current changes its direction is diagnostic for the ion species that carries the current. The I/V plots of $hVDAC_{CF/ND}$ shown in Fig. 5, *A–E* clearly indicate negative V_{rev}-values, which underpin the anion selectivity of the "open state." The "closed state," in contrast, reveals positive V_{rev}-values corresponding to cation selectivity. The permeability ratio of Cl^- to K^+ (P_{Cl^-}/P_{K+}) in the "open" and "closed" conformations of human VDAC isoforms was determined from the reversal potential using the Goldman-Hodgkin-Katz

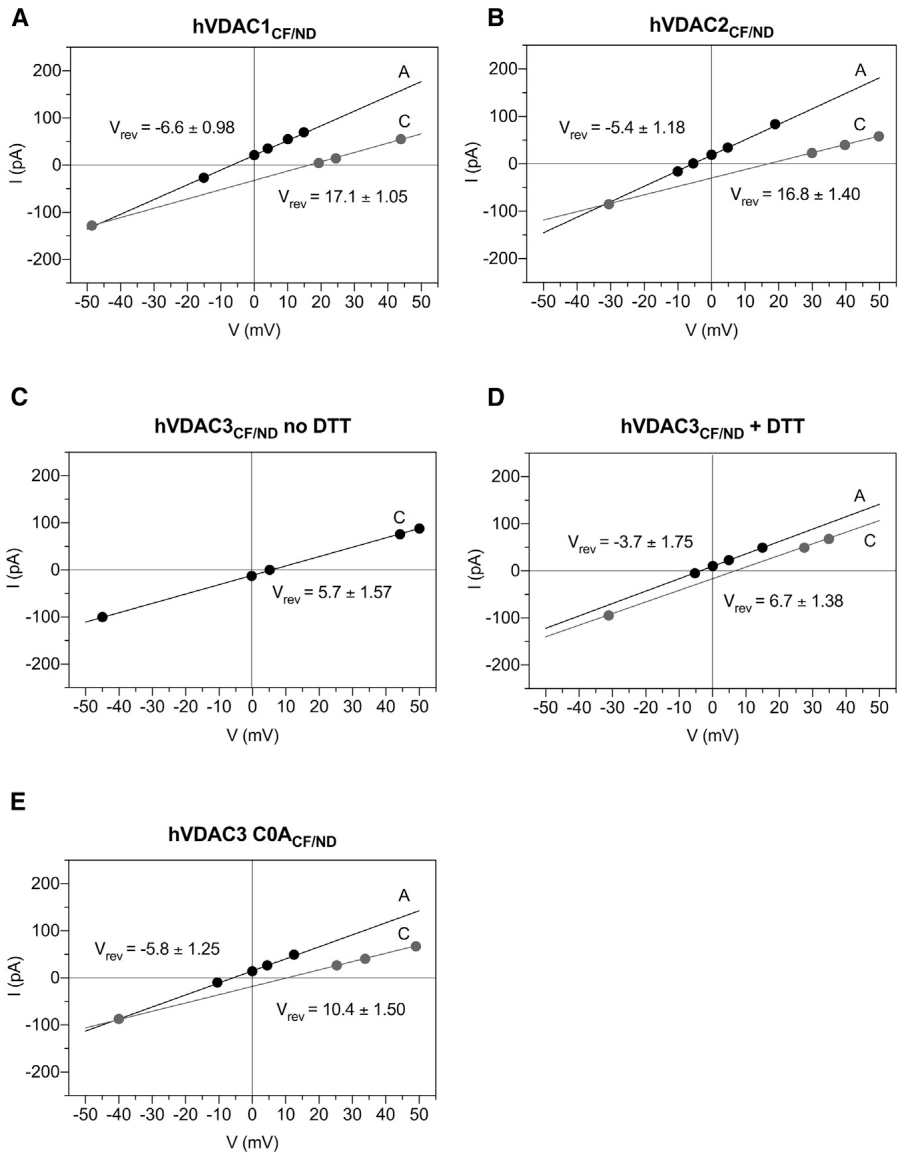

FIGURE 5 Ion selectivity of $hVDAC_{CF/ND}$s. (*A–E*) Representative I/V plots of human $VDAC_{CF/ND}$s performed in a 10-fold gradient of 0.1/1 M KCl. Currents were obtained by application of triangular voltage wave (amplitude ±50 mV). The two different regression lines (*solid lines*), correspond to the canonical anion high-conducting state (A, *black*) and to the cationic low-conducting state (C, *gray*). The intercepts of A and C lines with the I/axis identify the V_{rev}-values.

equation. In agreement with the literature (20,21,23,24), $hVDAC1_{CF/ND}$ featured a mild anion selectivity in the open state ($P_{Cl^-}/P_{K+} = 1.39 \pm 0.06$, $V_{rev} = -6.60 \pm 0.98$ mV). This preference for anions is reversed to a preferred movement of K^+ over Cl^- ($P_{Cl^-}/P_{K+} = 0.45 \pm 0.02$, $V_{rev} = 17.10 \pm 1.05$ mV) when the channel adopted the lower conducting conformation ("closed state") (Fig. 5 *A*; Table 2). For $hVDAC2_{CF/ND}$, the calculated V_{rev}-values were -5.4 ± 1.18 mV in the open state, corresponding to a permeability ratio $P_{Cl^-}/P_{K+} = 1.31 \pm 0.08$, and 16.8 ± 1.40 mV in the closed state, which is equivalent to a P_{Cl^-}/P_{K+} ratio of 0.43 ± 0.03 (Fig. 5 *B*; Table 2). hVDAC3 deserves a separate discussion.

As demonstrated in the previous paragraph, untreated human $hVDAC3_{CF/ND}$ is voltage-insensitive, which provides the possibility to determine the reversal potential exclusively for the conformation in which it inserted. In Fig. 5 *C*, it is indicated that the channel has a V_{rev}-value of 5.7 ± 1.57 mV. This corresponds to a permeability ratio P_{Cl^-}/P_{K+} of 0.76 ± 0.06 indicating cation selectivity (Table 2). This finding, however, is not surprising: it is conceivable that a channel with a very small conductance (~0.64 nS) promotes the passage of K^+ over Cl^- also because of steric hindrance.

TABLE 2 Permeability ratio of $hVDAC_{CF/ND}$ complexes

	P_{Cl^-}/P_{k+} (A)	P_{Cl^-}/P_{k+} (C)
$hVDAC1_{CF/ND}$	1.39 ± 0.06	0.45 ± 0.02
$hVDAC2_{CF/ND}$	1.31 ± 0.08	0.43 ± 0.03
$hVDAC3_{CF/ND}$ no DTT	–	0.76 ± 0.06
$hVDAC3_{CF/ND}$ + DTT	1.24 ± 0.12	0.66 ± 0.06
hVDAC3 $C0A_{CF/ND}$	1.27 ± 0.13	0.64 ± 0.10

The permeability ratio (P_{Cl^-}/P_{K+}) of $hVDAC_{CF/ND}$ complexes calculated from corresponding V_{rev} using the Goldman-Hodgkin-Katz equation. Data are means of at least three independent experiments ± SD.

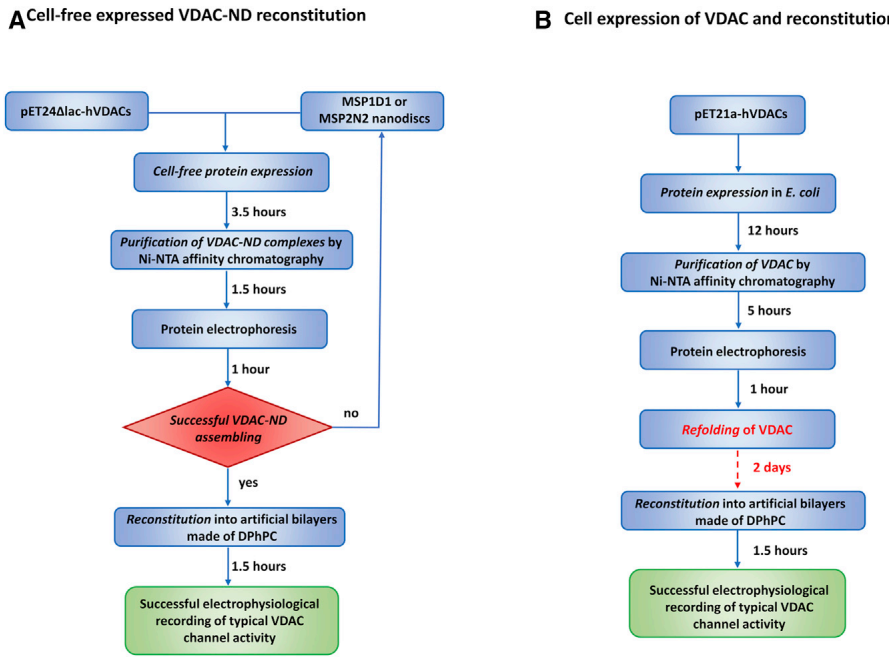

FIGURE 6 Flowcharts comparing the traditional method consisting of recombinant VDAC expression in microbial systems (right) and the new protocol that combines in vitro translation with nanodisc reconstitution (left). The lack of any type of refolding procedure is responsible for the substancial time gain experienced with the cell-free protein synthesis system.

Preincubation with DTT, which confers the large conductance state, then makes the fully open channel anion-selective with a $P_{Cl^-}/P_{K+} = 1.24 \pm 0.12$ ($V_{rev} = -3.7 \pm 1.75$ mV). The low conductance state reverses in this condition at $V_{rev} = 6.7 \pm 1.38$ mV translating into a cation selectivity of $P_{Cl^-}/P_{K+} = 0.66 \pm 0.06$ (Fig. 5 *D*; Table 2). The fact that the large conductance promotes anion selectivity was further supported by selectivity measurements of $hVDAC3C0A_{CF/ND}$. The reversal potential values of this mutant ($V_{rev} = -5.8 \pm 1.25$ mV) are in the fully open state more similar to $hVDAC1_{CF/ND}$ and $hVDAC2_{CF/ND}$, than to $hVDAC3_{CF/ND}$ no DTT. This reversal voltage translates into a permeability ratio $P_{Cl^-}/P_{K+} = 1.27 \pm 0.13$ in the large-conducting open conformation. The lower conducting closed state of this mutant exhibits a reversal voltage of $V_{rev} = 10.4 \pm 1.50$ mV indicating a cation selectivity with P_{Cl^-}/P_{K+} ratio of 0.64 ± 0.10 (Fig. 5 *E*; Table 2).

DISCUSSION

The first attempt to reconstitute VDAC into a PLB dates back to 1976 (19), when Schein and co-workers accidentally discovered a voltage-dependent and anion-selective channel in the mitochondria extract of *Paramecium Aurelia*. Since then, VDAC electrophysiology has been thoroughly investigated exploiting PLB measures. Today, well-established protocols exist for VDAC incorporation into artificial membranes and all of them involve the use of proteins isolated from tissue mitochondria (20,21,57) or protein produced by microbial systems (26,47). *Escherichia coli* is undoubtedly the most widely used expression platform for the highly efficient production of heterologous proteins. Despite its wide utilization, this technology has limitations that mainly concern the intracellular accumulation of improperly folded proteins in insoluble inclusion bodies and, possibly, the lack of physiological posttranslational modifications. Because functional and structural studies, however, need bioactive proteins, numerous strategies were established to counteract any denaturation process. In the specific case of VDAC, these methods include on-column refolding (30) or dropwise dilution (14,16,26) in the presence of detergents, along with gel filtration, ion exchange, and size exclusion chromatography (17). Overall, the reported procedures circumvent the difficulties associated with the transmembrane nature of VDAC though, at the same time, substantially prolonging the protein preparation workflow. Furthermore, the presence of contaminants, i.e., channel proteins of the bacterial host, is not absolutely abolished. In the last decades, CFPS has proven to be an excellent platform for in vitro protein expression that avoid all complications associated with living cells. Here, we report, for the first time, CF production of human VDACs and their insertion into NDs. Subsequent reconstitution into PLBs confirms that this procedure maintains the channel function of the proteins. Unlike detergent micelles and liposomes, NDs provide a native-like membrane environment that overcomes heterogeneity and aggregation (58,59). The ND also provides a greater stability for the membrane protein compared with liposomes (60).

Furthermore, this technology paves the way for a more accurate control of the local lipid compositions around the integral protein, that, besides, results more active (61). The literature already contains some examples of ND-stabilized VDACs (in particular, VDAC1 (45) and VDAC2 (46)), but all of them still involved the use of conventional bacterial protein expression systems. On the contrary, the results presented in this manuscript indicate the extraordinary advantages in terms of experimental effectiveness in combining in vitro VDAC translation with ND technology. To give a practical example, in vivo VDAC expression systems often require from 4 to 5 days to obtain active recombinant proteins, whereas CF/ND technology extremely cuts down working time to few hours (Fig. 6). The electrophysiological data confirm that human $VDAC1_{CF/ND}$, $VDAC2_{CF/ND}$, and $VDAC3_{CF/ND}$ form pores with robust channel properties. In this regard, $VDAC_{CF/ND}$s registered a higher probability to insert into artificial membranes when compared with VDAC proteins expressed via heterologous system (~90–70%). The functional features of these channels are undistinguishable from those obtained from recombinant proteins analyzed by canonical PLB protocols. We also checked the influence of PLB lipid composition on the pore-forming activity, by reconstituting $hVDAC1_{CF/ND}$ in a membrane made of 1:1 DiphPG/DiphPC as in (62). There was no difference between the protein produced with the new protocol presented here and the result reported in (62) (data not shown). Accordingly, at low membrane potentials $hVDAC1_{CF/ND}$ and $hVDAC2_{CF/ND}$ easily inserted into Diph-PC membranes as fully "open" channels with average conductance values between 3.47 $\pm$ 0.43 nS ($n = 35$) and 3.28 $\pm$ 0.36 nS ($n = 30$), respectively. An analysis of the voltage-dependence demonstrated that membrane potentials higher than $\pm$30 mV switched both isoform 1 and 2 to the low-conducting "closed" conformation. Also, the analysis of ion selectivity of channels obtained from the combined CF synthesis/ND system resembled data obtained with conventional methods (63). In both experimental systems the channels provide a weak preference for anion over cations in the high-conducting state that shifts to a distinct cation selectivity in the low conductance state. As expected, human $hVDAC3_{CF/ND}$ exhibited the same peculiar electrophysiological features previously reported for this channel (14,26,28). In the absence of any reductants, the average conductance of reconstituted channels was much lower than those of $hVDAC1_{CF/ND}$ and $VDAC2_{CF/ND}$. Furthermore, the open probability of $hVDAC3_{CF/ND}$ was insensitive to voltage over a wide voltage range. This condition allowed measurements of ion selectivity in a unique channel conformation that emerged as cation-selective. Addition of DTT or replacement of cysteines by alanine (hVDAC3 C0A mutant) converted the human $VDAC3_{CF/ND}$ into the same functional mode of the other two isoforms: the mean current across the $hVDAC3_{CF/ND}$ channel considerably increased both in DTT-treated (3.01 $\pm$ 0.47 nS ($n = 30$)) and Cys-less protein (3.57 nS $\pm$ 0.64 ($n = 33$)) although with different incorporation rates. Under the aforementioned experimental conditions, $hVDAC3_{CF/ND}$ acquired a voltage-dependence and anion selectivity in the open conformation similar to that of the two other isoforms. The results of these experiments further corroborate the importance of cysteine redox state in pore function (14,26) and they foster the hypothesis that the selectivity of the channel is correlated to the size of the unitary conductance. On the other hand, these experiments show that the new protocol for expression and reconstitution of VDAC pores can perfectly replicates the "classical" one also in altered conditions. In conclusion, we presented here a new protocol of expression and reconstitution of VDAC pores, based on CF expression of the protein and incorporation into NDs, that has the following advantages over the previous methods: 1) it is quicker because it takes only few hours from the expression to the reconstitution in PLB. This is mainly due to the lack of a dedicated refolding procedure, which is quite long and complex for bacterially expressed proteins; 2) consequently it is cheaper; 3) it is easier because the expression and NDs incorporation do not need any complex step in the laboratory; 4) the most interesting future perspective is that a combination of CFPS and reconstitution of active VDACs in NDs paves the way for site-specific incorporation of noncanonical amino acids. This will be interesting for studying structure/function correlations in these channel proteins and for understanding the effects of specific labeling (64). Finally, VDAC forming pores are more stable than those obtained with previous protocols, lasting many days at 4°C without loss of activity or precipitation and are more active in terms of ease of insertion in the PLB and incorporation of undamaged pore-forming protein. All these factors make our protocol an even better strategy than the liposome-fusion proposed by Liguori et al. (65). These authors set up a method for CF production of VDAC within liposomes that, however, requires much longer preparation times because of the need of preventing aggregation of the integral proteins.

The flowcharts in Fig. 6 summarize step by step protocols for the combined in vitro translation and ND reconstitution of VDACs and the conventional approach comprising recombinant VDAC synthesis and purification with advantages and disadvantages of both techniques. In the light of these findings, and of the successful confirmation of full activity recovery

showed by the three VDAC isoforms in PLB, which overlaps and even improves recordings of the functional properties reported in conventional system, we believe that our new protocol, combining CF synthesis with NDs reconstitution, will open up new opportunities in VDAC electrophysiology.

AUTHOR CONTRIBUTIONS

S.C.N. and O.R. performed the electrophysiological experiments on $VDAC_{CF}$ and analyzed the data. M.C.D.R. produced recombinant proteins. G.T., V.D.P., and S.R. designed the experiments and wrote the manuscript.

ACKNOWLEDGMENTS

The authors acknowledge funding by the European Research Council (2015 Advanced Grant 495) n. 695078 noMAGIC (to G.T.), the project POC-MUR 2018 DD 467, and the University of Catania, Progetto PIACERI 2020 "VDAC," Fondi di Ateneo 2020–2022, Linea Open Access and Linea CHANCE.

DECLARATION OF INTERESTS

The authors declare no competing interests.

REFERENCES

1. De Pinto, V. 2021. Renaissance of VDAC: new insights on a protein family at the interface between mitochondria and cytosol. *Biomolecules.* 11:107.
2. Brdiczka, D. 1994. Function of the outer mitochondrial compartment in regulation of energy metabolism. *Biochim. Biophys. Acta.* 1187:264–269.
3. Fiek, C., R. Benz, …, D. Brdiczka. 1982. Evidence for identity between the hexokinase-binding protein and the mitochondrial porin in the outer membrane of rat liver mitochondria. *Biochim. Biophys. Acta.* 688:429–440.
4. Campbell, A. M., and S. H. P. Chan. 2008. Mitochondrial membrane cholesterol, the voltage dependent anion channel (VDAC), and the Warburg effect. *J. Bioenerg. Biomembr.* 40:193–197.
5. Lee, A. C., X. Xu, …, M. Colombini. 1998. The role of yeast VDAC genes on the permeability of the mitochondrial outer membrane. *J. Membr. Biol.* 161:173–181.
6. Lemasters, J. J. 2017. Evolution of voltage-dependent anion channel function: from molecular sieve to governator to actuator of ferroptosis. *Front. Oncol.* 7:303.
7. Lemasters, J. J., and E. Holmuhamedov. 2006. Voltage-dependent anion channel (VDAC) as mitochondrial governator–thinking outside the box. *Biochim. Biophys. Acta.* 1762:181–190.
8. Messina, A., S. Reina, …, V. De Pinto. 2012. VDAC isoforms in mammals. *Biochim. Biophys. Acta.* 1818:1466–1476.
9. Shimizu, S., Y. Matsuoka, …, Y. Tsujimoto. 2001. Essential role of voltage-dependent anion channel in various forms of apoptosis in mammalian cells. *J. Cell Biol.* 152:237–250.
10. Huang, H., X. Hu, …, C. White. 2013. An interaction between Bcl-xL and the voltage-dependent anion channel (VDAC) promotes mitochondrial Ca2+ uptake. *J. Biol. Chem.* 288:19870–19881.
11. Cheng, E. H. Y., T. V. Sheiko, …, S. J. Korsmeyer. 2003. VDAC2 inhibits BAK activation and mitochondrial apoptosis. *Science.* 301:513–517.
12. Chin, H. S., M. X. Li, …, G. Dewson. 2018. VDAC2 enables BAX to mediate apoptosis and limit tumor development. *Nat. Commun.* 9:4976.
13. De Pinto, V., S. Reina, …, R. Mahalakshmi. 2016. Role of cysteines in mammalian VDAC isoforms' function. *Biochim. Biophys. Acta.* 1857:1219–1227.
14. Reina, S., V. Checchetto, …, V. De Pinto. 2016. VDAC3 as a sensor of oxidative state of the intermembrane space of mitochondria: the putative role of cysteine residue modifications. *Oncotarget.* 7:2249–2268.
15. Bayrhuber, M., T. Meins, …, K. Zeth. 2008. Structure of the human voltage-dependent anion channel. *Proc. Natl. Acad. Sci. USA.* 105:15370–15375.
16. Hiller, S., R. G. Garces, …, G. Wagner. 2008. Solution structure of the integral human membrane protein VDAC-1 in detergent micelles. *Science.* 321:1206–1210.
17. Ujwal, R., D. Cascio, …, J. Abramson. 2008. The crystal structure of mouse VDAC1 at 2.3 A resolution reveals mechanistic insights into metabolite gating. *Proc. Natl. Acad. Sci. USA.* 105:17742–17747.
18. Villinger, S., R. Briones, …, M. Zweckstetter. 2010. Functional dynamics in the voltage-dependent anion channel. *Proc. Natl. Acad. Sci. USA.* 107:22546–22551.
19. Schein, S. J., M. Colombini, and A. Finkelstein. 1976. Reconstitution in planar lipid bilayers of a voltage-dependent anion-selective channel obtained from paramecium mitochondria. *J. Membr. Biol.* 30:99–120.
20. Benz, R. 1994. Permeation of hydrophilic solutes through mitochondrial outer membranes: review on mitochondrial porins. *Biochim. Biophys. Acta.* 1197:167–196.
21. Colombini, M. 2007. Measurement of VDAC permeability in intact mitochondria and in reconstituted systems. *Methods Cell Biol.* 80:241–260.
22. Colombini, M., C. L. Yeung, …, T. König. 1987. The mitochondrial outer membrane channel, VDAC, is regulated by a synthetic polyanion. *Biochim. Biophys. Acta.* 905:279–286.
23. Benz, R., L. Wojtczak, …, D. Brdiczka. 1988. Inhibition of adenine nucleotide transport through the mitochondrial porin by a synthetic polyanion. *FEBS Lett.* 231:75–80.
24. Rostovtseva, T., and M. Colombini. 1996. ATP flux is controlled by a voltage-gated channel from the mitochondrial outer membrane. *J. Biol. Chem.* 271:28006–28008.
25. Xu, X., W. Decker, …, M. Colombini. 1999. Mouse VDAC isoforms expressed in yeast: channel properties and their roles in mitochondrial outer membrane permeability. *J. Membr. Biol.* 170:89–102.
26. Checchetto, V., S. Reina, …, V. De Pinto. 2014. Recombinant human voltage dependent anion selective channel isoform 3 (hVDAC3) forms pores with a very small conductance. *Cell. Physiol. Biochem.* 34:842–853.
27. Okazaki, M., K. Kurabayashi, …, M. Sodeoka. 2015. VDAC3 gating is activated by suppression of disulfide-bond formation between the N-terminal region and the bottom of the pore. *Biochim. Biophys. Acta.* 1848:3188–3196.
28. Queralt-Martín, M., L. Bergdoll, …, T. K. Rostovtseva. 2020. A lower affinity to cytosolic proteins reveals VDAC3 isoform-specific role in mitochondrial biology. *J. Gen. Physiol.* 152:e201912501.
29. Gincel, D., H. Zaid, and V. Shoshan-Barmatz. 2001. Calcium binding and translocation by the voltage-dependent anion channel: a possible regulatory mechanism in mitochondrial function. *Biochem. J.* 358:147–155.
30. Shi, Y., C. Jiang, …, H. Tang. 2003. One-step on-column affinity refolding purification and functional analysis of recombinant human VDAC1. *Biochem. Biophys. Res. Commun.* 303:475–482.

31. Singh, A., V. Upadhyay, …, A. K. Panda. 2015. Protein recovery from inclusion bodies of *Escherichia coli* using mild solubilization process. *Microb. Cell Fact.* 14:41.
32. Endo, Y., and T. Sawasaki. 2006. Cell-free expression systems for eukaryotic protein production. *Curr. Opin. Biotechnol.* 17:373–380.
33. Katzen, F., G. Chang, and W. Kudlicki. 2005. The past, present and future of cell-free protein synthesis. *Trends Biotechnol.* 23:150–156.
34. Jiang, X., Y. Ookubo, …, T. Yamane. 2002. Expression of Fab fragment of catalytic antibody 6D9 in an *Escherichia coli* in vitro coupled transcription/translation system. *FEBS Lett.* 514:290–294.
35. Ryabova, L. A., D. Desplancq, …, A. Plückthun. 1997. Functional antibody production using cell-free translation: effects of protein disulfide isomerase and chaperones. *Nat. Biotechnol.* 15:79–84.
36. Spirin, A. S., V. I. Baranov, …, Y. B. Alakhov. 1988. A continuous cell-free translation system capable of producing polypeptides in high yield. *Science.* 242:1162–1164.
37. Kalmbach, R., I. Chizhov, …, M. Engelhard. 2007. Functional cell-free synthesis of a seven helix membrane protein: in situ insertion of bacteriorhodopsin into liposomes. *J. Mol. Biol.* 371:639–648.
38. Shimono, K., M. Goto, …, S. Yokoyama. 2009. Production of functional bacteriorhodopsin by an *Escherichia coli* cell-free protein synthesis system supplemented with steroid detergent and lipid. *Protein Sci.* 18:2160–2171.
39. Denisov, I. G., and S. G. Sligar. 2016. Nanodiscs for structural and functional studies of membrane proteins. *Nat. Struct. Mol. Biol.* 23:481–486.
40. Katzen, F., J. E. Fletcher, …, W. Kudlicki. 2008. Insertion of membrane proteins into discoidal membranes using a cell-free protein expression approach. *J. Proteome Res.* 7:3535–3542.
41. Shim, J. W., M. Yang, and L.-Q. Gu. 2007. In vitro synthesis, tetramerization and single channel characterization of virus-encoded potassium channel Kcv. *FEBS Lett.* 581:1027–1034.
42. Rauh, O., U. P. Hansen, …, I. Schroeder. 2018. Site-specific ion occupation in the selectivity filter causes voltage-dependent gating in a viral K^+ channel. *Sci. Rep.* 8:10406.
43. Winterstein, L.-M., K. Kukovetz, …, O. Rauh. 2021. Distinct lipid bilayer compositions have general and protein-specific effects on K+ channel function. *J. Gen. Physiol.* 153:e202012731.
44. Winterstein, L.-M., K. Kukovetz, …, G. Thiel. 2018. Reconstitution and functional characterization of ion channels from nanodiscs in lipid bilayers. *J. Gen. Physiol.* 150:637–646.
45. Raschle, T., S. Hiller, …, G. Wagner. 2009. Structural and functional characterization of the integral membrane protein VDAC-1 in lipid bilayer nanodiscs. *J. Am. Chem. Soc.* 131:17777–17779.
46. Yu, T.-Y., T. Raschle, …, G. Wagner. 2012. Solution NMR spectroscopic characterization of human VDAC-2 in detergent micelles and lipid bilayer nanodiscs. *Biochim. Biophys. Acta.* 1818:1562–1569.
47. Magrì, A., R. Belfiore, …, A. Messina. 2016. Hexokinase I N-terminal based peptide prevents the VDAC1-SOD1 G93A interaction and re-establishes ALS cell viability. *Sci. Rep.* 6:34802.
48. Magrì, A., A. Karachitos, …, V. De Pinto. 2019. Recombinant yeast VDAC2: a comparison of electrophysiological features with the native form. *FEBS Open Bio.* 9:1184–1193.
49. Braun, C. J., T. Baer, …, G. Thiel. 2014. Pseudo painting/air bubble technique for planar lipid bilayers. *J. Neurosci. Methods.* 233:13–17.
50. Bayburt, T. H., and S. G. Sligar. 2003. Self-assembly of single integral membrane proteins into soluble nanoscale phospholipid bilayers. *Protein Sci.* 12:2476–2481.
51. Yokogawa, M., M. Fukuda, and M. Osawa. 2019. Nanodiscs for structural biology in a membranous environment. *Chem. Pharm. Bull. (Tokyo).* 67:321–326.
52. Denisov, I. G., Y. V. Grinkova, …, S. G. Sligar. 2004. Directed self-assembly of monodisperse phospholipid bilayer Nanodiscs with controlled size. *J. Am. Chem. Soc.* 126:3477–3487.
53. Grinkova, Y. V., I. G. Denisov, and S. G. Sligar. 2010. Engineering extended membrane scaffold proteins for self-assembly of soluble nanoscale lipid bilayers. *Protein Eng. Des. Sel.* 23:843–848.
54. Colombini, M. 1980. Structure and mode of action of a voltage dependent anion-selective channel (VDAC) located in the outer mitochondrial membrane. *Ann. N. Y. Acad. Sci.* 341:552–563.
55. Dubey, A. K., A. Godbole, and M. K. Mathew. 2016. Regulation of VDAC trafficking modulates cell death. *Cell Death Discov.* 2:16085.
56. Vander Heiden, M. G., N. S. Chandel, …, C. B. Thompson. 2000. Outer mitochondrial membrane permeability can regulate coupled respiration and cell survival. *Proc. Natl. Acad. Sci. USA.* 97:4666–4671.
57. de Pinto, V., G. Prezioso, and F. Palmieri. 1987. A simple and rapid method for the purification of the mitochondrial porin from mammalian tissues. *Biochim. Biophys. Acta.* 905:499–502.
58. Borch, J., and T. Hamann. 2009. The nanodisc: a novel tool for membrane protein studies. *Biol. Chem.* 390:805–814.
59. Lyukmanova, E. N., Z. O. Shenkarev, …, M. P. Kirpichnikov. 2012. Lipid-protein nanodiscs for cell-free production of integral membrane proteins in a soluble and folded state: comparison with detergent micelles, bicelles and liposomes. *Biochim. Biophys. Acta.* 1818:349–358.
60. Denisov, I. G., M. A. McLean, …, S. G. Sligar. 2005. Thermotropic phase transition in soluble nanoscale lipid bilayers. *J. Phys. Chem. B.* 109:15580–15588.
61. Ritchie, T. K., Y. V. Grinkova, …, S. G. Sligar. 2009. Chapter 11 - Reconstitution of membrane proteins in phospholipid bilayer nanodiscs. *Methods Enzymol.* 464:211–231.
62. Queralt-Martín, M., L. Bergdoll, …, T. K. Rostovtseva. 2019. Assessing the role of residue E73 and lipid headgroup charge in VDAC1 voltage gating. *Biochim. Biophys. Acta Bioenerg.* 1860:22–29.
63. Shoshan-Barmatz, V., V. De Pinto, …, N. Arbel. 2010. VDAC, a multi-functional mitochondrial protein regulating cell life and death. *Mol. Aspects Med.* 31:227–285.
64. Dondapati, S. K., M. Stech, …, S. Kubick. 2020. Cell-free protein synthesis: a promising option for future drug development. *BioDrugs.* 34:327–348.
65. Liguori, L., B. Stidder, …, D. K. Martin. 2016. Cell-free production of VDAC directly into liposomes for integration with biomimetic membrane systems. *Prep. Biochem. Biotechnol.* 46:546–551.

Article 2.

Redox Biology

Voltage Dependent Anion Channel 3 (VDAC3) protects mitochondria from oxidative stress

Simona Reina[1,4,#], Stefano Conti Nibali[2,#], Marianna Flora Tomasello[3], Andrea Magrì[1,4], Angela Messina[1,4], Vito De Pinto[2,4,5]

[1] Department of Biological, Geological and Environmental Sciences, Section of Molecular Biology, University of Catania, Viale A. Doria 6, 95125 Catania, Italy.
[2] Department of Biomedical and Biotechnological Sciences, University of Catania, Via S. Sofia 64, 95123 Catania, Italy.
[3] Institute of Crystallography, National Council of Research, Catania Unit, Catania 95126, Italy
[4] We.MitoBiotech S.R.L., c.so Italia 172, 95129 Catania, Italy
[5] National Institute for Biostructures and Biosystems, Section of Catania, Rome, Italy.

#: These authors equally contributed to the work.

Redox Biology 51 (2022) 102264

Contents lists available at ScienceDirect

Redox Biology

journal homepage: www.elsevier.com/locate/redox

Voltage Dependent Anion Channel 3 (VDAC3) protects mitochondria from oxidative stress

Simona Reina [a,d,*,1], Stefano Conti Nibali [a,1], Marianna Flora Tomasello [b], Andrea Magrì [c,d], Angela Messina [c,d], Vito De Pinto [a,d,e]

[a] Department of Biomedical and Biotechnological Sciences, University of Catania, Via S. Sofia 64, 95123, Catania, Italy
[b] Institute of Crystallography, National Council of Research, Catania Unit, Catania, 95126, Italy
[c] Department of Biological, Geological and Environmental Sciences, Section of Molecular Biology, University of Catania, Viale A. Doria 6, 95125, Catania, Italy
[d] We.MitoBiotech S.R.L., c.so Italia 172, 95129, Catania, Italy
[e] National Institute for Biostructures and Biosystems, Section of Catania, Rome, Italy

ARTICLE INFO

Keywords:
VDAC3
Cysteine
ROS
Mitochondria
Complex I
High-resolution respirometry

ABSTRACT

Unraveling the role of VDAC3 within living cells is challenging and still requires a definitive answer. Unlike VDAC1 and VDAC2, the outer mitochondrial membrane porin 3 exhibits unique biophysical features that suggest unknown cellular functions. Electrophysiological studies on VDAC3 carrying selective cysteine mutations and mass spectrometry data about the redox state of such sulfur containing amino acids are consistent with a putative involvement of isoform 3 in mitochondrial ROS homeostasis. Here, we thoroughly examined this issue and provided for the first time direct evidence of the role of VDAC3 in cellular response to oxidative stress. Depletion of isoform 3 but not isoform 1 significantly exacerbated the cytotoxicity of redox cyclers such as menadione and paraquat, and respiratory complex I inhibitors like rotenone, promoting uncontrolled accumulation of mitochondrial free radicals. High-resolution respirometry of transiently transfected HAP1-ΔVDAC3 cells expressing the wild type or the cysteine-null mutant VDAC3 protein, unequivocally confirmed that VDAC3 cysteines are indispensable for protein ability to counteract ROS-induced oxidative stress.

1. Introduction

Mitochondria are a major source of reactive oxygen species (ROS) as well as a critical target of the harmful effects of oxidative stress [1–3]: because of this they are equipped with multiple defense mechanisms [4]. These range from antioxidants enzymes, able to directly quench radical species (i.e. superoxide dismutases (SODs), glutathione peroxidase (GSH-Px) and peroxiredoxin/thioredoxin (PRX/Trx) systems [5,6]) to complex pathways including mitophagy and mitochondrial unfolded protein response (mtURP) [7,8]. Mitochondria communicate their redox state to targets located in the cytosol and in the nucleus (retrograde redox signaling) via mechanisms that are not fully understood but mostly rely on the modulation of redox sensitive proteins such as protein kinases [9,10]. In 2016, the Voltage Dependent Anion Channel isoform 3 (VDAC3) was suggested as a putative sensor of mitochondrial ROS levels [11,12]. Hitherto, VDAC1 had been considered a key player in ROS-induced apoptosis [13] as the responsible for the translocation of superoxide anion from mitochondria to cytosol [14]. Located in the outer membrane of eukaryotes mitochondria, VDACs form large aqueous channels that mediate metabolites exchange across the organelle [15,16]. They also participate in a wide range of pathways thanks to the interaction with cytosolic enzymes and both pro-apoptotic and anti-apoptotic factors [17,18]. The three VDAC isoforms (VDAC1, VDAC2 and VDAC3) that exist in mammals are considered functionally distinct, despite showing a high sequence similarity [19]. VDAC1 and VDAC2 are mainly involved in the regulation of bioenergetic and of mitochondria-mediated apoptosis, and also, they feature well-established electrophysiological properties which have been thoroughly investigated in artificial membranes [20]. Knowledge about isoform 3 is limited and its biophysical characteristics are still debated. The group of Colombini first reported that VDAC3 rarely inserted into planar lipid membranes as fully open pores that did not exhibit typical voltage-dependent gating [21]. Subsequently, Checchetto et al. described very small and ungated channels upon VDAC3 reconstitution

* Corresponding author. Department of Biomedical and Biotechnological Sciences, University of Catania, Via S. Sofia 64, 95123 Catania, Italy.
E-mail address: simona.reina@unict.it (S. Reina).
[1] These authors equally contributed to the work.

https://doi.org/10.1016/j.redox.2022.102264
Received 17 January 2022; Received in revised form 3 February 2022; Accepted 8 February 2022
Available online 12 February 2022

under non-reducing conditions [22]. The addition of reductants to the refolding procedures [23] or pre-incubation with DTT before electrophysiological analysis [24] significantly increased the current through VDAC3 which behaves as canonical voltage-gated VDAC pores albeit with a much lower insertion rate than isoform 1 and 2. Swapping experiments had previously suggested the involvement of cysteine residues in VDAC3 pore-activity [25]: the replacement of the VDAC3 N-terminus, containing two cysteines, with the homologous sequence of VDAC1, which has none, allowed isoform 3 to completely rescue the porin-less yeast temperature-sensitive phenotype [25]. However, the proof about the key function of these residues in the gating modulation of VDAC3 channels came later in Refs. [26,27]. The diverse content in cysteines is, indeed, a distinctive feature of the three isoforms: e.g. in human, VDAC1 has two, VDAC2 has nine and VDAC3 has six cysteines [28,29]. According to mass spectrometry analysis [30,31], all of these residues follow an evolutionarily conserved redox modification pattern, being oxidated or reduced probably depending on their location with respect to cytosol or IMS. In particular, the observation that the whole cysteine content of the isoform 3 is never detected as totally oxidized suggests that specific residues may undergo continuous oxidation-reduction cycles and strengthens the idea that they might be regulated or regulate intracellular ROS levels. However, experimental evidence is still missing. Clues from literature support the idea that VDAC3 may function as a redox-sensing protein. To date, a comprehensive proteomic analysis listed stress sensors and redox-mediating enzymes among the cytosolic proteins associated with VDAC3 [32] and a redox DIGE proteomic study performed on rat heart mitochondria identified VDAC3 as a preferred target of mitochondrial ROS generated by the complex III [33]. Furthermore, in a VDAC3 knock out mice, Zou et al. associated the lack of this isoform with the increase of mitochondrial ROS following a high-salt diet [34]. In another work [35], the authors speculated that the substantial increase of VDAC3 expression in non-metastatic endometrial cancers may correlate with dyslipidemia, a metabolic risk factor associated with the development of this type of tumor. Dyslipidemia could stimulate VDAC3 up-regulation through fatty acids and amine synthesis pathways responsible for ROS production within mitochondria. Very recently, VDAC3 was identified as severely oxidized in HEK293T and HeLa cells exposed to a photosensitizer compound that substantially increases mitochondria-specific oxidative stress [36].

In this work, near-haploid human HAP1 cells devoid of VDAC3 (HAP1-ΔVDAC3) were compared to VDAC1 knock out (HAP1-ΔVDAC1) and parental cell lines to test VDAC3 contribution in oxidative stress response. Along with a greater basal ROS production and a remarkable increase in the expression of the main antioxidant and detoxifying enzymes, the absence of VDAC3 considerably worsened cell resistance against mitochondrial ROS inducers. As confirmation, transfection of HAP1-ΔVDAC3 cell line with a cysteine-null (C0A) VDAC3 showed that cysteines are essential for the cell oxidative homeostasis. We here provide compelling evidence of the involvement of VDAC3 in mitochondrial redox-regulatory networks.

2. Results

2.1. VDAC3 knock out down-regulates mitochondrial biogenesis

HAP1 are a near-haploid cell line, of human leukemia origin, harboring a single copy of each chromosome, except for a disomic fragment of chromosome 15. Haploidy renders these cells a powerful tool for functional studies as genome editing ensures the full knock out of the target gene. In this work, HAP1 cells, devoid of VDAC1 or VDAC3, were exploited to analyze the contribution of isoform 3 in mitochondrial ROS metabolism and signaling. To this aim, we initially performed a phenotypic and molecular characterization of the novel cell lines. As shown in Supp. Fig. 1A, B and C, no appreciable differences were observed in morphology, proliferation (at least within the first 72 h) and survival rate among HAP1-ΔVDAC1, HAP1-ΔVDAC3 and parental cells. However, the quantification of both mRNA and protein levels demonstrated a significant dysregulation in the expression profiles of the other two isoforms in the absence of VDAC3: compared to the parental cell line, HAP1-ΔVDAC3 displayed an approximate 50% decrease and a concomitant approximate 70% increase of VDAC1 and VDAC2 proteins, respectively (Fig. 1A and B). VDAC1 knock out, conversely, did not considerably alter the expression levels of VDAC2 and VDAC3 (Fig. 1A and B). As changes in VDAC function/expression have been related to mitochondrial biogenesis dysfunction [37], the effects of VDAC1 and VDAC3 depletion on mitochondrial content were assessed by investigating the PGC-1α (peroxisome proliferator-activated receptor *gamma* coactivator 1a) signaling cascade. PGC-1α controls mitochondrial respiration and biogenesis by coactivating numerous transcription factors, including the nuclear respiratory factors NRF-1. PGC-1α also indirectly regulates the mtDNA transcription by modulating the expression of the mitochondrial transcription factor A (TFAM), which is coactivated by NRF-1. As illustrated in Fig. 1C, the expression of all these genes is significantly reduced in both HAP1 K.O. cell lines, although the lack of VDAC3 is associated with the greatest variations (more than 50% reduction in mitochondrial biogenesis markers). However, mtDNA copy number quantification by determining the mtDNA/nDNA ratio and western blot analysis of Succinate Dehydrogenase Complex Flavoprotein Subunit A (SDHA) (Fig. 1D–E) demonstrated a similar effect of VDAC1 and VDAC3 knock out on mitochondrial deregulation. The significant fall in the mitochondrial mass of both K.O. cell lines was accompanied by a considerable hyperpolarization across their inner mitochondrial membranes (Fig. 1F, G and 1H), which was more pronounced (approximately 38%) in cells devoid of VDAC1 and could be related to ADP exhaustion [38].

2.2. VDAC3 depletion weakens cellular defenses against ROS and stimulates expression of antioxidant enzymes

Clues about the involvement of VDAC3 in ROS homeostasis have been reported elsewhere [32,34–36]. To examine whether or not the absence of VDAC3 can influence the intracellular redox state, we measured the relative abundance of three antioxidant enzymes. As shown in Fig. 2A, catalase, superoxide dismutase 1 (SOD1) and thioredoxin (TRX) were significantly overexpressed in HAP1-ΔVDAC3 compared to parental cell line (0.59 ± 0.15, 1.18 ± 0.10 and 1.10 ± 0.11-fold increase, respectively). HAP1-ΔVDAC1 also exhibited an increment in catalase and TRX expression (0.74 ± 0.13 and 0.58 ± 0.12-fold increase, respectively) with respect to control cells, whereas a reduction of SOD1 (0.30 ± 0.14-fold decrease) was observed, in agreement with [39]. Overall, the expression pattern of these major antioxidant enzymes demonstrates that cells devoid of VDAC3 experience a greater oxidative stress. MitoSOX-Based Flow Cytometry, which specifically detect mitochondrial superoxide, confirmed the highest basal level of mitochondrial ROS in HAP1-ΔVDAC3 cells with respect to the parental cell line and to cells lacking VDAC1 (Fig. 2B) [40–43]. Interestingly, both VDAC1 and VDAC3 depletion led to a diminished amount of cytosolic ROS with respect to control cells, as revealed by flow cytometry quantification with DCFH probe (Fig. 2C). These findings could be a consequence of the enhanced expression of antioxidant enzymes that quickly remove the excess of ROS from the cytosol or otherwise be explained by the minor permeability of superoxide across the outer membrane of VDAC1 and VDAC3 K.O. mitochondria.

2.3. Challenge with ROS producing drugs reveals the importance of VDAC3 in fighting oxidative stress

The impact of drugs that trigger mitochondrial superoxide accumulation (i.e. rotenone, menadione and paraquat) was evaluated in HAP1 cells devoid of VDAC1 or VDAC3. The results suggest that VDAC3 has a role in oxidative stress response. According to Fig. 3A, cell survival of

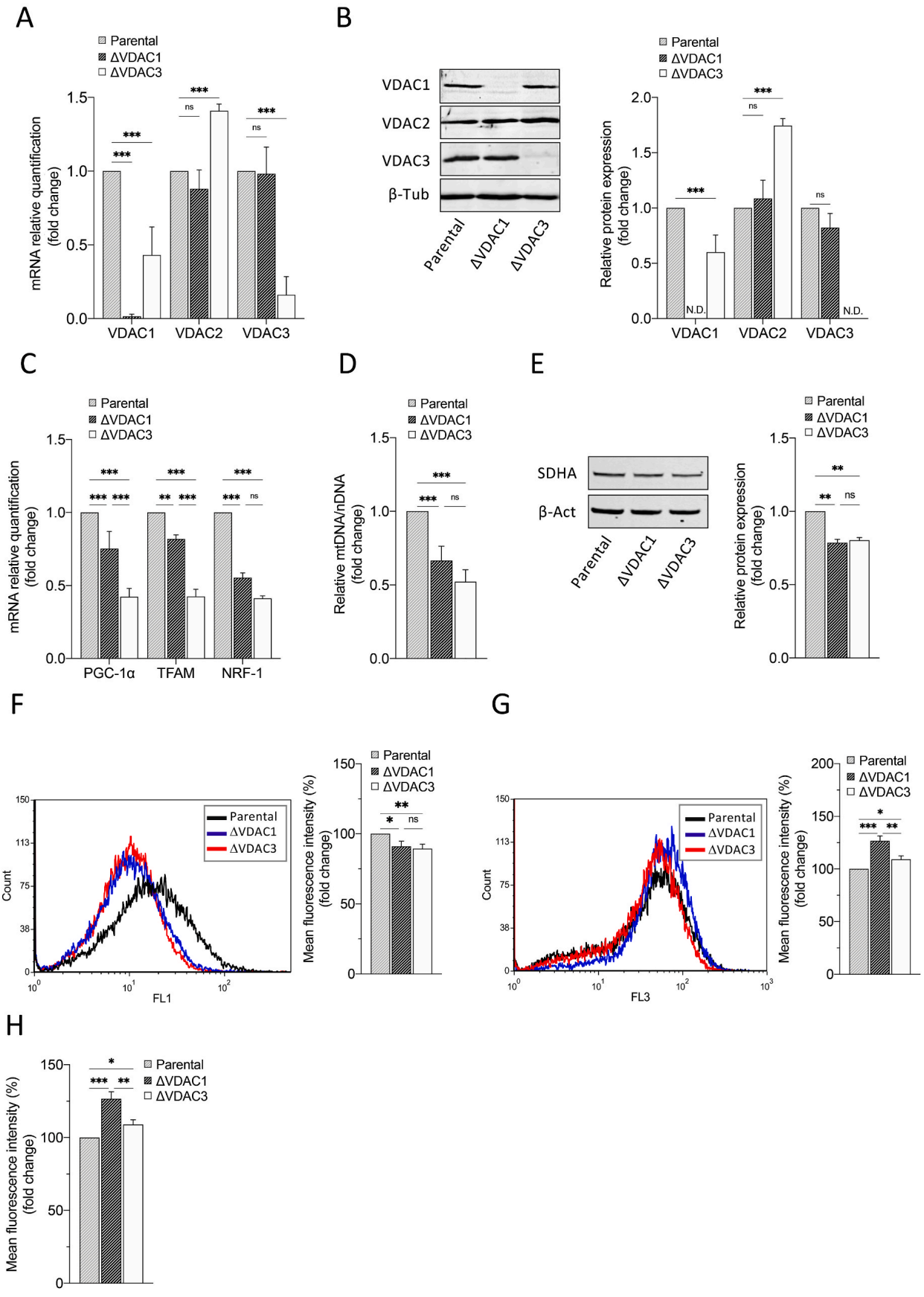

(caption on next page)

Fig. 1. Molecular characterization of HAP1 cell lines. A. Relative quantification of VDAC1, VDAC2 and VDAC3 mRNAs in HAP1-ΔVDAC1 and HAP1-ΔVDAC3. Data are normalized to the β-actin and expressed as means ± SEM (n = 3) and compared to HAP1 parental cells (equals one). B. Western blot illustration and relative quantification of VDAC1, VDAC2 and VDAC3 protein levels in HAP1-ΔVDAC1 and HAP1-ΔVDAC3. Data are normalized to the β-tubulin, expressed as means ± SEM (n = 3) and compared to HAP1 parental cells. C. Relative quantification of PGC-1α, NRF1 and TFAM (mitochondrial biogenesis markers) mRNAs in HAP1-ΔVDAC1 and HAP1-ΔVDAC3. Data are normalized to the β-actin and expressed as means ± SEM (n = 4) and compared to HAP1 parental cells. D. Quantification of mitochondrial DNA (mtDNA) in HAP1 cell lines devoid of VDAC1 or VDAC3. mtDNA amount was measured by Real-Time PCR of the mitochondrial gene COXII and normalized to the nuclear gene APP. Data are expressed as means ± SEM (n = 3) and compared to HAP1 parental cells. E. Quantification of mitochondrial content. Western blot illustration and relative quantification of mitochondrion-specific protein SDHA level in HAP1-ΔVDAC1 and HAP1-ΔVDAC3. Data are normalized to the β-Actin, expressed as means ± SEM (n = 3) and compared to HAP1 parental cells. F. Measurement of mitochondrial mass using MitoTracker Green. Representative fluorescence profiles of cells populations for the three cells lines. Histogram reports the average of fluorescence intensity measured by flow cytometry for the three HAP1 cell lines after proper gating of fluorescence. Gates were established based on negative and positive controls. Data are indicated as means ± SEM (n = 3) and compared to HAP1 parental cells. G. Detection of mitochondrial membrane potential by Mitotracker Red and measured by flow cytometry in each population of the three HAP1 cell lines. Histograms show the average fluorescence intensity measured for each gated cell population analyzed. Data are indicated as means ± SEM (n = 3) and compared to HAP1 parental cells. H. Quantification of mitochondrial membrane potential normalized for mitochondrial mass in HAP1 cell lines devoid of VDAC1 and VDAC3. Data are expressed as means ± SEM (n = 3) and compared to parental cell line. Data were analyzed with One-Way or Two-Way ANOVA; with *p < 0.05 **p < 0.01 and ***p < 0.001. (For interpretation of the references to colour in this figure legend, the reader is referred to the Web version of this article.)

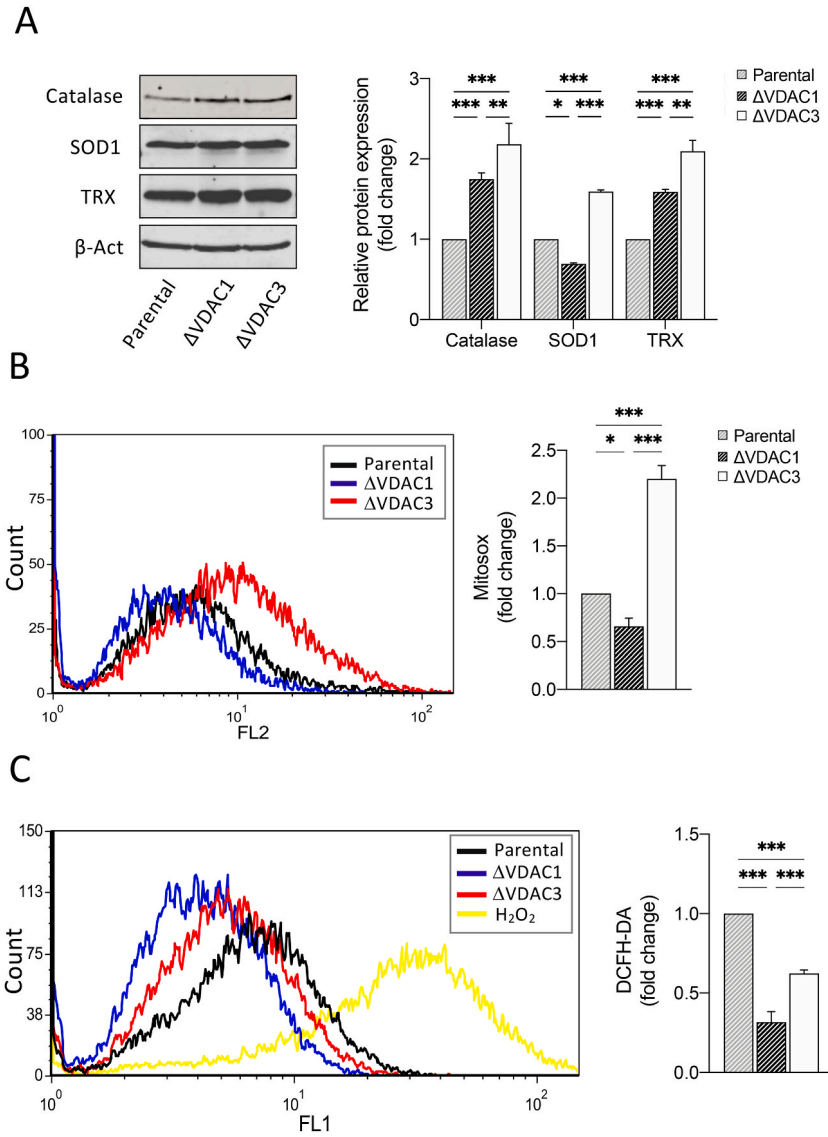

Fig. 2. Analysis of mitochondrial superoxide content and quantification of the expression levels of the main antioxidant enzymes in HAP1 cell lines. A. Representative immunoblot and relative protein quantification of antioxidant enzymes (Catalase, superoxide dismutase 1 (SOD1) and Thioredoxin (TRX)) in HAP1-ΔVDAC1 and HAP1-ΔVDAC3. Data are normalized to the β-actin, expressed as means ± SEM (n = 3) and compared to HAP1 parental cell line. B. Mitochondrial superoxide determination by MitoSOX red probe. Representative MitoSOX Red fluorescence profiles evaluated by flow cytometry in each population of HAP1 cell lines (left). Quantitative analysis of the mean fluorescence intensity MitoSOX Red in each population of HAP1 cell line. Results are expressed as the mean ± SD (n = 3) and compared to HAP1 parental cells (right). Results are expressed as the mean ± SD (n = 3) and compared to HAP1 parental cells. C. Intracellular ROS detected by DCFH-DA fluorescence measured by flow cytometer. Representative fluorescence profiles detected by flow cytometry for each cell line (left). Quantitative analysis of the average fluorescence intensity of DCFH-DA (%) in each gated population of HAP1 cell lines (right). Results are expressed as the mean ± SD (n = 3) and compared to HAP1 parental cell line. Data were analyzed with Two-Way ANOVA or One-Way ANOVA; with *p < 0.05 **p < 0.01 and ***p < 0.001. (For interpretation of the references to colour in this figure legend, the reader is referred to the Web version of this article.)

wild type HAP1 following paraquat, rotenone and menadione exposure, (MTT assay), ranged from 50 to 80%. VDAC3 knock out significantly reduced the percentage of viable cells by approx. 15% after paraquat and menadione treatments and by 40% upon rotenone administration. VDAC1 depletion did not affect cell sensitivity to rotenone and menadione, albeit, enhanced cell resistance to paraquat toxicity in accordance with Shimada et al. [44]. Relative quantification of protein levels in the parental cell line revealed that exposure to rotenone, menadione and paraquat mainly affected the expression profile of VDAC3 which is substantially up-regulated compared to VDAC1 and VDAC2 (Fig. 3B). To examine the endogenous mitochondrial superoxide production after a drug challenge in HAP1, control and K.O. cells were loaded with the

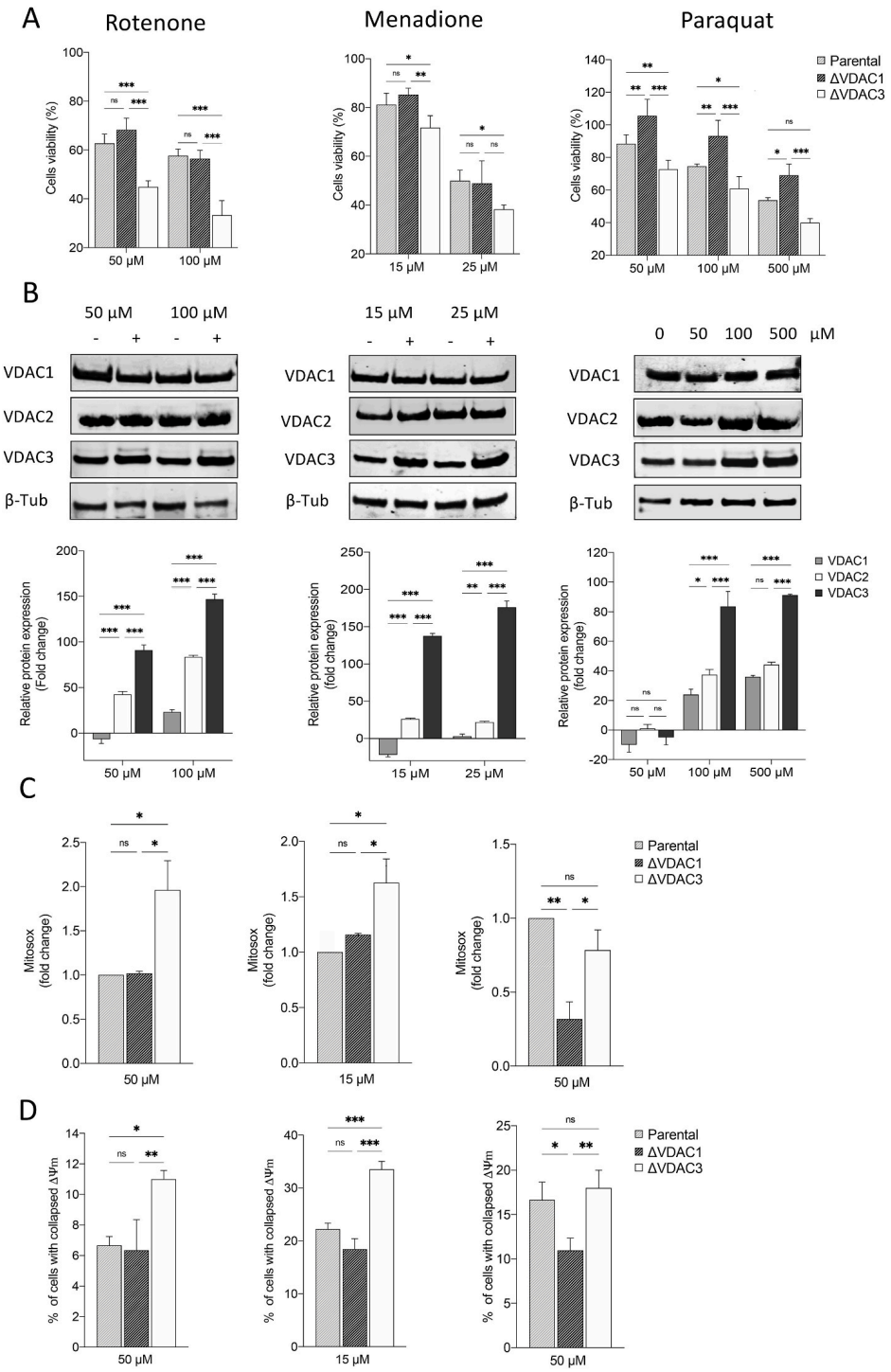

Fig. 3. Effect of mitochondrial ROS-inducers on cell viability, VDAC isoforms expression and mitochondria functionality. A. Cell viability of HAP1 cell lines treated with different concentrations of mitochondrial ROS-inducers (i.e., rotenone, menadione and paraquat). Data are indicated as the mean ± SE (n = 6) and expressed as the percentage ratio of the treated cells to the untreated ones. B. Relative quantification of VDAC1, VDAC2 and VDAC3 protein levels in HAP1 parental cells treated with increasing concentrations of rotenone, menadione and paraquat. All values are normalized to the β-tubulin endogenous control and expressed as means ± SEM (n = 3). C. Measurement of mitochondrial superoxide production via staining with MitoSOX Red after treatments with drugs. Data are expressed as mean ± SD (n = 3) and compared to HAP1 parental cell line. D. Mitochondrial membrane potential estimated by TMRM fluorescence measured with flow cytometry in HAP1 cell lines after drug administrations. Quantifications of percentage of cells with collapsed Δψm are indicated as means ± SEM (n = 3); mitochondrial membrane potential is normalized to mitochondrial mass value and expressed as the ratio of the treated cells to the untreated. Data were analyzed with Two-Way ANOVA or One-Way ANOVA; with *p < 0.05 **p < 0.01 and ***p < 0.001.

MitoSOX probe: following treatment with rotenone and menadione, flow cytometry measurements detected a significant increase (1.1 ± 0.10 and 0.65 ± 0.12-fold increase, respectively) in the amount of oxidized probe within HAP1-ΔVDAC3 cells with respect to the parental cell line (Fig. 3C). These same drugs did not remarkably enhance mitochondrial ROS production in VDAC1 K.O. cell line, where, on the contrary, a conspicuous reduction (0.68 ± 10 - fold decrease) in superoxide content was observed upon paraquat administration, compared to parental cell line (Fig. 3C). To this regard, unvaried ROS production in VDAC3-free cells compared to the wild-type cell line following treatment with paraquat may be explained by the down regulation of VDAC1, which mediates PQ toxicity. Consistent with the fact that oxidative stress caused by ROS can promote the rapid depolarization of the inner mitochondrial membrane potential, rotenone and menadione, but not paraquat, markedly increased the percentage of HAP1-ΔVDAC3 cells with collapsed ΔΨm (Fig. 3D). As expected, the mitochondrial membrane potential of parental and VDAC1 K.O cells was similarly affected by rotenone and menadione, whereas paraquat induced a considerable hyperpolarization of HAP1-ΔVDAC1 mitochondria compared to the other cell lines (Fig. 3D).

2.4. Cysteine residues are responsible for the ability of VDAC3 to counteract mitochondrial ROS overload

Previous reports led us to speculate that VDAC3 can modulate mitochondrial ROS content through the redox modifications of its

cysteine residues: most of them are indeed exposed towards the inter membrane space, an acidic and oxidative environment where ROS are released by Complex I [28]. To confirm this, HAP1-ΔVDAC3 cells were transiently transfected with plasmids encoding HA-tagged VDAC3 or VDAC3 C0A (i.e. a mutant where all cysteine residues were replaced with alanine residues), together with the mitochondrial-targeted Red Fluorescent Protein (mtDsRed) used as transfection reporter and as a mitochondrial marker. Before transfections, Mito Tracker Red DsRed staining allowed to portray the characteristic of mitochondrial network in parental and VDAC3 K.O. cells (Suppl. Fig. 2A). Flow cytometry and western blot confirmed the expression of the exogenous genes and revealed an approx. 70% transfection efficiency for both VDAC3 and VDAC3 C0A, which were also properly targeted to mitochondria (Fig. 4 A, B and Suppl. Fig. 2B). Strikingly, expression of VDAC3 induced nearly a 40% increase in HAP1-ΔVDAC3 cell survival after 24h exposure to 50 and 100 μM rotenone (Fig. 4C). Under the same experimental conditions, VDAC3 C0A did not considerably affect the susceptibility of VDAC3 knock out cells to the drug. These results are particularly impressive since neither VDAC3 nor VDAC3 C0A transfections altered mitochondrial content (Fig. 4D and E); furthermore, they did not stimulate a compensatory increase in VDAC1 protein level which could eventually disguise VDAC3 depletion (Suppl. Fig. 3). The boost in cell survival registered upon transfection with the wild type VDAC3 isoform is therefore unequivocally due to its cysteine residues that can counteract rotenone-induced mitochondrial injury. In support of these data, VDAC3 down-regulated catalase, thioredoxin and SOD1 expression more than the cysteine-null mutant, suggesting once again that restoring the wild-type protein expression is sufficient and necessary to reduce oxidative stress (Fig. 4F).

2.5. *VDAC3 preserves mitochondrial respiration upon oxidative stress conditions*

Rotenone is a powerful inhibitor of the mitochondrial electron transport system (ETS) complex I and exerts its toxicity by increasing mitochondrial ROS in the presence of NADH-linked substrates, through a mechanism not completely understood [45,46]. Given previous results, we queried whether VDAC3 could protect the mitochondrial respiration upon rotenone exposure. To this aim, High-Resolution Respirometry (HRR) was used to assay oxygen consumption of HAP1 cells.

Fig. 5A displays a representative respirometric curve of untreated parental HAP1 cells along with the specific protocol used herein. Briefly, oxygen consumption was first measured in intact cells, i.e., in the presence of endogenous substrates (ROUTINE state). Then, cells were permeabilized and the oxidative phosphorylation sustained by complex I was achieved in the presence of NADH-linked substrates (N-pathway, i.e. the contribution of complex I to the oxidative phosphorylation). Finally, the maximal electron transport (ET) capacity was obtained by the complete dissipation of the proton gradient through uncoupler titration.

In order to identify a sublethal rotenone dose, parental HAP1 cells were first exposed to increasing concentration of the toxin. In parallel, experiments were repeated using myxothiazol as a control. Myxothiazol blocks the ETS specifically acting on complex III [47] but without exerting any significant effect on ROS level [48,49]. As reported in Suppl. Fig. 4A–B, both drugs promoted a similarly significant decrease of parental HAP1 oxygen consumption in all the analyzed respiratory states in a dose-dependent manner starting from 100 nM, with the effect of rotenone being more pronounced than that of myxothiazol. On the other hand, no significant variation was observed at 10 nM rotenone. Additionally, this concentration did not affect cell viability (Suppl. Fig. 4C) nor in the case of rotenone neither upon myxothiazol treatment. Contrariwise, while the exposure of HAP1 cells to 10 nM rotenone correlated with an increase of about 58% in Mitosox signal in comparison to the untreated control, upon myxothiazol the Mitosox signal decreased (Suppl. Fig. 4D), suggesting a reduction of ROS production upon blockage of the ETS, in accordance with previous observations [50]. HRR experiments were also performed in HAP1-ΔVDAC3 cells transfected with constructs encoding VDAC3 or VDAC3 C0A, and exposed to the sublethal doses of rotenone and myxothiazol. While the transfections *per se* did not change respiration in any analyzed state (Suppl. Fig. 5), the absence of VDAC3 made HAP1 extremely sensitive to 10 nM rotenone: not only did the toxin halve cell viability (Fig. 5B) but significantly affected the respiration. As shown in Fig. 5C, VDAC3 knock out cells underwent a significant reduction of about 40% in the oxygen consumption during ROUTINE state, and of 65% and 70% in N-pathway and ET capacity, respectively. In contrast, absence of VDAC3 had no impact for cell viability or respiration of HAP1 (Fig. 5D–E) when cells are exposed to myxothiazol, since no significative variations were observed in all the conditions tested here. In any case, the re-introduction of VDAC3 with transient transfection almost nullified the harmful effect of rotenone, restoring cell survival and oxygen consumption in all the analyzed states (Fig. 5B–C). The expression of the *cys-null* mutant also improved both cell survival (Fig. 5B) and respiration (Fig. 5C) although the oxygen consumption levels never reached those of cells expressing VDAC3 WT. Again, no significative variations were observed upon VDAC3 WT or C0A mutant expression in VDAC3 knock out cells exposed to 10 nM myxothiazol (see Supplementary Table S1 for raw data).

Overall, these results indicate that VDAC3, and particularly the cysteine residues, is pivotal in maintaining mitochondrial functionality upon oxidative stress conditions.

3. Discussion

VDAC3 is the most recently discovered VDAC isoform [50]. Its existence raised questions about porin redundancy in the outer mitochondrial membrane. As for gram-negative bacteria, where many outer membrane porins absolve to specialized functions [51], mammalian VDAC isoforms accomplish distinct roles within the cell [52]. In particular, VDAC3 has recently been proposed to function as a sensor for the oxidation-reduction potential present in the mitochondrion [26,28]. To challenge this hypothesis, we deeply investigated the behavior of the human HAP1 cell lines devoid of VDAC1 or VDAC3 in response to ROS. Indeed, VDAC1 has been suggested to be involved in ROS homeostasis as well [41,53,54]: however, unlike VDAC3, isoform 1 would promote oxidative stress as speculated by Maldonado et al. [55] and demonstrated by Yang et al. [56]. The near haploid chromosomal status of HAP1 ensures the complete removal of the target gene: notwithstanding, in the particular case of VDAC, the remaining isoforms can potentially compensate for the knockout of a specific isoform and hence mask the effects of its depletion. For instance, in mouse embryonic stem (ES) cells, upon VDACs knock out a compensatory increase in VDAC1 expression was registered in VDAC2$^{-/-}$ and VDAC3$^{-/-}$ [56].

The preliminary characterization of HAP1-ΔVDAC1 and HAP1-ΔVDAC3 cells revealed no significant changes in the protein levels of VDAC2 and VDAC3 in HAP1-ΔVDAC1, whereas a simultaneous down-regulation of VDAC1 and up-regulation of VDAC2 was registered in HAP1-ΔVDAC3 cells. Interestingly, these data are in agreement with the positive association between VDAC1 and VDAC3 protein expression and the negative correlation of VDAC2 with VDAC1 detected in endometrial cancer cells [35]. Both knock out cell lines exhibited a considerable reduction in mitochondrial content with a concomitant increase in mitochondrial membrane potential. In other words, cells lacking VDAC1 or VDAC3 share a fewer number of mitochondria that, however, are more polarized. In accordance with our data, Magrì et al. previously reported that the absence of the endogenous yeast VDAC1 induces a metabolic rewiring through the down-regulation of mitochondria [37]. On the other hand, explaining the reasons for mitochondrial hyperpolarization upon VDACs knock out is arduous: one hypothesis is that it could be correlated to ADP depletion and loss of F_OF_1 ATPase activity,

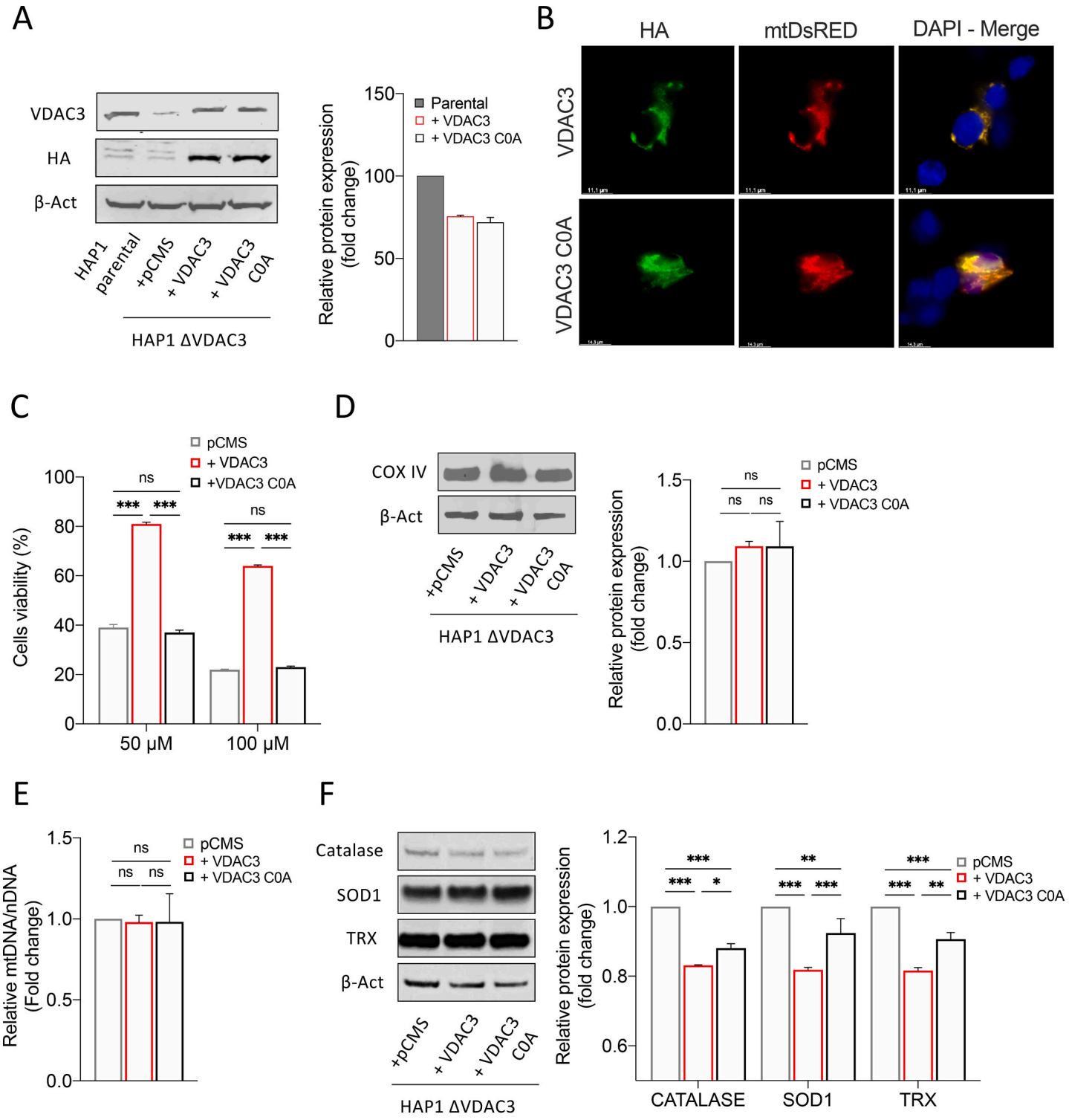

Fig. 4. Evaluation of HAP1-ΔVDAC3 cell profile upon transfection with VDAC3 wild type and VDAC3 *cys-null* mutant. A. Transfection efficiency of HAP1-ΔVDAC3 transfected with VDAC3 wild type (+VDAC3) and VDAC3 cys-null (+VDAC3 C0A) mutant was calculated by relative western blot quantification of VDAC3 proteins in HAP1-ΔVDAC3 compared to the endogenous protein level in HAP1 parental cells. Data were normalized with β-actin, expressed as means ± SEM (n = 3). Anti-HA is shown as control. B. Fluorescence microscopy analysis of subcellular distribution of VDAC3 and VDAC3 C0A in HAP1- ΔVDAC3 by indirect immunofluorescence targeting the HA tag. Mitochondria were visualized by expressing the mitochondrial-targeted mtDsRed protein. Both exogenous proteins are co-localized with mitochondria. C. Cell viability of HAP1-ΔVDAC3 upon transfection with an empty vector (pCMS) or plasmid encoding either for the VDAC3 (+VDAC3) or the VDAC3 C0A (+VDAC3 C0A) and treated with different concentration of rotenone. Data show the mean ± SE (n = 3) and are expressed as a percentage ratio of the treated cells to the untreated ones. D. Quantification of mitochondrial content. Immunoblot illustration and relative quantification of mitochondria-specific protein COX IV level in HAP1-ΔVDAC3 upon transfection. Data are normalized to the β-Actin, expressed as means ± SEM (n = 3) and compared to HAP1-ΔVDAC3 transfected with empty vector. E. Quantification of mtDNA in HAP1-ΔVDAC3 upon transfection. mtDNA amount was measured by Real-Time PCR of the mitochondrial gene COXII and normalized to the nuclear gene APP. Data are expressed as means ± SEM (n = 3) and compared to HAP1-ΔVDAC3 transfected with empty vector. F. Quantification of the main antioxidant enzymes in HAP1-ΔVDAC3 upon transfection. Representative immunoblot and relative protein quantification of Catalase, superoxide dismutase 1 (SOD1) and thioredoxin (TRX). Data are normalized to the β-Actin, expressed as means ± SEM (n = 3) and compared to HAP1-ΔVDAC3 transfected with the empty vector. Data were analyzed with One-Way or Two-Way ANOVA; *p < 0.05 **p < 0.01 and ***p < 0.001.

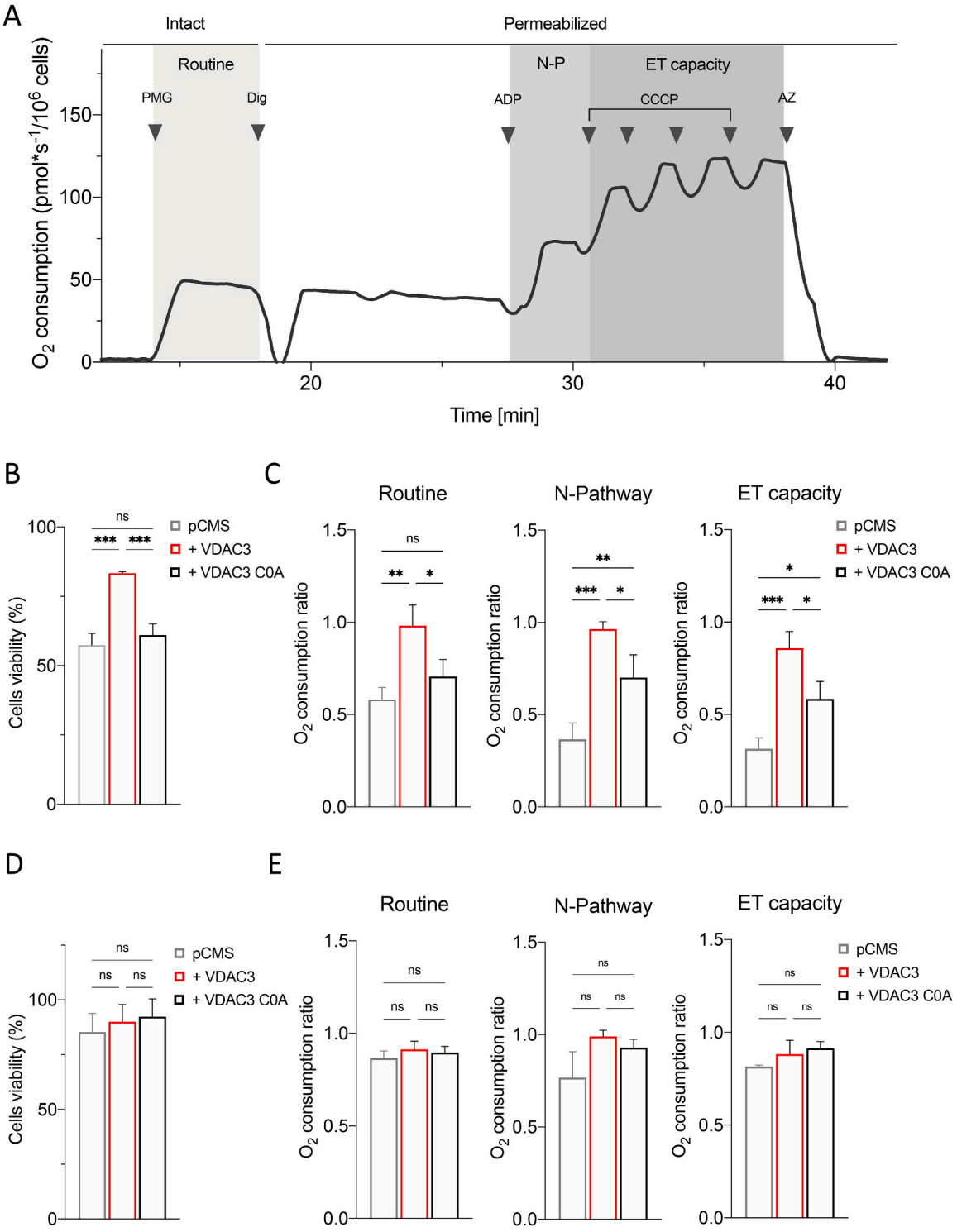

Fig. 5. Oxygen consumption analysis upon rotenone and myxothiazol exposure. A. Representative curve displaying the respirometry profile of untreated HAP1 parental cells and the SUIT protocol applied. The respiratory states Routine, N-pathway and ET capacity were achieved in intact or permeabilized cells with the specific addition of substrates and inhibitors, as following: PMG, pyruvate, malate and glutamate; Dig, digitonin; CCCP, carbonyl cyanide 3-chlorophenylhydrazone; AZ, sodium azide. B. Cell viability of HAP1-ΔVDAC3 upon transfection with an empty vector (pCMS) or plasmid encoding either for the VDAC3 (+VDAC3) or the VDAC3 C0A (+VDAC3 C0A) and treated with 10 nM rotenone. Data show the mean ± SE (n = 3) and are expressed as a percentage ratio of the treated cells to the untreated ones. C. Quantitative analysis of the oxygen consumption in the analyzed states of HAP1-ΔVDAC3 transfected with empty vector (pCMS) or construct carrying VDAC3 (+VDAC3) or VDAC3 C0A mutant (+VDAC3 C0A) attained after the exposure to 10 nM rotenone. Data are indicated as the mean ± SE (n = 3) and expressed as the ratio of the treated cells to the untreated ones. D. Cell viability of HAP1-ΔVDAC3 upon transfection with an empty vector (pCMS) or plasmid encoding either for the VDAC3 (+VDAC3) or the VDAC3 C0A (+VDAC3 C0A) and treated with 10 nM myxothiazol. Data show the mean ± SE (n = 3) and are expressed as a percentage ratio of the treated cells to the untreated ones. E. Quantitative analysis of the oxygen consumption in the analyzed states of HAP1-ΔVDAC3 transfected with empty vector (pCMS) or construct carrying VDAC3 (+VDAC3) or VDAC3 C0A mutant (+VDAC3 C0A) attained after the exposure to 10 nM myxothiazol. Data are indicated as the mean ± SE (n = 3) and expressed as the ratio of the treated cells to the untreated ones. Data were analyzed by one-way ANOVA, with *p < 0.05, **p < 0.01 and ***p < 0.001.

which in turn decreases the utilization of the electrochemical gradient [38]. An alternative interpretation may involve the so-called "incomplete mitochondrial outer membrane permeabilization (MOMP)" which occurs under caspase-inhibited conditions. As widely reported, VDAC1 is essential for mitochondria-mediated apoptosis [18]: for instance, it is required for full processing and activation of caspase-8 [57]. Hence, cells totally devoid of VDAC1 (ΔVDAC1) or carrying a 50% reduction in the expression level of this protein (ΔVDAC3) likely fail to undergo mitochondrial permeabilization. Accordingly, depletion of VDAC1 or VDAC2 by small interfering RNA have been reported to prevent mitochondrial membrane potential dissipation in H460 cells exposed to the cytotoxic isoflavone ME-344 [43]. Moreover, it is worthy of note, that the hyperpolarization of the mitochondrial inner membrane has been demonstrated to anticipate excessive ROS generation [58]. VDAC3 knock out cells effectively disclosed a significant boost in mitochondrial ROS under physiological conditions, as previously observed in H460 cells where VDAC3 was reduced by silencing [43]. This finding perfectly matches with changes in the expression levels of the main intracellular antioxidant enzymes that were all up-regulated within HAP1-ΔVDAC3 cells: this is evidence of an enhanced imbalance between production and accumulation of intracellular ROS. The absence of VDAC1 also increased catalase and thioredoxin expression, although, differently from VDAC3 depletion, down-regulated SOD1 and lowered the basal level of mitochondrial ROS.

Treatments with drugs triggering mitochondrial ROS generation clearly pointed out the extreme vulnerability of cells lacking VDAC3 compared to the control and to the cells devoid of VDAC1. Consistent with these observations, the parental cell line drastically overexpressed VDAC3 in response to prolonged exposure to rotenone, menadione and paraquat, stressing the importance of this specific VDAC isoform in fighting oxidative stress. To this regard, it should be outlined that, under physiological conditions, VDAC3 transcript is the less abundant isoform, despite its promoter retains the greater transcriptional activity compared to those of VDAC1 and VDAC2 [59]. As proposed by Zinghirino et al. [59], this discrepancy could be related to the minor stability of VDAC3 transcripts. Alternatively, cells would maintain the activity of VDAC3 promoter constitutively high in order to promptly increase protein expression upon specific stimuli [59]. However, the mechanism by which VDAC3 is up-regulated following oxidative insults needs to be elucidated: in the light of above, we speculate that this mechanism may include both an increase of mRNA stability and the modulation of gene expression, through the use of a polypyrimidine stretch localized within VDAC3 promoter and identified as a target of oxidative and metabolic stress [60].

Furthermore, HAP1-ΔVDAC3 mitochondria showed the highest increment in superoxide content, upon rotenone and menadione challenge, which proves they failed to counterbalance the overproduction of free-radical species. Rotenone and menadione also induced a sharp collapse of $\Delta\Psi_m$ in these cells suggesting a severe impaired mitochondrial function. Paraquat did not generate the same output, presumably because of VDAC1 down-regulation associated to VDAC3 depletion. VDAC1 is indeed fundamental for paraquat-mediated cytoxicity as, upon toxin-mediated redox cycling, VDAC1-deficient mitochondria experience the lowest amount of superoxide [43]. The role of rotenone, menadione and paraquat-generated mitochondrial ROS in apoptosis has been confirmed [45,61,62]. Our MTT assays proved that, after drug treatments, VDAC3 depletion yields the lowest cell viability compared to the other cell lines. These data, at first suggesting just a greater propension of VDAC3 K.O. cells to apoptosis, are particularly meaningful as removal of isoform 3 is accompanied by the down-regulation of the pro-apoptotic VDAC1 and the up-regulation of the anti-apoptotic VDAC2. Complementation of HAP1-ΔVDAC3, by reintroducing the wild type protein, restored most of the analyzed parameters approximately to levels measured in the HAP1 parental cell line. Interestingly, removal of all cysteine residues abolishes the protective effect of VDAC3 against mitochondrial oxidative damage, leaving only the canonical pore-forming activity [22,23,25,26]. This undoubtedly implies that the involvement of VDAC3 in mitochondrial ROS-sensing is strictly dependent on its cysteine content. HRR measurements of HAP1 cells challenged by ROS producing drugs additionally supported our conclusions. VDAC3 knock out significantly affected mitochondrial respiration of HAP1 cells exposed to rotenone, even at sublethal doses. Interestingly, we found that at nanomolar concentration rotenone promotes only a partial and not significant inhibition of complex I activity, with no effect on cell viability, but a still significative impact for mitochondrial ROS production. 10 nM rotenone had a negligible impact on oxygen flow of HAP1 parental or HAP1-ΔVDAC3 cells transfected with a plasmid encoding VDAC3, while dramatically affecting oxygen consumption of cells transfected with the empty vector. This suggests that VDAC3 is essential for the proper functioning of mitochondria upon oxidative stress. This finding is reinforced by two distinct aspects. First, no comparable effects were observed upon exposure to myxothiazol. Similarly, to rotenone, myxothiazol promoted a significant inhibition of ETS in a dose-dependent manner without increasing mitochondrial ROS production. In this case, the absence of VDAC3 had no effect for oxygen consumption, once again underlining the pivotal role of VDAC3 in counteracting ROS triggered by rotenone. Second, the expression of the cys-null VDAC3 in HAP1-ΔVDAC3 cells did not restore the physiological oxygen flow in presence of endogenous substrates, while partially improved oxygen consumption of permeabilized VDAC3 knock out cells. This indicates that the absence of cysteine residues makes VDAC3 unable to efficiently counteract the rotenone effect. The partial improvement in oxygen flows here observed could depends on the cys-null mutant ability to form canonical VDAC-like channels [23,26]. It has been recently shown that VDAC overexpression counteracts mitochondrial respiratory impairment by increasing the availability of adenylates and substrates. As a result, the respiration was overall improved [63]. Anyhow, cys-null VDAC3 is not able to fully recover oxygen flow as VDAC3, and this strengthens once again the pivotal role exerted by cysteine residues.

In conclusion, as hypothesized before [29–31], we demonstrate that VDAC3 protects mitochondria from oxidative stress-induced impairment, although the underlying molecular mechanism remains elusive. In particular, experimental results obtained with the VDAC3 mutant completely devoid of cysteine residues suggest that these amino acids are crucial for the protein ability to perceives changes in the amount of mitochondrial reactive oxygen species. Accumulation of oxidative modifications within VDAC3 cysteines may be used indeed as a *redox-state marker* of mitochondria by inducing conformational changes which, in turn, could signal the ROS load of the single mitochondrion to other proteins or organelles. Accordingly, VDAC3 could contribute to mitochondrial quality control in two ways: i) over-oxidated VDAC3 may undergo ubiquitination [64] and promote the clearance of defective mitochondria or, ii), ROS-induced conformational changes could drive protein incorporation into membranous structures secreted by mitochondria under oxidative stress called mitochondria-derived vesicles (MDVs), that participate in maintaining a healthy and functional mitochondrial network. Another possible explanation is that, in response to increased levels of mitochondrial ROS, VDAC3 is "sacrified" through the retro-translocation pathway (N-end rule pathway) which translocates a protein containing an oxidated N-terminal cysteine (i.e. VDAC3 contains a cys in position 2 which becomes the actual N-terminal residue following removal of the starting methionine) to the cytosolic proteasome for its degradation [12]. The lack of evidence of VDAC3 cys2 oxidation, suggests, that indeed, each protein containing this altered amino acid residue could be immediately destroyed by the N-end rule pathway. To this regard, Messina et al. [32], identified the valosin-containing protein (VCP) also known as transitional endoplasmic reticulum ATPase (TER ATPase) or p97 in mammals, as a VDAC3 interactor. VCP is part of the ubiquitin-proteasome system [65] and is also required for the proper functioning of the lysosomal system and autophagy [66], hence it is involved in the "extraction" of proteins

from the outer mitochondrial membrane (OMM) and other membranes to be subsequently ubiquitinated and degraded.

4. Methods

4.1. Cell culture and treatment

Near-haploid human HAP1 cell (C631), and derived cell lines HAP1 VDAC1 knock out (HZGHC005706c002) and HAP1 VDAC3 knock out (HZGHC005689c006) cells were obtained from Horizon Discovery. Knockout clones were edited by CTRISPR/Cas system. VDAC1 knock out clone contains a 2 pb deletion in exon 6 while, VDAC3 knock out clone contains a 17 bp deletion in exon 7. HAP1 cell lines were maintained at 37 °C in the presence of 5% CO2 in Iscove's modified Dulbecco's media (IMDM) supplemented with 10% (v/v) fetal bovine serum (FBS), 100 U/ml penicillin and 100 μg/ml streptomycin. Each cell line was treated with different compound: Menadione (15 or 25 μM dissolved in 0,01% DMSO) for 3 h; Rotenone (50 or 100 μM dissolved in 0,01% DMSO) for 24 h and Paraquat (50, 100 or 500 μM dissolved in H_2O) for 24 h. Subsequently, the cells were used for cell viability assay describe below.

4.2. Cell viability assay

Cell viability was evaluated by 3-(4,5-dimethylthiazolyl-2)-2,5-diphenyltetrazoliumbromide (MTT) assay. HAP1 cell lines were plated in 96-well plates at 10,000 cell/well and after 24 h received the indicated treatment. Subsequently, MTT was added to the culture medium to reach final concentration of 5 mg/ml. After incubation at 37 °C for 3 h, the medium was removed and the formazan crystals produced were dissolved by adding 100 μl of dimethyl sulfoxide. The absorbance at 590 nm was determined using the microplates reader Varioskan (Thermo Scientific). Data were statistically analyzed by two-way ANOVA followed by Dunnett's multiple comparisons test.

4.3. Quantitative Real-time PCR

Quantitative Real-time PCR was used to analyze the level of expression of the following genes: VDAC1, VDAC2, VDAC3, NRF-1, TFAM, PCG-1α. Total RNA was extracted using TRIzol® Reagent (ThermoFisher Scientific) according to manufacturer's instructions. RNA concentration and purity were measured by a spectrophotometer and 1 μg was used to synthesize cDNA by QuantiTect Reverse Transcription kit (Qiagen). For each experiment, three independent Real-Time PCR runs were performed in triplicate using the QuantiTec SYBR Green PCR Kit (QIAGEN). Analysis was performed in the Mastercycler ep realplex (Eppendorf) in 96-well plates. Thermocycling program consisted in a first activation at 95 °C for 15 min, followed by 40 cycles at 95 °C for 15 s, annealing at 57 °C for 15 s, extension at 68 °C for 15 s and a final step at 72 °C for 10 min. Analysis of relative expression level was performed using the housekeeping β-actin gene as internal calibrator by the ΔΔCt method [67]. Data were statistically analyzed by one-way ANOVA followed by Dunnett's multiple comparisons test.

4.4. Mitochondrial DNA analysis

To determinate the relative amount of mitochondrial DNA in the HAP1 cell lines, total DNA was extracted as described in Ref. [68]. Briefly, total DNA (20 ng) was used as a template in real-time PCR with primers for the COXII gene in mitochondrial DNA and nuclear gene for APP. Analysis of mtDNA/nDNA ratio was calculated by following the classical ΔΔCt method. Data were statistically analyzed by one-way ANOVA.

4.5. Measurement of the mitochondrial membrane potential, mitochondrial mass and mitochondrial superoxide

$\Delta\Psi_m$ was measured using alternatively two different probes suitable for determining mitochondrial membrane potential changes: tetramethyl-rhodamine methyl ester (TMRM), and Mito Tracker red. Both probes accumulate into active mitochondria due their positive charge whereby the reduction of $\Delta\Psi_m$ leads to the release of them. Conventional fluorescent stains for mitochondria, such as TMRM, are readily sequestered by functioning mitochondria and they are subsequently washed out of the cells once the mitochondrion's membrane potential is lost. This characteristic makes TMRM very useful in experiments where sudden changes must be detected. However, when using dual staining of mitochondria, TMRM should be used paying attention to its spectral features. Here we used the Mito Tracker Green (ThermoFisher) probe that allow measurements of mitochondrial mass being a probe that accumulates into mitochondria independently of the mitochondrial membrane potential status. Thus, when using flow cytometry, values measured for mitochondrial membrane potential could be normalized to the mitochondrial content per cell. In this case, to avoid false interpretation of results due to the overlap between Mito tracker Green emission spectrum and TMRM excitation spectrum, we used Mito tracker red, because of its spectral properties which allow a better signal detection when using simultaneously to others green probes.

After treatments, adherent cells were washed with PBS and then incubated for 30 min at 37 °C with Krebs Ringer Buffered Saline (130 mM NaCl, 3.6 mM KCl, 10 mM HEPES, 2 mM $NaHCO_3$, 0.5 mM NaH_2PO_4, 0.5 mM $MgCl_2$, 1.5 mM $CaCl_2$, 4.5 g/l glucose, pH 7.42) supplemented with mitochondrial probes (either 200 nM TMRM or 300 nM Mito tracker Green and 300 nm Mito tracker Red). In all cases 20 μM verapamil were added as a multi drug-resistant pump inhibitor (Sigma). Cells were then detached by a short treatment with trypsin–EDTA, resuspended in the above described buffer, supplemented with 1% FCS to neutralize the trypsin and immediately analyzed on a CyFlow® ML flow cytometer (Partec) in FL3 and FL1 log mode. Only viable cells detected by reading the scattering indicated as FSC and SSC, were considered for our analysis.The threshold physiological value of $\Delta\Psi_m$ was estimated by using cells exposed to 10 μM of the uncoupling agent FCCP as a negative control. Compensation algorithms were applied between FL1 and FL3 channels, when signals from Mito tracker Green and Mito tracker Red were read in the same cells, to normalize $\Delta\Psi_m$/mitochondrion/cell.

Mitochondrial superoxide, was measured by using MitoSOX Red (ThermoFisher) whose specificity for superoxide has been shown by the manufacturer. Briefly, cells were stained with 5 μM MitoSOX Red in Krebs Ringer Buffered Saline for 10 min at 37 °C, and FL2 median fluorescence intensity was measured by flow cytometry.

4.6. Growth curve

The day 0, 80000 cells from each HPA1 cell lines (parental, DVDAC1 and DVADC3) were seeded in 12 well plates. Then cells were collected and counted each 24h for 5 days by using flow cytometry. The CyFlow® ML analyses concentrations of any particle or cell subpopulations of interest using True Volumetric Absolute Counting. This unique method is solely based on the fundamental definition of absolute counting respectively the particle concentration (c) which is equal to the counted number (N) of particles (e.g. cells) in a given volume (V), $c = N/V$. In the CyFlow® ML, the volume is measured directly by mechanical means, rather than by calibration with expensive beads eliminating any errors related to varying bead concentrations or bead aggregation. The CyFlow® ML allows the analysis of a fixed volume as defined by the distance between two platinum electrodes reaching into the sample tube with a given diameter.

4.7. Flow cytometry

20,000 cells per sample were analyzed using a CyFlow® ML flow cytometer (Partec) system equipped with three laser sources and 10 optical parameters with dedicated filter settings and a high numerical aperture microscope objective (50 × NA 0.82) for the detection of different scatter and fluorescence signals. The cells were excited by an air-cooled argon 488 nm laser and then the signal from Mitotracker Green was read on FL1, Mitosox on FL2, detectors while the signal from TMRM, Mitotracker Red DsRed on FL3 detector. Data obtained were acquired, gated, compensated, and analyzed using the FlowMax software (Partec) and FCS Express 4 software (DeNovo). Data reported were obtained for three sets of independent experiments, each performed in triplicate and based on 20,000 events for each group. Cytometric profiles reported in each Figure are representative of one of the three sets of measurements. Data were statistical analyzed by chi-square test. A $p <$ 0,001 was taken as significant.

4.8. Western blots

1×10^6 cells for each line were collected and lysed in extraction buffer (50 mM Tris pH 7.4, 150 mM NaCl, EDTA 1 mM, 1% TRITON X-100 and protease inhibitors). After lysis, the supernatant was collected and the protein content was measured in triplicate using the Bradford reagent with bovine serum albumin (BSA) as a standard. 50 μg of total protein of each sample were separated using SDS/PAGE electrophoresis, transferred to a PDVF membrane (Amersham Hybond P 0.45; GE Healthcare Life Sciences) and blocked in 2,5% BSA at room temperature for 1h. The membranes were incubated overnight at 4 °C with primary antibodies against VDAC1 (1:1000, ab34726, Abcam), VDAC1 (1:200, ab154856, Abcam), VDAC2 (1:300, ab37985, Abcam), VDAC3 (1:100, ab130561, Abcam), COX IV (1:3000 #3E11, Cell Signaling Technology), HA-Tag (1:1000, #3724, Cell Signaling Technology), Oxidative Stress Defense (Catalase, SOD1, TRX, smooth muscle Actin) western blot cocktail (1:1000, ab179843, Abcam), SDHA (1:000, ab14715, Abcam), β-Actin (1:1000, #3700, Cell Signaling Technology), β-Tubulin (1:2000, #2146, Cell Signaling Technology) and after the washing step with secondary antibodies IRDye® 800CW Donkey anti-Mouse IgG (1:20000, 926–32212, Li-Cor Biosciences), IRDye® 680RD Donkey anti-Rabbit IgG (1:20000, 926–68073, Li-Cor Biosciences) and IRDye® 800CW Donkey anti-Goat IgG (1:20000, 926–32214, Li-Cor Biosciences). The membranes were scanned using the Odyssey CLx imaging system (Li-Cor Biosciences). Data were analyzed with ImageStudioLite software (Li-Cor Biosciences) and β-Tubulin or β-Actin was used as an internal control for normalizing protein loading. Data were statistically analyzed by one-way ANOVA followed by Dunnett's multiple comparisons test.

4.9. Cell transfection

HAP1 ΔVDAC3 cells were transfected with the pCMS-MtDsRed [69] carrying the encoding sequence of human VDAC3 or VDAC3 C0A in frame with the HA-tag at the C-terminus. The empty pCMS plasmid was used as control. Cells were seeded in a 6-well or 96-well plates and transfected using 5 μg DNA per well by Lipofectamine 3000 (Life Technologies) according to manufacturer's instructions. Further analyzes were performed after 48 h.

4.10. Indirect immunofluorescence of adherent cells

In order to detect the expression of VDAC3, following transfection with pCMS-MtDsRed-VDAC3-HA, we used indirect immunofluorescence. 48h post-transfection, cells growth on coverslips, were fixed in 4% formaldehyde, washed three times in PBS 1x, and incubated 10 min in 50 mM NH_4Cl. Cells were then permeabilized by using 0.3% Triton X-100. Unspecific binding was blocked by 30 min in 0.2% gelatine in PBS. To detect the expression and localization of VDAC3-HA in mtDsRed overexpressing cells, coverslips were incubated overnight with anti-HA (rabbit 1:100, Santa Cruz Biotechnology, Inc.). After PBS washing, cells were exposed for 1h at RT to the secondary anti-rabbit antibody AlexaFluor 488. After PBS washing, cells were exposed for 1 h at RT to the secondary antibody (anti-rabbit 1:2000, ThermoFischer). Coverslips were mounted by using DAPI-Fluoromount-G to stain nuclear DNA. Co-localization with mitochondria was obtained by merging the HA signal with the signal from the fluorescent reporter mtDsRed. A Leica DMI 6000B epifluorescence inverted microscope with Adaptive Focus Control was used. This system is outfitted with a controllable X-cite mercury lamp and an extensive collection of filter cubes (360, 488, 560, 604 nm excitation) for fluorescent microscopy, and a halogen lamp for bright field and DIC. It is equipped with 4 bright lenses (10, 20, 40, 63x), a high-resolution Hamamatsu Orca R2 CCD camera (1344 × 1024 pixels), and motorized stage (XY only). Images were obtained by using the Leica LAS Extended Annotation software.

4.11. High-Resolution Respirometry

Effect of rotenone and myxothiazol for the respiratory capacity of parental or ΔVDAC3 HAP1 cells was investigated by High-Resolution Respirometry using the two-chamber system O2k-FluoRespirometer (Oroboros Instruments). Parental HAP1 were exposed for 24 h to increasing concentration of rotenone or myxothiazol ranging from 10 nM to 10 μM. 24 h transfected ΔVDAC3 HAP1 cells were incubated with 10 nM rotenone, 10 nM myxothiazol or DMSO for additional 24 h and the respiratory states were then determined by a specific substrate-uncoupler-inhibitor titration (SUIT) protocol modified from Ref. [58]. Briefly, oxygen consumption in intact cells was first analyzed. Next, plasma membranes were permeabilized with 4 μM digitonin, without disturbing mitochondrial membranes, and the oxygen flow related to oxidative phosphorylation driven by the complex I activity (N-pathway) was attained by the addition of pyruvate (5 mM), glutamate (10 mM), malate (2 mM) and ADP (2.5 mM). The maximal capacity of electron transport (ET) was finally determined by titration with the uncoupler carbonyl cyanide 3-chlorophenylhydrazone (CCCP, 0.5 μM) up to the complete dissipation of the proton gradient. The activity of the respiratory chain enzymes was inhibited by the addition of 100 mM sodium azide. All substrates were purchased by Sigma Aldrich.

At least three independent experiments for each condition tested were performed in mitochondrial respiration buffer Mir05 (Oroboros Instruments) at 37 °C under constant stirring of 750 rpm. Instrumental and chemical background fluxes were calibrated as a function of the oxygen concentration using DatLab software (Oroboros Instruments). Oxygen consumption in intact cells or correspondent to N-pathway and maximal ET capacity in cells exposed to rotenone or myxothiazol was expressed as pmol/s per million cells and normalized to their respective untreated controls.

4.12. Statistical analysis

Data are presented as mean ± standard error of the mean (SEM). Dependent variables were analyzed by one-way or two-way ANOVA followed by Dunnett's multiple comparisons test using GraphPad Prism version 9.0.0 (GraphPad Software, San Diego, California USA). A value of $P < 0.05$ was considered significant. In particular, * indicates a $P <$ 0.05, ** indicates a $P < 0.01$, *** indicates a $P < 0.001$.

Author contributions

S.R. designed and supervised the experiments and analyzed the results. S.C.N. performed cell cultures, western blot and prepared figures. M.F.T. performed the flow cytometry experiments. A. Magrì conducted the high resolution respirometry measurements. S.R. and V.D.P wrote the original draft of the manuscript. M.F.T., A. Magrì., S.C.N. and A. Messina reviewed and edited the text. The authors acknowledge Rigel

Villagonzalo Rountree for language editing.

Fundings

The authors acknowledge funding by the Italian Ministry of University and Research to project Proof of Concept 2018, grant number PEPSLA POC 01_00054 (to A.M.), the University of Catania - linea PIACERI, grant number ARVEST (to A.M) and the AIM Linea 1-Salute (AIM1833071).

Declaration of competing interest

The authors declare that they have no affiliations with or involvement in any organization or entity with any financial interest (such as honoraria; educational grants; participation in speakers' bureaus; membership, employment, consultancies, stock ownership, or other equity interest; and expert testimony or patent-licensing arrangements), or non-financial interest (such as personal or professional relationships, affiliations, knowledge or beliefs) in the subject matter or materials discussed in this manuscript.

Appendix A. Supplementary data

Supplementary data to this article can be found online at https://doi.org/10.1016/j.redox.2022.102264.

References

[1] J.F. Turrens, Mitochondrial formation of reactive oxygen species, J. Physiol. 552 (2003) 335–344, https://doi.org/10.1113/jphysiol.2003.049478.
[2] R.S. Balaban, S. Nemoto, T. Finkel, Mitochondria, oxidants, and aging, Cell 120 (2005) 483–495, https://doi.org/10.1016/j.cell.2005.02.001.
[3] V. Adam-Vizi, C. Chinopoulos, Bioenergetics and the formation of mitochondrial reactive oxygen species, Trends Pharmacol. Sci. 27 (2006) 639–645, https://doi.org/10.1016/j.tips.2006.10.005.
[4] M.P. Murphy, Mitochondrial thiols in antioxidant protection and redox signaling: distinct roles for glutathionylation and other thiol modifications, Antioxidants Redox Signal. 16 (2012) 476–495, https://doi.org/10.1089/ars.2011.4289.
[5] E.-M. Hanschmann, J.R. Godoy, C. Berndt, C. Hudemann, C.H. Lillig, Thioredoxins, glutaredoxins, and peroxiredoxins–molecular mechanisms and health significance: from cofactors to antioxidants to redox signaling, Antioxidants Redox Signal. 19 (2013) 1539–1605, https://doi.org/10.1089/ars.2012.4599.
[6] J.N. Peoples, A. Saraf, N. Ghazal, T.T. Pham, J.Q. Kwong, Mitochondrial dysfunction and oxidative stress in heart disease, Exp. Mol. Med. 51 (2019) 1–13, https://doi.org/10.1038/s12276-019-0355-7.
[7] W.-X. Ding, X.-M. Yin, Mitophagy: mechanisms, pathophysiological roles, and analysis, Biol. Chem. 393 (2012) 547–564, https://doi.org/10.1515/hsz-2012-0119.
[8] T. Shpilka, C.M. Haynes, The mitochondrial UPR: mechanisms, physiological functions and implications in ageing, Nat. Rev. Mol. Cell Biol. 19 (2018) 109–120, https://doi.org/10.1038/nrm.2017.110.
[9] P. Storz, H. Döppler, A. Toker, Protein kinase D mediates mitochondrion-to-nucleus signaling and detoxification from mitochondrial reactive oxygen species, Mol. Cell Biol. 25 (2005) 8520–8530, https://doi.org/10.1128/MCB.25.19.8520-8530.2005.
[10] P. Storz, Mitochondrial ROS–radical detoxification, mediated by protein kinase D, Trends Cell Biol. 17 (2007) 13–18, https://doi.org/10.1016/j.tcb.2006.11.003.
[11] S. Reina, V. Checchetto, R. Saletti, A. Gupta, D. Chaturvedi, C. Guardiani, F. Guarino, M.A. Scorciapino, A. Magrì, S. Foti, M. Ceccarelli, A.A. Messina, R. Mahalakshmi, I. Szabo, V. De Pinto, VDAC3 as a sensor of oxidative state of the intermembrane space of mitochondria: the putative role of cysteine residue modifications, Oncotarget 7 (2016) 2249–2268, https://doi.org/10.18632/oncotarget.6850.
[12] S. Reina, F. Guarino, A. Magrì, V. De Pinto, VDAC3 as a potential marker of mitochondrial status is involved in cancer and pathology, Front. Oncol. 6 (2016) 264, https://doi.org/10.3389/fonc.2016.00264.
[13] M.C. Brahimi-Horn, S. Giuliano, E. Saland, S. Lacas-Gervais, T. Sheiko, J. Pelletier, I. Bourget, F. Bost, C. Féral, E. Boulter, M. Tauc, M. Ivan, B. Garmy-Susini, A. Popa, B. Mari, J.-E. Sarry, W.J. Craigen, J. Pouysségur, N.M. Mazure, Knockout of Vdac1 activates hypoxia-inducible factor through reactive oxygen species generation and induces tumor growth by promoting metabolic reprogramming and inflammation, Cancer Metabol. 3 (2015) 8, https://doi.org/10.1186/s40170-015-0133-5.
[14] D. Han, F. Antunes, R. Canali, D. Rettori, E. Cadenas, Voltage-dependent anion channels control the release of the superoxide anion from mitochondria to cytosol, J. Biol. Chem. 278 (2003) 5557–5563, https://doi.org/10.1074/jbc.M210269200.
[15] N. Roos, R. Benz, D. Brdiczka, Identification and characterization of the pore-forming protein in the outer membrane of rat liver mitochondria, Biochim. Biophys. Acta 686 (1982) 204–214, https://doi.org/10.1016/0005-2736(82)90114-6.
[16] M. Colombini, E. Blachly-Dyson, M. Forte, VDAC, a channel in the outer mitochondrial membrane, Ion Channel. 4 (1996) 169–202, https://doi.org/10.1007/978-1-4899-1775-1_5.
[17] G.C. Shore, Apoptosis: it's BAK to VDAC, EMBO Rep. 10 (2009) 1311–1313, https://doi.org/10.1038/embor.2009.249.
[18] V. Shoshan-Barmatz, E.N. Maldonado, Y. Krelin, VDAC1 at the crossroads of cell metabolism, apoptosis and cell stress, Cell Stress 1 (2017) 11–36, https://doi.org/10.15698/cst2017.10.104.
[19] A. Messina, S. Reina, F. Guarino, V. De Pinto, VDAC isoforms in mammals, Biochim. Biophys. Acta 1818 (2012) 1466–1476, https://doi.org/10.1016/j.bbamem.2011.10.005.
[20] R. Benz, Permeation of hydrophilic solutes through mitochondrial outer membranes: review on mitochondrial porins, Biochim. Biophys. Acta 1197 (1994) 167–196, https://doi.org/10.1016/0304-4157(94)90004-3.
[21] X. Xu, W. Decker, M.J. Sampson, W.J. Craigen, M. Colombini, Mouse VDAC isoforms expressed in yeast: channel properties and their roles in mitochondrial outer membrane permeability, J. Membr. Biol. 170 (1999) 89–102, https://doi.org/10.1007/s002329900540.
[22] V. Checchetto, S. Reina, A. Magrì, I. Szabo, V. De Pinto, Recombinant human voltage dependent anion selective channel isoform 3 (hVDAC3) forms pores with a very small conductance, Cell. Physiol. Biochem. 34 (2014) 842–853, https://doi.org/10.1159/000363047.
[23] M. Queralt-Martín, L. Bergdoll, O. Teijido, N. Munshi, D. Jacobs, A.J. Kuszak, O. Protchenko, S. Reina, A. Magrì, V. De Pinto, S.M. Bezrukov, J. Abramson, T. K. Rostovtseva, A lower affinity to cytosolic proteins reveals VDAC3 isoform-specific role in mitochondrial biology, J. Gen. Physiol. 152 (2020), e201912501, https://doi.org/10.1085/jgp.201912501.
[24] S. Conti Nibali, M.C. Di Rosa, O. Rauh, G. Thiel, S. Reina, V. De Pinto, Cell-free electrophysiology of human VDACs incorporated into nanodiscs: an improved method, Biophys Rep 1 (2021), https://doi.org/10.1016/j.bpr.2021.100002. None.
[25] S. Reina, V. Palermo, A. Guarnera, F. Guarino, A. Messina, C. Mazzoni, V. De Pinto, Swapping of the N-terminus of VDAC1 with VDAC3 restores full activity of the channel and confers anti-aging features to the cell, FEBS Lett. 584 (2010) 2837–2844, https://doi.org/10.1016/j.febslet.2010.04.066.
[26] S. Reina, V. Checchetto, R. Saletti, A. Gupta, D. Chaturvedi, C. Guardiani, F. Guarino, M.A. Scorciapino, A. Magrì, S. Foti, M. Ceccarelli, A.A. Messina, R. Mahalakshmi, I. Szabo, V. De Pinto, VDAC3 as a sensor of oxidative state of the intermembrane space of mitochondria: the putative role of cysteine residue modifications, Oncotarget 7 (2016) 2249–2268, https://doi.org/10.18632/oncotarget.6850.
[27] M. Okazaki, K. Kurabayashi, M. Asanuma, Y. Saito, K. Dodo, M. Sodeoka, VDAC3 gating is activated by suppression of disulfide-bond formation between the N-terminal region and the bottom of the pore, Biochim. Biophys. Acta 1848 (2015) 3188–3196, https://doi.org/10.1016/j.bbamem.2015.09.017.
[28] V. De Pinto, S. Reina, A. Gupta, A. Messina, R. Mahalakshmi, Role of cysteines in mammalian VDAC isoforms' function, Biochim. Biophys. Acta 1857 (2016) 1219–1227, https://doi.org/10.1016/j.bbabio.2016.02.020.
[29] S. Reina, M.G.G. Pittalà, F. Guarino, A. Messina, V. De Pinto, S. Foti, R. Saletti, Cysteine oxidations in mitochondrial membrane proteins: the case of VDAC isoforms in mammals, Front. Cell Dev. Biol. 8 (2020) 397, https://doi.org/10.3389/fcell.2020.00397.
[30] R. Saletti, S. Reina, M.G.G. Pittalà, R. Belfiore, V. Cunsolo, A. Messina, V. De Pinto, S. Foti, High resolution mass spectrometry characterization of the oxidation pattern of methionine and cysteine residues in rat liver mitochondria voltage-dependent anion selective channel 3 (VDAC3), Biochim. Biophys. Acta Biomembr. 1859 (2017) 301–311, https://doi.org/10.1016/j.bbamem.2016.12.003.
[31] M.G.G. Pittalà, R. Saletti, S. Reina, V. Cunsolo, V. De Pinto, S. Foti, A high resolution mass spectrometry study reveals the potential of disulfide formation in human mitochondrial voltage-dependent anion selective channel isoforms (hVDACs), Int. J. Mol. Sci. 21 (2020) E1468, https://doi.org/10.3390/ijms21041468.
[32] A. Messina, S. Reina, F. Guarino, A. Magrì, F. Tomasello, R.E. Clark, R.R. Ramsay, V. De Pinto, Live cell interactome of the human voltage dependent anion channel 3 (VDAC3) revealed in HeLa cells by affinity purification tag technique, Mol. Biosyst. 10 (2014) 2134–2145, https://doi.org/10.1039/c4mb00237g.
[33] L. Bleier, I. Wittig, H. Heide, M. Steger, U. Brandt, S. Dröse, Generator-specific targets of mitochondrial reactive oxygen species, Free Radic. Biol. Med. 78 (2015) 1–10, https://doi.org/10.1016/j.freeradbiomed.2014.10.511.
[34] L. Zou, V. Linck, Y.-J. Zhai, L. Galarza-Paez, L. Li, Q. Yue, O. Al-Khalili, H.-F. Bao, H.-P. Ma, T.L. Thai, J. Jiao, D.C. Eaton, Knockout of mitochondrial voltage-dependent anion channel type 3 increases reactive oxygen species (ROS) levels and alters renal sodium transport, J. Biol. Chem. 293 (2018) 1666–1675, https://doi.org/10.1074/jbc.M117.798645.
[35] P. Jóźwiak, P. Ciesielski, E. Forma, K. Kozal, K. Wójcik-Krowiranda, Ł. Cwonda, A. Bieńkiewicz, M. Bryś, A. Krześlak, Expression of voltage-dependent anion channels in endometrial cancer and its potential prognostic significance, Tumour Biol. 42 (2020), https://doi.org/10.1177/1010428320951057, 1010428320951057.
[36] C. Lee, J.S. Nam, C.G. Lee, M. Park, C.-M. Yoo, H.-W. Rhee, J.K. Seo, T.-H. Kwon, Analysing the mechanism of mitochondrial oxidation-induced cell death using a multifunctional iridium(III) photosensitiser, Nat. Commun. 12 (2021) 26, https://doi.org/10.1038/s41467-020-20210-3.

[37] A. Magrì, M.C. Di Rosa, I. Orlandi, F. Guarino, S. Reina, M. Guarnaccia, G. Morello, A. Spampinato, S. Cavallaro, A. Messina, M. Vai, V. De Pinto, Deletion of Voltage-Dependent Anion Channel 1 knocks mitochondria down triggering metabolic rewiring in yeast, Cell. Mol. Life Sci. 77 (2020) 3195–3213, https://doi.org/10.1007/s00018-019-03342-8.
[38] A. Perl, P. Gergely, G. Nagy, A. Koncz, K. Banki, Mitochondrial hyperpolarization: a checkpoint of T-cell life, death and autoimmunity, Trends Immunol. 25 (2004) 360–367, https://doi.org/10.1016/j.it.2004.05.001.
[39] M.S. Baghel, M.K. Thakur, Vdac1 downregulation causes mitochondrial disintegration leading to hippocampal neurodegeneration in scopolamine-induced amnesic mice, Mol. Neurobiol. 56 (2019) 1707–1718, https://doi.org/10.1007/s12035-018-1164-z.
[40] N. Tajeddine, L. Galluzzi, O. Kepp, E. Hangen, E. Morselli, L. Senovilla, N. Araujo, G. Pinna, N. Larochette, N. Zamzami, N. Modjtahedi, A. Harel-Bellan, G. Kroemer, Hierarchical involvement of Bak, VDAC1 and Bax in cisplatin-induced cell death, Oncogene 27 (2008) 4221–4232, https://doi.org/10.1038/onc.2008.63.
[41] F. Tomasello, A. Messina, L. Lartigue, L. Schembri, C. Medina, S. Reina, D. Thoraval, M. Crouzet, F. Ichas, V. De Pinto, F. De Giorgi, Outer membrane VDAC1 controls permeability transition of the inner mitochondrial membrane in cellulo during stress-induced apoptosis, Cell Res. 19 (2009) 1363–1376, https://doi.org/10.1038/cr.2009.98.
[42] A. Tikunov, C.B. Johnson, P. Pediaditakis, N. Markevich, J.M. Macdonald, J. J. Lemasters, E. Holmuhamedov, Closure of VDAC causes oxidative stress and accelerates the Ca(2+)-induced mitochondrial permeability transition in rat liver mitochondria, Arch. Biochem. Biophys. 495 (2010) 174–181, https://doi.org/10.1016/j.abb.2010.01.008.
[43] L. Zhang, D.M. Townsend, M. Morris, E.N. Maldonado, Y.-L. Jiang, A.-M. Broome, J.R. Bethard, L.E. Ball, K.D. Tew, Voltage-dependent anion channels influence cytotoxicity of ME-344, a therapeutic isoflavone, J. Pharmacol. Exp. Therapeut. 374 (2020) 308–318, https://doi.org/10.1124/jpet.120.000009.
[44] H. Shimada, K.-I. Hirai, E. Simamura, T. Hatta, H. Iwakiri, K. Mizuki, T. Hatta, T. Sawasaki, S. Matsunaga, Y. Endo, S. Shimizu, Paraquat toxicity induced by voltage-dependent anion channel 1 acts as an NADH-dependent oxidoreductase, J. Biol. Chem. 284 (2009) 28642–28649, https://doi.org/10.1074/jbc.M109.033431.
[45] N. Li, K. Ragheb, G. Lawler, J. Sturgis, B. Rajwa, J.A. Melendez, J.P. Robinson, Mitochondrial complex I inhibitor rotenone induces apoptosis through enhancing mitochondrial reactive oxygen species production, J. Biol. Chem. 278 (2003) 8516–8525, https://doi.org/10.1074/jbc.M210432200.
[46] A.A. Starkov, G. Fiskum, Regulation of brain mitochondrial H2O2 production by membrane potential and NAD(P)H redox state, J. Neurochem. 86 (2003) 1101–1107, https://doi.org/10.1046/j.1471-4159.2003.01908.x.
[47] T. Tron, M. Crimi, A.M. Colson, M. Degli Esposti, Structure/function relationships in mitochondrial cytochrome b revealed by the kinetic and circular dichroic properties of two yeast inhibitor-resistant mutants, Eur. J. Biochem. 199 (1991) 753–760, https://doi.org/10.1111/j.1432-1033.1991.tb16180.x.
[48] A.M. Gusdon, G.A. Fernandez-Bueno, S. Wohlgemuth, J. Fernandez, J. Chen, C. E. Mathews, Respiration and substrate transport rates as well as reactive oxygen species production distinguish mitochondria from brain and liver, BMC Biochem. 16 (2015) 22, https://doi.org/10.1186/s12858-015-0051-8.
[49] T.V. Votyakova, I.J. Reynolds, ΔΨm-Dependent and -independent production of reactive oxygen species by rat brain mitochondria, J. Neurochem. 79 (2001) 266–277, https://doi.org/10.1046/j.1471-4159.2001.00548.x.
[50] J.F. Turrens, A. Alexandre, A.L. Lehninger, Ubisemiquinone is the electron donor for superoxide formation by complex III of heart mitochondria, Arch. Biochem. Biophys. 237 (1985) 408–414, https://doi.org/10.1016/0003-9861(85)90293-0.
[51] J. Vergalli, I.V. Bodrenko, M. Masi, L. Moynié, S. Acosta-Gutiérrez, J.H. Naismith, A. Davin-Regli, M. Ceccarelli, B. van den Berg, M. Winterhalter, J.-M. Pagès, Porins and small-molecule translocation across the outer membrane of Gram-negative bacteria, Nat. Rev. Microbiol. 18 (2020) 164–176, https://doi.org/10.1038/s41579-019-0294-2.
[52] V. De Pinto, F. Guarino, A. Guarnera, A. Messina, S. Reina, F.M. Tomasello, V. Palermo, C. Mazzoni, Characterization of human VDAC isoforms: a peculiar function for VDAC3? Biochim. Biophys. Acta 1797 (2010) 1268–1275, https://doi.org/10.1016/j.bbabio.2010.01.031.
[53] J. Gatliff, D. East, J. Crosby, R. Abeti, R. Harvey, W. Craigen, P. Parker, M. Campanella, TSPO interacts with VDAC1 and triggers a ROS-mediated inhibition of mitochondrial quality control, Autophagy 10 (2014) 2279–2296, https://doi.org/10.4161/15548627.2014.991665.
[54] V. Shoshan-Barmatz, A. Shteinfer-Kuzmine, A. Verma, VDAC1 at the intersection of cell metabolism, apoptosis, and diseases, Biomolecules 10 (2020) E1485, https://doi.org/10.3390/biom10111485.
[55] E.N. Maldonado, VDAC-tubulin, an anti-warburg pro-oxidant switch, Front. Oncol. 7 (2017) 4, https://doi.org/10.3389/fonc.2017.00004.
[56] M. Yang, J. Sun, D.F. Stowe, E. Tajkhorshid, W.-M. Kwok, A.K.S. Camara, Knockout of VDAC1 in H9c2 cells promotes oxidative stress-induced cell apoptosis through decreased mitochondrial hexokinase II binding and enhanced glycolytic stress, Cell. Physiol. Biochem. 54 (2020) 853–874, https://doi.org/10.33594/000000274.
[57] A.D. Chacko, F. Liberante, I. Paul, D.B. Longley, D.A. Fennell, Voltage dependent anion channel-1 regulates death receptor mediated apoptosis by enabling cleavage of caspase-8, BMC Cancer 10 (2010) 380, https://doi.org/10.1186/1471-2407-10-380.
[58] M. Poppe, C. Reimertz, H. Düßmann, A.J. Krohn, C.M. Luetjens, D. Böckelmann, A.-L. Nieminen, D. Kögel, J.H.M. Prehn, Dissipation of potassium and proton gradients inhibits mitochondrial hyperpolarization and cytochrome c release during neural apoptosis, J. Neurosci. 21 (2001) 4551–4563, https://doi.org/10.1523/JNEUROSCI.21-13-04551.2001.
[59] F. Zinghirino, X.G. Pappalardo, A. Messina, G. Nicosia, V. De Pinto, F. Guarino, VDAC genes expression and regulation in mammals, Front. Physiol. 12 (2021) 708695, https://doi.org/10.3389/fphys.2021.708695.
[60] C. Nepal, Y. Hadzhiev, P. Balwierz, E. Tarifeño-Saldivia, R. Cardenas, J.W. Wragg, A.-M. Suzuki, P. Carninci, B. Peers, B. Lenhard, J.B. Andersen, F. Müller, Dual-initiation promoters with intertwined canonical and TCT/TOP transcription start sites diversify transcript processing, Nat. Commun. 11 (2020) 168, https://doi.org/10.1038/s41467-019-13687-0.
[61] Y.J. Jang, J.H. Won, M.J. Back, Z. Fu, J.M. Jang, H.C. Ha, S. Hong, M. Chang, D. K. Kim, Paraquat induces apoptosis through a mitochondria-dependent pathway in RAW264.7 cells, Biomol Ther (Seoul) 23 (2015) 407–413, https://doi.org/10.4062/biomolther.2015.075.
[62] D.N. Criddle, S. Gillies, H.K. Baumgartner-Wilson, M. Jaffar, E.C. Chinje, S. Passmore, M. Chvanov, S. Barrow, O.V. Gerasimenko, A.V. Tepikin, R. Sutton, O. H. Petersen, Menadione-induced reactive oxygen species generation via redox cycling promotes apoptosis of murine pancreatic acinar cells, J. Biol. Chem. 281 (2006) 40485–40492, https://doi.org/10.1074/jbc.M607704200.
[63] A. Magrì, P. Risiglione, A. Caccamo, B. Formicola, M.F. Tomasello, C. Arrigoni, S. Zimbone, F. Guarino, F. Re, A. Messina, Small hexokinase 1 peptide against toxic SOD1 G93A mitochondrial accumulation in ALS rescues the ATP-related respiration, Biomedicines 9 (2021) 948, https://doi.org/10.3390/biomedicines9080948.
[64] Y. Sun, A.A. Vashisht, J. Tchieu, J.A. Wohlschlegel, L. Dreier, Voltage-dependent anion channels (VDACs) recruit Parkin to defective mitochondria to promote mitochondrial autophagy, J. Biol. Chem. 287 (2012) 40652–40660, https://doi.org/10.1074/jbc.M112.419721.
[65] H. Meyer, M. Bug, S. Bremer, Emerging functions of the VCP/p97 AAA-ATPase in the ubiquitin system, Nat. Cell Biol. 14 (2012) 117–123, https://doi.org/10.1038/ncb2407.
[66] J.-S. Ju, C.C. Weihl, Inclusion body myopathy, Paget's disease of the bone and fronto-temporal dementia: a disorder of autophagy, Hum. Mol. Genet. 19 (2010) R38–R45, https://doi.org/10.1093/hmg/ddq157.
[67] K.J. Livak, T.D. Schmittgen, Analysis of relative gene expression data using real-time quantitative PCR and the 2(-Delta Delta C(T)) Method, Methods 25 (2001) 402–408, https://doi.org/10.1006/meth.2001.1262.
[68] P.M. Quiros, A. Goyal, P. Jha, J. Auwerx, Analysis of mtDNA/nDNA ratio in mice, Curr. Protoc Mouse Biol. 7 (2017) 47–54, https://doi.org/10.1002/cpmo.21.
[69] M.F. Tomasello, F. Guarino, S. Reina, A. Messina, V.D. Pinto, The voltage-dependent anion selective channel 1 (VDAC1) topography in the mitochondrial outer membrane as detected in intact cell, PLoS One 8 (2013), e81522, https://doi.org/10.1371/journal.pone.0081522.

Supplementary data:

“Voltage Dependent Anion Channel 3 (VDAC3) protects mitochondria from oxidative stress”.

HAP1 parental cell line

	Untreated	10 nM Myxothiazol	Untreated	10 nM Rotenone
Routine	61.18 ± 2.32	60.32 ± 1.8	40.08 ± 1.27	35.99 ± 3.39
Leak	44.16 ± 1.58	42.64 ± 1.65	21.75 ± 1.25	23.89 ± 1.20
N-Pathway	75.36 ± 2.65	72.79 ± 2.52	50.57 ± 2.38	42.60 ± 2.55
ET-capacity	130.6 ± 7.2	120.18 ± 8.2	117.4 ± 1.79	111.4 ± 4.57
ROX	2.06 ± 0.18	3.63 ± 0.89	2.43 ± 2.30	3.79 ± 1.78

HAP1-ΔVDAC3 + empty vector

	Untreated	10 nM Myxothiazol	Untreated	10 nM Rotenone
Routine	49.80 ± 3.51	43.15 ± 3.86	46.33 ± 6.42	28.56 ± 2.35
Leak	30.98 ± 2.95	31.38 ± 2.74	39.50 ± 7.26	22.34 ± 3.09
N-Pathway	64.16 ± 4.71	49.19 ± 10.01	56.66 ± 11.30	23.35 ± 6.64
ET-capacity	102.1 ± 3.89	83.26 ± 12.37	99.02 ± 18.53	32.95 ± 1.69
ROX	2.18 ± 1.54	7.09 ± 3.06	2.05 ± 0.40	6.51 ± 1.23

HAP1-ΔVDAC3 + pCMS + VDAC3

	Untreated	10 nM Myxothiazol	Untreated	10 nM Rotenone
Routine	49.13 ± 3.89	44.84 ± 4.3	43.36 ± 1.66	43.02 ± 5.64
Leak	27.81 ± 4.33	27.75 ± 3.38	34.01 ± 7.30	39.52 ± 7.31
N-Pathway	59.35 ± 4.66	58.16 ± 3.03	55.88 ± 5.99	55.03 ± 6.17
ET-capacity	118.2 ± 7.5	104.40 ± 11.4	105.51 ± 20.44	96.84 ± 10.37
ROX	1.96 ± 2.58	2.54 ± 1.99	2.17 ± 2.02	1.59 ± 2.61

HAP1-ΔVDAC3 + pCMS + VDAC3 C0A

	Untreated	10 nM Myxothiazol	Untreated	10 nM Rotenone
Routine	57.87 ± 3.67	51.68 ± 5.8	40.49 ± 7.49	30.69 ± 8.83
Leak	28.98 ± 3.38	29.86 ± 2.77	35.33 ± 8.53	26.28 ± 6.91
N-Pathway	70.08 ± 4.65	64.73 ± 7.52	50.71 ± 5.50	35.71 ± 4.75
ET-capacity	121.06 ± 5.6	110.11 ± 9.27	99.24 ± 9.92	59.58 ± 4.78
ROX	0.43 ± 9.11	1.06 ± 2.88	1.66 ± 0.89	2.98 ± 1.74

Table S1. Respirometry flux row data. Oxygen flux calculated for each respiratory state in untreated and treated cells. Data are reported as mean ± standard deviation of independent experiments.

Sup. Figure 1 Reina et al.

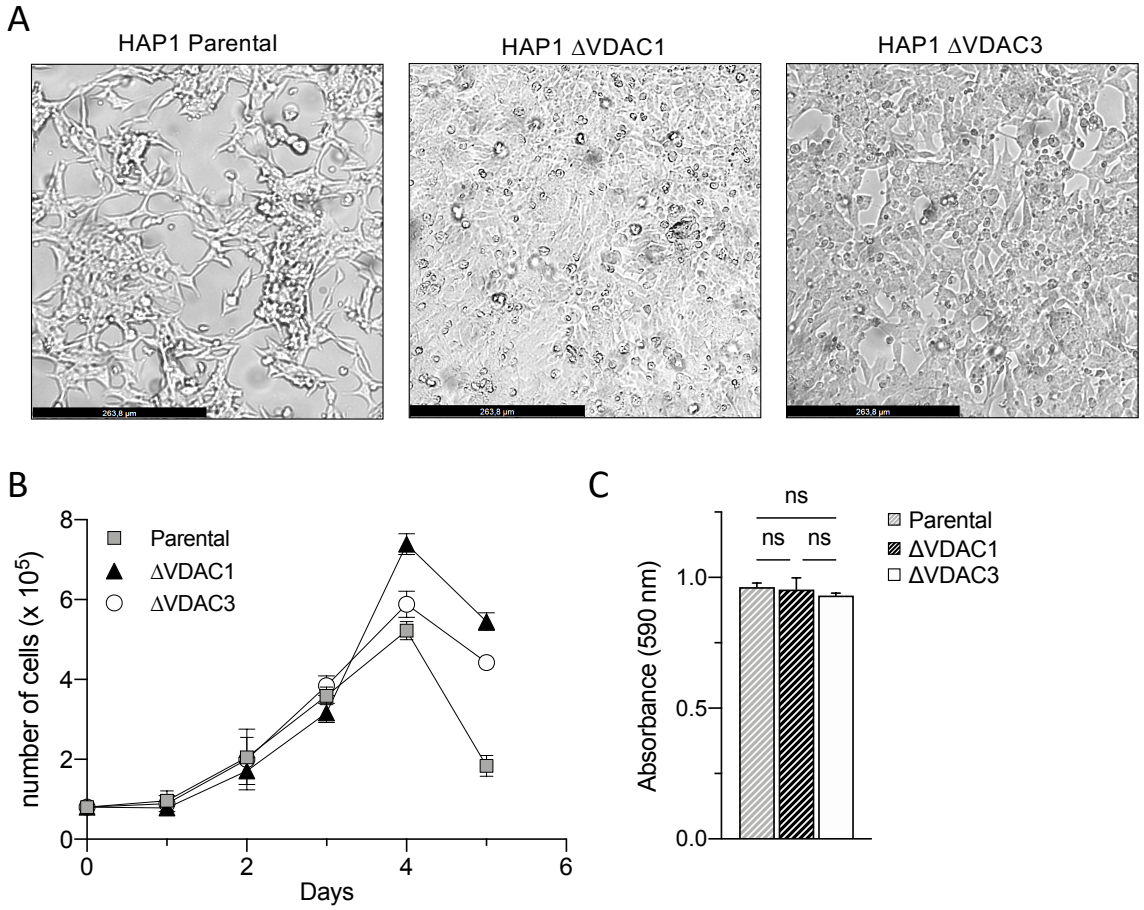

Fig. S1. **Phenotypic characterization of HAP1 cell lines.** A. Bright field images of HAP1 Parental, ΔVDAC1 and ΔVDAC3 cell lines seeding 48 before the pictures were taken. B. Proliferation of HAP1 cells measured over the time (5 days, each 24h) by flow cytometry true volumetric counting. C. Formazan absorbance expressed as a measure of the three cell lines in basal conditions. Data are expressed as mean ± SE (n = 3) and analyzed by one-way ANOVA.

Sup. Figure 2 Reina et al.

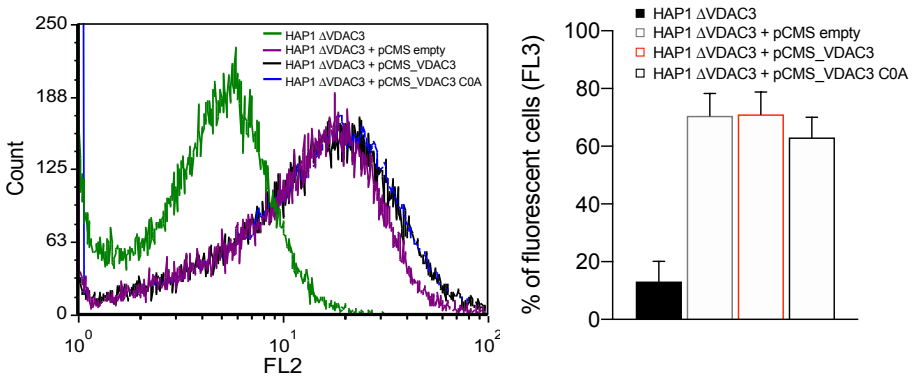

Fig. S2**.** *Mitochondrial morphology of parental and ΔVDAC3 HAP1 cell lines and flow cytometric determination of transfection efficiency***.** A. Fluorescence microscopyimaging of parental and ΔVDAC3 HAP1 mitochondria stained with the mitochondrial marker Mito Tracker Red DsRed. B. Representative fluorescence profiles evaluated by flow cytometry in HAP1- ΔVDAC3 upon cell transfection (left panel). Transfection yield of HAP1-ΔVDAC3 cells estimated by flow cytometry as the percentage of cells in FL3, based on the fluorescent emission of the transfection marker DsRed. Data are expressed as mean ± SE (n = 3).

Sup. Figure 3 Reina et al.

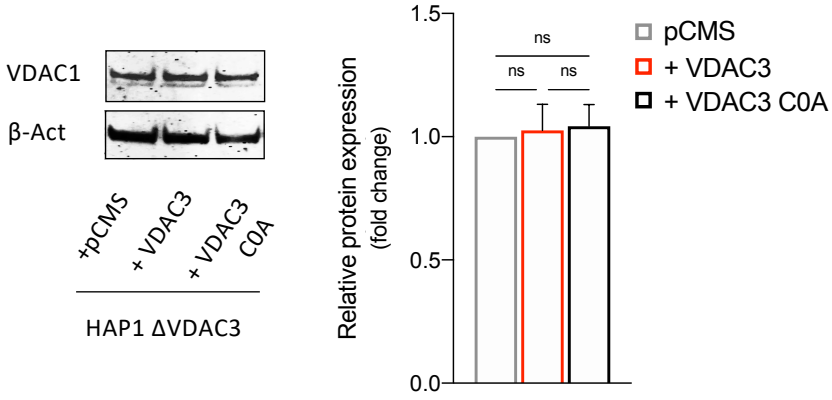

Fig. S3. Analysis of VDAC1 protein expression in HAP1-ΔVDAC3 upon cell transfection. Immunoblot and densitometry quantification of VDAC1 protein level in HAP1-ΔVDAC3 upon transfection with empty vector (pCMS) or plasmid carrying VDAC3 (+VDAC3) or VDAC3 C0A mutant (+VDAC3 C0A). Data are normalized to the β-Actin, expressed as means ± SD (n = 3) and compared to HAP1-ΔVDAC3 transfected with empty vector. Data were analyzed by one-way ANOVA.

Sup. Figure 4 Reina et al.

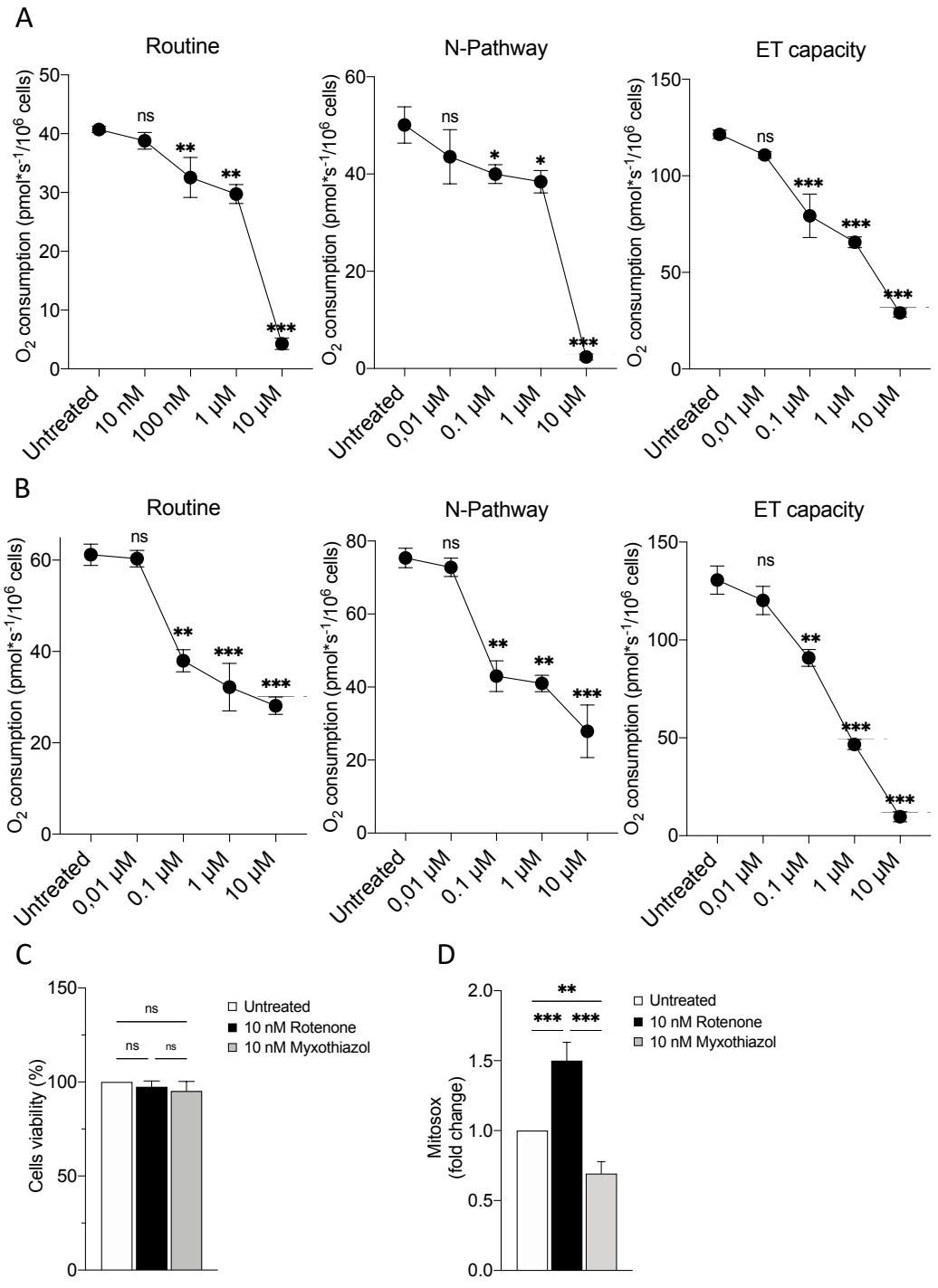

Fig. S4. Characterization of HAP1 parental cell line treated with rotenone and myxothiazol. A. Quantitative analysis of the oxygen consumption in the analyzed states of HAP1 parental cells before and after the exposure to different concentrations of rotenone. Data are expressed as means ± SD (n = 3) and compared to untreated cells. B. Quantitative analysis of the oxygen consumption in the analyzed states of HAP1 parental cells before and after the exposure to different concentrations of myxothiazol. Data are expressed as means ± SD (n = 3) and compared to untreated cells. C. Cell viability of HAP1 cell lines treated with 10 nM rotenone or 10 nM myxothiazol. Data are indicated as the mean ± SE (n = 3) and compared to untreated cells. D. Measurement of mitochondrial superoxide production via staining with MitoSOX Red after treatments with 10 nM rotenone or 10 nM myxothiazol. Data were expressed as mean ± SD (n = 3) and compared to untreated cells. Data were analyzed by one-way ANOVA, with *p < 0.05, **p < 0.01 and ***p < 0.001.

Sup. Figure 5 Reina et al.

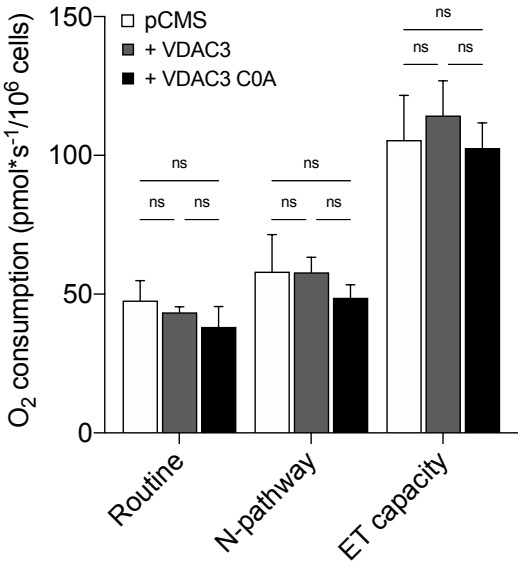

Fig. S5. **Impact of cell transfection on the respirometry profile of HAP1-ΔVDAC3 cells.** Quantitative analysis of the oxygen consumption performed by HRR in the respiratory states Routine, N-pathway and ET capacity upon cell transfection with empty vector (pCMS) or construct carrying VDAC3 (+VDAC3) or VDAC3 CoA mutant (+VDAC3 CoA). Data are expressed as means ± SD (n = 4) and analyzed by one-way ANOVA.

Article 3.

FEBS Open Bio

Recombinant yeast VDAC2: a comparison of electrophysiological features with the native form

Andrea Magrì[1,2], Andonis Karachitos[3], Maria Carmela Di Rosa[2], Simona Reina[2], Stefano Conti Nibali[1], Angela Messina[2,4], Hanna Kmita[3] and Vito De Pinto[1,4]

1 Department of Biomedical and Biotechnological Sciences, University of Catania, Italy
2 Department of Biological, Geological and Environmental Sciences, Section of Molecular Biology, University of Catania, Italy
3 Department of Bioenergetics, Faculty of Biology, Institute of Molecular Biology and Biotechnology, Adam Mickiewicz University, Poznan, Poland
4 National Institute for Biomembranes and Biosystems, Section of Catania, Italy

FEBS openbio

FEBS PRESS science publishing by scientists

Recombinant yeast VDAC2: a comparison of electrophysiological features with the native form

Andrea Magrì[1,2], Andonis Karachitos[3], Maria Carmela Di Rosa[2], Simona Reina[2], Stefano Conti Nibali[1], Angela Messina[2,4], Hanna Kmita[3] and Vito De Pinto[1,4]

1 Department of Biomedical and Biotechnological Sciences, University of Catania, Italy
2 Department of Biological, Geological and Environmental Sciences, Section of Molecular Biology, University of Catania, Italy
3 Department of Bioenergetics, Faculty of Biology, Institute of Molecular Biology and Biotechnology, Adam Mickiewicz University, Poznan, Poland
4 National Institute for Biomembranes and Biosystems, Section of Catania, Italy

Keywords
electrophysiology; heterologous expression; mitochondria; mitochondrial porins; planar lipid bilayer; VDAC2; yeast; yeastVDAC2; yVDAC2

Correspondence
A. Magrì, Department of Biological, Geological and Environmental Sciences, Section of Molecular Biology, University of Catania, V. le Andrea Doria, 6, Cittadella Universitaria, 95125, Catania, Italy
E-mail: andrea.magri@unict.it

Andrea Magrì and Andonis Karachitos contributed equally to this work

(Received 6 August 2018, revised 4 December 2018, accepted 10 December 2018)

doi:10.1002/2211-5463.12574

Voltage-dependent anion channel isoform 2 of the yeast *Saccharomyces cerevisiae* (yVDAC2) was believed for many years to be devoid of channel activity. Recently, we isolated yVDAC2 and showed that it exhibits channel-forming activity in the planar lipid bilayer system when in its so-called native form. Here, we describe an alternative strategy for yVDAC2 isolation, through heterologous expression in bacteria and refolding *in vitro*. Recombinant yVDAC2, like its native form, is able to form voltage-dependent channels. However, some differences between native and recombinant yVDAC2 emerged in terms of voltage dependence and ion selectivity, suggesting that, in this specific case, the recombinant protein might be depleted of post-translational modification(s) that occur in eukaryotic cells.

The voltage-dependent anion channel (VDAC) proteins, also known as mitochondrial porins, are the most abundant proteins in the mitochondrial outer membrane (MOM) of all eukaryotes. Characterized by a molecular mass of 30–32 kDa, VDAC proteins allow for the continuous exchange of metabolites (ATP/ADP, NAD^+/NADH, Krebs cycle intermediates) and ions (Na^+, Cl^-, Mg^{2+}, Ca^{2+}) between mitochondria and cytosol. Therefore, they play a crucial role in mitochondrial bioenergetics [1–3]. In mammals, where three different but conserved isoforms are expressed (VDAC1, VDAC2 and VDAC3) [4], evolution has conferred to each isoform peculiar additional functions beyond the metabolic role. For example, VDAC1 and VDAC2 participate differently in the regulation of cell death [5–8], while recent literature suggests the involvement of VDAC3 in reactive oxygen species (ROS) homeostasis [9,10]. The three-dimensional structure of mammalian VDAC1 has been shown to involve a transmembrane β-barrel structure, formed by 19

Abbreviations
LDAO, lauryldimethylamine oxide; MOM, mitochondrial outer membrane; PLB, planar lipid bilayer; PTM, post-translational modification; ROS, reactive oxygen species; VDAC, voltage-dependent anion channel; yVDAC2, yeast voltage-dependent anion channel isoform 2.

amphipathic, mostly anti-parallel β-strands, with the exception of the N-terminal domain, which is structured as an α-helix and partially exposed to the cytosol [11–13]. A similar result was obtained for zebrafish VDAC2 [14] and for other species by homology modeling studies [15], suggesting a conserved structure of VDAC across evolution.

Differently from mammals, the budding yeast *Saccharomyces cerevisiae* has only two distinct VDAC genes, *POR1* and *POR2*, encoding two different VDAC isoforms. However, only yVDAC1 is widely considered essential for mitochondrial metabolism. Indeed, the inactivation of the *POR1* gene, as in the Δ*por1* mutant strain, resulted in a strong inhibition of cell growth in non-fermentable conditions, especially at the restrictive temperature of 37 °C [16]. On the contrary, the inactivation of the *POR2* gene resulted in an undetectable phenotype, since Δ*por2* cells were able to grow in a comparable way to the wild-type [16]. Overall, the channel-forming ability of yeast voltage-dependent anion channel isoform 2 (yVDAC2) has been questioned for many years. Contrasting results were indeed obtained upon *POR2* overexpression; namely, a complete recovery of Δ*por1* yeast growth on glycerol was detected [16,17], suggesting a channel activity for yVDAC2, at least under particular conditions. Only recently, an electrophysiological analysis has clearly shown that yVDAC2 is able to form channels in artificial membranes, with features resembling many other members of the VDAC family [18].

In a previous work, we purified yVDAC2 directly from mitochondria extracted from Δ*por1* cells overexpressing *POR2*, under native conditions [18]. In parallel, the same protein was prepared by heterologous expression in a bacterial system, purified and refolded as previously performed for many other VDAC isoforms and mutants [19–22]. In this work, we analyzed the electrophysiological features of the recombinant yVDAC2. Our results indicate that the protein is able to form channels in artificial membranes, with similar features to native one but, at the same time, with differences in terms of voltage sensitivity and ion selectivity.

Materials and methods

Cloning of yVDAC2

The sequence encoding yVDAC2 was obtained by reverse transcription from the total RNA previously extracted from *S. cerevisiae* BY4742 (EUROSCARF, Frankfurt, Germany). Reverse transcription was performed by using the AffinityScript Multi-Temp RT and RT-PCR system (Agilent, Santa Clara, CA, USA) according to the manufacturer's protocol. The corresponding cDNA was amplified by PCR using the following primers: forward 5′-TTTTGCTAGCATGGCACTACGATTTTTCAACGAT-3′ and reverse 5′-TTTTCTCGAGGGGCGAGAACGATAGAGACCA-3′. The yVDAC2 cDNA was cloned in the bacterial expression vector pET-21b (Novagen, Madison, WI, USA) by NheI/XhoI digestion, in frame with the His-tag at the C-terminal part. The construct was verified by sequencing.

Expression, purification and refolding of yVDAC2 protein

Escherichia coli BL21 (DE3) cells were transformed with pET-21b plasmid containing the yVDAC2 sequence. Transformed cells were grown to an optical density (λ = 600 nm) of 0.6, and the protein expression was induced by addition of 0.4 mM isopropyl-β-D-thiogalactopyranoside (IPTG) (Sigma-Aldrich, Saint Louis, MO, USA), for 3 h at 30 °C. Cells were harvested by centrifugation and lysed in buffer B (8 M urea, 1 mM NaH_2PO_4, 0.01 mM Tris/HCl, pH 8.0) overnight at 4 °C. The total protein lysate was clarified by centrifugation and loaded onto Ni-NTA agarose (Thermo Fisher Scientific, Waltham, MA, USA) packed column, previously equilibrated with buffer B. The column was then washed twice with five volumes of buffer C (8 M urea, phosphate buffer, pH 6.3), and proteins were purified by elution with five volumes of buffer E (8 M urea, phosphate buffer, pH 3.5). The eluted protein was refolded by incubation at 4 °C in a 10-fold volume of refolding buffer [25 mM Tris, 100 mM NaCl, 1 mM EDTA, 1% (v/v) lauryldimethylamine oxide (LDAO, Sigma-Aldrich), pH 7.0]. Then, the protein solution was dialyzed against 100 volumes of a dialysis buffer (25 mM Tris, 1 mM EDTA, 0.1% LDAO, pH 7.0) with Thermo Scientific Slide-A-Lyzer Dialysis Cassettes (Thermo Fisher Scientific) (3.5 K MWCO). The solution containing the refolded proteins was clarified by centrifugation (60 000 ***g***, 1 h) and loaded into a size exclusion chromatography column (Superdex 200 Increase 30/100, GE Healthcare, Chicago, IL, USA) in SEC buffer (150 mM NaCl, 20 mM Tris/HCl, pH 8.0, 1 mM DTT 0.1% LDAO) to separate aggregates from monomers. Elution fractions, corresponding exclusively to the monomer peak, were collected.

Electrophysiological analysis of recombinant yVDAC2

The refolded yVDAC2 was reconstituted into a planar lipid bilayer (PLB) system as previously described in [20–22]. Bilayers of approximately 80–100 pF capacity made of asolectin from a soybean phospholipid mixture (Sigma-Aldrich) at a concentration of 20 $mg \cdot mL^{-1}$ in *n*-decane were used. Channel insertion was obtained by addition of

0.5–5 μL of protein solution to the *cis* side of the cuvette containing approximately 3 mL of aqueous solution (1 M KCl, 10 mM Hepes, pH 7.0). Data were acquired using a Bilayer Clamp amplifier (Warner Instruments, Hamden, CT, USA) at 100 μs per point, filtered at 300 Hz and analyzed offline using the PCLAMP program set (version 10; Molecular Devices, San Jose, CA, USA). Channel conductance (G) was calculated from current (I) measurements in the presence of an applied constant voltage (V_m) of +10 mV, as the I/V_m ratio. Distribution of conductance was obtained from six independent reconstitution experiments, each showing several channel insertions.

Voltage dependence analysis of yVDAC proteins

Analysis of voltage dependence of recombinant yVDAC2 was performed in 1 M KCl, 10 mM Hepes, pH 7.0, by application of two distinct voltage ramps including positive and negative potentials (amplitude ±90 mV, time 100 s). At least three independent multi-channel experiments were performed. Values of G and G_{max}, indicating respectively the conductance value at a given V_m and the maximal conductance, were calculated for the recombinant yVDAC2. Control experiments were performed using the native yVDAC1 and yVDAC2 produced as previously described [18]. The relative conductance was calculated as the G/G_{max} ratio and plotted as a function of the voltage using PRISM 7 software (GraphPad Software Inc., La Jolla, CA, USA). Three independent experiments were performed for each protein and data are shown as the mean ± SEM.

Ion selectivity measurement of yVDAC2

Selectivity measurements were performed for the recombinant yVDAC2 in a 0.1 M/1 M *cis*/*trans* gradient of KCl in a voltage range of ±90 mV, by increasing V_m with discrete steps of ±5 mV for 45 s. Values of conductance were plotted as a function of V_m, and linear regression was applied with PRISM 7 software. The permeability ratio of cation K^+ (P_C) over anion Cl^- (P_A) was calculated from the reversal potential (V_r) using the Goldman–Hodgkin–Katz equation, according to [23]. Six independent selectivity measurements were performed with both a single- and a multi-channel approach.

Results

Reconstituted recombinant yVDAC2 forms channels of conductance similar to the native protein

To analyze the electrophysiological properties of recombinant yVDAC2, the corresponding encoding sequence was introduced into *E. coli* BL21 (DE3) cells and the protein expression was achieved by IPTG induction, as verified by SDS/PAGE (Fig. 1A). The recombinant protein was extracted directly from inclusion bodies and purified by nickel affinity chromatography, exploiting the 6×His tag (Fig. 1B). Since the heterologous expression of membrane proteins in bacterial systems leads to loss of proper conformation and activity, the purified yVDAC2 was refolded and dialyzed. In order to avoid the presence of aggregates in the final protein solution, size exclusion chromatography was performed and the elution fractions, corresponding to the monomers (Fig. 1C), were collected and used in our study. Finally, the electrophysiological features of recombinant yVDAC2 were analyzed at the PLB.

The representative current trace displayed in Fig. 2A clearly shows that recombinant yVDAC2 was able to form channels in artificial membrane, since insertion of three different channels of similar size in a short time was obtained after the addition of the protein solution to the *cis* side of the cuvette. The histogram in Fig. 2B shows the distribution of conductance values calculated for $n = 36$ channels. The analysis, performed in 1 M KCl, 10 mM Hepes, pH 7, in the presence of an applied constant voltage of +10 mV, allowed for calculation of the average conductance, estimated as 3.76 ± 0.94 nS (SD, $n = 36$). This value perfectly overlaps our previous measurements showing an average conductance for the native yVDAC2 of about 3.6 nS in the same experimental conditions [18]. Overall, our results indicate that, in artificial membrane, recombinant yVDAC2 forms channels of conductance similar to the native protein.

Recombinant yVDAC2 is less sensitive to the applied voltage than the native protein

It is known that the conductance of VDAC proteins changes depending on the applied voltage. This feature, well conserved through evolution from yeast to human, is known as voltage dependence. In general, yeast or mammalian VDAC1 persists at low potentials in a stable highly conductive state, called the 'open' state. However, as the applied voltage rises (starting from ±20–30 mV), VDAC1 switches to several low-conducting states, called 'closed' states [24–27]. We demonstrated previously that the native yVDAC2 shows a less pronounced voltage dependence in comparison to yVDAC1, because yVDAC2-formed channel closure began from ±40–50 mV of applied voltage [18].

In order to analyze the effect of voltage on recombinant yVDAC2 conductance, PLB experiments were

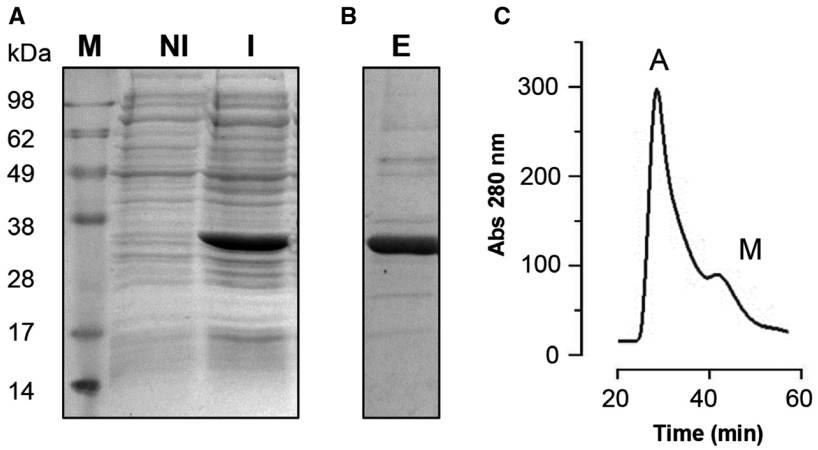

Fig. 1. Expression and purification of yVDAC2 in bacterial system. (A) SDS/PAGE analysis of whole *Escherichia coli* BL21 (DE3) lysate from cells transformed with the pET-21b-yVDAC2 construct, obtained in the presence of 0.4 M IPTG (I, induced). As a control, a sample that was not induced (NI) was used. Addition of IPTG allowed the expression of recombinant yVDAC2 as demonstrated by the strong band of the expected molecular mass (28–32 kDa) exclusively found in the induced sample. 'M' indicates the molecular mass marker. (B) SDS/PAGE of eluate (E) obtained after Ni-NTA chromatography of the total induced lysate. As shown, a predominant band of the expected molecular mass was detected. (C) Elution profile obtained by size-exclusion chromatography of refolded protein. 'A' indicates the peak corresponding to aggregated proteins; 'M' indicates the peak corresponding to the monomeric protein. Only fractions corresponding to monomeric protein were collected and used going forward.

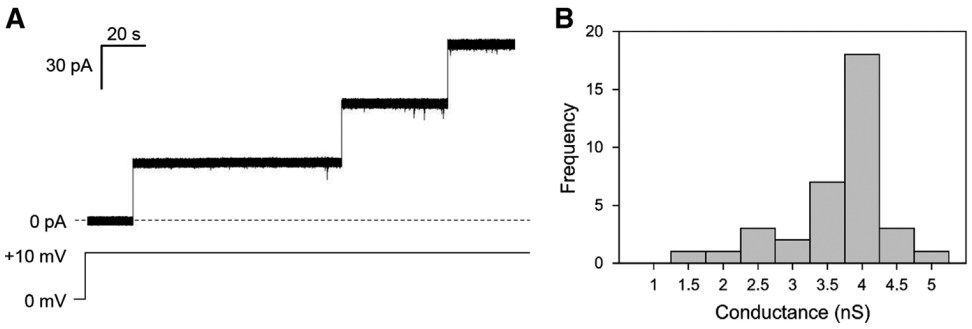

Fig. 2. Pore-forming activity analysis of recombinant yVDAC2 in artificial membranes. (A) Representative trace of yVDAC2 activity recorded at the PLB. Channels insertion was achieved after addition of 0.5–5 μL of protein solution into the *cis* side of the cuvette, in presence of a lipid bilayer. Discrete steps indicate single channel insertion. Experiment was performed in 1 M KCl, 10 mM Hepes, pH 7, at a constant applied voltage of +10 mV. (B) Distribution of conductance values obtained for $n = 36$ channels inserted in the membrane. Most of the channels showed conductance values between 3.5 and 4 nS, resulting in an average conductance value of 3.76 ± 0.94 nS (SD, $n = 36$).

performed by the application of voltage ramps from 0 to ±90 mV. The curves, displayed in Fig. 3A, indicate that recombinant yVDAC2 is completely insensible to low positive and negative voltages, since no closure was detected either at potentials that normally close yeast or mammalian VDAC1 or at voltages able to close native yVDAC2. Only the application of high voltages, starting from ±70–80 mV, induced a channel closure, which occurred symmetrically at both positive and negative potentials, suggesting that recombinant yVDAC2 is significantly less voltage sensitive than the native protein. Furthermore, current across recombinant yVDAC2 was monitored upon application of the constant voltage +90 mV. As shown in the representative trace in Fig. 3B, a complete closure of the channels occurred only after a prolonged exposure to high potential, highlighting the recombinant yVDAC2 limited sensitivity to voltage.

The electrophysiological behavior of the native protein was then analyzed in the presence of similar high voltages, by applying a voltage ramp from 0 to +90 mV. According to our previous data [18], native yVDAC2 began to close around +40–50 mV, as shown by the trace in Fig. 4A. However, the application of higher potentials (i.e. +80 mV) promoted a further channel closure, similarly to that previously shown by the recombinant

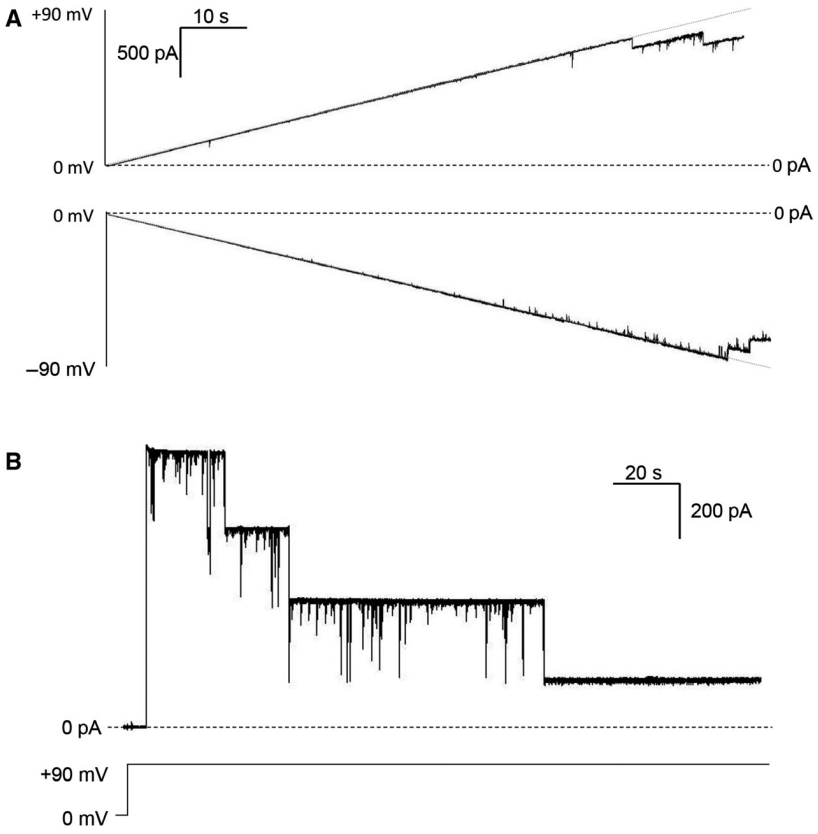

Fig. 3. Voltage dependence of recombinant yVDAC2. (A) Representative traces of yVDAC2 activity at the PLB in presence of voltage ramps from 0 to +90 mV (upper trace) and from 0 to −90 mV (lower trace). Traces show that no change in the conductance was obtained at low positive or negative potentials. A significant reduction of channel conductance was obtained starting from ±80 mV. Experiments were performed in 1 M KCl, 10 mM Hepes, pH 7. (B) Representative trace of recombinant yVDAC2 recorded at the constant voltage of +90 mV for a prolonged time; $n = 3$ different channels inserted in the membrane. It is clear that application of high voltage promotes a step-by-step closure of yVDAC2 channels. The experiment was performed in 1 M KCl, 10 mM Hepes, pH 7.

protein (see Fig. 3A). To deeply analyze this aspect, the values of conductance (G) obtained at each applied voltage for both native and recombinant proteins, as well as for the native yVDAC1, were normalized relative to the maximal conductance (G_{max}). Then, as shown in Fig. 4B, relative conductance values (G/G_{max}) were plotted as a function of the applied voltage (amplitude of ±90 mV). As expected, yVDAC1 conductance (pale green circles) significantly decreased starting from ±20–30 mV, reaching a stable level of closure characterized by a decrease at about 50% of the maximal conductance. Native yVDAC2 (orange circles) began to close around ±40–50 mV and its conductance at these voltages showed a decrease of about 20%, in a similar manner to that shown previously [18]. It is clear that this channel is not able to reach a channel closure similar to that observed for yVDAC1. However, the application of high voltages, up to ±80–90 mV, promoted a further 10–15% decrease of its relative conductance.

The results shown in Fig. 4B also confirmed the overall attenuation of voltage dependence in the case of recombinant yVDAC2 (red circles) observed in Fig. 3. Furthermore, the application of voltages up to ±60–70 mV did not promote any significant decrease in the channel conductance. Conversely, the application of potentials ±80–90 mV caused channel closure, as G/G_{max} values almost overlap those calculated for both native yVDAC1 and yVDAC2 at similar voltages. Although the recombinant yVDAC2 still shows voltage dependence, our results suggest a decrease of voltage sensitivity even with respect to the native form.

Recombinant yVDAC2 displays exclusively cation-selective states

It is known that VDAC displays an anionic selectivity in the high-conducting 'open' state and a less anionic or more cationic selectivity in the low-conducting

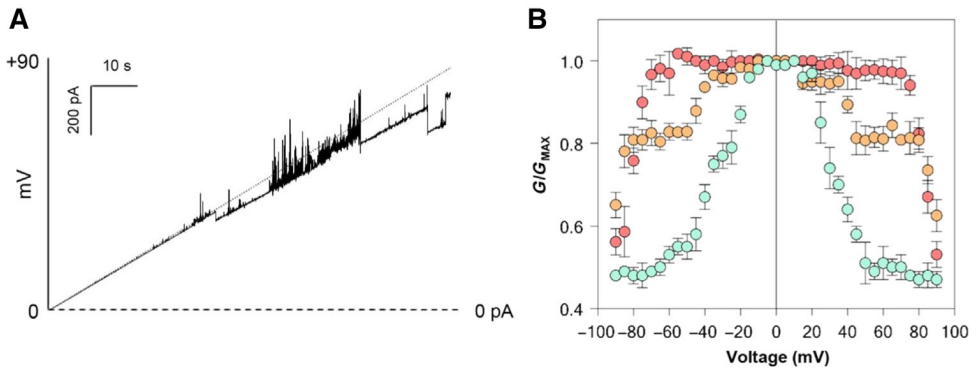

Fig. 4. Comparative analysis of relative conductance for yVDAC proteins. (A) A representative trace of native yVDAC2 activity in presence of voltage ramps from 0 to +90 mV. The trace shows that the protein undergoes to partial closure at +40–50 mV and, as the voltage increases, channels become noisy. However, a stable reduction of channel conductance was obtained starting from ±80 mV. Experiments were performed in 1 M KCl, 10 mM Hepes, pH 7. (B) Analysis of relative conductance (G/G_{max}) (±SEM) of $n = 3$ independent experiments showing the different voltage-dependent features of yVDAC proteins. Pale green circles refer to yVDAC1, orange circles refer to native yVDAC2 results, and red circles refer to recombinant yVDAC2. As reported, both native and recombinant yVDAC2 remain in an open state up to application of high voltages, starting from ±80–90 mV, when they switch to the closed state. Experiments were performed in 1 M KCl, 10 mM Hepes, pH 7.

'closed' state [28,29]. In the previous work, the presence of 1 and 0.1 M KCl in the *cis* and *trans* side of the cuvette, respectively, allowed for detection of the presence of different selectivity states, three in total for native yVDAC2. Two of them appeared to be high-conducting states but with an opposite selectivity, while the third was a very low-conducting state characterized by an extremely pronounced cation selectivity [18]. In order to analyze the ion selectivity of recombinant yVDAC2, current values, measured in a 10-fold gradient of KCl and obtained upon application of discrete voltages in the range of ±90 mV, were plotted as a function of the applied voltage. Linear regressions of the obtained data (Fig. 5) indicated the presence of only two distinct states of recombinant yVDAC2, i.e. a main high-conducting state (called state 1 in Fig. 5) and a low-conducting state (state 2 in Fig. 5) and that both states displayed a cation selectivity.

The Goldman–Hodgkin–Katz equation was then used to calculate the ratio between permeability of cations over anions (P_C/P_A) for the two states of recombinant yVDAC2, using a reversal potential corresponding to the voltage at zero current [23]. The P_C/P_A value obtained for state 1 was 1.94 ± 0.19 and the value obtained for state 2 was 11.2 ± 2.8. For comparison, the corresponding P_C/P_A values obtained for native yVDAC2 were 2.17 ± 0.11 and 16.24 ± 6, respectively [18]. This clearly indicates that recombinant and native yVDAC2 are very similar in terms of cationic strength. In particular, the lowest conducting state determined for both variants of yVDAC2 is characterized by a pronounced selectivity for cations over anions, a feature found exclusively for yVDAC2. At the same time, a significant difference between native and recombinant protein emerged, since no anionic state was found for the recombinant one.

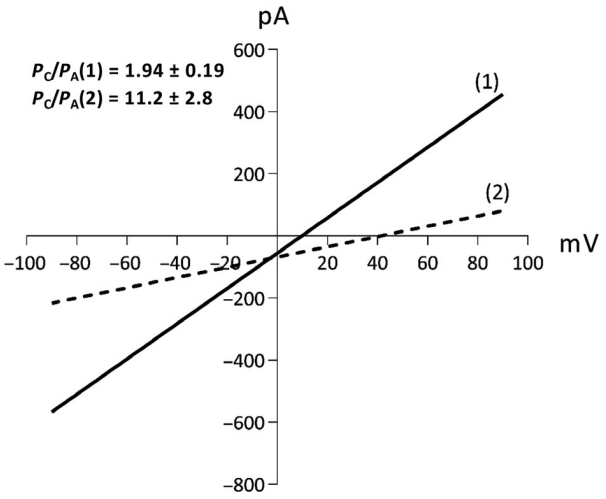

Fig. 5. Ion selectivity of recombinant yVDAC2. Representative graph of current–voltage relationship of yVDAC2 recombinant protein performed in 10-fold gradient of 1 M KCl obtained by application of voltage steps for a prolonged time. The conductance (slope) and the reversal potentials were calculated from the extrapolated regression lines of the different conducting states of the channel. The multi-channel experiment shown was performed with $n = 8$ channels inserted in the membrane. Numbers indicate the different states: 1, cationic high-conducting state; 2, cationic low-conducting state.

Discussion

So far, the second VDAC isoform of the yeast *S. cerevisiae* has been considered to be one of the most elusive members of the VDAC family. Indeed, since the *POR2* gene discovery, the story of yVDAC2 has been controversial. Differently from *POR1*, the genetic inactivation of *POR2* has no consequence for yeast growth on non-fermentable carbon sources [16]. Furthermore, no data about yVDAC2 reconstitution in liposomes and/or artificial membranes were available for a long time, raising the suspicion (now proved wrong [18]) that the yVDAC2 protein was completely devoid of channel function. On the contrary, the overexpression of the *POR2* gene in Δ*por1* cells promoted the restoration of the yeast wild-type growth phenotype. This effect can be achieved when the *POR2* sequence is transcribed under the control of a strong promoter [16] or is activated by an external factor, such as the serendipitously found human SOD1, which stimulates *POR2* overexpression [17]. These findings in turn suggest that the contribution of yVDAC2 to the permeability of the yeast MOM is a consequence of its expression level, providing a logical explanation for the recovery of Δ*por1* cell growth [16] and of the mitochondrial functionality [17]. To definitively clarify the functional properties of yVDAC2, we have recently analyzed the electrophysiological features of this protein reconstituted into artificial membranes by using two parallel approaches. As shown in our previous work, we isolated yVDAC2 directly from Δ*por1* mitochondria, after yeast cell transformation with an expression plasmid carrying the corresponding yVDAC2 cDNA sequence. This strategy allowed us to increase *POR2* transcript concentration and consequently the corresponding protein amount, which simplified the protein isolation under the native condition [18]. Alternatively, yVDAC2 was produced as a recombinant protein in *E. coli* cells, a procedure commonly used for large-scale protein production, since it allows a high yield of protein to be obtained in a relatively short time with minimal cost and effort. The same approach was previously used by our group for the characterization of human VDAC3 [20] and its cysteine mutants [21], and for the production of human VDAC1 suitable for interaction studies with proteins involved in neurodegenerative diseases [22,30]. Furthermore, an identical approach was used by Hiller and coauthors to obtain the human VDAC1 preparation for NMR studies aimed at identifying its three-dimensional structure [11,31] and by Abramson's group to purify the mouse VDAC1, later crystalized [13], confirming the strength of this method. With this perspective, the yVDAC2 cDNA was cloned into a specific expression vector and the protein was expressed in bacterial cells. Since membrane proteins localize into inclusion bodies, bacterial lysis occurred upon denaturing conditions, with the loss of the native conformation. Therefore, once isolated, in order to obtain a perfectly active protein, the recombinant protein must undergo a refolding procedure using a well-established protocol [11,19–22].

Recombinant yVDAC2 was then characterized by reconstitution in a PLB system and previous data were used as a reference. Our reconstitution experiments clearly indicate the ability of the recombinant protein to form channels in artificial membranes, with an average conductance value identical to that previously found for the native protein. This result confirmed also the appropriateness of our refolding method. The analyses of voltage dependence indicate that the recombinant yVDAC2 is less sensitive to voltage than native yVDAC1 and yVDAC2, although the voltage dependence of the latter is also weaker than that of the former. Accordingly, only application of a high potential is able to promote a strong attenuation (approximately halving) of relative conductance of native yVDAC2, allowing the protein to reach a similar closure level to that displayed by yVDAC1. Similarly, the recombinant yVDAC2 undergoes a complete and stable closure exclusively at high potentials, such as ±80–90 mV.

Another significant difference among native and recombinant yVDAC2 concerns ion selectivity. In our previous work, we found that native yVDAC2 displays the anion-selective state typical of most VDAC proteins, and two different cation-selective states [18]. Importantly, both cation-selective states are observed for recombinant yVDAC2 as indicated by values of P_C/P_A, but no anion-selective state was found for the recombinant protein. Although the presence of the highly conductive cationic state was already observed in VDAC1 extracted from *Neurospora crassa* or rat liver mitochondria [32], such a difference between native and recombinant VDAC1 from yeast or human has not been detected so far; rather many papers agree with the fact that both samples behave similarly upon PLB analysis in terms of conductance, voltage dependence and selectivity. Conversely, specific functional differences were noticed in the case of human VDAC3. The first electrophysiological characterization of VDAC3 was obtained by heterologous expression in bacteria, which produced proteins able to form pores in artificial membranes with a very low conductance (100 pS in 1 M KCl, channels about 35–40 times smaller than both VDAC1 and VDAC2) [20]. However, the work by Okazaki *et al.* showed that the

recombinant VDAC3 could form channels with conductance similar to the other isoforms [33]. In this work, although the proteins were obtained with very similar protocols, the presence of reducing agents in preparation buffers and in PLB experiments led to the formation of channels of normal conductance. Moreover, channels of regular conductance were also obtained by using human VDAC3 directly extracted in the same conditions from yeast mitochondria [27]. At variance was that VDAC3 purified in the absence of reducing agents showed different electrophysiological features [21]. The reason for such differences was later attributed to the presence of specific post-translational modifications (PTMs), in particular to irreversible oxidation states of cysteine residues, as demonstrated by electrophysiological characterization in [21] and recently confirmed by high-resolution mass spectrometry [34,35].

We thus hypothesize that also the differences between native and recombinant yVDAC2 could be explained by naturally occurring PTMs. While the native protein is isolated directly from yeast mitochondria under native conditions, the recombinant protein is produced in a heterologous system lacking any eukaryotic PTMs. Beyond oxidation, VDAC proteins undergo phosphorylation of specific amino acid in both physiological and pathological conditions [36,37], which could be responsible for modulation of voltage sensitivity, as well as other electrophysiological parameters, as has been recently proposed [38,39]. Furthermore, it is known that modifications of amino acid residues change VDAC features. For instance, the treatment of VDAC1 with succinic anhydride abolishes the voltage dependence and changes its selectivity from an anionic to a cationic one [40].

In conclusion, the slight functional differences found in the specific case of *S. cerevisiae* VDAC2 between the native and recombinant proteins do not affect the biological significance of our findings, indicating that yVDAC2 is definitely another member of the VDAC family, being able to form voltage-dependent channel of about 3.6 nS conductance under our experimental conditions. The behavior of the recombinant protein supports our hypothesis of the presence of specific PTMs in the native one. As a further, intriguing consequence, our results indicate that such differences could be associated to the still unknown role of yVDAC2. Its encoding gene is under-expressed in normal conditions. It is not the first time, indeed, that an under-expressed isoform of VDAC was noticed, as was recently found in *Drosophila melanogaster*: in that case, a regulatory function has been associated to the alternative isoform [41].

Acknowledgements

The authors acknowledge the financial support of MIUR PRIN, project 2015795S5W_005, Piano della Ricerca UNICT 2017 to VDP and A. Messina, Fondazione Umberto Veronesi for a post-doctoral fellowship to A Magrì.

Conflict of interest

The authors declare no conflict of interest.

Author contributions

A. Magrì, AK, and SR performed electrophysiological experiments. A. Magrì, MCDR, and SCN performed protein purification. A. Magrì, A. Messina, HK, and VDP analyzed the data and wrote the manuscript.

References

1 Benz R (1994) Permeation of hydrophilic solutes through mitochondrial outer membranes: review on mitochondrial porins. *Biochim Biophys Acta* **1197**, 167–196.
2 Colombini M (2004) VDAC: the channel at the interface between mitochondria and the cytosol. *Mol Cell Biochem* **256–257**, 107–115.
3 Shoshan-Barmatz V, De Pinto V, Zweckstetter M, Raviv Z, Keinan N and Arbel N (2010) VDAC, a multi-functional mitochondrial protein regulating cell life and death. *Mol Asp Med* **31**, 227–285.
4 Messina A, Reina S, Guarino F and De Pinto V (2012) VDAC isoforms in mammals. *Biochim Biophys Acta* **1818**, 1466–1476.
5 Granville DJ & Gottlieb RA (2003) The mitochondrial voltage-dependent anion channel (VDAC) as a therapeutic target for initiating cell death. *Curr Med Chem* **16**, 1527–1533.
6 Shoshan-Barmatz V, Zakar M, Rosenthal K & Abu-Hamad S (2009) Key regions of VDAC1 functioning in apoptosis induction and regulation by hexokinase. *Biochim Biophys Acta* **1787**, 421–430.
7 Magrì A, Reina S and De Pinto V (2018) VDAC1 as pharmacological target in cancer and neurodegeneration: focus on its role in apoptosis. *Front Chem* **6**, 108.
8 Cheng EH, Sheiko TV, Fisher JK, Craigen WJ and Korsmeyer SJ (2003) VDAC2 inhibits BAK activation and mitochondrial apoptosis. *Science* **301**, 513–517.
9 De Pinto V, Reina S, Gupta A, Messina A and Mahalakshmi R (2016) Role of cysteines in mammalian VDAC isoforms' function. *Biochim Biophys Acta* **1857**, 1219–1227.

10 Reina S, Guarino F, Magrì A and De Pinto V (2016) VDAC3 as a potential marker of mitochondrial status is involved in cancer and pathology. *Front Oncol* **6**, 264.
11 Hiller S, Graces RG, Malia TJ, Orekhov VY, Colombini M and Wagner G (2008) Solution structure of the integral human membrane protein VDAC-1 in detergent micelles. *Science* **321**, 1206–1210.
12 Bayrhuber M, Menis T, Habeck M, Becker S, Giller K, Villinger S, Vonrhein C, Griesinger C, Zweckstetter M and Zeth K (2008) Structure of the human voltage-dependent anion channel. *Proc Natl Acad Sci USA* **105**, 15370–15375.
13 Ujwal R, Cascio D, Colletier JP, Fahama S, Zhanga J, Torod L, Pinga P and Abramson J (2008) The crystal structure of mouse VDAC1 at 2.3 Å resolution reveals mechanistic insights into metabolite gating. *Proc Natl Acad Sci USA* **105**, 17742–17747.
14 Schredelseker J, Paz A, López CJ, Altenbach C, Leung CS, Drexler MK, Chen JN, Hubbell WL and Abramson J (2014) High resolution structure and double electron-electron resonance of the zebrafish voltage-dependent anion channel 2 reveal an oligomeric population. *J Biol Chem* **289**, 12566–12577.
15 De Pinto V, Guarino F, Guarnera A, Messina A, Reina S, Tomasello MF, Palermo V and Mazzoni C (2010) Characterization of human VDAC isoforms: a peculiar function for VDAC3? *Biochim Biophys Acta* **1797**, 1268–1275.
16 Blachly-Dyson E, Song J, Wolfgang WJ, Colombini M and Forte M (1997) Multicopy suppressors of phenotypes resulting from the absence of yeast VDAC encode a VDAC-like protein. *Mol Cell Biol* **17**, 5727–5738.
17 Magrì A, Di Rosa MC, Tomasello MF, Guarino F, Reina S, Messina A and De Pinto V (2016) Overexpression of human SOD1 in VDAC1-less yeast restores mitochondrial functionality modulating beta-barrel outer membrane protein genes. *Biochim Biophys Acta* **1857**, 789–798.
18 Guardiani C, Magrì A, Karachitos A, Di Rosa MC, Reina S, Bodrenko I, Messina A, Kmita H, Ceccarelli M and De Pinto V (2018) yVDAC2, the second mitochondrial porin isoform of *Saccharomyces cerevisiae*. *Biochim Biophys Acta* **1859**, 270–279.
19 Reina S, Magrì A, Lolicato M, Guarino F, Impellizzari A, Maier E, Benz R, Ceccarelli M, De Pinto V and Messina A (2013) Deletion of β-strands 9 and 10 converts VDAC1 voltage-dependence in an asymmetrical process. *Biochim Biophys Acta* **1827**, 793–805.
20 Checchetto V, Reina S, Magrì A, Szabò I and De Pinto V (2014) Recombinant human voltage dependent anion selective channel isoform 3 (hVDAC3) forms pores with a very small conductance. *Cell Physiol Biochem* **34**, 842–853.
21 Reina S, Checchetto V, Saletti R, Gupta A, Chaturvedi D, Guardiani C, Guarino F, Scorciapino MA, Magrì A, Foti S *et al*. (2016) VDAC3 as a sensor of oxidative state of the intermembrane space of mitochondria: the putative role of cysteine residue modifications. *Oncotarget* **7**, 2249–2268.
22 Magrì A, Belfiore R, Reina S, Tomasello MF, Di Rosa MC, Guarino F, Leggio L, De Pinto V and Messina A (2016) Hexokinase I N-terminal based peptide prevents the VDAC1-SOD1 G93A interaction and re-establishes ALS cell viability. *Sci Rep* **6**, 34802.
23 Krammer EM, Saidani H, Prévost M and Homblè F (2014) Origin of ion selectivity in *Phaseolus coccineus* mitochondrial VDAC. *Mitochondrion* **19**, 206–213.
24 Colombini M (1980) Structure and mode of action of a voltage dependent anion-selective channel (VDAC) located in the outer mitochondrial membrane. *Ann N Y Acad Sci* **341**, 552–563.
25 Benz R, Schmid A and Dihanich M (1989) Pores from mitochondrial outer membranes of yeast and a porin-deficient yeast mutant: a comparison. *J Bioenerg Biomembr* **21**, 439–450.
26 De Pinto V, Benz R, Caggese C and Palmieri F (1989) Characterization of the mitochondrial porin from *Drosophila melanogaster*. *Biochim Biophys Acta* **987**, 1–7.
27 Karachitos A, Grobys D, Antoniewicz M, Jedut S, Jordan J and Kmita H (2016) Human VDAC isoforms differ in their capability to interact with minocycline and to contribute to its cytoprotective activity. *Mitochondrion* **28**, 38–48.
28 Schein SJ, Colombini M and Finkelstein A (1976) Reconstitution in planar lipid bilayers of a voltage-dependent anion-selective channel obtained from paramecium mitochondria. *J Membr Biol* **30** (2), 99–120.
29 Colombini M (2016) The VDAC channel: molecular basis for selectivity. *Biochim Biophys Acta* **1863** (10), 2498–2502.
30 Magrì A and Messina A (2017) Interactions of VDAC with proteins involved in neurodegenerative aggregation: an opportunity for advancement on therapeutic molecules. *Curr Med Chem* **24** (40), 4470–4487.
31 Hiller S and Wagner G (2009) The role of solution NMR in the structure determinations of VDAC-1 and other membrane proteins. *Curr Opin Struct Biol* **19** (4), 396–401.
32 Pavlov E, Grigoriev SM, Dejean LM, Zweihorn CL, Mannella CA and Kinnally KW (2005) The mitochondrial channel VDAC has a cation-selective open state. *Biochim Biophys Acta* **1710**, 96–102.

33 Okazaki M, Kurabayashi K, Asanuma M, Saito Y, Dodo K and Sodeoka M (2015) VDAC3 gating is activated by suppression of disulfide-bond formation between the N-terminal region and the bottom of the pore. *Biochim Biophys Acta* **1848**, 3188–3196.
34 Saletti R, Reina S, Pittalà MG, Belfiore R, Cunsolo V, Messina A, De Pinto V and Foti S (2017) High resolution mass spectrometry characterization of the oxidation pattern of methionine and cysteine residues in rat liver mitochondria voltage-dependent anion selective channel 3 (VDAC3). *Biochim Biophys Acta* **1859**, 301–311.
35 \Saletti R, Reina S, Pittalà MGG, Magrì A, Cunsolo V, Foti Sand De Pinto V (2018) Post-translational modification of VDAC1 and VDAC2 cysteines from rat liver mitochondrial. *Biochim Biophys Acta* **1859**, 806–816.
36 Kerner J, Lee K, Tandler B and Hoppel CL (2012) VDAC proteomics: post-translation modifications. *Biochim Biophys Acta* **1818**, 1520–1525.
37 Lee H, Lara P, Ostuni A, Presto J, Johansson J, Nilsson I and Kim H (2014) Live-cell topology assessment of URG7, $MRP6_{102}$ and SP-C using glycosylatable green fluorescent protein in mammalian cells. *Biochem Biophys Res Commun* **450** (4), 1587–1592.
38 Gupta R and Ghosh S (2017) Phosphorylation of purified mitochondrial Voltage-Dependent Anion Channel by c-Jun N-terminal Kinase-3 modifies channel voltage-dependence. *Biochim Open* **4**, 78–87.
39 Miglionico R, Gerbino A, Ostuni A, Armentano MF, Monné M, Carmosino M and Bisaccia F (2016) New insights into the roles of the N-terminal region of the ABCC6 transporter. *J Bioenerg Biomembr* **48** (3), 259–267.
40 Doring D and Colombini M (1985) Voltage dependence and ion selectivity of the mitochondrial channel, VDAC, are modified by succinic anhydride. *J Membrain Biol* **83** (1–2), 81–86.
41 Leggio L, Guarino F, Magrì A, Accardi-Gheit R, Reina S, Specchia V, Damiano F, Tomasello MF, Tommasino M and Messina A (2018) Mechanism of translation control of the alternative *Drosophila melanogaster* Voltage Dependent Anion Channel 1 mRNAs. *Sci Rep* **8**, 5347.

Article 4.

Frontiers in Physiology

Voltage-Dependent Anion Selective Channel Isoforms in Yeast: Expression, Structure, and Functions

Maria Carmela Di Rosa[1†], Francesca Guarino[1,2†], Stefano Conti Nibali[1], Andrea Magrì[2,3] and Vito De Pinto[1,2]

1 Department of Biomedical and Biotechnological Sciences, University of Catania, Catania, Italy,
2 we.MitoBiotech S.R.L., Catania, Italy,
3 Department of Biological, Geological and Environmental Sciences, University of Catania, Catania, Italy

frontiers in Physiology

MINI REVIEW
published: 19 May 2021
doi: 10.3389/fphys.2021.675708

Voltage-Dependent Anion Selective Channel Isoforms in Yeast: Expression, Structure, and Functions

Maria Carmela Di Rosa[1†], Francesca Guarino[1,2†], Stefano Conti Nibali[1], Andrea Magrì[2,3] and Vito De Pinto[1,2]*

[1] Department of Biomedical and Biotechnological Sciences, University of Catania, Catania, Italy, [2] we.MitoBiotech S.R.L., Catania, Italy, [3] Department of Biological, Geological and Environmental Sciences, University of Catania, Catania, Italy

Mitochondrial porins, also known as voltage-dependent anion selective channels (VDACs), are pore-forming molecules of the outer mitochondrial membranes, involved in the regulation of metabolic flux between cytosol and mitochondria. Playing such an essential role, VDAC proteins are evolutionary conserved and isoforms are present in numerous species. The quest for specific function(s) related to the raise of multiple isoforms is an intriguing theme. The yeast *Saccharomyces cerevisiae* genome is endowed with two different VDAC genes encoding for two distinct porin isoforms, definitely less characterized in comparison to mammalian counterpart. While yVDAC1 has been extensively studied, the second isoform, yVDAC2, is much less expressed, and has a still misunderstood function. This review will recapitulate the known and poorly known information in the literature, in the light of the growing interest about the features of VDAC isoforms in the cell.

Keywords: porin, VDAC, mitochondria, electrophyiology, yeast, outer mitochondrial membrane

OPEN ACCESS

Edited by:
Clara De Palma, University of Milan, Italy

Reviewed by:
Yasuo Shinohara, Tokushima University, Japan
Tatiana Rostovtseva, National Institutes of Health (NIH), United States

***Correspondence:**
Andrea Magrì
andrea.magri@unict.it

† These authors have contributed equally to this work

Specialty section:
This article was submitted to Mitochondrial Research, a section of the journal Frontiers in Physiology

Received: *03 March 2021*
Accepted: *20 April 2021*
Published: *19 May 2021*

Citation:
Di Rosa MC, Guarino F, Conti Nibali S, Magrì A and De Pinto V (2021) Voltage-Dependent Anion Selective Channel Isoforms in Yeast: Expression, Structure, and Functions. Front. Physiol. 12:675708. doi: 10.3389/fphys.2021.675708

INTRODUCTION

The passive diffusion of small hydrophilic molecules throughout outer membranes (OM) of Gram-negative bacteria, mitochondria and chloroplast is provided by the presence of integral membrane proteins commonly named *porins*. Characterized by a cylindrical shape, porins were firstly discovered in prokaryotes (Nakae, 1976) and subsequently in mitochondria (Schein et al., 1976; Colombini, 1979) and chloroplast (Smack and Colombini, 1985), supporting the endosymbiotic theory. Porins are generally arranged in a conserved β-barrel structure, with polar amino acids facing the hydrophilic compartments counterbalanced by non-polar residues in the hydrophobic membrane core (Benz, 1989; Rosenbusch, 1990; Zeth and Thein, 2010).

The first mitochondrial porin was identified in the unicellular ciliate *Paramecium tetraurelia* by Schein et al. (1976). In artificial membranes, the protein showed a maximal conductance at the transmembrane potential close to zero, which decreased as a function of both positive and negative voltage applied (Schein et al., 1976). Furthermore, the channel exhibited a slight preference for anions over cations in the high-conducting state (Schein et al., 1976; Benz et al., 1988). Given these electrophysiological features, mitochondrial porin was then named Voltage-Dependent Anion selective Channel (VDAC).

VDACs are ubiquitously expressed proteins of about 28–32 kDa, with an estimated pore dimension of ∼3–3.5 nm in diameter and ∼4–4.5 nm in height. The

number of VDAC isoforms varies significantly in many species, ranging from one or two in yeast, three in mammals and up to five in plants (Young et al., 2007). Anyway, they represent the most abundant protein family of the outer mitochondrial membrane (OMM), accounting for ∼50% of the total protein content (Mannella, 1998; Gonçalves et al., 2007). This confers the typical sieve-like aspect to the OMM, as revealed by atomic force microscopy experiments (Gonçalves et al., 2007, 2008).

While human and murine VDACs were extensively studied, the same was not for the *Saccharomyces cerevisiae* counterpart. *S. cerevisiae*, also known as the Baker's yeast, is a unicellular organism widely employed as a eukaryotic model. Its genome was completely sequenced in 1996 (Goffeau et al., 1996), making the genetic manipulation simpler through recombination techniques. Furthermore, most of the metabolic and cellular pathways, especially those involving mitochondria biogenesis and function, are conserved. This has led to define yeast "a smaller but not lower eukaryote" (Rine, 1989).

In the lights of these considerations, in this review we summarized all the literature information available so far about the structure, the electrophysiological features and the peculiar functions of the two VDAC isoforms expressed by the yeast *S. cerevisiae*.

THE STRUCTURE AND FUNCTIONS OF VDAC PROTEINS

From the time of their discovery, many hypotheses were formulated about VDAC three-dimensional structure. The alternation of hydrophobic and hydrophilic residues, as revealed by the sequence analysis, and a set of single-point mutagenesis experiments allowed the development of the first model, consisting in a transmembrane barrel made of 12 antiparallel β-strands and one amphipathic is α-helix (Blachly-Dyson et al., 1990; Thomas et al., 1993). In the early 2000s, by using computational approaches, *Neurospora crassa* and *S. cerevisiae* VDACs were modeled onto bacterial porins structures available at that time, predicting a 16 β-strands barrel structure with a globular α-helix corresponding to the first amino acid residues of the N-terminal domain (Casadio et al., 2002). The specific structure of N-terminus, already predicted by the first studies (Blachly-Dyson et al., 1990; Thomas et al., 1993), was experimentally confirmed by circular dichroism experiments performed by independent groups (Guo et al., 1995; Bay and Court, 2002; De Pinto et al., 2007). However, only several years later the three-dimensional structures of murine and human VDAC1 (Bayrhuber et al., 2008; Hiller et al., 2008; Ujwal et al., 2008) and zebrafish VDAC2 (Schredelseker et al., 2014) were determined by NMR spectroscopy, X-ray crystallography or a combination of these two techniques.

The β-barrel pore structure of VDAC proteins is built by 19 β-strands connected to each other by short turns and loops. This makes mitochondrial porins significantly different from bacterial general porins, which have an even, variable number of β-strands, commonly between 14 and 18 (Achouak et al., 2001; Nikaido, 2003). In VDAC, strands are anti-parallel except for the first and the last one, showing instead a parallel orientation. As predicted, in the first 26 N-terminal residues two short α-helix stretches were found. Although there are several differences in the specific location among the models, all authors agree that N-terminus does not take part in the barrel formation, as evinced also from the superposition of human and murine VDAC1 (Zeth and Zachariae, 2018). According to Bayrhuber et al. (2008) the sequence 7–17 (at the N-terminal end) is horizontally oriented inside the barrel and the sequence 3–7 contacts the pore wall. Similar findings have been found in the other models, where the presence of N-terminus within the channel lumen was justified by the presence of a specific hydrogen-bonding pattern between it and several specific residues located in different strands of the barrel (Ujwal et al., 2008) and/or by hydrophobic interactions (Hiller and Wagner, 2009).

As farther detailed, a putative role in the channel gating was assigned to the N-terminus (Shuvo et al., 2016). In fact, the domain is connected to the barrel by a glycine-rich motif, which confers flexibility. It is thus believed that N-terminal domain is capable to leave the lumen and to partially expose itself to the cytosolic environment, possibly mediating the interaction with the membrane or other proteins (Geula et al., 2012; Manzo et al., 2018). This hypothesis is supported by the transmission electron microscopy work by Guo et al. (1995) and, more recently, by the definition of VDAC topology within the OMM (Tomasello et al., 2013).

The pore allows the passive diffusion through the OMM of small ions (Na^+, Cl^-, and K^+) and metabolites up to ∼5,000 Da, including ATP/ADP and nucleotides, intermediates of Krebs' cycle (glutamate, pyruvate, succinate, malate) and NAD^+/NADH (Benz, 1994; Hodge and Colombini, 1997; Rostovtseva and Colombini, 1997; Gincel and Shoshan-Barmatz, 2004). Other small molecules are instead capable to modulate the pore activity and/or interaction of VDACs with cytosolic proteins and enzymes. By binding the channel, cholesterol preserves the structural integrity of VDAC and facilitates its insertion in lipid bilayers (De Pinto et al., 1989a; Popp et al., 1995; Hiller et al., 2008). Being a component of the OMM, cholesterol amount may vary according to the conditions, affecting in turn VDAC functionality (Baggetto et al., 1992; Pastorino and Hoek, 2008).

In this perspective, VDACs are widely considered essential for the maintenance of the mitochondrial bioenergetic and the communication between the organelle and the rest of the cell (as reviewed in Shoshan-Barmatz et al., 2010; De Pinto, 2021).

VOLTAGE-DEPENDENT ANION SELECTIVE CHANNELS HAVE ISOFORM-SPECIFIC FUNCTIONS

Both VDAC genes and proteins are evolutionary conserved. The three different mammalian VDAC isoforms are encoded by independent genes, each characterized by a similar intron-exon organization. VDAC2 gene has an additional pre-sequence placed upstream of the first exon that confers to the protein a 11-amino acids longer N-terminus (Messina et al., 2012). Furthermore, the proteins are characterized by high intra- and

inter-species sequence conservation. For instance, mammalian isoforms show up to ∼75% of sequence similarity, while yeast and human VDAC1 share about 70% of similar sequence (Young et al., 2007; Messina et al., 2012). This implies that all VDAC proteins should have similar structure/functions, as arises from computational simulations made for all the proteins for which the three-dimensional structure is not available yet (De Pinto et al., 2010; Guardiani et al., 2018). Accordingly, VDACs from mice, yeast, fruit fly, and human can substitute for each other in the regulation of metabolic fluxes if expressed in yeast mitochondria, as demonstrated by complementation assays performed in porin-less strain(s) on non-fermentable carbon sources (i.e., glycerol) at the restrictive temperature of 37°C (Sampson et al., 1997; Xu et al., 1999; Reina et al., 2010; Leggio et al., 2018). At the same time, the simultaneous presence of different isoforms has raised the question of distinct and non-redundant functions for each VDAC. While this issue is unexplained for yeast, several hypotheses have been put forward for high eukaryotes.

In mammals, VDACs show a tissue-specific distribution in which VDAC1 is the most ubiquitous (Cesar and Wilson, 2004; De Pinto et al., 2010). While controlling the overall permeability of OMM (Tomasello et al., 2009) and participating in Ca^{2+} homeostasis (De Stefani et al., 2012), VDAC1 interacts with proteins of Bcl-2 family and hexokinases, playing a crucial role for the activation of apoptosis (Shimizu et al., 2001; Abu-Hamad et al., 2008; Huang et al., 2013). Upon specific stimuli, VDAC1 undergoes oligomerization allowing MOM permeabilization, as well as the release of cytochrome c and/or mitochondrial DNA fragments (Keinan et al., 2010;. Kim et al., 2019).

VDAC2 was initially indicated as a pro-survival protein, being able to prevent the activation of the pro-apoptotic protein Bak (Cheng et al., 2003). In the last years, however, a mechanism in which VDAC2 is necessary for the activation of Bax, another pro-apoptotic member of Bcl-2 family, was proposed (Ma et al., 2014; Chin et al., 2018).

On the contrary, the specific role of VDAC3 remains not completely clarified yet. This isoform has specific and peculiar features: for example, in non-reducing conditions it forms small pores of about 90 pS in artificial membranes (Checchetto et al., 2014) while, in yeast devoid of endogenous porins, it complements the growth defect only partially (Sampson et al., 1997; Reina et al., 2010). In the last years, our group carried out site-direct mutagenesis experiments on human VDAC3 aimed at replacing cysteine with alanine residues. Cysteines, indeed, can undergo oxidation/reduction according to the environment. Mutations of single or multiple cysteines significantly increased the conductance of VDAC3 up to similar or identical values to those shown by the other isoforms (Reina et al., 2016a; Queralt-Martín et al., 2020), suggesting that the pattern of post-translational modifications (PTMs) modulates VDAC3 activity (Okazaki et al., 2015; Reina et al., 2016a). This hypotesis was later confirmed by mass spectrometry (Saletti et al., 2017; Pittalà et al., 2020). Given also the specific interaction of VDAC3 with stress sensor and redox-mediating enzymes (Messina et al., 2014), this isoform was indicated as a putative mitochondrial sensor of the oxidative stress (De Pinto et al., 2016; Reina et al., 2016b, 2020).

The pattern of cysteine oxidation was never studied in yeast. Isoform 1 has only two cysteines similar to mammal VDAC1. The same holds for yVDAC2, whose PTMs study by mass spectrometry is practically hindered by its paucity in the usual yeast strains.

THE VDAC GENES AND PROTEINS IN YEAST

Differently from mammals, *S. cerevisiae* genome is endowed with two different genes encoding for two distinct porin isoforms. As summarized in **Table 1**, the so-called *POR* genes are located in different chromosomes and they are very similar in length. A comparative genomic analysis has suggested that isoforms have been originated from genome duplication during the evolution. This phenomenon was postulated for *S. cerevisiae* and *Candida glabrata* but not for other Saccharomycetales fungi such as *Kluyveromyces lactis* or *S. pombe* in which VDAC paralogs were not detected (Kellis et al., 2004). At the same time, in *C. glabrata* the gene encoding for the second VDAC isoform is highly degenerate, raising the specific question about the maintenance of both *POR* copies in *S. cerevisiae* (Young et al., 2007).

Being encoded by the nuclear genome, all VDACs are synthesized by cytosolic ribosomes and subsequently imported into the OMM by specific evolutionary conserved protein complexes (Ulrich and Rapaport, 2015). This process was in-depth studied using the yeast as a cellular model. Briefly, the translocase of outer membrane (TOM) complex recognizes VDAC precursors onto OMM surface and drives the protein translocation through the main TOM complex subunit, Tom40 (Pfanner et al., 2004; Chacinska et al., 2009), which is itself a β-barrel protein (Araiso et al., 2019; Tucker and Park, 2019). The signal allowing the mitochondrial targeting is a hydrophobic β-harpin motif that interacts with Tom20, another subunit of TOM complex (Jores et al., 2016). The final assembly of VDAC into the OMM is achieved by the presence of a second complex, the sorting and assembly machinery (SAM) complex (also known with the acronym of TOB complex). Again, the main SAM complex subunit is the β-barrel protein Sam50/Tob55 (Kozjak et al., 2003; Takeda et al., 2021).

The expression levels of the two yeast VDAC isoforms appears profoundly different. A recent determination of the mitochondrial proteome at high-confidence identified an average copy number of 16,000 for yVDAC1 and 1–2 copy for yVDAC2 per single mitochondria (Morgenstern et al., 2017). This difference was attributed to the promoter strength, as hypothesized immediately after *POR* genes discovery (Blachly-Dyson et al., 1997). In fact, if *POR2* sequence is cloned downstream *POR1* promoter, yVDAC2 protein levels resemble those of yVDAC1 in physiological condition (Blachly-Dyson et al., 1997).

The primary sequences of yVDACs were determined after their identification. Multialigment analysis shown in **Figure 1A** revealed less than 50% of sequence identity between the two VDAC isoforms of *S. cerevisiae*. However, the computational analysis indicates high similarity in term

TABLE 1 | Main features of POR genes and proteins.

Gene	ORF	Location	Position	Size (bp)	Protein length (aa)
POR1	YNL055C	chrXIV	517.994–518.845	852	283
POR2	YIL114C	chrIX	149.143–149.988	846	281

Genetic information about POR genes and the coorrespondent proteins. Data were taken from Saccharomices Genome Database (https://www.yeastgenome.org).

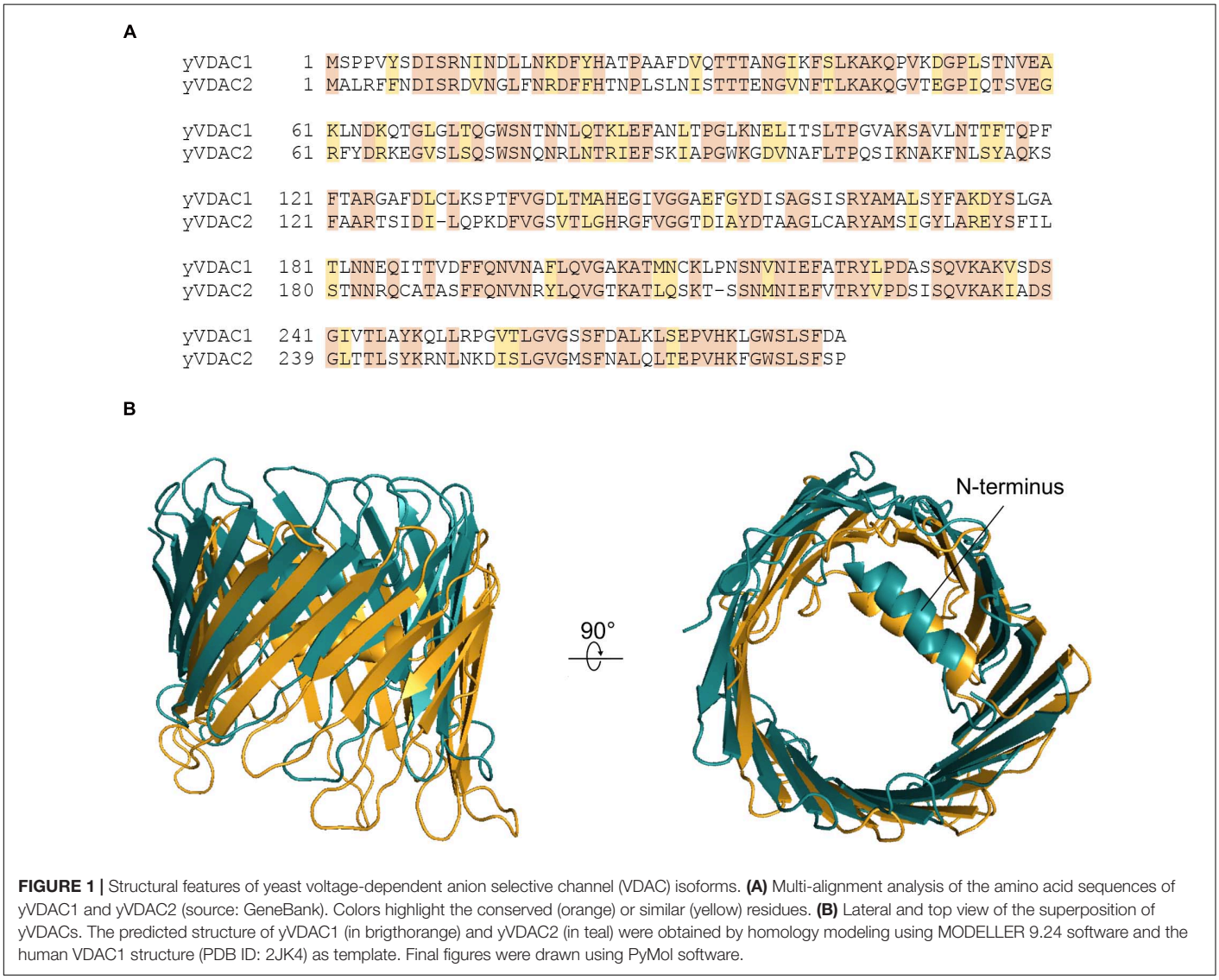

FIGURE 1 | Structural features of yeast voltage-dependent anion selective channel (VDAC) isoforms. **(A)** Multi-alignment analysis of the amino acid sequences of yVDAC1 and yVDAC2 (source: GeneBank). Colors highlight the conserved (orange) or similar (yellow) residues. **(B)** Lateral and top view of the superposition of yVDACs. The predicted structure of yVDAC1 (in brigthorange) and yVDAC2 (in teal) were obtained by homology modeling using MODELLER 9.24 software and the human VDAC1 structure (PDB ID: 2JK4) as template. Final figures were drawn using PyMol software.

of three-dimensional structures, as strengthened by homology modeling predictions (Guardiani et al., 2018) displayed in **Figure 1B**. Despite this, many substantial differences exist in the electrophysiological features, as fully described in the next paragraphs.

YEAST VDAC1: FROM THE DISCOVERY TO THE ELECTROPHYSIOLOGICAL CHARACTERIZATION

The first evidence of porin existence in yeast was observed by Mihara et al. (1982). They described a porin-like activity in isolated OMM fractions attributed to the presence of a single predominant ∼29 kDa protein comparable to that previously found in rat liver mitochondria (Mihara et al., 1982). This protein was generically called "porin" by analogy to the other similar proteins of Gram-negative bacteria. Only after the discovery of a second porin isoform it was formally named yVDAC1 or POR1.

The primary structure of yVDAC1 was deduced from the nucleotide sequence, revealing a 283 amino acid long molecule (Mihara and Sato, 1985). In comparison to the human homologous, it has similarity and identity values of 67 and 24%, respectively (Hiller et al., 2010).

The electrophysiological properties of yVDAC1 were then investigated after protein isolation from mitochondria and

incorporation into planar lipid bilayer (PLB). The protein showed a high propensity to form pores in artificial membranes, characterized by an average conductance of ∼4 nS in 1 M KCl solution (Forte et al., 1987a). In a similar manner to what previously observed for VDACs extracted from *N. crassa* (Freitag et al., 1982), rat brain (Ludwig et al., 1986), and other mammalian tissues (De Pinto et al., 1987), the application of increasing positive and negative voltages, from 0 to ±60 mV, promoted a significative reduction of yVDAC1 conductance. In particular, a high-conducting or open state was observed at low voltages. Conversely, the application of potential, starting from ±10–20 mV, resulted in a symmetrical switch toward low-conducting or closed state(s) (Forte et al., 1987a). Notably, these data were recently confirmed by our group. In particular, we observed an average value of yVDAC1 conductance of ∼4.2 nS and a voltage-dependent behavior starting from ±20–30 mV (Guardiani et al., 2018).

The ion selectivity of yVDAC1 was also investigated. The protein prefers anion over cations in the open state, while in the closed state it becomes less anionic or more cation selective (Schein et al., 1976; Forte et al., 1987b; Colombini, 2016). These observations are in agreement with our recent report showing a ratio Cl^-:K^+ of 2:1 in the open state and 1:4 in the closed state (Guardiani et al., 2018). Similar electrophysiological features were detected for human VDAC1 (Reina et al., 2013) and for *Drosophila melanogaster* VDAC1 (De Pinto et al., 1989b).

A summary of the main electrophysiological features, as well as a comparison with those of yVDAC2, is shown in **Figure 2**.

Particularly interesting for the maintenance of electrophysiological features of VDACs is the N-terminal domain, as revealed by mutagenesis experiments. E.g., the mutations of Asp 15 to Lys or Lys 19 to Glu modified the sensitivity of yVDAC1 to the voltage applied, as well as the ion selectivity (Blachly-Dyson et al., 1990; Thomas et al., 1993). Remarkably, these residues are conserved in mammalian VDACs suggesting that they are essential for the proper functioning and gating of the channel. Also truncation or substitution of specific part of the N-terminus has similar effects. E.g., the truncated yVDAC1, missing the first 8 amino acids, showed an abnormal channel activity and a pronounced instability of the open state, which rapidly switched toward multiple low-conducting states (Koppel et al., 1998).

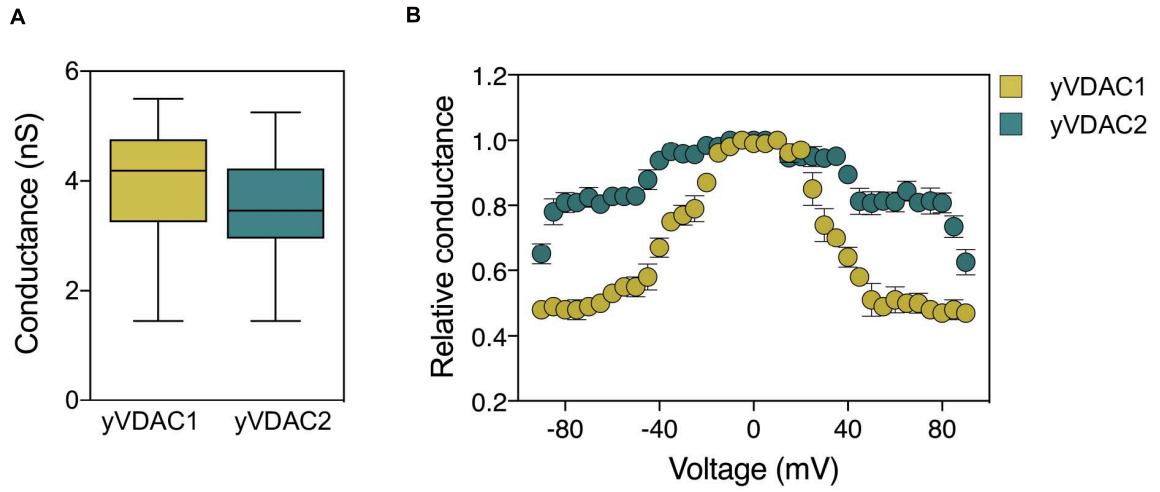

C

	P_K/P_{Cl} ratio		
	Anionic state	Cationic state 1	Cationic state 2
yVDAC1	0.57 ± 0.09	3.9 ± 0.4	-
yVDAC2	0.30 ± 0.03	2.17 ± 0.11	16.24 ± 6

FIGURE 2 | Comparative analysis of the electrophysiological features of native yVDAC1 and yVDAC2 at the Planar Lipid Bilayer. **(A)** Analysis of conductance after yVDACs reconstitution into the artificial membrane. Experiments were performed with an applied constant voltage of +10 mV in 1 M KCl solution. **(B)** Analysis of the voltage-dependence of yVDACs isoforms. Experiments were performed by gradually increasing the voltage from 0 to ±100 mV. Data are expressed as mean of the relative conductance ± SEM. The relative conductance was calculated as the G/G_0, where G is the conductance at the given voltage while G_0 is the conductance values calculated at 0 mV applied. **(C)** Analysis of current-voltage performed in a 10-fold gradient 1/0.1 M cis/trans KCl in a voltage ramp with amplitude ± 60 mV. Values of reversal potential were used to estimate the permeability ratio of cations (P_K) over anions (P_{Cl}) by using the Goldman-Hodgkin-Katz equation in the three states.

The importance of the N-terminus for the channel function was demonstrated also for human VDAC isoforms. It is known that VDAC3 is the less active one in complementation assay of porin-less yeast performed on glycerol at 37°C or in the presence of acetic acid (a cell death inductor, Reina et al., 2010). Swapping experiments in which the first 20 N-terminal residues of VDAC3 were replaced with those from VDAC1 or VDAC2, showed increased life span and resistance to oxidative stress than porin-less yeast transformed with plasmids carrying wild-type VDAC3 sequence (Reina et al., 2010).

YEAST VDAC1 IS ESSENTIAL FOR THE PROPER MAINTENANCE OF MITOCHONDRIA

VDAC1 is by far the most abundant protein of yeast mitochondria, accounting for 7,000–19,000 copies per organelle, as for growth on glucose and glycerol, respectively (Morgenstern et al., 2017). Notably, this number overcomes of one and two orders of magnitude the copy number of the second and the third OMM most represented proteins, Tom40 and Sam50. From this study, we tried to estimate the overall OMM conductance, given by all the β-barrel proteins, and the specific contribution of yVDAC1. In this calculation, we included the putative pore-forming proteins recently discovered by Krüger et al. (2017), such as Mim1, Ary1, OMC7, and OMC8 as well as the β-barrel component of TOM and SAM complexes that can mediate small molecules exchanges across the OMM (Kmita and Budzińska, 2000; Antos et al., 2001). From this analysis emerged that the outer membrane of a single mitochondrion has an estimated permeability of ∼30 μS, 27 of which are provided by yVDAC1 (Magrì et al., 2020). It thus is clear that this isoform is mainly involved in the metabolic exchanges and in the maintenance of the communication between mitochondria and the rest of the cell.

Many information about yVDAC1 function arose from the study of Δ*por1* mutant, in which *POR1* was genetically inactivated. The strain was still viable, but it showed a marked growth impairment on media containing non-fermentable carbon sources (i.e., substrates which are mainly metabolized in mitochondria) at temperature of 37°C (Blachly-Dyson et al., 1990). More recently, our group performed an extensive characterization of Δ*por1* yeast in order to expand the knowledge of this model. Our results indicate that mitochondrial respiration is dramatically compromised in the absence of yVDAC1, since the expression of the respiratory chain subunits encoded by mtDNA, but not nuclear DNA, was completely abolished, as a consequence of the dramatic reduction of mtDNA (Magrì et al., 2020). In this context, the metabolites commonly addressed to the mitochondria, as pyruvate, are pushed toward a cytosolic utilization and the whole cell metabolism undergoes a complete rearrangement aimed to by-pass mitochondria. To survive in the absence of yVDAC1, the cells enhance the biosynthesis of phospholipids, which are then stored into lipid droplets (as an energy reserve) or in the plasma membrane, as schematized in **Figure 3** (Magrì et al., 2020). Overall, these results revealed once again the irreplaceable role of yVDAC1 for the OMM permeability and for mitochondrial metabolism.

An increasing body of evidence suggests an equally important function of yVDAC1 in mitochondrial biogenesis. It is known since many years that the inactivation of *POR1* affects the expression of specific subunits of TOM and SAM complexes (Galganska et al., 2008; Karachitos et al., 2009). However, only recently a direct involvement of yVDAC1 in this mechanism was demonstrated. The assembly of TOM complexes requires the presence of the constituent protein Tom40 and Tom22 (Model et al., 2001). Sakaue et al. (2019) demonstrated that yVDAC1 interacts with Tom22, preventing the transition from a dimeric to a trimeric form of the complex, essential for the import of specific proteins. Furthermore, yVDAC1 antagonizes Tom6, another regulator of TOM assembly (Sakaue et al., 2019). At the same time, yVDAC1 modulates also the Translocase of the inner membrane (TIM) complex activity, by its direct interaction with Tim22. In this contest, yVDAC1 was individuated as a coupling factor for protein translocation of carrier precursors into the inner mitochondrial membrane (IMM) (Ellenrieder et al., 2019). Notably, both these works supported this brand new role of yVDAC1 independent of its metabolic function (Edwards and Tokatlidis, 2019).

As a last point, the role of yVDAC1 in the regulation of yeast redox homeostasis is less characterized than in mammals. VDAC are intrinsically sensitive to oxidation (Saletti et al., 2017, 2018) and during the exponential and/or stationary growth phases they undergo oxidation/carbonylation (O'Brien et al., 2004). However, this effect is exacerbated in yeast strains devoid of the antioxidant enzymes superoxide dismutase (SOD), as expected. The cytosolic Cu/Zn SOD (SOD1), however, not only protects yVDAC1 from oxidation but it is required for the proper channel activity and expression of yVDAC1 (Karachitos et al., 2009). At the same time, the inactivation of *POR1* affects the expression of the mitochondrial Mn-SOD (SOD2) (Galganska et al., 2008, 2010), suggesting a mutual regulation between the two proteins.

THE CONTROVERSIAL STORY OF YVDAC2

Until 1996, yVDAC1 was believed the only porin isoform of *S. cerevisiae*. Two different events contributed to the discovery of the second VDAC: the availability of yeast genomic sequences and the increasing use of recombinant techniques aimed to inactivate specific genes. By the insertion of a functional *LEU2* gene in the *POR1* sequence, yVDAC1 was knocked-out and the Δ*por1* mutant was obtained (Dihanich et al., 1987). The mutant showed normal levels of other OMM proteins but reduced levels of cytochrome c_1 and cytochrome oxidase subunit IV (Dihanich et al., 1987). Surprisingly, Δ*por1* strain was still viable, even if it grew slower than the wild-type at 30°C (Dihanich et al., 1987). This result suggested the existence of some unknown alternative pathway through which small metabolites and ions could cross the OMM.

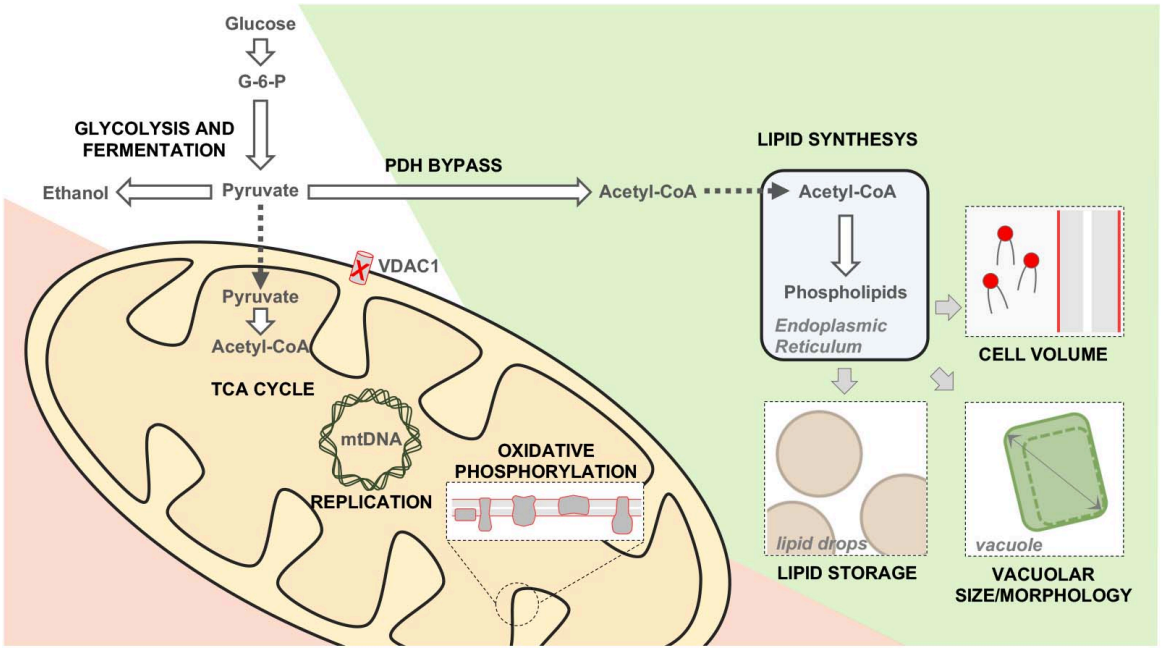

FIGURE 3 | Metabolic and phenotypic changes occurring in Δ*por1* cells. Schematic representation of the main changes occurring in yeast upon *POR1* gene inactivation. Metabolic down-regulated, upregulated or unchanged pathways are displayed in red, green and white, respectively. The absence of yVDAC1 reduces the nucleotides trafficking within mitochondria, affecting the replication/expression of the mtDNA. The mitochondrial utilization of pyruvate, TCA cycle and the functioning of the electron transport system are strongly compromised. On the other hand, the cytosolic conversion of pyruvate into acetyl-coA is enhanced (PDH by-pass). The latter is addressed toward the synthesis of phospholipids, which are then stored into lipid drops (an energy reservoir). Furthermore, the newly synthetized phospholipids contribute to build plasma membrane and to increase the vacuole dimension. As a consequence, the size of Δ*por1* cells is increased of about 30% in comparison to the wild-type.

The analysis of Δ*por1* growth on glycerol at the elevated temperature of 37 °C has revealed a specific defect (Blachly-Dyson et al., 1990). Glycerol, indeed, is a non-fermentable carbon source that forces the utilization of mitochondria (Gancedo et al., 1968). By screening a genomic *S. cerevisiae* library, Blachly-Dyson et al. (1997) identified a second VDAC isoform through its ability to correct this Δ*por1* growth defect. Then, a second porin gene, called *POR2* and encoding for yVDAC2, was individuated.

yVDAC2 was immediately indicated as a potential yVDAC1 substitute, even if some peculiarities emerged. For instance, the second yeast VDAC isoform was able to restore the growth defect of Δ*por1* only upon specific conditions. If *POR2* is present in low copy number (one or two copies per cell) it fails to substitute yVDAC1. Conversely, when *POR2* sequence is cloned downstream the *POR1* promoter it can successfully restore the yeast growth as in wild-type (Blachly-Dyson et al., 1997). Notably, Δ*por1* transformation with single copy plasmid, carrying the encoding sequences of mouse VDAC isoforms 1 and 2, completely recovers the yeast growth on glycerol at 37°C (Sampson et al., 1997). This suggested that yVDAC2 had pore-forming activity but such compensation was strictly depended on its concentration. However, all the efforts made by Blachly-Dyson et al. (1997) to isolate and incorporate yVDAC2 in artificial membrane failed, prompting the scientific community to question the pore-forming ability of yVDAC2 and its involvement in mitochondrial bioenergetics. This idea was supported by the low level of similarity between VDAC isoforms, consisting in only 49% (see **Figure 1A**). Also, not many information was obtained from deletion studies: differently from Δ*por1*, the genetic inactivation of *POR2* gene does not affect yeast growth in any condition, while the simultaneous absence of both endogenous porins, as in the double mutant Δ*por1*Δ*por2*, only exacerbates the yeast growth defect on glycerol typical of Δ*por1*.

YEAST VDAC2 HAS PORE FORMING ACTIVITY AND A PECULIAR ION SELECTIVITY

After its discovery, the interest in yVDAC2 has waned for almost two decades. However, in 2016, investigating the role of human SOD1 in yeast, we casually noticed a complete recovery of Δ*por1* growth defect on glycerol at 37°C in the presence of overexpressed hSOD1. In this condition, the expression level of *POR2*, as well as of other genes encoding for OMM β-barrel proteins (Tom40 and Sam50), was found significantly increased (Magrì et al., 2016b). Since the same results did not appear in Δ*por1*Δ*por2* yeast, we hypothesized that yVDAC2 might re-establish the OMM pore activity.

To definitely clarify this aspect, we established a collaboration with the group of prof. Hanna Kmita (Poznan, PL), aimed at purify with high yield yVDAC2. In the first attempt Δ*por1* strain was transfected with a plasmid carrying *POR2*

sequence and the protein was purified from Δ*por1* mitochondria, avoiding yVDAC1 contamination (Guardiani et al., 2018). It was called *native* yVDAC2. The second strategy applied the heterologous expression of a 6xHis-tagged yVDAC2 in *E. coli* (Magrì et al., 2019). Being a membrane protein, yVDAC2 localized in the inclusion bodies and needed high concentrations of denaturant to be purified, followed by a refolding step in presence of specific detergents (Engelhardt et al., 2007). Remarkably, this refolding method was successfully applied many times and by different groups, producing VDAC proteins with indistinguishable features from those native (Ujwal et al., 2008, Checchetto et al., 2014; Okazaki et al., 2015; Magrì et al., 2016a; Reina et al., 2016a; Queralt-Martín et al., 2020).

The electrophysiology at the PLB revealed that both native and recombinant proteins were able to form pores with the same, typical VDAC-like conductance of ∼3.6 nS in 1 M KCl, as displayed in **Figure 2A**) (Guardiani et al., 2018; Magrì et al., 2019). As for voltage-dependence, native yVDAC2 resembled yeast or human VDAC1, even if it began to close at ±40–50 mV. This suggests that yVDAC2 is slightly less sensitive to the applied voltage (**Figure 2B**). However, this specific aspect was amplified in the recombinant protein, which began to close only at ± 80–90 mV (Magrì et al., 2019). The difference between the native and recombinant forms of yVDAC2 raises the interesting question of whether the native yVDAC2 was subject to specific PTMs, not occurring in the heterologous expression in *E. coli*. The influence of PTMs in VDAC activity is indeed a rather unexplored subject.

Ion selectivity of yVDAC2 was particularly interesting. The computational analysis revealed a similar tridimensional structure for the two yeast VDAC isoforms but a net charge of +11 in the case of yVDAC2, in comparison to +1 of yVDAC1. Thus, anion selectivity was expected for yVDAC2 in the open state, as also predicted by bioinformatic analysis, with a chloride selectivity estimated 2–3 times higher than that displayed by isoform 1 (Guardiani et al., 2018). The analysis of native yVDAC2 at the PLB allowed the identification of up three states with different parameters of ionic selectivity: two of them appeared to be high-conductance states but with opposite selectivity (Guardiani et al., 2018; Magrì et al., 2019). In the open state, the ratio Cl^-: K^+ for yVDAC2 was 3:1, definitely more anionic than the corresponding state displayed by yVDAC1. The second high-conducting state showed a prominent cation selectivity (Cl^-: K^+ = 1:2) (Guardiani et al., 2018). This oddity is not entirely new with VDACs: a similar state was already observed for VDAC1 from mammals (Pavlov et al., 2005). The third state detected by studying yVDAC2 ion selectivity was a low-conducting and very cation-selective state (Cl^-: K^+ = 1:16, Guardiani et al., 2018). Such state was previously unseen in any studied VDAC. The ion selectivity of yVDAC isoforms is detailed in **Figure 2C**.

WHAT IS YVDAC2 FUNCTION?

Despite its demonstrated pore-forming activity, all evidences suggest that yVDAC2 plays only a marginal role in mitochondria bioenergetics. Indeed, the deletion of *POR2* does not significantly affect yeast growth on glycerol at 37°C although its simultaneous inactivation with *POR1* aggravates the growth defect (Blachly-Dyson et al., 1997). The involvement of yVDAC2 in mediating the OMM permeability to small molecules, such as NADH, was studied in Δ*por1* cells. Here, NADH permeability was found 20 times lower than in wild-type (Lee et al., 1998). However, similar results were obtained for the double mutant Δ*por1*Δ*por2*, excluding definitely the involvement of yVDAC2 in this pathway. Later, Tom40 was indicated as a valid substitute of yVDAC1 in Δ*por1* cells (Kmita and Budzińska, 2000; Antos et al., 2001).

A participation in the maintenance of energy homeostasis was also proposed for yVDAC2. SNF1 protein kinase is the orthologue of the mammalian AMP-activated protein kinase (AMPK), both important players in the regulation of cell growth and glucose metabolism in response to the energy limitation (Hedbacker and Carlson, 2008; Mihaylova and Shaw, 2011). It was shown that SNF1 co-precipitated with both yeast VDACs and SNF1 function was significantly affected only when both porin genes are simultaneously inactivated (Strogolova et al., 2012). For this reason, yVDAC2 was identified as a "co-sensor" of a stress signal upstream of SNF1, even if the precise mechanism was still unclear.

Anyway, given the pacucity of literature information, the residual hypothesis is that yVDAC2 acts as a rescue permeability mitochondrial pathway, expressed in presence of some undefined stimulus. In fact, the absence of yVDAC1 *per se* is not able to activate *POR2* gene expression (Magrì et al., 2020). On the contrary, the co-presence of an additional factor, such as the overexpressed hSOD1, induces *POR2* expression and restores the yeast growth defect of Δ*por1* cells (Magrì et al., 2016b).

Δ*POR1* YEAST, AN OPPORTUNITY TO STUDY VDAC ROLE IN HUMAN PATHOLOGIES

Despite the obvious absence of a nervous system in yeast, basic mechanisms and pathways underlying neurodegenerative diseases, such as mitochondrial dysfunction, transcriptional dysregulation, trafficking defects and proteasomal dysfunction, are extremely well conserved between humans and yeast, enabling detailed studies of the molecular events involved in those conditions.

Mitochondrial dysfunctions, along with defects in proteasomal activity and misfolded protein aggregations, are well-known molecular hallmarks of neurodegenerative disorders that can be easily recapitulated in a relatively simple system as the yeast. This is made possible by the presence of disease-associated human orthologues or by the introduction of a human protein directly linked to the disease of interested with easy manipulation techniques. For instance, yeast has been successfully used to investigate TDP43 and FUS dysfunction in amyotrophic lateral sclerosis (ALS), amyloid-β peptide and Tau in Alzheimer's disease, α-synuclein (αSyn) and Lrrk2 in Parkinson's disease, and Huntingtin in Huntington's disease (as reviewed in Miller-Fleming et al., 2008; Bharadwaj et al., 2010; Pereira et al., 2012; Rencus-Lazar et al., 2019). In this contest, VDAC proteins (and VDAC1 in particular) play a

crucial role in mediating mitochondrial dysfunction. In fact, most of the previously cited proteins are able to aggregate onto the cytosolic surface of mitochondria using VDAC as an anchor point (Magrì and Messina, 2017). Thus, the use of Δ*por1* mutant, transformed or not with plasmids carrying encoding sequences for human VDAC isoforms or mutants, represents an important opportunity to clarify the specific roles of porins in pathological contexts.

The involvement of human VDAC1 in mediating αSyn toxicity in Parkinson's disease was demonstrated for the first time in yeast. Rostovtseva et al. (2015) introduced αSyn expression in the Δ*por1* mutant, noticing a yeast growth defect on galactose only when the protein was expressed together with the human VDAC1. This finding supports the idea that mitochondrial dysfunction mediated by αSyn occurs through the modulation of VDAC1 permeability (Rostovtseva et al., 2015). Also, the specific ability of the three VDAC isoforms to counteract oxidative stress was investigated in yeast (Galganska et al., 2008), as well as the antibiotic minocycline specificity to interact with VDACs. These last studies revealed that minocycline interacts in a different manner with VDAC proteins and only isoform 3 is able to mediate the cytoprotective effect counteracting H_2O_2-mediated toxicity (Karachitos et al., 2012, 2016).

In the light of the emerging consideration of VDAC proteins as a pharmacological target in many diseases (Magrì et al., 2018; Shoshan-Barmatz et al., 2020), these few examples highlight the potential usage and the versatility of Δ*por1* cells for biotechnological and biomedical application.

CONCLUSION

Along with the increased interest of the scientific community in understanding VDACs role in apoptosis and mitochondrial dysfunctions, many studies have been carried out on mammalian or human porins, but significantly fewer for the yeast counterparts. Nevertheless, the complete understanding of *S. cerevisiae* VDACs functioning is equally important, especially considering its potential use as biomedical/biotechnological tool. The aim of this review was to collect all the information present in the literature about both yeast VDAC isoforms and to depict a framework as complete as possible. Despite this, several questions need to be addressed yet and deserved to be answered. One of above all: what is the physiological role of yVDAC2? Given the peculiar electrophysiological features here listed, it is indeed hard to believe that this protein is only a genetic heritage from a duplication event.

AUTHOR CONTRIBUTIONS

MCDR, FG, and SCN collected the information and prepared the reference list for the manuscript. AM drow the figures and wrote the manuscript. VDP supervised the work. All authors have read and approved the manuscript.

FUNDING

This research was conducted with the support of Università di Catania–linea PIACERI (Grants VDAC and ARVEST), Proof of Concept (Grant No. PEPSLA POC 01_00054) and AIM Linea 1 Salute (AIM1833071).

ACKNOWLEDGMENTS

Authors acknowledge Salvatore A. M. Cubisino for providing the help in the homology modeling figures preparation and Fondi di Ateneo 2020–2022, Universitaì di Catania, linea Open Access.

REFERENCES

Abu-Hamad, S., Zaid, H., Israelson, A., Nahon, E., and Shoshan-Barmatz, V. (2008). Hexokinase-I protection against apoptotic cell death is mediated via interaction with the voltage-dependent anion channel-1: mapping the site of binding. *J. Biol. Chem.* 283, 13482–13490. doi: 10.1074/jbc.M708216200

Achouak, W., Heulin, T., and Pagès, J. M. (2001). Multiple facets of bacterial porins. *FEMS Microbiol. Lett.* 199, 1–7. doi: 10.1016/S0378-1097(01)00127-6

Antos, N., Stobienia, O., Budzińska, M., and Kmita, H. (2001). Under conditions of insufficient permeability of VDAC1, external NADH may use the TOM complex channel to cross the outer membrane of Saccharomyces cerevisiae mitochondria. *J. Bioenerg. Biomembr.* 33, 119–126. doi: 10.1023/A:1010748431000

Araiso, Y., Tsutsumi, A., Qiu, J., Imai, K., Shiota, T., Song, J., et al. (2019). Structure of the mitochondrial import gate reveals distinct preprotein paths. *Nature* 575, 395–401. doi: 10.1038/s41586-019-1680-7

Baggetto, L. G., Clottes, E., and Vial, C. (1992). Low mitochondrial proton leak due to high membrane cholesterol content and cytosolic creatine kinase as two features of the deviant bioenergetics of ehrlich and AS30-D tumor cells. *Cancer Res.* 52, 4935–4941.

Bay, D. C., and Court, D. A. (2002). Origami in the outer membrane: the transmembrane arrangement of mitochondrial porins. *Biochem. Cell Biol.* 80, 551–562. doi: 10.1139/o02-149

Bayrhuber, M., Meins, T., Habeck, M., Becker, S., Giller, K., Villinger, S., et al. (2008). Structure of the human voltage-dependent anion channel. *Proc. Natl. Acad. Sci. U.S.A.* 105, 15370–15375. doi: 10.1073/pnas.0808115105

Benz, R. (1989). "Porins from mitochondrial and bacterial outer membranes: structural and functional aspects," in *Anion Carriers of Mitochondrial Membranes*, eds A. Azzi, K. A. Nałęz, M. J. Nałęcz, and L. Wojtczak (Berlin: Springer), 199–214. doi: 10.1007/978-3-642-74539-3_16

Benz, R. (1994). Permeation of hydrophilic solutes through mitochondrial outer membranes: review on mitochondrial porins. *Biochim. Biophys. Acta Rev. Biomembr.* 1197, 167–196. doi: 10.1016/0304-4157(94)90004-3

Benz, R., Wojtczak, L., Bosch, W., and Brdiczka, D. (1988). Inhibition of adenine nucleotide transport through the mitochondrial porin by a synthetic polyanion. *FEBS Lett.* 231, 75–80. doi: 10.1016/0014-5793(88)80706-3

Bharadwaj, P., Martins, R., and Macreadie, I. (2010). Yeast as a model for studying Alzheimer's disease. *FEMS Yeast Res.* 10, 961–969. doi: 10.1111/j.1567-1364.2010.00658.x

Blachly-Dyson, E., Peng, S., Colombini, M., and Forte, M. (1990). Selectivity changes in site-directed mutants of the VDAC ion channel: structural implications. *Science* 247, 1233–1236. doi: 10.1126/science.1690454

Blachly-Dyson, E., Song, J., Wolfgang, W. J., Colombini, M., and Forte, M. (1997). Multicopy suppressors of phenotypes resulting from the absence of yeast VDAC encode a VDAC-like protein. *Mol. Cell. Biol.* 17, 5727–5738. doi: 10.1128/mcb.17.10.5727

Casadio, R., Jacoboni, I., Messina, A., and De Pinto, V. (2002). A 3D model of the voltage-dependent anion channel (VDAC). *FEBS Lett.* 520, 1–7. doi: 10.1016/S0014-5793(02)02758-8

Cesar, M. D. C., and Wilson, J. E. (2004). All three isoforms of the voltage-dependent anion channel (VDAC1, VDAC2, and VDAC3) are present in mitochondria from bovine, rabbit, and rat brain. *Arch. Biochem. Biophys.* 422, 191–196. doi: 10.1016/j.abb.2003.12.030

Chacinska, A., Koehler, C. M., Milenkovic, D., Lithgow, T., and Pfanner, N. (2009). Importing mitochondrial proteins: machineries and mechanisms. *Cell* 138, 628–644. doi: 10.1016/j.cell.2009.08.005

Checchetto, V., Reina, S., Magrì, A., Szabo, I., and De Pinto, V. (2014). Recombinant human voltage dependent anion selective channel isoform 3 (hVDAC3) forms pores with a very small conductance. *Cell Physiol. Biochem.* 34, 842–853. doi: 10.1159/000363047

Cheng, E. H. Y., Sheiko, T. V., Fisher, J. K., Craigen, W. J., and Korsmeyer, S. J. (2003). VDAC2 inhibits BAK activation and mitochondrial apoptosis. *Science* 301, 513–517. doi: 10.1126/science.1083995

Chin, H. S., Li, M. X., Tan, I. K. L., Ninnis, R. L., Reljic, B., Scicluna, K., et al. (2018). VDAC2 enables BAX to mediate apoptosis and limit tumor development. *Nat. Commun.* 9:4976. doi: 10.1038/s41467-018-07309-4

Colombini, M. (1979). A candidate for the permeability pathway of the outer mitochondrial membrane. *Nature* 279, 643–645. doi: 10.1038/279643a0

Colombini, M. (2016). The VDAC channel: molecular basis for selectivity. *Biochim. Biophys. Acta* 1863, 2498–2502. doi: 10.1016/j.bbamcr.2016.01.019

De Pinto, V. (2021). Renaissance of VDAC: new insights on a protein family at the interface between mitochondria and cytosol. *Biomolecules* 11:107. doi: 10.3390/biom11010107

De Pinto, V., Benz, R., Caggese, C., and Palmieri, F. (1989a). Characterization of the mitochondrial porin from *Drosophila melanogaster*. *Biochim. Biophys. Acta Biomembr.* 987, 1–7. doi: 10.1016/0005-2736(89)90447-1

De Pinto, V., Benz, R., and Palmieri, F. (1989b). Interaction of non-classical detergents with the mitochondrial porin. *Eur. J. Biochem.* 183, 179–187. doi: 10.1111/j.1432-1033.1989.tb14911.x

De Pinto, V., Guarino, F., Guarnera, A., Messina, A., Reina, S., Tomasello, F. M., et al. (2010). Characterization of human VDAC isoforms: a peculiar function for VDAC3? *Biochim. Biophys. Acta Bioenerg.* 1797, 1268–1275. doi: 10.1016/j.bbabio.2010.01.031

De Pinto, V., Ludwig, O., Krause, J., Benz, R., and Palmieri, F. (1987). Porin pores of mitochondrial outer membranes from high and low eukaryotic cells: biochemical and biophysical characterization. *Biochim. Biophys. Acta Bioenerg.* 894, 109–119. doi: 10.1016/0005-2728(87)90180-0

De Pinto, V., Reina, S., Gupta, A., Messina, A., and Mahalakshmi, R. (2016). Role of cysteines in mammalian VDAC isoforms' function. *Biochim. Biophys. Acta Bioenerg.* 1857, 1219–1227. doi: 10.1016/j.bbabio.2016.02.020

De Pinto, V., Tomasello, F., Messina, A., Guarino, F., Benz, R., La Mendola, D., et al. (2007). Determination of the conformation of the human VDAC1 N-terminal peptide, a protein moiety essential for the functional properties of the pore. *ChemBioChem* 8, 744–756. doi: 10.1002/cbic.200700009

De Stefani, D., Bononi, A., Romagnoli, A., Messina, A., De Pinto, V., Pinton, P., et al. (2012). VDAC1 selectively transfers apoptotic Ca 2 signals to mitochondria. *Cell Death Differ.* 19, 267–273. doi: 10.1038/cdd.2011.92

Dihanich, M., Suda, K., and Schatz, G. (1987). A yeast mutant lacking mitochondrial porin is respiratory-deficient, but can recover respiration with simultaneous accumulation of an 86-kd extramitochondrial protein. *EMBO J.* 6, 723–728. doi: 10.1002/j.1460-2075.1987.tb04813.x

Edwards, R., and Tokatlidis, K. (2019). The yeast voltage-dependent anion channel porin: more important than just metabolite transport. *Mol. Cell* 73, 861–862. doi: 10.1016/j.molcel.2019.02.028

Ellenrieder, L., Dieterle, M. P., Doan, K. N., Mårtensson, C. U., Floerchinger, A., Campo, M. L., et al. (2019). Dual role of mitochondrial porin in metabolite transport across the outer membrane and protein transfer to the inner membrane. *Mol. Cell* 73, 1056–1065.e7. doi: 10.1016/j.molcel.2018.12.014

Engelhardt, H., Meins, T., Poynor, M., Adams, V., Nussberger, S., Welte, W., et al. (2007). High-level expression, refolding and probing the natural fold of the human voltage-dependent anion channel isoforms I and II. *J. Membr. Biol.* 216, 93–105. doi: 10.1007/s00232-007-9038-8

Forte, M., Adelsberger-Mangan, D., and Colombini, M. (1987a). Purification and characterization of the voltage-dependent anion channel from the outer mitochondrial membrane of yeast. *J. Membr. Biol.* 99, 65–72. doi: 10.1007/BF01870622

Forte, M., Guy, H. R., and Mannella, C. A. (1987b). Molecular genetics of the VDAC ion channel: Structural model and sequence analysis. *J. Bioenerg. Biomembr.* 19, 341–350. doi: 10.1007/BF00768537

Freitag, H., Neupert, W., and Benz, R. (1982). Purification and characterisation of a pore protein of the outer mitochondrial membrane from neurospora crassa. *Eur. J. Biochem.* 123, 629–636. doi: 10.1111/j.1432-1033.1982.tb06578.x

Galganska, H., Budzinska, M., Wojtkowska, M., and Kmita, H. (2008). Redox regulation of protein expression in *Saccharomyces cerevisiae* mitochondria: possible role of VDAC. *Arch. Biochem. Biophys.* 479, 39–45. doi: 10.1016/j.abb.2008.08.010

Galganska, H., Karachitos, A., Wojtkowska, M., Stobienia, O., Budzinska, M., and Kmita, H. (2010). Communication between mitochondria and nucleus: putative role for VDAC in reduction/oxidation mechanism. *Biochim. Biophys. Acta Bioenerg.* 1797, 1276–1280. doi: 10.1016/j.bbabio.2010.02.004

Gancedo, C., Gancedo, J. M., and Sols, A. (1968). Glycerol metabolism in yeasts: pathways of utilization and production. *Eur. J. Biochem.* 5, 165–172. doi: 10.1111/j.1432-1033.1968.tb00353.x

Geula, S., Ben-Hail, D., and Shoshan-Barmatz, V. (2012). Structure-based analysis of VDAC1: N-terminus location, translocation, channel gating and association with anti-apoptotic proteins. *Biochem. J.* 444, 475–485. doi: 10.1042/BJ20112079

Gincel, D., and Shoshan-Barmatz, V. (2004). Glutamate interacts with VDAC and modulates opening of the mitochondrial permeability transition pore. *J. Bioenerg. Biomembr.* 36, 179–186. doi: 10.1023/B:JOBB.0000023621.72873.9e

Goffeau, A., Barrell, G., Bussey, H., Davis, R. W., Dujon, B., Feldmann, H., et al. (1996). Life with 6000 genes. *Science* 274, 546–567. doi: 10.1126/science.274.5287.546

Gonçalves, R. P., Buzhynskyy, N., Prima, V., Sturgis, J. N., and Scheuring, S. (2007). Supramolecular assembly of VDAC in native mitochondrial outer membranes. *J. Mol. Biol.* 369, 413–418. doi: 10.1016/j.jmb.2007.03.063

Gonçalves, R. P., Buzhysnskyy, N., and Scheuring, S. (2008). Mini review on the structure and supramolecular assembly of VDAC. *J. Bioenerg. Biomembr.* 40, 133–138. doi: 10.1007/s10863-008-9141-2

Guardiani, C., Magrì, A., Karachitos, A., Di Rosa, M. C., Reina, S., Bodrenko, I., et al. (2018). yVDAC2, the second mitochondrial porin isoform of Saccharomyces cerevisiae. *Biochim. Biophys. Acta Bioenerg.* 1859, 270–279. doi: 10.1016/j.bbabio.2018.01.008

Guo, X. W., Smith, P. R., Cognon, B., D'Arcangelis, D., Dolginova, E., and Mannella, C. A. (1995). Molecular design of the voltage-dependent, anion-selective channel in the mitochondrial outer membrane. *J. Struct. Biol.* 114, 41–59. doi: 10.1006/jsbi.1995.1004

Hedbacker, K., and Carlson, M. (2008). SNF1/AMPK pathways in yeast. *Front. Biosci.* 13:2408–2420. doi: 10.2741/2854

Hiller, S., Abramson, J., Mannella, C., Wagner, G., and Zeth, K. (2010). The 3D structures of VDAC represent a native conformation. *Trends Biochem. Sci.* 35, 514–521. doi: 10.1016/j.tibs.2010.03.005

Hiller, S., Garces, R. G., Malia, T. J., Orekhov, V. Y., Colombini, M., and Wagner, G. (2008). Solution structure of the integral human membrane protein VDAC-1 in detergent micelles. *Science* 321, 1206–1210. doi: 10.1126/science.1161302

Hiller, S., and Wagner, G. (2009). The role of solution NMR in the structure determinations of VDAC-1 and other membrane proteins. *Curr. Opin. Struct. Biol.* 19, 396–401. doi: 10.1016/j.sbi.2009.07.013

Hodge, T., and Colombini, M. (1997). Regulation of metabolite flux through voltage-gating of VDAC channels. *J. Membr. Biol.* 157, 271–279. doi: 10.1007/s002329900235

Huang, H., Hu, X., Eno, C. O., Zhao, G., Li, C., and White, C. (2013). An interaction between Bcl-xL and the voltage-dependent anion channel (VDAC) promotes mitochondrial Ca2+ uptake. *J. Biol. Chem.* 288, 19870–19881. doi: 10.1074/jbc.M112.448290

Jores, T., Klinger, A., Groß, L. E., Kawano, S., Flinner, N., Duchardt-Ferner, E., et al. (2016). Characterization of the targeting signal in mitochondrial β-barrel proteins. *Nat. Commun.* 7:12036. doi: 10.1038/ncomms12036

Karachitos, A., Galganska, H., Wojtkowska, M., Budzinska, M., Stobienia, O., Bartosz, G., et al. (2009). Cu,Zn-superoxide dismutase is necessary for proper function of VDAC in *Saccharomyces cerevisiae* cells. *FEBS Lett.* 583, 449–455. doi: 10.1016/j.febslet.2008.12.045

Karachitos, A., Grobys, D., Antoniewicz, M., Jedut, S., Jordan, J., and Kmita, H. (2016). Human VDAC isoforms differ in their capability to interact with minocycline and to contribute to its cytoprotective activity. *Mitochondrion* 28, 38–48. doi: 10.1016/j.mito.2016.03.004

Karachitos, A., Jordan, J., and Kmita, H. (2012). Cytoprotective activity of minocycline includes improvement of mitochondrial coupling: the importance

of minocycline concentration and the presence of VDAC. *J. Bioenerg. Biomembr.* 44, 297–307. doi: 10.1007/s10863-012-9441-4

Keinan, N., Tyomkin, D., and Shoshan-Barmatz, V. (2010). Oligomerization of the mitochondrial protein voltage-dependent anion channel is coupled to the induction of apoptosis. *Mol. Cell Biol.* 30, 5698–5709. doi: 10.1128/mcb.00165-10

Kellis, M., Birren, B. W., and Lander, E. S. (2004). Proof and evolutionary analysis of ancient genome duplication in the yeast *Saccharomyces cerevisiae*. *Nature* 428, 617–624. doi: 10.1038/nature02424

Kim, J., Gupta, R., Blanco, L. P., Yang, S., Shteinfer-Kuzmine, A., Wang, K., et al. (2019). VDAC oligomers form mitochondrial pores to release mtDNA fragments and promote lupus-like disease. *Science* 366, 1531–1536. doi: 10.1126/science.aav4011

Kmita, H., and Budzińska, M. (2000). Involvement of the TOM complex in external NADH transport into yeast mitochondria depleted of mitochondrial porin1. *Biochim. Biophys. Acta Biomembr.* 1509, 86–94. doi: 10.1016/S0005-2736(00)00284-4

Koppel, D. A., Kinnally, K. W., Masters, P., Forte, M., Blachly-Dyson, E., and Mannella, C. A. (1998). Bacterial expression and characterization of the mitochondrial outer membrane channel: effects of N-terminal modifications. *J. Biol. Chem.* 273, 13794–13800. doi: 10.1074/jbc.273.22.13794

Kozjak, V., Wiedemann, N., Milenkovic, D., Lohaus, C., Meyer, H. E., Guiard, B., et al. (2003). An essential role of Sam50 in the protein sorting and assembly machinery of the mitochondrial outer membrane. *J. Biol. Chem.* 278, 48520–48523. doi: 10.1074/jbc.C300442200

Krüger, V., Becker, T., Becker, L., Montilla-Martinez, M., Ellenrieder, L., Vögtle, F. N., et al. (2017). Identification of new channels by systematic analysis of the mitochondrial outer membrane. *J. Cell Biol.* 216, 3485–3495. doi: 10.1083/jcb.201706043

Lee, A. C., Xu, X., Blachly-Dyson, E., Forte, M., and Colombini, M. (1998). The role of yeast VDAC genes on the permeability of the mitochondrial outer membrane. *J. Membr. Biol.* 161, 173–181. doi: 10.1007/s002329900324

Leggio, L., Guarino, F., Magrì, A., Accardi-Gheit, R., Reina, S., Specchia, V., et al. (2018). Mechanism of translation control of the alternative *Drosophila melanogaster* voltage dependent anion-selective channel 1 mRNAs. *Sci. Rep.* 8:5347. doi: 10.1038/s41598-018-23730-7

Ludwig, O., De Pinto, V., Palmieri, F., and Benz, R. (1986). Pore formation by the mitochondrial porin of rat brain in lipid bilayer membranes. *Biochim. Biophys. Acta Biomembr.* 860, 268–276. doi: 10.1016/0005-2736(86)90523-7

Ma, S. B., Nguyen, T. N., Tan, I., Ninnis, R., Iyer, S., Stroud, D. A., et al. (2014). Bax targets mitochondria by distinct mechanisms before or during apoptotic cell death: a requirement for VDAC2 or Bak for efficient Bax apoptotic function. *Cell Death Differ.* 21, 1925–1935. doi: 10.1038/cdd.2014.119

Magrì, A., Belfiore, R., Reina, S., Tomasello, M. F., Di Rosa, M. C., Guarino, F., et al. (2016a). Hexokinase i N-terminal based peptide prevents the VDAC1-SOD1 G93A interaction and re-establishes ALS cell viability. *Sci. Rep.* 6:34802. doi: 10.1038/srep34802

Magrì, A., Di Rosa, M. C., Orlandi, I., Guarino, F., Reina, S., Guarnaccia, M., et al. (2020). Deletion of voltage-dependent anion channel 1 knocks mitochondria down triggering metabolic rewiring in yeast. *Cell Mol. Life Sci.* 77, 3195–3213. doi: 10.1007/s00018-019-03342-8

Magrì, A., Di Rosa, M. C., Tomasello, M. F., Guarino, F., Reina, S., Messina, A., et al. (2016b). Overexpression of human SOD1 in VDAC1-less yeast restores mitochondrial functionality modulating beta-barrel outer membrane protein genes. *Biochim. Biophys. Acta Bioenerg.* 1857, 789–798. doi: 10.1016/j.bbabio.2016.03.003

Magrì, A., Karachitos, A., Di Rosa, M. C., Reina, S., Conti Nibali, S., Messina, A., et al. (2019). Recombinant yeast VDAC2: a comparison of electrophysiological features with the native form. *FEBS Open Biol.* 9, 1184–1193. doi: 10.1002/2211-5463.12574

Magrì, A., and Messina, A. (2017). Interactions of VDAC with proteins involved in neurodegenerative aggregation: an opportunity for advancement on therapeutic molecules. *Curr. Med. Chem.* 24, 4470–4487. doi: 10.2174/0929867324666170601073920

Magrì, A., Reina, S., and De Pinto, V. (2018). VDAC1 as pharmacological target in cancer and neurodegeneration: focus on its role in apoptosis. *Front. Chem.* 6:108. doi: 10.3389/fchem.2018.00108

Mannella, C. A. (1998). Conformational changes in the mitochondrial channel protein, VDAC, and their functional implications. *J. Struct. Biol.* 121, 207–218. doi: 10.1006/jsbi.1997.3954

Manzo, G., Serra, I., Magrí, A., Casu, M., De Pinto, V., Ceccarelli, M., et al. (2018). Folded structure and membrane affinity of the N-terminal domain of the three human isoforms of the mitochondrial voltage-dependent anion-selective channel. *ACS Omega* 3, 11415–11425. doi: 10.1021/acsomega.8b01536

Messina, A., Reina, S., Guarino, F., and De Pinto, V. (2012). VDAC isoforms in mammals. *Biochim. Biophys. Acta Biomembr.* 1818, 1466–1476. doi: 10.1016/j.bbamem.2011.10.005

Messina, A., Reina, S., Guarino, F., Magrì, A., Tomasello, F., Clark, R. E., et al. (2014). Live cell interactome of the human voltage dependent anion channel 3 (VDAC3) revealed in HeLa cells by affinity purification tag technique. *Mol. Biosyst.* 10, 2134–2145. doi: 10.1039/c4mb00237g

Mihara, K., Blobel, G., and Sato, R. (1982). In vitro synthesis and integration into mitochondria of porin, a major protein of the outer mitochondrial membrane of Saccharomyces cerevisiae. *Proc. Natl. Acad. Sci. U.S.A.* 79, 7102–7106. doi: 10.1073/pnas.79.23.7102

Mihara, K., and Sato, R. (1985). Molecular cloning and sequencing of cDNA for yeast porin, an outer mitochondrial membrane protein: a search for targeting signal in the primary structure. *EMBO J.* 4, 769–774. doi: 10.1002/j.1460-2075.1985.tb03695.x

Mihaylova, M. M., and Shaw, R. J. (2011). The AMPK signalling pathway coordinates cell growth, autophagy and metabolism. *Nat. Cell Biol.* 13, 1016–1023. doi: 10.1038/ncb2329

Miller-Fleming, L., Giorgini, F., and Outeiro, T. F. (2008). Yeast as a model for studying human neurodegenerative disorders. *Biotechnol. J.* 3, 325–338. doi: 10.1002/biot.200700217

Model, K., Meisinger, C., Prinz, T., Wiedemann, N., Truscott, K. N., Pfanner, N., et al. (2001). Multistep assembly of the protein import channel of the mitochondrial outer membrane. *Nat. Struct. Biol.* 8, 361–370. doi: 10.1038/86253

Morgenstern, M., Stiller, S. B., Lübbert, P., Peikert, C. D., Dannenmaier, S., Drepper, F., et al. (2017). Definition of a high-confidence mitochondrial proteome at quantitative scale. *Cell Rep.* 19, 2836–2852. doi: 10.1016/j.celrep.2017.06.014

Nakae, T. (1976). Outer membrane of *Salmonella*. Isolation of protein complex that produces transmembrane channels. *J. Biol. Chem.* 251, 2176–2178. doi: 10.1016/s0021-9258(17)33673-6

Nikaido, H. (2003). Molecular basis of bacterial outer membrane permeability revisited. *Microbiol. Mol. Biol. Rev.* 67, 593–656. doi: 10.1128/mmbr.67.4.593-656.2003

O'Brien, E. M., Dirmeier, R., Engle, M., and Poyton, R. O. (2004). Mitochondrial protein oxidation in yeast mutants lacking manganese- (MnSOD) or copper- and zinc-containing superoxide dismutase (CuZnSOD): evidence that mnsod and cuznsod have both unique and overlapping functions in protecting mitochondrial proteins from. *J. Biol. Chem.* 279, 51817–51827. doi: 10.1074/jbc.M405958200

Okazaki, M., Kurabayashi, K., Asanuma, M., Saito, Y., Dodo, K., and Sodeoka, M. (2015). VDAC3 gating is activated by suppression of disulfide-bond formation between the N-terminal region and the bottom of the pore. *Biochim. Biophys. Acta Biomembr.* 1848, 3188–3196. doi: 10.1016/j.bbamem.2015.09.017

Pastorino, J. G., and Hoek, J. B. (2008). Regulation of hexokinase binding to VDAC. *J. Bioenerg. Biomembr.* 40, 171–182. doi: 10.1007/s10863-008-9148-8

Pavlov, E., Grigoriev, S. M., Dejean, L. M., Zweihorn, C. L., Mannella, C. A., and Kinnally, K. W. (2005). The mitochondrial channel VDAC has a cation-selective open state. *Biochim. Biophys. Acta Bioenerg.* 1710, 96–102. doi: 10.1016/j.bbabio.2005.09.006

Pereira, C., Bessa, C., Soares, J., Leo, M., and Saraiva, L. (2012). Contribution of yeast models to neurodegeneration research. *J. Biomed. Biotechnol.* 2012:941232. doi: 10.1155/2012/941232

Pfanner, N., Wiedemann, N., Meisinger, C., and Lithgow, T. (2004). Assembling the mitochondrial outer membrane. *Nat. Struct. Mol. Biol.* 11, 1044–1048. doi: 10.1038/nsmb852

Pittalà, M. G. G., Saletti, R., Reina, S., Cunsolo, V., De Pinto, V., and Foti, S. (2020). A high resolution mass spectrometry study reveals the potential of disulfide formation in human mitochondrial voltage-dependent anion selective channel isoforms (hVDACs). *Int. J. Mol. Sci.* 21:1468. doi: 10.3390/ijms21041468

Popp, B., Schmid, A., and Benz, R. (1995). Role of sterols in the functional reconstitution of water-soluble mitochondrial porins from different organisms. *Biochemistry* 34, 3352–3361. doi: 10.1021/bi00010a026

Queralt-Martín, M., Bergdoll, L., Teijido, O., Munshi, N., Jacobs, D., Kuszak, A. J., et al. (2020). A lower affinity to cytosolic proteins reveals VDAC3 isoform-specific role in mitochondrial biology. *J. Gen. Physiol.* 152:e201912501. doi: 10.1085/JGP.201912501

Reina, S., Checchetto, V., Saletti, R., Gupta, A., Chaturvedi, D., Guardiani, C., et al. (2016a). VDAC3 as a sensor of oxidative state of the intermembrane space of mitochondria: the putative role of cysteine residue modifications. *Oncotarget* 7, 2249–2268. doi: 10.18632/oncotarget.6850

Reina, S., Guarino, F., Magrì, A., and De Pinto, V. (2016b). VDAC3 as a potential marker of mitochondrial status is involved in cancer and pathology. *Front. Oncol.* 6:264. doi: 10.3389/fonc.2016.00264

Reina, S., Magrì, A., Lolicato, M., Guarino, F., Impellizzeri, A., Maier, E., et al. (2013). Deletion of β-strands 9 and 10 converts VDAC1 voltage-dependence in an asymmetrical process. *Biochim. Biophys. Acta Bioenerg.* 1827, 793–805. doi: 10.1016/j.bbabio.2013.03.007

Reina, S., Palermo, V., Guarnera, A., Guarino, F., Messina, A., Mazzoni, C., et al. (2010). Swapping of the N-terminus of VDAC1 with VDAC3 restores full activity of the channel and confers anti-aging features to the cell. *FEBS Lett.* 584, 2837–2844. doi: 10.1016/j.febslet.2010.04.066

Reina, S., Pittalà, M. G. G., Guarino, F., Messina, A., De Pinto, V., Foti, S., et al. (2020). Cysteine oxidations in mitochondrial membrane proteins: the case of VDAC isoforms in mammals. *Front. Cell Dev. Biol.* 8:397. doi: 10.3389/fcell.2020.00397

Rencus-Lazar, S., DeRowe, Y., Adsi, H., Gazit, E., and Laor, D. (2019). Yeast models for the study of amyloid-associated disorders and development of future therapy. *Front. Mol. Biosci.* 6:15. doi: 10.3389/fmolb.2019.00015

Rine, J. (1989). The yeast *Saccharomyces cerevisiae* in molecular and cellular biology: a smaller but not lower eucaryote. *Integr. Comp. Biol.* 29, 605–616. doi: 10.1093/icb/29.2.605

Rosenbusch, J. P. (1990). Structural and functional properties of porin channels in E. coli outer membranes. *Experientia* 46, 167–173.

Rostovtseva, T., and Colombini, M. (1997). Vdac channels mediate and gate the flow of ATP: implications for the regulation of mitochondrial function. *Biophys. J.* 72, 1954–1962. doi: 10.1016/S0006-3495(97)78841-6

Rostovtseva, T. K., Gurnev, P. A., Protchenko, O., Hoogerheide, D. P., Yap, T. L., Philpott, C. C., et al. (2015). α-synuclein shows high affinity interaction with voltage-dependent anion channel, suggesting mechanisms of mitochondrial regulation and toxicity in Parkinson disease. *J. Biol. Chem.* 290, 18467–18477. doi: 10.1074/jbc.M115.641746

Sakaue, H., Shiota, T., Ishizaka, N., Kawano, S., Tamura, Y., Tan, K. S., et al. (2019). Porin associates with Tom22 to regulate the mitochondrial protein gate assembly. *Mol. Cell* 73, 1044–1055.e8. doi: 10.1016/j.molcel.2019.01.003

Saletti, R., Reina, S., Pittalà, M. G. G., Belfiore, R., Cunsolo, V., Messina, A., et al. (2017). High resolution mass spectrometry characterization of the oxidation pattern of methionine and cysteine residues in rat liver mitochondria voltage-dependent anion selective channel 3 (VDAC3). *Biochim. Biophys. Acta Biomembr.* 1859, 301–311. doi: 10.1016/j.bbamem.2016.12.003

Saletti, R., Reina, S., Pittalà, M. G. G., Magrì, A., Cunsolo, V., Foti, S., et al. (2018). Post-translational modifications of VDAC1 and VDAC2 cysteines from rat liver mitochondria. *Biochim. Biophys. Acta Bioenerg.* 1859, 806–816. doi: 10.1016/j.bbabio.2018.06.007

Sampson, M. J., Lovell, R. S., and Craigen, W. J. (1997). The murine voltage-dependent anion channel gene family. Conserved structure and function. *J. Biol. Chem.* 272, 18966–18973. doi: 10.1074/jbc.272.30.18966

Schein, S. J., Colombini, M., and Finkelstein, A. (1976). Reconstitution in planar lipid bilayers of a voltage-dependent anion-selective channel obtained from paramecium mitochondria. *J. Membr. Biol.* 30, 99–120. doi: 10.1007/BF01869662

Schredelseker, J., Paz, A., López, C. J., Altenbach, C., Leung, C. S., Drexler, M. K., et al. (2014). High resolution structure and double electron-electron resonance of the zebrafish voltage-dependent anion channel 2 reveal an oligomeric population. *J. Biol. Chem.* 289, 12566–12577. doi: 10.1074/jbc.M113.497438

Shimizu, S., Matsuoka, Y., Shinohara, Y., Yoneda, Y., and Tsujimoto, Y. (2001). Essential role of voltage-dependent anion channel in various forms of apoptosis in mammalian cells. *J. Cell Biol.* 152, 237–250. doi: 10.1083/jcb.152.2.237

Shoshan-Barmatz, V., De Pinto, V., Zweckstetter, M., Raviv, Z., Keinan, N., and Arbel, N. (2010). VDAC, a multi-functional mitochondrial protein regulating cell life and death. *Mol. Aspects Med.* 31, 227–285. doi: 10.1016/j.mam.2010.03.002

Shoshan-Barmatz, V., Shteinfer-Kuzmine, A., and Verma, A. (2020). VDAC1 at the intersection of cell metabolism, apoptosis, and diseases. *Biomolecules* 10:1485. doi: 10.3390/biom10111485

Shuvo, S. R., Ferens, F. G., and Court, D. A. (2016). The N-terminus of VDAC: structure, mutational analysis, and a potential role in regulating barrel shape. *Biochim. Biophys. Acta Biomembr.* 1858, 1350–1361. doi: 10.1016/j.bbamem.2016.03.017

Smack, D. P., and Colombini, M. (1985). Voltage-dependent channels found in the membrane fraction of corn mitochondria. *Plant Physiol.* 79, 1094–1097. doi: 10.1104/pp.79.4.1094

Strogolova, V., Orlova, M., Shevade, A., and Kuchin, S. (2012). Mitochondrial porin Por1 and its homolog Por2 contribute to the positive control of snf1 protein kinase in *Saccharomyces cerevisiae*. *Eukaryot. Cell* 11, 1568–1572. doi: 10.1128/EC.00127-12

Takeda, H., Tsutsumi, A., Nishizawa, T., Lindau, C., Busto, J. V., Wenz, L. S., et al. (2021). Mitochondrial sorting and assembly machinery operates by β-barrel switching. *Nature* 590, 163–169. doi: 10.1038/s41586-020-03113-7

Thomas, L., Blachly-Dyson, E., Colombini, M., and Forte, M. (1993). Mapping of residues forming the voltage sensor of the voltage-dependent anion-selective channel. *Proc. Natl. Acad. Sci. U.S.A.* 90, 5446–5449. doi: 10.1073/pnas.90.12.5446

Tomasello, F., Messina, A., Lartigue, L., Schembri, L., Medina, C., Reina, S., et al. (2009). Outer membrane VDAC1 controls permeability transition of the inner mitochondrial membrane in cellulo during stress-induced apoptosis. *Cell Res.* 19, 1363–1376. doi: 10.1038/cr.2009.98

Tomasello, M. F., Guarino, F., Reina, S., Messina, A., and De Pinto, V. (2013). The voltage-dependent anion selective Channel 1 (VDAC1) topography in the mitochondrial outer membrane as detected in intact cell. *PLoS One* 8:e81522. doi: 10.1371/journal.pone.0081522

Tucker, K., and Park, E. (2019). Cryo-EM structure of the mitochondrial protein-import channel TOM complex at near-atomic resolution. *Nat. Struct. Mol. Biol.* 26, 1158–1166. doi: 10.1038/s41594-019-0339-2

Ujwal, R., Cascio, D., Colletier, J. P., Faham, S., Zhang, J., Toro, L., et al. (2008). The crystal structure of mouse VDAC1 at 2.3 Å resolution reveals mechanistic insights into metabolite gating. *Proc. Natl. Acad. Sci. U.S.A.* 105, 17742–17747. doi: 10.1073/pnas.0809634105

Ulrich, T., and Rapaport, D. (2015). Biogenesis of beta-barrel proteins in evolutionary context. *Int. J. Med. Microbiol.* 305, 259–264. doi: 10.1016/j.ijmm.2014.12.009

Xu, X., Decker, W., Sampson, M. J., Craigen, W. J., and Colombini, M. (1999). Mouse VDAC isoforms expressed in yeast: channel properties and their roles in mitochondrial outer membrane permeability. *J. Membr. Biol.* 170, 89–102. doi: 10.1007/s002329900540

Young, M. J., Bay, D. C., Hausner, G., and Court, D. A. (2007). The evolutionary history of mitochondrial porins. *BMC Evol. Biol.* 7:31. doi: 10.1186/1471-2148-7-31

Zeth, K., and Thein, M. (2010). Porins in prokaryotes and eukaryotes: common themes and variations. *Biochem. J.* 431, 13–22. doi: 10.1042/BJ20100371

Zeth, K., and Zachariae, U. (2018). Ten years of high resolution structural research on the voltage dependent anion channel (VDAC)-Recent developments and future directions. *Front. Physiol.* 9:108. doi: 10.3389/fphys.2018.00108

Conflict of Interest: FG, AM, and VDP are affiliated with we.MitoBiotech S.R.L, a spin-off company to the University of Catania.

All the authors declare that the research was conducted in the absence of any commercial of financial relationships that could be construed a potential conflict of interest.

Article 5.

International journal of molecular sciences

VDACs Post-Translational Modifications Discovery by Mass Spectrometry: Impact on Their Hub Function

Maria Gaetana Giovanna Pittalà [1], Stefano Conti Nibali [2], Simona Reina [2], Vincenzo Cunsolo [3] , Antonella Di Francesco [3], Vito De Pinto [2] , Angela Messina [1] , Salvatore Foti [3] and Rosaria Saletti [3,*]

1Molecular Biology Laboratory, Department of Biological, Geological and Environmental Sciences, University of Catania, Via S. Sofia 64, 95123 Catania, Italy; ti.oiligriv@ttip.alleniram (M.G.G.P.); ti.tcinu@ssem (A.M.)
2Department of Biomedical and Biotechnological Sciences, University of Catania, Via S. Sofia 64, 95123 Catania, Italy; ti.tcinu@ilabinitnoc.onafets (S.C.N.); ti.tcinu@anier.anomis (S.R.); ti.tcinu@afoibpdv (V.D.P.)
3Organic Mass Spectrometry Laboratory, Department of Chemical Sciences, University of Catania, Via S. Sofia 64, 95123 Catania, Italy; ti.tcinu@olosnucv (V.C.); moc.liamg@ocsecnarfdallenotna (A.D.F.); ti.tcinu@itofs (S.F.)
*Correspondence: ti.tcinu@ittelasr; Tel.: +39-095-738-5026

International Journal of
Molecular Sciences

MDPI

Review

VDACs Post-Translational Modifications Discovery by Mass Spectrometry: Impact on Their Hub Function

Maria Gaetana Giovanna Pittalà [1], Stefano Conti Nibali [2], Simona Reina [2], Vincenzo Cunsolo [3], Antonella Di Francesco [3], Vito De Pinto [2], Angela Messina [1], Salvatore Foti [3] and Rosaria Saletti [3,*]

[1] Molecular Biology Laboratory, Department of Biological, Geological and Environmental Sciences, University of Catania, Via S. Sofia 64, 95123 Catania, Italy; marinella.pitt@virgilio.it (M.G.G.P.); mess@unict.it (A.M.)
[2] Department of Biomedical and Biotechnological Sciences, University of Catania, Via S. Sofia 64, 95123 Catania, Italy; stefano.continibali@unict.it (S.C.N.); simona.reina@unict.it (S.R.); vdpbiofa@unict.it (V.D.P.)
[3] Organic Mass Spectrometry Laboratory, Department of Chemical Sciences, University of Catania, Via S. Sofia 64, 95123 Catania, Italy; vcunsolo@unict.it (V.C.); antonelladfrancesco@gmail.com (A.D.F.); sfoti@unict.it (S.F.)
* Correspondence: rsaletti@unict.it; Tel.: +39-095-738-5026

Abstract: VDAC (voltage-dependent anion selective channel) proteins, also known as mitochondrial porins, are the most abundant proteins of the outer mitochondrial membrane (OMM), where they play a vital role in various cellular processes, in the regulation of metabolism, and in survival pathways. There is increasing consensus about their function as a cellular hub, connecting bioenergetics functions to the rest of the cell. The structural characterization of VDACs presents challenging issues due to their very high hydrophobicity, low solubility, the difficulty to separate them from other mitochondrial proteins of similar hydrophobicity and the practical impossibility to isolate each single isoform. Consequently, it is necessary to analyze them as components of a relatively complex mixture. Due to the experimental difficulties in their structural characterization, post-translational modifications (PTMs) of VDAC proteins represent a little explored field. Only in recent years, the increasing number of tools aimed at identifying and quantifying PTMs has allowed to increase our knowledge in this field and in the mechanisms that regulate functions and interactions of mitochondrial porins. In particular, the development of nano-reversed phase ultra-high performance liquid chromatography (nanoRP-UHPLC) and ultra-sensitive high-resolution mass spectrometry (HRMS) methods has played a key role in this field. The findings obtained on VDAC PTMs using such methodologies, which permitted an in-depth characterization of these very hydrophobic trans-membrane pore proteins, are summarized in this review.

Keywords: voltage dependent anion channel; cysteine overoxidation; deamidation; hydroxyapatite; high-resolution mass spectrometry; post-translational modifications

Citation: Pittalà, M.G.G.; Conti Nibali, S.; Reina, S.; Cunsolo, V.; Di Francesco, A.; De Pinto, V.; Messina, A.; Foti, S.; Saletti, R. VDACs Post-Translational Modifications Discovery by Mass Spectrometry: Impact on Their Hub Function. *Int. J. Mol. Sci.* **2021**, *22*, 12833. https://doi.org/10.3390/ijms222312833

Academic Editor: Victor Muñoz

Received: 25 October 2021
Accepted: 23 November 2021
Published: 27 November 2021

1. Introduction

1.1. VDAC Isoforms: A Family of Hub Proteins

VDAC (voltage-dependent anion selective channel) proteins, also known as mitochondrial porins, are the most abundant proteins of the outer mitochondrial membrane (OMM) where they play a vital role in various cellular processes, in the regulation of metabolism, and in survival pathways. They mediate the ions and metabolites exchange between mitochondria and the rest of the cell, ensuring good functionality of mitochondrial complexes and energy production [1].

In higher eukaryotes, there are three VDAC isoforms (VDAC1, VDAC2, VDAC3) encoded by separate genes located on different chromosomes [2]. These pore-forming proteins have a similar molecular weight (30 kDa) and highly conserved sequences of

about 280 amino acids with the exception of VDAC2 which has the N-terminal moiety of 11 residues longer than the other isoforms.

The evolutionary analysis indicates VDAC3 as the oldest isoform, while VDAC1 is considered the youngest mitochondrial porin [3,4].

The experimental 3D structures of mouse and human VDAC1 isoform have been determined using X-ray crystallography and NMR [5–7]. These analyses revealed a structure constituted by 19 β-strands arranged to form a trans-membrane β-barrel and by a region containing α-helix at the N-terminus of the protein. The barrel is organized as a regular antiparallel array of β-strands with the exception of strands 1 and 19 that run in parallel. The amphipathic α-helix tail is located inside the pore. However, the exact position and local structure of this segment are still elusive since these features are not perfectly overlapping in the available X-ray and NMR structures [5–7].

Recently, the structure of zebrafish VDAC2 was solved at a high resolution, confirming the same β-barrel arrangement as VDAC1 [8]. Zebrafish VDAC2 has one cysteine residue in the sequence and lacks the 11 amino acid longer N-terminal sequence present in mammalian VDACs.

The VDAC3 structure has not yet been determined. Several bioinformatic predictions, based on the large sequence similarity, proposed a barrel core such as the other VDAC isoforms [9]. Despite the high sequence similarity and structural homology, VDAC isoforms display different functional properties within the cell.

Analysis of the expression levels of human VDAC isoforms in HeLa cells, determined by real-time PCR, suggests that VDAC1 is the most abundant isoform, ten times more abundant compared to VDAC2 and hundred times more abundant compared to VDAC3, the least characterized of the isoforms. In addition, the overexpression of each single VDAC isoform affects the mRNA levels of the other two isoforms, suggesting that the ratios between VDAC isoforms are subjected to a reciprocal control that avoids an imbalance among these proteins [10].

Although the three isoforms show a common involvement in cellular bioenergetics maintenance, VDAC1 and VDAC2 have specialized functions in programmed cell death. For VDAC3 isoform, recent studies indicate a central role in ROS metabolism and in mitochondrial quality control [11].

The functions of VDACs are several-fold and some of these depend on, or are affected by, interaction with other cytosolic and mitochondrial proteins. Due to their localization at the OMM, VDACs are considered to be hub proteins, interacting with over 200 proteins in order to integrate mitochondrial functions with the rest of the cellular activities [12,13]. Thus, VDAC isoforms appears to be a junction for a variety of signals associated with different pathways related to cell survival or programmed death. Furthermore, the function of VDACs and their interactions with other proteins are affected by post-translational modifications (PTMs) [14]. Unfortunately, PTMs of VDAC proteins represent a little explored field, mainly because discovery and characterization of PTM in these proteins is very challenging, due to their poor solubility and impossibility to isolate single isoforms. Only in recent years has the increasing number of tools aimed at identifying and quantifying PTMs increased, improving the knowledge in this field and in the mechanisms that regulate functions and interactions of mitochondrial porins. In particular, the development of nano-reversed phase ultra-high-performance liquid chromatography (nanoRP-UHPLC) and ultra-sensitive high-resolution mass spectrometry (HRMS) methods has played a key role in this field. The findings obtained on VDAC PTMs using such methodologies, which have permitted an in-depth characterization of these very hydrophobic trans-membrane pore proteins, are summarized in this review.

1.2. VDACs as Main Players in Mediating and Regulating Mitochondrial Functions with Cellular Activities

The location in the OMM allows the VDAC proteins to act as anchor points for diverse sets of molecules that interact with mitochondria. In this way, VDACs are able to mediate and regulate the integration of mitochondrial functions with cellular activities.

The VDAC interactome includes proteins located in OMM, inner mitochondrial membrane (IMM), intermembrane space (IMS), cytosol, endoplasmic reticulum, plasma membrane and nucleus that are involved in metabolism, apoptosis, signal transduction, protection against ROS, binding to RNA or DNA, and more.

Mobility of VDAC N-terminal α-helix region is important for channel gating but also for interactions with both pro-apoptotic and anti-apoptotic proteins such as Bax, Bak, and Bcl-xL [15–17]. VDAC1 is involved in the release of apoptotic factors located in the intermembrane space due to its ability of oligomerizing in dimers, hexamers, and higher-order structures, to form a large pore that allows the passage of cytochrome c and apoptosis inducing factor (AIF) to the cytosol and consequently the activation of programmed cell death. Instead, VDAC2 functions as anti-apoptotic factor and it is upregulated in several debilitating diseases including Alzheimer's and cancer [18]. This property is probably due to the unique ability of VDAC2 to sequester the pro-apoptotic protein Bak in the OMM and maintain it in the inactive state [11].

VDAC1 displays binding sites, located in its cytosolic moiety, for many metabolic enzymes, such as glyceraldehyde 3-phosphate dehydrogenase, creatine kinase, glycerol kinase, glucokinase, c-Raf kinase, and hexokinase isoforms (I and II), which need preferential access to mitochondrial ATP [19].

Hexokinase interacts through its hydrophobic N-terminal sequence with Glu^{73} of VDAC1, a binding site localized on one side of the barrel wall, buried in the hydrophobic environment of OMM [20].

It has been demonstrated that treatment of mitochondria with dicyclohexylcarbodiimide (DCCD) inhibits hexokinase–VDAC interaction due to selective chemical modification of Glu^{73} [21].

Glu^{73} residue is also the binding site for ceramides, tumor suppressor lipids able to act directly on mitochondria to trigger apoptotic cell death. It is interesting that both VDAC1 and 2 own, in a similar position, a cysteine residue (Cys^{127} in human VDAC1 and Cys^{138} in human VDAC2) in the form of sulfonic acid with a strong negative charge resembling that of the glutamate acid residue [22]. Instead, VDAC3 isoform does not show any residue homologous to $Cys^{127/138}$ or Glu^{73} embedded in the hydrophobic moiety of the OMM.

VDAC1 presents a cholesterol binding pocket formed, in human isoform, by Ile^{123}, Leu^{144}, Tyr^{146}, Ala^{151}, and Val^{171} residues [23].

Mitochondrial porins form complexes with other proteins, such as the adenine nucleotide translocase (ANT), the translocator protein (TSPO), also known as the peripheral-type benzodiazepine receptor (PBR), mitochondrial HSP70, and several cytoskeletal proteins such as tubulin, actin, dynein light chain, and gelsolin [11].

The translocator protein interacts directly with all VDAC isoforms. In particular, interaction between TSPO and VDAC1 contributes to regulate the efficiency of mitochondrial quality control mechanisms and inhibits mitophagy, preventing ubiquitination of proteins through downregulation of the PINK1/Parkin pathway [24]. The GxxxG motif presents both in VDAC and in TSPO, and is necessary for this interaction [25]. Moreover, VDAC1 and TSPO, in association with StAR (steroidogenic acute regulatory protein), form the transduceosome, a multi-protein complex involved in cholesterol transport. In a former hypothesis, VDAC1 and TSPO in OMM, ANT in IMM, and Cyclophilin D in the mitochondrial matrix were candidates to constitute the permeability transition pore (PTP), a high conductance and non-specific pore that allows mitochondrial swelling and release of apoptogenic proteins. More recently, it was proposed that PTP could be formed by dimers of the ATP synthase complex [26].

Recent studies have focused attention on the role of VDAC proteins in mitochondrial dysfunction typical of many pathological conditions including stroke, cancer, mitochondrial encephalomyopathies, and aging, as well as neurodegenerative disorders [27,28].

Mass spectrometry analysis revealed the association between VDACs and the ubiquitin ligase Parkin. In presence of damaged mitochondria, as in Parkinson's disease, Parkin is phosphorylated by PINK1 and consequently ubiquitinates proteins that reside on the OMM,

targeting the mitochondria for degradation. Parkin is a cytosolic protein but translocates to the mitochondria to participate in mitochondrial quality control mechanisms. VDAC proteins represent a docking site of Parkin on defective mitochondria [29].

Moreover, VDAC1 represents the main docking site at the mitochondrial level for misfolded and aggregated proteins, a common feature of neurodegenerative disorders known as proteinopathies, such as Alzheimer's disease (AD), Parkinson's disease (PD), Creutzfeldt–Jacob disease (CJD), dementia with Lewy bodies (DLB), Huntington disease (HD), and amyotrophic lateral sclerosis (ALS) [30].

For example, in AD post-mortem brains, in neuroblastoma cells and in an AD mouse model, a direct association was demonstrated between VDAC1, specifically its N-terminal region, and hyper-phosphorylated Tau but also with amyloid beta (Aβ), both in its monomeric and oligomeric forms [31]. These interactions can have a dramatic effect on mitochondrial functions in AD neuron because they block the PTP formation, disrupt the transport of mitochondrial proteins and metabolites, and impair gating, conductance, and physiological interactome of VDACs [32].

In Parkinson's disease, α-synuclein directly interacts with mitochondria, blocks VDAC1, and impairs metabolite fluxes leading, consequently, to an energetic crisis able to compromise cell viability [33].

In ALS, several SOD1 mutants are able to bind VDAC1 [34]. This interaction impairs ATP/ADP exchange, VDAC1 conductance and mitochondrial membrane potential. Recently, the competition between SOD1G93A and HK1 was demonstrated in binding VDAC1, in NSC34 motor-neuron cell lines [35].

In literature, the role of VDAC1 in neurodegeneration is rather well known; however, the involvement of the other two isoforms in these pathways remains poorly defined. This is likely associated with the relative abundance of VDAC1 compared to other isoforms which are more difficult to isolate in pure form.

Recent studies demonstrated that Cytoskeleton-associated protein 4 (CKAP4), a palmitoylated type II transmembrane protein localized to the endoplasmic reticulum (ER), regulates mitochondrial functions through an interaction with VDAC2 at ER-mitochondria contact sites [36].

VDAC2 binds inositol trisphosphate receptors (IP3R) and regulates the release of Ca^{2+} from the ER. In addition, several other interaction partners have been reported for VDAC2 isoform, which imply its effect in multiple cellular functions. Specifically, VDAC2 has been linked to many cellular proteins, including apoptotic factors as Bak and Bax, StAR, Metaxin2, eNOS (nitric oxide synthesize), GSK3β, tubulin, and Mcl1 [19]. In addition, VDAC2 and RACK1 (receptor of activated protein kinase C1) function as receptors for lymphocystis disease virus (LCDV) and for bursal disease virus in host cells [37].

VDAC2 together with VDAC3 binds Erastin, the activator of ferroptosis, a new pathway that regulates cell death characterized by the iron-dependent accumulation of lipid hydroperoxides. Interaction between VDAC2/3 and Erastin results in degradation of the channels following activation of ubiquitin protein ligase Nedd4 [38].

Finally, the VDAC3 isoform is associated with cytosolic proteins as tubulins and cytoskeletal proteins, stress sensors, chaperones, and proteasome components, redox-mediating enzymes such as protein disulfide isomerase [39].

2. MS-Based Techniques for Protein Analysis

The development in the late 1980s of the two "soft" desorption/ionization MS techniques electrospray ionization (ESI) and matrix-assisted laser desorption/ionization (MALDI) [40], which are able to convert large molecules, such as proteins, DNA, and carbohydrates, into gas-phase ions without affecting their integrity, has greatly broadened the applicability of MS to biology and revolutionized the analysis of biomolecules, making possible the high-throughput identification of thousands of proteins in only one experiment.

With respect to the ESI method, MALDI MS is commonly used for the characterization of relatively simple mixtures of peptides or proteins; it is quite resistant to interference with

targeting the mitochondria for degradation. Parkin is a cytosolic protein but translocates to the mitochondria to participate in mitochondrial quality control mechanisms. VDAC proteins represent a docking site of Parkin on defective mitochondria [29].

Moreover, VDAC1 represents the main docking site at the mitochondrial level for misfolded and aggregated proteins, a common feature of neurodegenerative disorders known as proteinopathies, such as Alzheimer's disease (AD), Parkinson's disease (PD), Creutzfeldt–Jacob disease (CJD), dementia with Lewy bodies (DLB), Huntington disease (HD), and amyotrophic lateral sclerosis (ALS) [30].

For example, in AD post-mortem brains, in neuroblastoma cells and in an AD mouse model, a direct association was demonstrated between VDAC1, specifically its N-terminal region, and hyper-phosphorylated Tau but also with amyloid beta (Aβ), both in its monomeric and oligomeric forms [31]. These interactions can have a dramatic effect on mitochondrial functions in AD neuron because they block the PTP formation, disrupt the transport of mitochondrial proteins and metabolites, and impair gating, conductance, and physiological interactome of VDACs [32].

In Parkinson's disease, α-synuclein directly interacts with mitochondria, blocks VDAC1, and impairs metabolite fluxes leading, consequently, to an energetic crisis able to compromise cell viability [33].

In ALS, several SOD1 mutants are able to bind VDAC1 [34]. This interaction impairs ATP/ADP exchange, VDAC1 conductance and mitochondrial membrane potential. Recently, the competition between SOD1G93A and HK1 was demonstrated in binding VDAC1, in NSC34 motor-neuron cell lines [35].

In literature, the role of VDAC1 in neurodegeneration is rather well known; however, the involvement of the other two isoforms in these pathways remains poorly defined. This is likely associated with the relative abundance of VDAC1 compared to other isoforms which are more difficult to isolate in pure form.

Recent studies demonstrated that Cytoskeleton-associated protein 4 (CKAP4), a palmitoylated type II transmembrane protein localized to the endoplasmic reticulum (ER), regulates mitochondrial functions through an interaction with VDAC2 at ER-mitochondria contact sites [36].

VDAC2 binds inositol trisphosphate receptors (IP3R) and regulates the release of Ca^{2+} from the ER. In addition, several other interaction partners have been reported for VDAC2 isoform, which imply its effect in multiple cellular functions. Specifically, VDAC2 has been linked to many cellular proteins, including apoptotic factors as Bak and Bax, StAR, Metaxin2, eNOS (nitric oxide synthesize), GSK3β, tubulin, and Mcl1 [19]. In addition, VDAC2 and RACK1 (receptor of activated protein kinase C1) function as receptors for lymphocystis disease virus (LCDV) and for bursal disease virus in host cells [37].

VDAC2 together with VDAC3 binds Erastin, the activator of ferroptosis, a new pathway that regulates cell death characterized by the iron-dependent accumulation of lipid hydroperoxides. Interaction between VDAC2/3 and Erastin results in degradation of the channels following activation of ubiquitin protein ligase Nedd4 [38].

Finally, the VDAC3 isoform is associated with cytosolic proteins as tubulins and cytoskeletal proteins, stress sensors, chaperones, and proteasome components, redox-mediating enzymes such as protein disulfide isomerase [39].

2. MS-Based Techniques for Protein Analysis

The development in the late 1980s of the two "soft" desorption/ionization MS techniques electrospray ionization (ESI) and matrix-assisted laser desorption/ionization (MALDI) [40], which are able to convert large molecules, such as proteins, DNA, and carbohydrates, into gas-phase ions without affecting their integrity, has greatly broadened the applicability of MS to biology and revolutionized the analysis of biomolecules, making possible the high-throughput identification of thousands of proteins in only one experiment.

With respect to the ESI method, MALDI MS is commonly used for the characterization of relatively simple mixtures of peptides or proteins; it is quite resistant to interference with

buffers commonly used in protein chemistry (e.g., phosphate, Tris, urea) and produces mass spectra that are simple to interpret because of the tendency of the method to generate predominantly singly charged molecular ions [41]. On the contrary, the most important feature of the ESI is the generation of multiply charged molecular ions. This feature allows the detection of proteins also using analyzers with limited mass range (e.g., quadrupoles and ion traps). ESI gained immediate popularity because it can be easily coupled on-line with high-performance separation techniques such as capillary electrophoresis and HPLC and currently represents the most used MS-based method in protein analysis [42,43].

In particular, chromatographic separation represents an essential step during protein analysis because highly complex samples, such as a total cellular protein fraction, may contain hundreds of components that must be, at least partially, separated before the MS analysis. Analogously, when a biological sample is digested, the complexity of the protein mixture increases because each protein component yields many peptides and a high-performing separation step is needed. A variety of liquid chromatographic (LC) separation methods, including reverse phase ultra-high-performance liquid chromatography (RP-UHPLC), strong cation exchange (SCX), affinity chromatography (AC), and size exclusion (SEC), have been developed [44]. Recently, UHPLC, operating with stationary phases consisting of small particles (size < 2 μm), was introduced for more efficient and faster peptide separation [44]. In order to improve the chromatographic resolving power, it is also possible to combine several separation techniques (i.e., multidimensional separation), in which each technique utilizes different physicochemical properties of molecules as a basis for separation (e.g., SCX joined with RP-HPLC) [45]. On the other hand, the development of high-resolution ion mobility mass spectrometry (IMMS), which allows ions to be separated on the basis of their size/charge ratios and their interactions with a buffer gas, adds a degree of orthogonality to MS, and it is now emerging as new powerful tool in the MS arena for the investigation of complex biological samples [46].

The implementation of separation techniques in miniaturized formats coupled on-line with high-performance mass spectrometers and the development of miniaturized ESI sprayers (nanoESI) have reduced the amount of analyte required for complete and routine sequence characterization below the attomole (10^{-18} mol) range. Moreover, the improved performance and versatility of the mass spectrometers nowadays allow to measure the molecular mass of proteins and peptides with high accuracy and to determine additional structural features, which include the primary structure or PTMs. In this respect, the mass analyzer plays a fundamental role in the mass spectrometer technology, together with its key parameters such as sensitivity, resolution, mass accuracy and the ability to generate MS/MS spectra.

Fundamentally, the mass analyzers currently used in protein studies are five: quadrupole (Q), ion trap (IT), time-of-flight (TOF), Fourier transform ion cyclotron resonance (FTICR), and Orbitrap. These mass analyzers differ considerably in design and performance, each with its own strength and weakness.

Ion trap, routinely coupled with ESI source, represents the unique analyzer which alone allows to perform both MS and tandem mass spectrometry (MS/MS) analysis. It is robust, sensitive, and moderately inexpensive, but shows a relatively low resolution and mass accuracy. TOF analyzer has a high sensitivity and high mass detection range that represent the main strengths of this type of analyzer in comparison with others [47]. This type of analyzer is dedicated for pulsed ionization methods, such as MALDI or secondary ion mass spectrometry (SIMS), whereas it cannot be directly interfaced with ESI sources. On the other hand, coupling quadrupole or ion trap analyzers with TOF (Q-q-TOF and LTQ-TOF, respectively) permits not only a direct interfacing with ESI but also allows MS/MS analysis.

Currently, FTICR MS [48] offers the highest resolution (more than 500,000 full width at half maximum, FWHM), resolving power, and accuracy greater than any other mass analyzer. Orbitrap [49], the unique mass analyzer developed during the last 20 years, uses the Fourier transform algorithm to obtain mass spectra with very high mass resolution

(FWHM > 150,000 at m/z 600) and mass accuracy (<2 ppm) [50]. In particular, in these instruments, detection is based on the production of an induced alternating current (AC) with the same frequency as that of the oscillation of the ions inside the instruments. The complex signal produced must be mathematically processed by the Fourier transform algorithm.

Stand-alone FTICR and Orbitrap analyzers cannot perform ion fragmentation requiring additional fragmentation devices. The most common MS platforms equipped with these mass analyzers are the LTQ-FTICR and the LTQ-Orbitrap. In these systems, the LTQ mass analyzer is used for ion isolation, ion storage, and ion fragmentation in MS/MS experiments.

Although the resolution and accuracy of Orbitrap analyzer is not as high as in the case FTICR -MS spectrometer discussed above, Orbitrap offers higher scan rate, is more compact, less costly, easier to maintain, and does not require expensive cryogenic liquids. For these reasons, the LTQ-Orbitrap is becoming the universal solution when high resolution and mass accuracy are required in protein research.

The development of many early hybrid instruments was also motivated by the desire for MS/MS spectral acquisition, which represents one of the most important and effective analytical techniques among MS methodologies. MS/MS usually couples two MS steps and this enables to obtain information about the sequence of peptides.

During MS/MS procedure, a selected ion is isolated and fragmented. Fragmentation occurs along the polypeptide chain in a precisely defined manner. Each resulting fragment has its own mass-to-charge ratio (m/z) related to the m/z of the parent ion. By interpreting the MS/MS data, it is possible to reconstruct the sequence of peptides so obtaining structural information. Consequently, tandem MS plays a key role for protein or peptide sequencing and for the characterization of their PTMs. For this purpose, different fragmentation methods were introduced, such as collision-induced dissociation (CID), electron-capture dissociation (ECD), electron-transfer dissociation (ETD), and higher-energy C-trap dissociation (HCD). CID is the most widely applied fragmentation method for MS/MS in proteomics, mainly resulting in cleavage of amide bonds [51,52]. CID is more effective for small, low-charged peptides, whereas it is not suitable for fragmentation of intact proteins and peptides with labile PTMs. In addition, in spite of its prevalence, CID provides limited sequence coverage when applied to peptide sequences carrying many basic residues. The recent development of the new fragmentation techniques of ECD, ETD, and HCD has greatly enlarged the capabilities of tandem MS strategies [53–55], providing data highly complementary to the conventional CID, better sequence coverage for small-sized to medium-sized peptides, and more comprehensive characterization of PTMs. Therefore, taking into account the complementary fragmentation information that can be obtained by these methods, the use of CID, ETD, or HCD alone, in alternating acquisition or by a decision-tree regulated combination, can provide the best performance for the analysis of distinct peptide populations [56].

Because a detailed description of the capabilities of the different mass analyzers, hybrid instruments, and fragmentation methods is out of the purpose of the present chapter, the reader is referred to a recently published review [57].

3. Proteomics of VDAC Isoforms

3.1. Sample Preparation

Sample preparation has a profound effect on the final results of a proteomic workflow. Protein extraction methods and protein separation techniques should provide an unbiased and reliable map representative of all proteins present in a specific sample. The different extraction and fractionation approaches are based on proteins physicochemical and structural characteristics, such as molecular weight, solubility, hydrophobicity, and isoelectric point. A specific protocol has to be optimized for each particular sample, to maximize protein recovery and minimize the possible proteolysis and amino acid modifications. For these reasons, there is no universal extraction protocol and not a unique buffer composition. Regarding the extraction method, the different strategies available need to be compatible

with both the amount of the processed material and the subsequent analytical approach (i.e., separation or MS).

The structural characterization of VDACs presents challenging issues due to their very high hydrophobicity, low solubility, and the impossibility to separate them from other mitochondrial proteins of similar hydrophobicity and to easily isolate each single isoform. In fact, isolation of VDACs has been possible exclusively for plant VDAC isoforms by chromatofocusing, thanks to the absence of phosphorylation sites in their structure [58]. Consequently, it is necessary to analyze them as components of a relatively complex mixture.

A bottom-up proteomic approach was used to investigate the VDAC3 from rat liver mitochondria (rVDAC3) [59]. According with a standard procedure [60], mitochondria were extracted and lysed with a buffer containing 3% Triton X-100 at pH 7.0. The VDAC proteins were partially purified by hydroxyapatite (HTP) chromatography, which allows to obtain a VDACs enriched fraction which comprises also other mitochondria hydrophobic proteins. After precipitation with cold acetone, the protein pellet was solubilized in SDS buffer and loaded on a 17% polyacrylamide gel (1D-SDS-PAGE). The bands in the range 30–35 kDa were manually excised from the gel, cut in small pieces, and subjected to reduction with DTT and alkylation by addition of IAA. Finally, the reduced and carboxyamidomethylated proteins were in gel-digested using trypsin and chymotrypsin, and the resulting peptide mixtures were analyzed by nUHPLC/HRMS [59]. MS data showed that rVDAC3 was found in the whole range 30–35 kDa, together with other proteins, mainly VDAC1, VDAC2, and several other mitochondrial proteins. The reason for VDAC3 electrophoretic heterogeneity probably stems from (i) the different pattern of cysteine oxidations that can modify the protein mobility; (ii) the different amount and quality of cysteine oxidations in various molecules ("redox isomers").

The gel-digestion procedure shows some disadvantages: (i) larger peptides can get trapped between the gel meshes and lost during the extraction phase of the peptides from the gel; (ii) the electrophoretic procedure itself could damage the samples and alter the redox state of the sulfur amino acids (due to possible over heating generated by the applied voltage and to the presence of residual quantities of the catalysts used for the polyacrylamide polymerization). Furthermore, electrophoresis requires a greater amount of sample and the utilization of dyes and detergents: These last molecules could interfere with subsequent MS analyses because these compounds are difficult to eliminate from the sample.

2-DE could potentially represent a useful alternative to 1-DE to improve the separation of VDAC isoforms, but its utilization presents other problems. Actually, this kind of proteins has been under-represented in 2-DE gels due to difficulties in extracting and solubilizing them in the isoelectric focusing sample buffer. In fact, the most effective solubilizing agent for highly hydrophobic membrane proteins is SDS, but this detergent is incompatible with 2-DE. In addition to the difficulties in entering IPG (immobilized pH gradient) gels, membrane proteins tend to precipitate at their isoelectric point during IEF. Furthermore, their tendency to absorb the IPG matrix prevents their migration into the SDS-PAGE gel.

An improvement in the rVDAC3 mass spectrometric analysis was obtained following the introduction of a gel-free shotgun proteomic approach [59]. According to this procedure, to avoid any possible artefact due to air exposure and manipulations, reduction/alkylation was carried out before VDACs purification from the mitochondria. Afterwards, all the proteins present in the HTP eluate, without previous electrophoretic separation, were purified from non-protein contaminating molecules with the PlusOne 2-D Clean-Up kit, and the desalted protein pellet was then re-dissolved in ammonium bicarbonate containing RapiGest SF to improve the solubility. In fact, this surfactant makes the proteins more susceptible to enzymatic cleavage without modifying the sample or inhibiting endoprotease activity. Furthermore, the RapiGest SF is compatible with enzymes such as trypsin or

chymotrypsin and does not influence subsequent MS analysis because it can be easily removed in acidic conditions.

Separate aliquots of reduced and alkylated proteins were then subjected to digestion with modified porcine trypsin and chymotrypsin. In this experiment, every protein in the HTP eluate was digested, producing a very complex peptide mixture, which was finally analyzed by nUHPLC/HR nESI-MS/MS.

The new "in solution-digestion" protocol associated with nUHPLC/HR ESI-MS/MS allowed to extend the coverage of the rat and human VDACs sequences with respect to that obtained with the previous procedure [61], so that it was possible to completely cover the rat and human VDAC1 sequences and almost completely the rat and humanVDAC2 and VDAC3 sequences [22,59,62]. It should be noted that the short regions not identified in VDAC2 and VDAC3 correspond to small tryptic or chymotryptic peptides or even to single amino acids, which cannot be detected in LC/MS analysis.

Moreover, by means of this new procedure a detailed characterization of PTMs of the three VDACs was obtained (see next paragraphs).

3.2. Mass Spectrometry Analysis of Post-Translational Modifications

The mammalian proteome is vastly more complex than the related genome. The reasons for this difference reside both in the molecular mechanisms that allow a single gene to encode for multiple proteins (genomic recombination, transcription initiation at alternative promoters, differential transcription termination, and alternative splicing of the transcript) and in the post-translational modifications (PTMs) which represent a wide range of chemical changes that proteins can undergo after synthesis. They include the specific cleavage of protein precursors, the covalent addition or removal of low-molecular groups (i.e., acetylation, glycosylation, hydroxylation, phosphorylation, ubiquitination) and the formation of disulfide bonds or other redox modifications [63–65].

PTMs play crucial roles in cell biology since they can change protein physical or chemical properties, activity, localization, and/or stability. Traditionally, PTMs have been identified by Edman degradation, amino acid analysis, isotopic labeling, or immunochemistry. Within recent years, MS has proven to be extremely useful in PTM discovery. Post-translationally modified amino acids always have a different molecular mass than the original, unmodified residues and this mass increment or deficit is usually the basis for the detection and characterization of PTM by MS (commonly by LC-ESI-MS/MS).

MS has several advantages for characterization of PTMs, including (i) very high sensitivity; (ii) discovery of novel PTMs; (iii) ability to identify PTMs and the modified sites, even in complex protein mixtures; and (iv) ability to quantify the relative changes in PTM occupancy at distinct sites. None of the other techniques provide all these features, so the greater majority of the known PTMs have been described by MS [66].

To improve sensibility, several methods have been developed to enrich the samples in proteins or peptides with specific PTMs prior to MS/MS analysis, such as anti-pY antibodies, IMAC (immobilized metal affinity chromatography) and TiO_2 for phosphorylation [67,68], affinity capture with lectins for glycosylated proteins [69], and resin coupled with anti-acetyl-lysine for acetylated proteins [70]. Although, as previously described, isolation of single isoforms of VDACs cannot be obtained, application of combined HPLC and high-resolution ESI-MSMS analysis has resulted in the identification of several PTM in these proteins. In the following, a summary of the MS-based PTMs characterized in VDACs is reported and the respective biological significance discussed. These results are resumed in Table 1 and Figure 1.

Table 1. Post-translational modifications in VDAC isoforms obtained using mass spectrometry. PTM type, mass shift (Da), source of the sample, modified residue, MS method and relative reference are reported. Studies are described by listing first author + year.

ISOFORM	PTM Type	ΔMass (Da)	Source	Residue	Method	Study
VDAC1	Protein N-terminal acetylation	42.0106	Rat liver	Ala 2	nUHPLC/high resolution nESI-MS/MS in a Q-QT-qIT MS	Saletti et al., 2018
			HAP1 cells	Ala 2		Pittalà et al., 2020
	Acetylation	42.0106	Mouse liver	Lys 33, 41, 74, 234	nHPLC MS/MS in an LTQ MS	Kim et al., 2006
				Lys 41, 122, 132	nHPLC MS/MS in an LTQ 2D ion-trap MS	Schwer et al., 2009
			Mouse liver and heart	Lys 237	UPLC Velos-FT MS	Yang et al., 2011
			Human liver	Lys 28	LC/LC-MS/MS in an FTICR/MS	Zhao et al., 2010
	Oxidation	15.9949	Rat liver	Met 155	LC/LC-MS/MS in an FTICR/MS	Guan et al., 2003
					nUHPLC/high resolution nESI-MS/MS in a Q-QT-qIT MS	Saletti et al., 2018
			HAP1 cells	Met 129, 155		Pittalà et al., 2020
	Trioxidation	47.9847	Rat liver	Cys 127, 232		Saletti et al., 2018
			HAP1 cells	Cys 127		Pittalà et al., 2020
	Phosphorylation	79.9663	Rat liver	Ser 12, 136	HPLC MS/MS in an LTQ MS	Distler et al., 2007
			Mouse liver	Ser 117	nHPLC MS/MS in an LTQ MS	Lee et al., 2007
			HeLa cells	Ser 101, 102, 104, Thr 107	nHPLC MS/MS in an LTQ-Orbitrap MS	Olsen et al., 2006
			Mouse brain	Tyr 80, 208	LC-MS/MS in an LTQ FT MS	Ballif et al., 2008
VDAC2	Protein N-terminal acetylation	42.0106	Rat liver	Ala 2	nUHPLC/high resolution nESI-MS/MS in a Q-QT-qIT MS	Saletti et al., 2018
			HAP1 cells	Ala 2		Pittalà et al., 2020
	Acetylation	42.0106	Mouse liver	Lys 32, 75	nHPLC MS/MS in an LTQ MS	Kim et al., 2006
				Lys 121	nHPLC MS/MS in an LTQ 2D ion-trap MS	Schwer et al., 2009
	Oxidation	15.9949	Rat liver	Met 167	nUHPLC/high resolution nESI-MS/MS in a Q-QT-qIT MS	Saletti et al., 2018
			HAP1 cells	Met 12, 166		Pittalà et al., 2020
	Trioxidation	47.9847	Rat liver	Cys 48, 77, 104, 211		Saletti et al., 2018
			HAP1 cells	Cys 47, 76, 103, 138, 210		Pittalà et al., 2020
	Succination	116.0110	Mouse brain	Cys 48, 77	LC-nESI-MS/MS in an LTQ-Orbitrap MS	Piroli et al., 2016
			Rat liver	Cys 48	nUHPLC/high resolution nESI-MS/MS in a Q-QT-qIT MS	Saletti et al., 2018
	Phosphorylation	79.9663	HeLa cells	Ser 115, Thr 118	nHPLC MS/MS in an LTQ-Orbitrap MS	Olsen et al., 2006
			Rat liver	Thr 109	SCX-RP-MS/MS in an LTQ-Orbitrap MS	Deng et al., 2010
			Rat liver	Tyr 237	HPLC MS/MS in an LTQ MS	Distler et al., 2007
			Mouse brain	Tyr 207	LC-MS/MS in an LTQ FT MS	Ballif et al., 2008

Table 1. *Cont.*

ISOFORM	PTM Type	ΔMass (Da)	Source	Residue	Method	Study
VDAC3	Protein N-terminal acetylation	42.0106	Rat liver	Cys 2	nUHPLC/high resolution nESI-MS/MS in a Q-QT-qIT MS	Saletti et al., 2016
			HAP1 cells	Cys 2		Pittalà et al., 2020
	Acetylation	42.0106	Mouse liver	Lys 20, 61, 226	nHPLC MS/MS in an LTQ MS	Kim et al., 2006
				Lys 63, 109	nHPLC MS/MS in an LTQ 2D ion-trap MS	Schwer et al., 2009
			Human liver	Lys 28	LC/LC-MS/MS in an FTICR-MS	Zhao et al., 2010
	Oxidation	15.9949	Rat liver	Met 26, 155	nUHPLC/high resolution nESI-MS/MS in a Q-QT-qIT MS	Saletti et al., 2016
			HAP1 cells	Met 26, 155, 226		Pittalà et al., 2020
	Trioxidation	47.9847	Rat liver	Cys 36, 65, 165, 229		Saletti et al., 2016
			HAP1 cells	Cys 36, 65		Pittalà et al., 2020
	Succination	116.0110	Rat liver	Cys 8, 36, 229		Saletti et al., 2018
	Phosphorylation	79.9663	Rat liver	Ser 241, Thr 33	HPLC MS/MS in an LTQ MS	Distler et al., 2007
			Mouse brain	Tyr 49	LC-MS/MS in an LTQ FT MS	Ballif et al., 2008

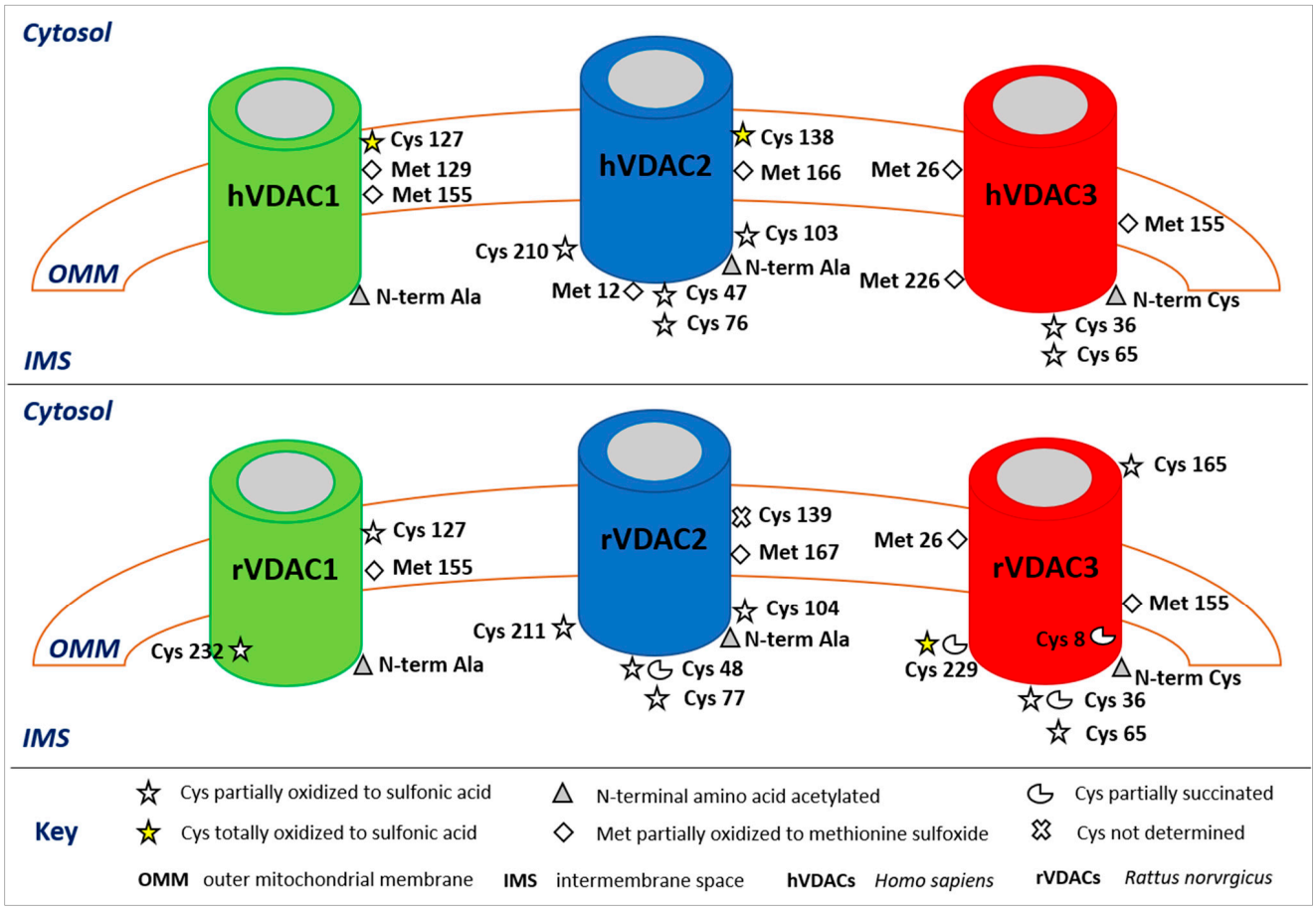

Figure 1. Post-translational modifications of human (upper panel) and rattus (lower panel) VDAC isoforms. The image shows only the modified amino acids and their positions with respect to the cytosol, the outer mitochondrial membrane (OMM), and the intermembrane space (IMS). In the rVDAC1 Cys^{232} faces the aqueous inside of the pore; in the rVDAC3 Cys^{8} is located inside of the pore.

3.2.1. Deletion of N-Terminal Methionine and Acetylation of Lysines

In all rat and human VDACs the HRMS data confirmed that the N-terminal Met, reported in the SwissProt database sequence, is missing in the mature proteins and that the N-terminal amino acid is always acetylated [22,59,62]. Although N-terminal acetylation is widespread in eukaryotes, the biological relevance of this modification is only known for a few substrates [71,72]. Unlike ε-lysine modification, N-terminal acetylation, catalyzed by N-terminal acetyltransferases, is irreversible and occurs co-translationally [73,74]. It has been suggested that co-translational N-acetylation modifies protein–protein interaction, affects accumulation of the mature protein(s) in target organelles [75], confers metabolic stability to the protein by providing general protection from peptidases and against irreversible oxidation, and seems to act as a degradation signal in the Ac/N–degron pathway [76]. Consequently, any dysregulation of N-terminal acetylation, leads to serious pathological conditions including neurodegenerative diseases, cancers, hypertension, and X-linked genetic disorders [77–79].

All data regarding the acetylation of the three different VDAC isoforms were obtained from proteomic studies of acetyl-lysine enriched fractions.

In liver of fed and starved mice, lysines 33, 41, 74, and 234 of VDAC1 were detected acetylated by immunoprecipitation enrichment of acetylated peptides with an anti-acetylated lysine antibody and nanoHPLC MS/MS in an LTQ mass spectrometer [70]. Analogously, using mass spectrometry and label-free quantitation, Schwer et al. found that, in mouse liver tryptic digest immunopurified with acetyl-lysine affinity matrix, lysines 41, 122, and 132 in VDAC1 were found acetylated during calorie restriction [80]. However, no significant quantitative difference in VDAC1 acetylation was highlighted between fed and starved and fed and calorie restricted animals, respectively. In addition to the above-mentioned sites, lysine 237 was also acetylated in mouse liver and heartVDAC1 analyzed with a built-in-house Velos-FT mass spectrometer [81].

Acetylation of lysines 32 and 75 [70] and 121 [80] was observed in mouse liver VDAC2. Again, no differences in acetylation between fed and starved and fed and calorie-restricted mice were revealed.

In contrast to VDAC1 and VDAC2, VDAC3 showed acetylation of lysines 20, 61, and 226 only in livers of starved but not of fed mice [70]. In addition, lysines 63 and 109 were identified acetylated in mouse liver, with no differences between fed and calorie-restricted animals [80]. However, none of the above studies addressed the potential physiological effect of VDAC acetylation.

In human liver mitochondria, VDAC1 and VDAC3 were found acetylated in position 28 after purification with an antibody to acetyl lysine and analysis by tandem liquid chromatography–tandem mass spectrometry (LC/LC-MS/MS) [82]. The amino acid sequence of the acetylated dodecapeptide in human VDAC1 and 3 (GYGFGLIK*LDLK and GYGFGMVK*IDLK, respectively) differs in three amino acid residues.

3.2.2. Oxidation States of Methionines

Even in mild conditions, methionine residues are highly susceptible to oxidation mediated by reactive oxygen (ROS) and nitrogen species (NOS) to generate in vivo Met sulfoxide (MetO), which can be further oxidized to methionine sulfone ($MetO_2$) under stronger oxidizing conditions [83]. MetO exists as a mixture of S and R diastereomers and its production is tightly regulated in vivo by ubiquitous sulfoxide reductases, which catalyze the thioredoxin-dependent reduction of MetO into methionine [84]. Conversely, $MetO_2$ cannot be reduced in vivo.

Cyclic Met oxidation/MetO reduction leads to consumption of ROS and thereby acts as a scavenging system to protect proteins from oxidative damage [85,86]. Moreover, MetO formation seems to have little or no effect on protein susceptibility to proteolytic degradation [87,88]. Numerous studies reported that MetO levels in proteins increase during aging and in certain disease, in particular in the neurodegenerative ones [89].

Evidence for an additional role of certain methionines as oxidation sensors in the redox regulation of enzyme activity is accumulating [90–92].

In rat and human VDAC isoforms, methionines oxidized to sulfoxide were detected by nUHPLC/HRnESI-MS/MS [22,59,62].

Considering the VDAC1 sequence, one methionine residue (Met^{155}) is conserved in rat and human. The mass spectral data indicated that among the peptides identified, besides the fragments containing Met^{155} in the normal form, peptides with this residue in the form of methionine sulfoxide (MetO) were also identified [93].

Although from these data a precise determination of the ratio between Met and Met sulfoxide could not be obtained, a rough estimation of their relative abundance was derived from the comparison of the absolute intensity of the multiply charged molecular ions of the respective peptides. These calculations demonstrated that in rat VDAC1 (rVDAC1) the conserved Met^{155} is oxidized to MetO in a remarkable higher amount (Ox/Red ratio 65:1) than in the human VDAC1 (hVDAC1) (Ox/Red ratio 0.8:1), while the Ox/Red ratio for the Met^{129}, which is present only in hVDAC1, resulted 1.5:1.

Analogously, VDAC2 sequence contains one internal conserved methionine, Met^{167} in rat and Met^{166} in human, respectively. Both the amino acid residues are partially oxidized to MetO in approximatively equal amount (Ox/Red ratio 3.2:1 in rVDAC2, and 1.4:1 in hVDAC2). On the contrary, the other Met^{12} in hVDAC2 is mainly in the oxidized form (Ox/Red ratio about 10:1).

Finally, in the hVDAC3 the Ox/Red ratio of the three methionines 26, 155, and 226 was about 0.1:1, 1:1, and 3:1, respectively. In particular, Met^{26} showed an oxidation state comparable to that of the analogous rVDAC3 methionine (Ox/Red ratio about 0.6:1), whereas the oxidation rate of Met^{155}, the latter conserved methionine, was not determined in the rat isoform.

Literature has highlighted a key role of VDACs in mitochondrial dysfunction typical of many neurodegenerative disorders. In particular, the principal isoform VDAC1 represents the main mitochondrial docking site of many misfolded proteins, such as amyloid-β and Tau in Alzheimer's disease, α-synuclein in Parkinson's disease, and several SOD1 mutants in ALS. The interaction of misfolded proteins with VDAC1 has a strong impact on both cellular bioenergetics and apoptosis' pathways alteration. Therefore, VDACs represent a promising therapeutic target in neurodegenerative diseases [28].

Very recently, by HRMS/MS analysis, possible signs of oxidative damage in VDAC1 from the NSC34-SOD1G93A cell line, a suitable ALS motor neuron cell model line, were investigated [94].

Interestingly, a higher amount of methionine sulfoxide and sulfone was observed for Met^{155} in the mutated line (MetO/Met ratio 61:1 and $MetO_2$/Met 4.7:1, respectively) in comparison with NSC34 and NSC34-SOD1WT cell lines (MetO/Met ratio 3–5:1 and $MetO_2$/Met0.1:1, respectively).

3.2.3. Oxidation States of Cysteines

Because of their redox-reactive thiol (–SH) side chain, cysteine residues are easily subjected to various Ox-PTMs including S-nitrosylation (or S-nitrosation, SNO), sulfhydration (SSH), S-acylation, S-glutathionylation, sulfenylation (SOH), and oxidation to sulfinic acid (SO_2H) and sulfonic acid (SO_3H) [65]. Except for sulfonic acid, all the reported Ox-PTMs are readily reversible and ruled by specific enzymatic activities. Moreover, cysteine oxidation has a structural relevance for proteins, since it can support the disulfide bridge formation (RS-SR), a physiological protein cross-linking, which is an essential PTM involved in protein folding and in the stabilization of tertiary and quaternary structure. Disulfide formation depends on the spatial proximity between two cysteines and can also occur through a reaction with sulfenic acid in the presence of high concentrations of ROS. They indeed convert SOH groups into thiol radicals (RS) which, in turn, react with other thiolates to form a disulfide bond [65].

In a recent paper, mitochondrial enrichment and subsequent cysteine-targeted MS analysis allowed to identify ~1500 reactive cysteine residues on ~450 mitochondrial proteins in HEK293T cells, and additionally, 22 highly S-nitrosoglutathione (GSNO)-sensitive cysteines also in VDAC proteins [95].

Through UHPLC/HR nESI-MS/MS analysis, cysteine PTMs were characterized in detail, and it was discovered that such cysteines can be subject to different oxidization degrees, ranging from the disulfide bridge to the most oxidized, the sulfonic acid one, an irreversible and permanent protein modification, and even harmful in the cell. In fact, as mentioned above, there are no known enzymes that can reverse this form back to any of the lower sulfur oxidative states (sulfenic and sulfinic forms) [96].

Interestingly, the insertion of a strong negative charges by $–SO_3H$ formation can modify the protein conformation by electric repulsions inside the chain or toward phospholipids. Some authors suggested that these conformational changes can initiate protein incorporation into mitochondria-derived vesicles (MDVs), later targeted to lysosomes. MDVs, whose production is induced by mitochondrial stress [97], contain numerous oxidized proteins derived mainly from the OMM.

Recent findings revealed a precise and evolution conserved pattern in oxidative status among human and rat VDACs [22,59,62].

VDAC1 presents only two cysteines in position 127 and 232, located far from each other. In rVDAC1 both these residues are moderately oxidized, with a ratio Ox/Red in the range of 0.1–0.26 [62]. Instead, in hVDAC1, Cys^{127} (in the β-strand 8), which protrudes in the hydrophobic, phospholipidic milieu, is totally trioxidized as $–SO_3H$, while Cys^{232} (in β-strand 16) facing the water-accessible side of the channel [5–7], is exclusively in the reduced and carboxyamidomethylated form [22].

VDAC2 is the longer isoform, with an N-terminal extension of 11 amino acids in mammals and is the richest in cysteines: 11 and 9 in rat and human, respectively. This difference is due to the presence of two additional Cys residues in the N-terminal sequence of the rat isoform.

In hVDAC2 Cys^8, Cys^{13}, and Cys^{133} were exclusively in the reduced form; these residues are exposed to the IMS and correspond to Cys^9, Cys^{14}, and Cys^{134} in rVDAC2, which have also been found to be reduced or not determined (Cys^{134}).

Cysteines in position 47, 76, 103, and 210, all in IMS loops, were instead identified as partially oxidized to $–SO_3H$. Among them, Cys^{76} was detected in the form of sulfonic acid with an Ox/Red ratio of about 0.1:1, similarly to the homologue Cys^{77} in rVDAC2. Cysteines 47, 103, and 210 are found partially trioxidized but with a lower Ox/Red ratio (about 0.1:1–0.01:1), reproducing the trend observed for the homologous cysteines 48, 104, and 211 of rVDAC2.

Cys^{227}, which is instead the only cysteine predicted to be in a hydrophilic turn exposed to the cytosol, resulted exclusively reduced, analogously to the Cys^{228} in rVDAC2, whose trioxidized form was detected in very low amount (rough ratio of 1:100 oxidized/reduced). It is tempting to speculate that it can be involved in some kind of docking function of this protein.

In rVDAC2, the additional Cys^4 and Cys^5 in the N-terminal moiety are also reduced; thus, VDAC2 has a cluster of cysteines oriented towards the IMS that are available to reversible oxidation.

Finally, hVDAC2 Cys^{138}, situated in a position similar to that of Cys^{127} in hVDAC1, and therefore embedded in the hydrophobic environment of the OMM, was found fully trioxidized to sulfonic acid as the homologous residue in hVDAC1.

It is important to underline that the preferred redox state of cysteines in general is conserved between rat and human VDAC3 [22,59]. Accordingly, Cys^{36} and Cys^{65} were detected in a reduced form and trioxidized to sulfonic acid in a similar extent in both organisms. Cys^2 and Cys^{122}, which are also facing the IMS, were identified entirely reduced, as Cys^8 which is inside the channel. In rat, the oxidation state of Cys^{122} remained undetermined because peptides containing this residue were not detectable. The only

exception was Cys^{229} that in hVDAC3 is completely reduced, whereas in the rat isoform was totally trioxidized.

Overoxidation can be required to target a protein to degradation. In particular, in the so called "N-end rule pathway", the presence of an oxidized N-terminal cysteine in certain mammalian proteins is required for arginylation by ATE1 R-transferases and subsequent ubiquitin-dependent degradation [98]. In VDAC3, Cys^2 becomes the N-terminal end after the elimination of Met^1 during the protein maturation [22,59]. Because the oxidized form of Cys^2 was never detected, this can mean that the potentially Cys^2-oxidized, if existing, is a marker used to remove the protein from the membrane for degradation.

On the contrary, the groups of Cys residues always in reduced form in all the three VDAC isoforms could have another function: The persistence of their reduction, together with the exposition to the IMS, an oxidative environment, prompts to speculate their involvement in disulfide bridge(s) formation, with conformational consequence for the pore.

In conclusion, it is important to underline that most of the HRMS data obtained for the oxidation states of cysteines in human VDACs are the same as those obtained for the rat ones, thus demonstrating that they do not depend on the type of organism, at least in mammals, but reflect a physiological condition.

Furthermore, the power of the deep mass spectrometric analysis reported us a list of other proteins present in the HTP eluate from Triton X-100 solubilized rat liver mitochondria. Among them, no evidence of over-oxidized cysteines was discovered, demonstrating that the overoxidation is a peculiarity of the VDAC isoforms [62]. Another validation of these data is that the application of the same methodologies to different kind of sources, living tissue from organism (rat liver), or cultured cells (human HAP cell) resulted in remarkably similar results.

3.2.4. Phosphorylation

Phosphorylation of VDACs was reported in pathological conditions and is associated with degradation and pro-apoptotic pathways [14,99]. Indeed, some results suggest that VDAC1 phosphorylation is involved in the genesis of apoptosis in brain of Alzheimer disease (AD) and Down syndrome (DS) patients [100]. In this work, the authors described protein levels of VDACs in individual post-mortem brain regions of patients with DS and AD using two-dimensional electrophoresis (2-DE) and MALDI TOF-MS. VDAC1 and VDAC2 were unambiguously identified and quantified, but VDAC3 was not found. It was noted an increase in the content of three VDAC1 isoforms, which differed in their isoelectric points, probably caused by post-translational modifications as, e.g., phosphorylation. However, no information regarding the type and site of phosphorylation was presented.

Through proteomic analysis followed by Western blotting and immunohistochemical techniques, it was demonstrated that VDAC1 is overexpressed in the hippocampus from amyloidogenic AD transgenic mice models [101]. VDAC1 was also overexpressed in post-mortem brain tissue from AD patients at an advanced stage of the disease. Interestingly, amyloid-β (Aβ) soluble oligomers were able to induce upregulation of VDAC1 in a human neuroblastoma cell line, further supporting a correlation between Aβ levels and VDAC1 expression. In hippocampal extracts from transgenic mice, a significant increase was observed in the levels of VDAC1 phosphorylated at an epitope susceptible to phosphorylation by glycogen synthase kinase-3β [101].

Protein phosphorylation is catalyzed by a family of protein kinases, with serine, threonine, and tyrosine side chains being the most frequently modified [102]. The reverse reaction is catalyzed by specific protein phosphatases, i.e., phosphoserine/phosphothreonine-specific and phosphotyrosine-specific families of phosphatases [103].

To study the PTMs of rVDACs, a method based on enrichment of the proteins by harvesting high-purity outer membrane from rat liver mitochondria, followed by isolation of the proteins of interest by semipreparative SD-PAGE/electroelution was developed [104]. Following this approach, all three isoforms were found phosphorylated at one or more sites, in particular, VDAC1 at serine 12 and 136, corresponding to CaM-II/GSK3 and PKC

consensus sites, respectively. Employing an improved IMAC method to examine mouse liver mitochondrial phosphoproteome, it was documented also the phosphorylation of serine 117 [105]. By a shotgun approach, phosphorylation of serine 101, 102, and 104, and of threonine 107 in HeLa cells were determined [106] as well as of tyrosine residues 80 and 208 in mouse brain [107].

VDAC2 phosphorylation of serine 115 and threonine 118 was demonstrated in HeLa cells [106]; in rat liver mitochondria Deng et al. reported that VDAC2 is phosphorylated at threonine 109 [108], whereas Distler et al. found phosphorylation at tyrosine 237 [104]. Subsequently, in mouse brain Ballif et al. documented tyrosine phosphorylation of residue 207 [107].

Finally, in VDAC3 from rat liver mitochondria, phosphorylation of serine 241 and threonine 33 was shown [104]. These sites correspond to PKA and PKC consensus sites. In mouse brain, VDAC3 is also tyrosine-phosphorylated at residue 49 [107].

Again, the phosphorylation of Ser^{104} in VDAC1 was evidenced in the three cellular lines (NSC34, NSC34-SOD1WT, and NSC34-SOD1G93A) recently investigated by nUH-PLC/HR ESI-MS/MS, even though in low amounts (Table 2 and Figure 2) [94].

Table 2. Post-translational modifications in VDAC1 from NSC34, NSC34-SOD1WT, and NSC34-SOD1G93A cell lines obtained using mass spectrometry. PTM type, mass shift (Da), cell line, residue, and modified/normal ratio are reported.

PTM Type	ΔMass (Da)	Cell Line	Residue	Modified/Normal Ratio
Protein N-terminal acetylation	42.0106	NSC34	Ala 2	Totally acetylated
		NSC34-SOD1WT		
		NSC34-SOD1G93A		
Oxidation	15.9949	NSC34	Met 155	5:1
		NSC34-SOD1WT		4:1
		NSC34-SOD1G93A		60:1
Dioxidation	31.9898	NSC34	Met 155	0.1:1
		NSC34-SOD1WT		0.1:1
		NSC34-SOD1G93A		5:1
Trioxidation	47.9847	NSC34	Cys 127	Totally trioxidized
		NSC34-SOD1WT	Cys 127	Totally trioxidized
		NSC34-SOD1G93A	Cys 127	30:1
Phosphorylation	79.9663	NSC34	Ser 104	0.01:1
		NSC34-SOD1WT		0.01:1
		NSC34-SOD1G93A		0.01:1
Deamidation	0.9840	NSC34	/	/
		NSC34-SOD1WT	/	/
		NSC34-SOD1G93A	Asn 37, 106, 207, 214, 239 Gln 166, 226	Asn = 0.01–0.6:1 Gln = deamidated in trace amount

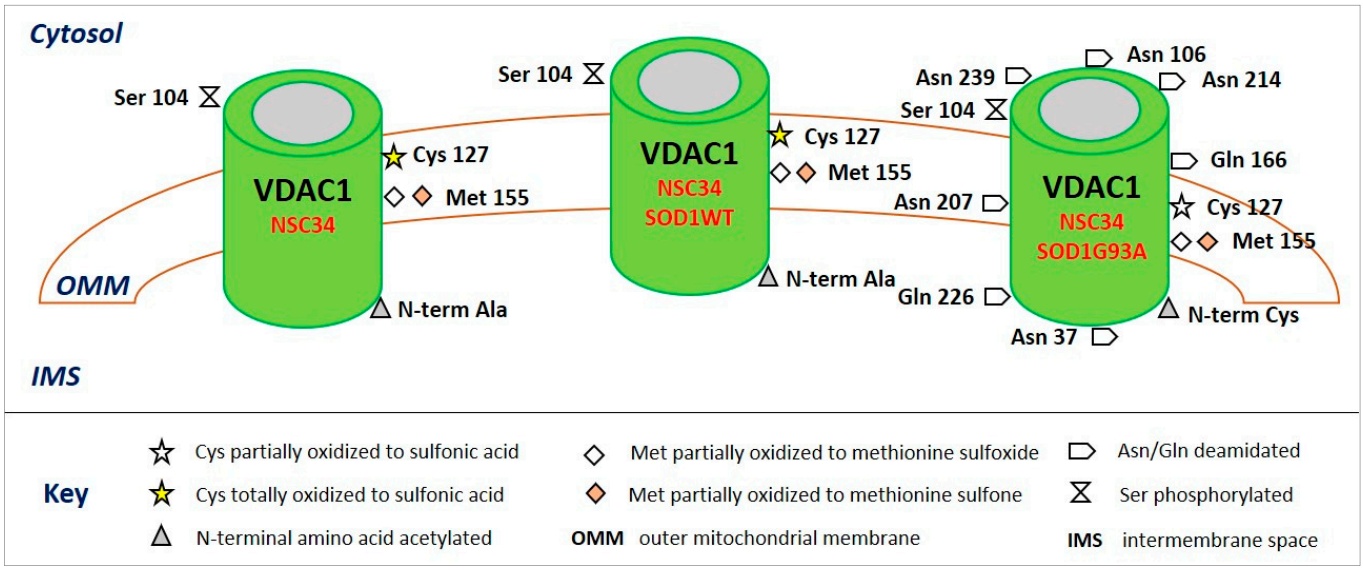

Figure 2. Post-translational modifications of VDAC1 from NSC34 (left), NSC34-SOD1WT (middle), and NSC34-SOD1G93A (right) cell lines. The image shows only the modified amino acids and their positions with respect to the cytosol, the outer mitochondrial membrane (OMM), and the intermembrane space (IMS).

3.2.5. Succination, Deamidation, Ubiquitin, Ubiquitination, and Presence of Selenocysteines

Elevated fumarate concentrations as a result of Krebs cycle inhibition lead to increases in protein succination, an irreversible post-translational modification that occurs when fumarate reacts with cysteine residues to generate S-(2-succino)cysteine (2SC). It has been verified in some mitochondrial diseases [109], cancer (with fumarate hydratase (FH) deficiency) [110], and diabetes [111].

Using the Ndufs4 knockout (Ndufs4 KO) mouse, a model of Leigh syndrome, it was demonstrated that protein succination increased in the brainstem (BS). 2D-SDS-PAGE followed by immunoblotting for succinated proteins and MS/MS analysis of BS proteins allowed to identify VDAC1 and 2 as specific targets of succination: in particular, Cys^{77} and Cys^{48} were identified as endogenous sites of succination in VDAC2. Given the important role of the VDACs in the exchange of ADP/ATP between the cytosol and the mitochondria, and the already decreased capacity for ATP synthesis in the Ndufs4 KO mice, the authors proposed that the increased protein succination observed in the BS of these animals would further decrease the already compromised mitochondrial function [109].

Identification of succinated cysteines in rVDAC2, but not in rVDAC1, was also reported [62]. In rVDAC2 only Cys^{48} was succinated in very low amount with a ratio succinated/normal about 0.04.

Selenocysteines were not observed in any of the rVDAC isoforms. In the nUHPLC/HRESI-MS/MS analysis of the PTMs of VDAC1 in ALS-SOD1 model cells [94], succinated cysteines were not found, as well as no evidence of ubiquitin and ubiquitination.

Notably, in the same work, the deamidation of five specific asparagine (Asn^{37}, Asn^{106}, Asn^{207}, Asn^{214}, and Asn^{239}) and two glutamine (Gln^{166} and Gln^{226}) residues was revealed exclusively in VDAC1 purified from NSC34-SOD1G93A cells but not in NSC34-SOD1WT or NSC34 cells. Deamidation is a non-inheritable PTM that introduces negative charges by removing amino groups from asparagine and, with a much lower frequency and rate, glutamine [112,113].

Because deamidation alters both peptide and protein structure and charge, it is suspected to contribute to the aging proteome in stability and to protein folding disorders such as those observed in Alzheimer's, Parkinson's, and many other degenerative diseases [114–118]. In particular, it has been found that deamidation is one of the most abundant modifications in long-lived proteins and can serve as disease biomarkers. More-

over, abnormal level of deamidation has also been associated with disease-related proteins in type 2 diabetes and cancers, and therefore, in-depth characterization of deamidation is of great biological significance [119].

The deamidation level of the Asn^{207} residue was much higher than for any other residue converted to aspartate. This residue is indeed located in the center of the β-strand 14 and is preceded and followed by non-bulky amino acid residues. As a consequence, the amido group of Asn^{207} can be particularly sensitive to ROS at the IMM, which are strongly increased in ALS, as well as being affected by the aggressive action of peroxidized lipids in the OMM.

Interestingly, the different charge distribution due to deamidation must have an impact on the physiological interactivity of VDAC1 and consequently on the functionality of the protein itself and of the whole mitochondrion.

In conclusion, these post-translational changes in VDAC1 may be involved in its specific interaction with ALS-related SOD1 mutants and it is reasonable to hypothesize a role of the modified isoform in the disease and as a biomarker of irreparably damaged mitochondria, and at the same time for the early diagnosis of this pathology.

4. Conclusions

The remarkable difficulties in the analysis of VDAC are related to their very high hydrophobicity, low solubility and the impossibility to separate them from each other. Currently available combination of nUHPLC and HRMS provides a powerful and indispensable tool for the detailed structural characterization of a single protein in a complex mixture without previous isolation, including the fine characterization of PTMs. Future advances in technology are expected in the next years. New instrumentation able to performs faster scanning speeds and higher mass accuracy will allow for more peptide identifications and ultimately higher proteome coverage which will facilitate the analysis of membrane proteins.

Presently, the association of an originally developed "in-solution" protocol with nUHPLC/HRMS for the analysis of an enriched VDACs fraction has permitted a fine determination of a number of PTMs in these proteins. As a result, the use of specific PTMs as possible biomarkers for an early diagnosis of degenerative diseases can be envisaged.

The assignment of a functional role to these modifications of VDACs will be a further step towards the full understanding of the roles of these proteins in the cell, leading to an even more detailed knowledge of the molecular basis of the degenerative disorders which are still poorly understood.

Author Contributions: R.S. and M.G.G.P. conceived the review organization. S.C.N., S.R., V.C. and A.D.F. revised the experimental data. R.S., M.G.G.P. and S.R. wrote most of text. M.G.G.P., S.F. and V.D.P. selected the references. A.M., V.D.P. and S.F. reviewed and revised the text. All authors have read and agreed to the published version of the manuscript.

Funding: This research was partly supported by the "Piano della Ricerca di Ateneo PIACERI 2020" of the University of Catania, Italy to all the participants, and by the MIUR PNR "Proof of Concept 2018" grant (codex: PEPSLA POC 01_00054) to A.M.

Institutional Review Board Statement: Not applicable.

Informed Consent Statement: Not applicable.

Acknowledgments: The authors gratefully acknowledge the Bio-Nanotech Research and Innovation Tower of the University of Catania (BRIT; PON project financed by the Italian Ministry for Education. University and Research MIUR).

Conflicts of Interest: The authors declare no conflict of interest.

References

1. Shoshan-Barmatz, V.; De Pinto, V.; Zweckstetter, M.; Raviv, Z.; Keinan, N.; Arbel, N. VDAC, a multi-functional mitochondrial protein regulating cell life and death. *Mol. Aspects Med.* **2010**, *31*, 227–285. [CrossRef]
2. Messina, A.; Reina, S.; Guarino, F.; De Pinto, V. VDAC isoforms in mammals. *Biochim. Biophys. Acta* **2012**, *1818*, 1466–1476. [CrossRef]
3. Young, M.J.; Bay, D.C.; Hausner, G.; Court, D.A. The evolutionary history of mitochondrial porins. *BMC Evol. Biol.* **2007**, *7*, 31. [CrossRef]
4. De Pinto, V.; Reina, S.; Gupta, A.; Messina, A.; Mahalakshmi, R. Role of cysteines in mammalian VDAC isoforms' function. *Biochim. Biophys. Acta Bioenerg.* **2016**, *1857*, 1219–1227. [CrossRef]
5. Hiller, S.; Garces, R.G.; Malia, T.J.; Orekhov, V.Y.; Colombini, M.; Wagner, G. Solution structure of the integral human membrane protein VDAC-1 in detergent micelles. *Science* **2008**, *321*, 1206–1210. [CrossRef] [PubMed]
6. Bayrhuber, M.; Meins, T.; Habeck, M.; Becker, S.; Giller, K.; Villinger, S.; Vonrhein, C.; Griesinger, C.; Zweckstetter, M.; Zeth, K. Structure of the human voltage-dependent anion channel. *Proc. Natl. Acad. Sci. USA* **2008**, *105*, 15370–15375. [CrossRef] [PubMed]
7. Ujwal, R.; Cascio, D.; Colletier, J.P.; Faham, S.; Zhang, J.; Toro, L.; Ping, P.; Abramson, J. The crystal structure of mouse VDAC1 at 2.3 angstrom resolution reveals mechanistic insights into metabolite gating. *Proc. Natl. Acad. Sci. USA* **2008**, *105*, 17742–17747. [CrossRef] [PubMed]
8. Schredelseker, J.; Paz, A.; Lopez, C.J.; Altenbach, C.; Leung, C.S.; Drexler, M.K.; Chen, J.N.; Hubbell, W.L.; Abramson, J. High resolution structure and double electron-electron resonance of the zebrafish voltage-dependent anion channel 2 reveal an oligomeric population. *J. Biol. Chem.* **2014**, *289*, 12566–12577. [CrossRef] [PubMed]
9. Amodeo, G.F.; Scorciapino, M.A.; Messina, A.; De Pinto, V.; Ceccarelli, M. Charged residues distribution modulates selectivity on the open state of human isoforms of the voltage dependent anion-selective channel. *PLoS ONE* **2014**, *9*, e103879. [CrossRef]
10. De Pinto, V.; Guarino, F.; Guarnera, A.; Messina, A.; Reina, S.; Tomasello, M.F.; Palermo, V.; Mazzoni, C. Characterization of human VDAC isoforms: A peculiar function for VDAC3? *Biochim. Biophys. Acta-Bioenergetics* **2010**, *1797*, 1268–1275. [CrossRef]
11. Naghdi, S.; Várnai, P.; Hajnóczky, G. Motifs of VDAC2 required for mitochondrial Bak import and tBid-induced apoptosis. *Proc. Natl. Acad. Sci. USA* **2015**, *112*, E5590–E5599. [CrossRef]
12. Shoshan-Barmatz, V.; Maldonado, E.N.; Krelin, Y. VDAC1 at the crossroads of cell metabolism, apoptosis and cell stress. *Cell Stress* **2017**, *1*, 1. [CrossRef]
13. Shoshan-Barmatz, V.; Pittala, S.; Mizrachi, D. VDAC1 and the TSPO: Expression, Interactions, and Associated Functions in Health and Disease States. *Int. J. Mol. Sci.* **2019**, *20*, 3348. [CrossRef] [PubMed]
14. Kerner, J.; Lee, K.; Tandler, B.; Hoppel, C.L. VDAC proteomics: Post-translation modifications. *Biochim. Biophys. Acta* **2012**, *1818*, 1520–1525. [CrossRef] [PubMed]
15. Geula, S.; Ben-Hail, D.; Shoshan-Barmatz, V. Structure-based analysis of vdac1: N-terminus location, translocation, channel gating and association with anti-apoptotic proteins. *Biochem. J.* **2012**, *444*, 475–485. [CrossRef] [PubMed]
16. Abu-Hamad, S.; Arbel, N.; Calo, D.; Arzoine, L.; Israelson, A.; Keinan, N.; Ben-Romano, R.; Friedman, O.; Shoshan-Barmatz, V. The vdac1 n-terminus is essential both for apoptosis and the protective effect of anti-apoptotic proteins. *J. Cell Sci.* **2009**, *122*, 1906–1916. [CrossRef]
17. Shi, Y.; Chen, J.; Weng, C.; Chen, R.; Zheng, Y.; Chen, Q.; Tang, H. Identification of the protein-protein contact site and interaction mode of human vdac1 with bcl-2 family proteins. *Biochem. Biophys. Res. Commun.* **2003**, *305*, 989–996. [CrossRef]
18. Naghdi, S.; Hajnóczky, G. VDAC2-specific cellular functions and the underlying structure. *Biochim. Biophys. Acta* **2016**, *1863*, 2503–2514. [CrossRef]
19. Shoshan-Barmatz, V.; Ben-Hail, D. VDAC, a multi-functional mitochondrial protein as a pharmacological target. *Mitochondrion* **2012**, *12*, 24–34. [CrossRef]
20. Abu-Hamad, S.; Zaid, H.; Israelson, A.; Nahon, E.; Shoshan-Barmatz, V. Hexokinase-I protection against apoptotic cell death is mediated via interaction with the voltage-dependent anion channel-1: Mapping the site of binding. *J. Biol. Chem.* **2008**, *283*, 13482–13490. [CrossRef]
21. De Pinto, V.; al Jamal, J.A.; Palmieri, F. Location of the dicyclohexylcarbodiimide-reactive glutamate residue in the bovine heart mitochondrial porin. *J. Biol. Chem.* **1993**, *268*, 12977–12982. [CrossRef]
22. Pittalà, M.G.G.; Saletti, R.; Reina, S.; Cunsolo, V.; De Pinto, V.; Foti, S. A High Resolution Mass Spectrometry Study Reveals the Potential of Disulfide Formation in Human Mitochondrial Voltage-Dependent Anion Selective Channel Isoforms (hVDACs). *Int. J. Mol. Sci.* **2020**, *21*, 1468. [CrossRef]
23. Budelier, M.M.; Cheng, W.W.L.; Bergdoll, L.; Chen, Z.W.; Janetka, J.W.; Abramson, J.; Krishnan, K.; Mydock-McGrane, L.; Covey, D.F.; Whitelegge, J.P.; et al. Photoaffinity labeling with cholesterol analogues precisely maps a cholesterol-binding site in voltage-dependent anion channel-1. *J. Biol. Chem.* **2017**, *292*, 9294–9304. [CrossRef] [PubMed]
24. Gatliff, J.; East, D.; Crosby, J.; Abeti, R.; Harvey, R.; Craigen, W.; Parker, P.; Campanella, M. Tspo interacts with vdac1 and triggers a ros-mediated inhibition of mitochondrial quality control. *Autophagy* **2015**, *10*, 2279–2296. [CrossRef] [PubMed]
25. Mueller, B.K.; Subramaniam, S.; Senes, A. A frequent, GxxxG-mediated, transmembrane association motif is optimized for the formation of interhelical Cα-H hydrogen bonds. *Proc. Natl. Acad. Sci. USA* **2014**, *111*, E888–E895. [CrossRef] [PubMed]
26. Bernardi, P.; Di Lisa, F.; Fogolari, F.; Lippe, G. From ATP to PTP and back: A dual function for the mitochondrial ATP synthase. *Circ. Res.* **2015**, *116*, 1850–1862. [CrossRef]

27. Reina, S.; Guarino, F.; Magrì, A.; De Pinto, V. VDAC3 as a potential marker of mitochondrial status is involved in cancer and pathology. *Front. Oncol.* **2016**, *6*, 264. [CrossRef]
28. Magrì, A.; Messina, A. Interactions of VDAC with Proteins Involved in Neurodegenerative Aggregation: An Opportunity for Advancement on Therapeutic Molecules. *Curr. Med. Chem.* **2017**, *24*, 4470–4487. [CrossRef] [PubMed]
29. Sun, Y.; Vashisht, A.A.; Tchieu, J.; Wohlschlegel, J.A.; Dreier, L. Voltage-dependent Anion Channels (VDACs) recruit Parkin to defective mitochondria to promote mitochondrial autophagy. *J. Biol. Chem.* **2012**, *287*, 40652–40660. [CrossRef]
30. Sheikh, S.; Haque, E.; Snober, S.M. Neurodegenerative diseases: Multifactorial conformational diseases and their therapeutic interventions. *J. Neurodegen. Dis.* **2013**, *2013*, 563481. [CrossRef]
31. Smilansky, A.; Dangoor, L.; Nakdimon, I.; Ben-Hail, D.; Mizrachi, D.; Shoshan-Barmatz, V. The voltage-dependent anion channel 1 mediates amyloid beta toxicity and represents a potential target for Alzheimer's disease therapy. *J. Biol. Chem.* **2015**, *290*, 30670–30683. [CrossRef] [PubMed]
32. Hemachandra Reddy, P. Is the mitochondrial outer membrane protein VDAC1 therapeutic target for Alzheimer's disease? *Biochim. Biophys. Acta* **2013**, *1832*, 67–75. [CrossRef] [PubMed]
33. Rostovtseva, T.K.; Gurnev, P.A.; Protchenko, O.; Hoogerheide, D.P.; Yap, T.L.; Philpott, C.C.; Lee, J.C.; Bezrukov, S.M. α-Synuclein shows high affinity interaction with Voltage-dependent Anion Channel, suggesting mechanisms of mitochondrial regulation and toxicity in Parkinson Disease. *J. Biol. Chem.* **2015**, *290*, 18467–18477. [CrossRef] [PubMed]
34. Israelson, A.; Arbel, N.; Da Cruz, S.; Ilieva, H.; Yamanaka, K.; Shoshan-Barmatz, V.; Cleveland, D.W. Misfolded mutant SOD1 directly inhibits VDAC1 conductance in a mouse model of inherited ALS. *Neuron* **2010**, *67*, 575–587. [CrossRef] [PubMed]
35. Magrì, A.; Belfiore, R.; Reina, S.; Tomasello, M.F.; Di Rosa, M.C.; Guarino, F.; Leggio, L.; De Pinto, V.; Messina, A. Hexokinase I N-terminal based peptide prevents the VDAC1-SOD1G93A interaction and re-establishes ALS cell viability. *Sci. Rep.* **2016**, *6*, 34802. [CrossRef]
36. Harada, T.; Sada, R.; Osugi, Y.; Matsumoto, S.; Matsuda, T.; Hayashi-Nishino, M.; Nagai, T.; Harada, A.; Kikuchi, A. Palmitoylated CKAP4 regulates mitochondrial functions through an interaction with VDAC2 at ER–mitochondria contact sites. *J. Cell Sci.* **2020**, *133*, jcs249045. [CrossRef]
37. Zhong, Y.; Tang, X.; Sheng, X.; Xing, J.; Zhan, W. Voltage-Dependent Anion Channel Protein 2 (VDAC2) and Receptor of Activated Protein C Kinase 1 (RACK1) Act as Functional Receptors for Lymphocystis Disease Virus Infection. *J. Virol.* **2019**, *93*, e00122-19. [CrossRef]
38. Yang, Y.; Luo, M.; Zhang, K.; Zhang, J.; Gao, T.; O'Connell, D.; Yao, F.; Mu, C.; Cai, B.; Shang, Y.; et al. Nedd4 ubiquitylates VDAC2/3 to suppress erastin-induced ferroptosis in melanoma. *Nat. Commun.* **2020**, *11*, 433. [CrossRef]
39. Messina, A.; Reina, S.; Guarino, F.; Magrì, A.; Tomasello, F.; Clark, R.E.; Ramsayc, R.R.; De Pinto, V. Live cell interactome of the human voltage dependent anion channel 3 (VDAC3) revealed in HeLa cells by affinity purification tag technique. *Mol. BioSyst.* **2014**, *10*, 2134–2145. [CrossRef]
40. Ytterberg, A.J.; Dunsmore, J.; Lomeli, S.H.; Thevis, M.; Xie, Y.; Loo, R.R.O.; Loo, J.A. The role of mass spectrometry for peptide, protein, and proteome characterization. In *Electrospray and MALDI Mass Spectrometry: Fundamentals, Instrumentation, Practicalities, and Biological Applications*, 2nd ed.; Cole, R.B., Ed.; Wiley and Sons: Hoboken, NJ, USA, 2010; Chapter 18; pp. 683–721.
41. Rosinke, B.; Strupat, K.; Hillenkamp, F.; Rosenbusch, J.; Dencher, N.; Krüger, U.; Galla, H.-J. Matrix-assisted laser desorption/ionization mass spectrometry (MALDI-MS) of membrane proteins and non-covalent complexes. *J. Mass Spectrom.* **1995**, *30*, 1462–1468. [CrossRef]
42. Barth, M.; Schmidt, C. Native mass spectrometry—A valuable tool in structural biology. *J. Mass Spectrom.* **2020**, *55*, e4578. [CrossRef]
43. Stolz, A.; Jooß, K.; Höcker, O.; Römer, J.; Schlecht, J.; Neusüß, C. Recent advances in capillary electrophoresis-mass spectrometry: Instrumentation, methodology and applications. Recent advances in capillary electrophoresis- • 1000e102 mass spectrometry: Instrumentation, methodology and applications. *Electrophoresis* **2019**, *40*, 79–112. [CrossRef]
44. Thakur, S.S.; Geiger, T.; Chatterjee, B.; Bandilla, P.; Frohlich, F.; Cox, J.; Mann, M. Deep and highly sensitive proteome coverage by LC-MS/MS without prefractionation. *Mol. Cell Proteomics* **2011**, *10*, M110.003699. [CrossRef] [PubMed]
45. Motoyama, A.; Yates III, J.R. Multidimensional LC separations in shotgun proteomics. *Anal. Chem.* **2008**, *80*, 7187–7193. [CrossRef] [PubMed]
46. Kanu, A.B.; Dwivedi, P.; Tam, M.; Matz, L.; Hill, H.H., Jr. Ion mobility-mass spectrometry. *J. Mass Spectrom.* **2008**, *43*, 1–22. [CrossRef] [PubMed]
47. De Hoffmann, E.; Stroobant, V. *Mass Spectrometry: Principles and Applications*, 3rd ed.; John Wiley: Hoboken, NJ, USA, 2007.
48. Loo, J.A.; Quinn, J.P.; Ryu, S.I.; Henry, K.D.; Senko, M.W.; McLafferty, F.W. High-resolution tandem mass spectrometry of large biomolecules. *Proc. Natl. Acad. Sci. USA* **1992**, *89*, 286–289. [CrossRef] [PubMed]
49. Hu, Q.; Noll, R.J.; Li, H.; Makarov, A.; Hardman, M.; Cooks, R.G. The Orbitrap: A new mass spectrometer. *J. Mass Spectrom.* **2005**, *40*, 430–443. [CrossRef] [PubMed]
50. Eliuk, S.; Makarov, A. Evolution of Orbitrap Mass Spectrometry Instrumentation. *Annu. Rev. Anal. Chem.* **2015**, *8*, 61–80. [CrossRef]
51. Johnson, R.S.; Martin, S.A.; Biemann, K.; Stults, J.T.; Watson, J.T. Novel fragmentation process of peptides by collision-induced decomposition in a tandem mass spectrometer: Differentiation of leucine and isoleucine. *Anal. Chem.* **1987**, *59*, 2621–2625. [CrossRef] [PubMed]

52. Roepstorff, P.; Fohlman, J. Proposal for a common nomenclature for sequence ions in mass spectra of peptides. *Biomed. Mass Spectrom.* **1984**, *11*, 601. [CrossRef] [PubMed]
53. Chi, H.; Sun, R.X.; Yang, B.; Song, C.Q.; Wang, L.H.; Liu, C.; Fu, Y.; Yuan, Z.F.; Wang, H.P.; He, S.M.; et al. pNovo: De novo peptide sequencing and identification using HCD spectra. *J. Proteome Res.* **2010**, *9*, 2713–2724. [CrossRef]
54. Good, D.M.; Wirtala, M.; McAlister, G.C.; Coon, J.J. Performance characteristics of electron transfer dissociation mass spectrometry. *Mol. Cell. Proteomics* **2007**, *6*, 1942–1951. [CrossRef] [PubMed]
55. Quan, L.; Liu, M. CID, ETD and HCD Fragmentation to Study Protein Post-Translational Modifications. *Mod. Chem. Appl.* **2013**, *1*, 1000e102.
56. Frese, C.K.; Altelaar, A.F.; Hennrich, M.L.; Nolting, D.; Zeller, M.; Griep-Raming, J.; Heck, A.J.R.; Mohammed, S. Improved peptide identification by targeted fragmentation using CID, HCD and ETD on an LTQ-OrbitrapVelos. *Proteome Res.* **2011**, *10*, 2377–2388. [CrossRef] [PubMed]
57. Cunsolo, V.; Foti, S. Mass Spectrometry in Proteomics. In *Mass Spectrometry: An Applied Approach*, 2nd ed.; Smoluch, M., Grasso, G., Suder, P., Silberring, J., Eds.; Wiley: Hoboken, NJ, USA, 2019; pp. 261–272.
58. Abrecht, H.; Wattiez, R.; Ruysschaert, J.M.; Homblé, F. Purification and characterization of two Voltage-Dependent Anion Channel Isoforms from plant seeds. *Plant Physiol.* **2000**, *124*, 1181–1190. [CrossRef]
59. Saletti, R.; Reina, S.; Pittalà, M.G.G.; Belfiore, R.; Cunsolo, V.; Messina, A.; De Pinto, V.; Foti, S. High resolution mass spectrometry characterization of the oxidation pattern of methionine and cysteine residues in rat liver mitochondria Voltage-Dependent Anion selective Channel 3 (VDAC3). *Biochim. Biophys. Acta-Biomembr.* **2017**, *1859*, 301–311. [CrossRef]
60. De Pinto, V.; Prezioso, G.; Palmieri, F. A simple and rapid method for the purification of the mitochondrial porin from mammalian tissues. *Biochim. Biophys. Acta* **1987**, *905*, 499–502. [CrossRef]
61. Distler, A.M.; Kerner, J.; Peterman, S.M.; Hoppel, C.L. A targeted proteomic approach for the analysis of rat liver mitochondrial outer membrane proteins with extensive sequence coverage. *Anal. Biochem.* **2006**, *356*, 18–29. [CrossRef]
62. Saletti, R.; Reina, S.; Pittalà, M.G.G.; Magrì, A.; Cunsolo, V.; Foti, S.; De Pinto, V. Post-translational modifications of VDAC1 and VDAC2 cysteines from rat liver mitochondria. *Biochim. Biophys. Acta-Bioenerg.* **2018**, *1859*, 806–816. [CrossRef]
63. Wang, Y.; Peterson, S.; Loring, J. Protein post-translational modifications and regulation of pluripotency in human stem cells. *Cell Res.* **2014**, *24*, 143–160. [CrossRef]
64. Duan, G.; Walther, D. The roles of post-translational modifications in the context of protein interaction networks. *PLoS Comput. Biol.* **2015**, *11*, e1004049. [CrossRef]
65. Reina, S.; Pittalà, M.G.G.; Guarino, F.; Messina, A.; De Pinto, V.; Foti, S.; Saletti, R. Cysteine oxidations in mitochondrial membrane proteins: The case of VDAC isoforms in mammals. *Front. Cell Dev. Biol.* **2020**, *8*, 397. [CrossRef] [PubMed]
66. Jensen, O.N. Modification-specific proteomics: Characterization of posttranslational modifications by mass spectrometry. *Curr. Opin. Chem. Biol.* **2004**, *8*, 33–41. [CrossRef] [PubMed]
67. Corthals, G.L.; Aebersold, R.; Goodlett, D.R. Identification of phosphorylation sites using microimmobilized metal affinity chromatography. *Meth. Enzymol.* **2005**, *405*, 66–81.
68. Larsen, M.R.; Thingholm, T.E.; Jensen, O.N.; Roepstorff, P.; Jørgensen, T.J. Highly selective enrichment of phosphorylated peptides from peptide mixtures using titanium dioxide microcolumns. *Mol. Cell. Proteomics* **2005**, *4*, 873–886. [CrossRef]
69. Yang, Z.; Hancock, W.S. Approach to the comprehensive analysis of glycoproteins isolated from human serum using a multi-lectin affinity column. *J. Chromatogr. A* **2004**, *1053*, 79–88. [CrossRef]
70. Kim, S.C.; Sprung, R.; Chen, Y.; Xu, Y.; Ball, H.; Pei, J.; Cheng, T.; Kho, Y.; Xiao, H.; Xiao, L.; et al. Substrate and functional diversity of lysine acetylation revealed by a proteomics survey. *Mol. Cell.* **2006**, *23*, 607–618. [CrossRef]
71. Caesar, R.; Warringer, J.; Blomberg, A. Physiological importance and identification of novel targets for the N-terminal acetyltransferase NatB. *Eukaryot. Cell* **2006**, *5*, 368–378. [CrossRef]
72. Polevoda, B.; Norbeck, J.; Takakura, H.; Blomberg, A.; Sherman, F. Identification and specificities of N-terminal acetyltransferases from *Saccharomyces cerevisiae*. *EMBO J.* **1999**, *18*, 6155–6168. [CrossRef]
73. Polevoda, B.; Sherman, F. N alpha-terminal acetylation of eukaryotic proteins. *J. Biol. Chem.* **2000**, *275*, 36479–36482. [CrossRef]
74. Polevoda, B.; Sherman, F. N-terminal acetyltransferases and sequence requirements for N-terminal acetylation of eukaryotic proteins. *J. Mol. Biol.* **2003**, *325*, 595–622. [CrossRef]
75. Pesaresi, P.; Gardner, N.A.; Masiero, S.; Dietzmann, A.; Eichacker, L.; Wickner, R.; Salamini, F.; Leister, D. Cytoplasmic N-Terminal Protein Acetylation Is Required for Efficient Photosynthesis in Arabidopsis. *Plant Cell* **2003**, *15*, 1817–1832. [CrossRef]
76. Hershko, A.; Heller, H.; Eytan, E.; Kaklij, G.; Rose, I.A. Role of the alpha-amino group of protein in ubiquitin-mediated protein breakdown. *Proc. Natl. Acad. Sci. USA* **1984**, *81*, 7021–7025. [CrossRef]
77. Rope, A.F.; Wang, K.; Evjenth, R.; Xing, J.; Johnston, J.J.; Swensen, J.J.; Johnson, W.E.; Moore, B.; Huff, C.D.; Bird, L.M.; et al. Using VAAST to identify an X-linked disorder resulting in lethality in male infants due to N-terminal acetyltransferase deficiency. *Am. J. Hum. Genet.* **2011**, *89*, 28–43. [CrossRef]
78. Aksnes, H.; Drazic, A.; Arnesen, T. (Hyper)tension release by N-terminal acetylation. *Trends Biochem. Sci.* **2015**, *40*, 422–424. [CrossRef]
79. Aksnes, H.; Drazic, A.; Marie, M.; Arnesen, T. First things first: Vital protein marks by N-terminal acetyltransferases. *Trends Biochem. Sci.* **2016**, *41*, 746–760. [CrossRef] [PubMed]

80. Schwer, B.; Eckersdorf, M.; Li, Y.; Silva, J.C.; Fermin, D.; Kurtev, M.V.; Giallourakis, C.; Comb, M.J.; Alt, F.W.; Lombard, D.B. Calorie restriction alters mitochondrial protein acetylation. *Aging Cell* **2009**, *8*, 604–606. [CrossRef] [PubMed]
81. Yang, L.; Vaitheesvaran, B.; Hartil, K.; Robins, A.J.; Hoopmann, M.R.; Eng, J.K.; Kurland, I.J.; Bruce, J.E. The fasted/fed mouse metabolic acetylome: N6-acetylation differences suggest acetylation coordinates organ-specific fuel switching. *J. Proteome Res.* **2011**, *10*, 4134–4149. [CrossRef] [PubMed]
82. Zhao, S.; Xu, W.; Jiang, W.; Yu, W.; Lin, Y.; Zhang, T.; Yao, J.; Zhou, L.; Zeng, Y.; Li, H.; et al. Regulation of cellular metabolism by protein lysine acetylation. *Science* **2010**, *327*, 1000–1004. [CrossRef]
83. Levine, R.L.; Moskovitz, J.; Stadtman, E.R. Oxidation of methionine in proteins: Roles in antioxidant defense and cellular regulation. *IUBMB Life* **2000**, *50*, 301–307. [CrossRef] [PubMed]
84. Stadtman, E.R.; Moskovitz, J.; Levine, R.L. Oxidation of methionine residues of proteins: Biological consequences. *Antioxid. Redox Signal.* **2003**, *5*, 577–582. [CrossRef]
85. Stadtman, E.R. Protein oxidation and aging. *Free Radic. Res.* **2006**, *40*, 1250–1258. [CrossRef]
86. Ugarte, N.; Petropoulos, I.; Friguet, B. Oxidized mitochondrial protein degradation and repair in aging and oxidative stress. *Antioxid. Redox Signal.* **2010**, *13*, 539–549. [CrossRef]
87. Levine, R.L.; Mosoni, L.; Berlett, B.S.; Stadtman, E.R. Methionine residues as endogenous antioxidants in proteins. *Proc. Natl. Acad. Sci. USA* **1996**, *93*, 15036–15040. [CrossRef]
88. Stadtman, E.R.; Moskovitz, J.; Berlett, B.S.; Levine, R.L. Cyclic oxidation and reduction of protein methionine residues is an important antioxidant mechanism. *Mol. Cell Biochem.* **2002**, *234*, 3–9. [CrossRef] [PubMed]
89. Stadtman, E.R.; Van Remmen, H.; Richardson, A.; Wehr, N.B.; Levine, R.L. Methionine oxidation and aging. *Biochim. Biophys. Acta* **2005**, *1703*, 135–140. [CrossRef]
90. Bartlett, R.K.; Urbauer, R.J.B.; Anbanandam, A.; Smallwood, H.S.; Urbauer, J.L.; Squier, T.C. Oxidation of Met(144) and Met(145) in calmodulin blocks calmodulin dependent activation of the plasma membrane Ca-ATPase. *Biochemistry* **2003**, *42*, 3231–3238. [CrossRef] [PubMed]
91. Bigelow, D.J.; Squier, T.C. Redox modulation of cellular signaling and metabolism through reversible oxidation of methionine sensors in calcium regulatory proteins. *Biochim. Biophys. Acta* **2005**, *1703*, 121–134. [CrossRef]
92. Erickson, J.R.; Joiner, M.L.; Guan, X.; Kutschke, W.; Yang, J.; Oddis, C.V.; Bartlett, R.K.; Lowe, J.S.; O'Donnell, S.E.; Aykin-Burns, N.; et al. A dynamicpathway for calcium-independent activation of CaMKII by methionine oxidation. *Cell* **2008**, *133*, 462–474. [CrossRef] [PubMed]
93. Guan, Z.Q.; Yates, N.A.; Bakhtiar, R. Detection and characterization of methionine oxidation in peptides by collision-induced dissociation and electron capture dissociation. *J. Am. Soc. Mass Spectrom.* **2003**, *14*, 605–613. [CrossRef]
94. Pittalà, M.G.G.; Reina, S.; Cubisino, S.A.M.; Cucina, A.; Formicola, B.; Cunsolo, V.; Foti, S.; Saletti, R.; Messina, A. Post-translational modification analysis of VDAC1 in ALS-SOD1 model cells reveals specific asparagines and glutamine deamidation. *Antioxidants* **2020**, *9*, 1218. [CrossRef]
95. Bak, D.W.; Pizzagalli, M.D.; Weerapana, E. Identifying functional cysteine residues in the mitochondria. *ACS Chem. Biol.* **2017**, *12*, 947–957. [CrossRef]
96. Bachi, A.; Dalle-Donne, I.; Scaloni, A. Redox proteomics: Chemical principles, methodological approaches and biological/biomedical promises. *Chem. Rev.* **2013**, *113*, 596–698. [CrossRef] [PubMed]
97. Sugiura, A.; McLelland, G.L.; Fon, E.A.; McBride, H.M. A new pathway for mitochondrial quality control: Mitochondrial-derived vesicles. *EMBO J.* **2014**, *33*, 2142–2156. [CrossRef] [PubMed]
98. Tasaki, T.; Kwon, Y.T. The mammalian N-end rule pathway: New insights into its components and physiological roles. *Trends Biochem. Sci.* **2007**, *32*, 520–528. [CrossRef] [PubMed]
99. Baines, C.P.; Kaiser, R.A.; Sheiko, T.; Craigen, W.J.; Molentkin, J.D. Voltage-dependent anion channels are dispensable for mitochondrial cell death. *Nat. Cell Biol.* **2007**, *9*, 550–555. [CrossRef] [PubMed]
100. Yoo, B.C.; Fountoulakis, M.; Cairns, N.; Lubec, G. Changes of Voltage-Dependent Anion-Selective Channel proteins VDAC1 and VDAC2 brain levels in patients with Alzheimer's disease and Down syndrome. *Electrophoresis* **2001**, *22*, 172–179. [CrossRef]
101. Cuadrado-Tejedor, M.; Vilarino, M.; Cabodevilla, F.; Del Rio, J.; Frechilla, D.; Perez- Mediavilla, A. Enhanced expression of the voltage-dependent anion channel 1 (VDAC1) in Alzheimer's disease transgenic mice: An insight into the pathogenic effects of amyloid-β. *J. Alzheimers Dis.* **2011**, *23*, 195–206. [CrossRef]
102. Hanks, S.K.; Hunter, T. The eukaryotic protein kinase superfamily: Kinase (catalytic) domain structure and classification. *FASEB J.* **1995**, *9*, 576–596. [CrossRef]
103. Moorhead, G.B.G.; De Wever, V.; Templeton, G.; Kerk, D. Evolution of protein phos-phatases in plants and animals. *Biochem. J.* **2009**, *417*, 401–409. [CrossRef]
104. Distler, A.M.; Kerner, J.; Hoppel, C.L. Posttranslational modifications of rat liver mitochondrial carnitine palmitoyltransferase-I, long-chain acyl-CoA synthetase, and voltage dependent anion channel. *Biochim. Biophys. Acta* **2007**, *1774*, 628–636. [CrossRef]
105. Lee, J.; Xu, Y.; Chen, Y.; Sprung, R.; Kim, S.C.; Xie, S.; Zhao, Y. Mitochondrial phosphoproteome revealed by an improved IMAC method and MS/MS/MS. *Mol. Cell. Proteomics* **2007**, *6*, 669–676. [CrossRef]
106. Olsen, J.V.; Blagoev, B.; Gnad, F.; Macek, B.; Kumar, C.; Mortensen, P.; Mann, M. Global, in vivo, and site-specific phosphorylation dynamics in signaling networks. *Cell* **2006**, *127*, 635–648. [CrossRef]

107. Ballif, B.A.; Carey, G.R.; Sunyaev, S.R.; Gygi, S.P. Large-scale identification and evolution indexing of tyrosine phosphorylation sites from murine brain. *J. Proteome Res.* **2008**, *7*, 311–318. [CrossRef]
108. Deng, W.J.; Nie, S.; Dai, J.; Wu, J.R.; Zeng, R. Proteome, phosphoproteome, and hydroxyproteome of liver mitochondria in diabetic rats at early pathogenic stages. *Mol. Cell. Proteomics* **2010**, *9*, 100–116. [CrossRef] [PubMed]
109. Piroli, G.G.; Manuel, A.M.; Clapper, A.C.; Walla, M.D.; Baatz, J.E.; Palmiter, R.D.; Quintana, A.; Frizzell, N. Succination is increased on select proteins in the brainstem of the NADH dehydrogenase (ubiquinone) Fe-S protein 4 (Ndufs4) knockout mouse, a model of Leigh syndrome. *Mol. Cell. Proteomics* **2016**, *15*, 445–461. [CrossRef] [PubMed]
110. Pollard, P.J.; Briere, J.J.; Alam, N.A.; Barwell, J.; Barclay, E.; Wortham, N.C.; Hunt, T.; Mitchell, M.; Olpin, S.; Moat, S.J.; et al. Accumulation of Krebs cycle intermediates and overexpression of HIF1α in tumours which result from germline FH and SDH mutations. *Hum. Mol. Genet.* **2005**, *14*, 2231–2239. [CrossRef] [PubMed]
111. Isaacs, J.S.; Jung, Y.J.; Mole, D.R.; Lee, S.; Torres-Cabala, C.; Chung, Y.L.; Merino, M.; Trepel, J.; Zbar, B.; Toro, J.; et al. HIF overexpression correlates with biallelic loss of fumarate hydratase in renal cancer: Novel role of fumarate in regulation of HIF stability. *Cancer Cell* **2005**, *8*, 143–153. [CrossRef] [PubMed]
112. Wright, H.T. Nonenzymatic deamidation of asparaginyl and glutaminyl residues in proteins. *Crit. Rev. Biochem. Mol. Biol.* **1991**, *26*, 1–52. [CrossRef]
113. Robinson, N.E.; Robinson, Z.W.; Robinson, B.R.; Robinson, A.L.; Robinson, J.A.; Robinson, M.L.; Robinson, A.B. Structure-dependent nonenzymatic deamidation of glutaminyl and asparaginyl pentapeptides. *J. Pept. Res.* **2004**, *63*, 426–436. [CrossRef]
114. Bastrup, J.; Kastaniegaard, K.; Asuni, A.A.; Volbracht, C.; Stensballe, A. Proteomic and Unbiased Post-Translational Modification Profiling of Amyloid Plaques and Surrounding Tissue in a Transgenic Mouse Model of Alzheimer's Disease. *J. Alzheimer's Dis.* **2020**, *73*, 393–411. [CrossRef] [PubMed]
115. Sadakane, Y.; Kawahara, M. Implications of Metal Binding and Asparagine Deamidation for Amyloid Formation. *Int. J. Mol. Sci.* **2018**, *19*, 2449. [CrossRef] [PubMed]
116. Shimizu, T.; Watanabe, A.; Ogawara, M.; Mori, H.; Shirasawa, T. Isoaspartate formation and neurodegeneration in Alzheimer's disease. *Arch. Biochem. Biophys.* **2000**, *381*, 225–234. [CrossRef] [PubMed]
117. Robinson, N.E.; Robinson, M.L.; Schulze, S.E.S.; Lai, B.T.; Gray, H.B. Deamidation of α-synuclein. *Protein Sci.* **2009**, *18*, 1766–1773. [CrossRef] [PubMed]
118. Vigneswara, V.; Cass, S.; Wayne, D.; Bolt, E.L.; Ray, D.E.; Carter, W.G. Molecular ageing of alpha- and beta-synucleins: Protein damage and repair mechanisms. *PLoS ONE* **2013**, *8*, e61442. [CrossRef]
119. Ying, Y.; Li, H. Recent progress in the analysis of protein deamidation using mass spectrometry. *Methods* **2020**. [CrossRef]